Academic year 2008-2009

Thesis submitted in partial fulfillment of the requirements
for the degree of Doctor in Science: Biology

A paleolimnological reconstruction of Late-Quaternary environmental change along a transect from South America to the Antarctic Peninsula

Een paleolimnologische reconstructie van Laat-Kwartaire milieuveranderingen langsheen een transect van Zuid-Amerika tot het Antarctisch Schiereiland

Mieke Sterken

Promotor: Prof. W. Vyverman
Co-promotor: Prof. K. Sabbe
Co-promotor: Prof. M. De Batist

Faculty of Sciences, Biology Department
Research group Protistology and Aquatic Ecology

Members of the examination committee:

Members of the reading committee:

Promotor: Prof. Dr. Wim Vyverman (Universiteit Gent)
Co-promotor: Prof. Dr. Koen Sabbe (Universiteit Gent)
Co-promotor: Prof. Dr. Marc De Batist (Universiteit Gent)
Dr. Elie Verleyen (Universiteit Gent)
Dr. Dominic Hodgson (British Antarctic Survey, Cambridge, UK)
Dr. Holger Cremer (TNO Geological Survey, Utrecht, Nl)

Other members of the examination committee:

Prof. Dr. Dominique Adriaens (Universiteit Gent) (Chairman)
Prof. Dr. Dirk Verschuren (Universiteit Gent)

Public thesis defence:

Friday, May 8th, 2009 at 4.00 p.m.
Ghent University
Auditorium Valère Billiet, Krijgslaan 281-S8, 9000 Gent

*This thesis was realised within the framework of the **Belspo**- (Belgian Science Policy) projects Holant, Bella, Laquan and ENSO-Chile.*

Contents

De Steen

(*Bram Vermeulen*)

Ik heb een steen verlegd, in een rivier op aarde,
Het water gaat er anders dan voorheen.
De stroom van een rivier, hou je niet tegen,
Het water vindt er altijd een weg omheen.

Misschien, eens gevuld door sneeuw en regen,
neemt de rivier mijn kiezel met zich mee,
om hem dan glad en rond gesleten,
te laten rusten in de luwte van de zee.

Ik heb een steen verlegd, in een rivier op aarde.
Nu weet ik dat ik nooit zal zijn vergeten.
Ik leverde bewijs van mijn bestaan,
omdat door het verleggen, van die ene steen,
de stroom nooit meer dezelfde weg kan gaan.

Ik hoop dat deze thesis één van de kiezels mag zijn in het geheel van klimaat- en diatomeeënstudies, en dat deze en andere studies in de toekomst nog zullen aangroeien, tot er een solide 'dam' van kennis over het klimaat en zijn onderliggende mechanismen ontstaat.

Gent, mei 2009 *Mieke*

Dankwoord

Woord vooraf: Tijdens het schrijven van dit doctoraat kostte het me dikwijls moeite om mijn teksten 'summier' te houden. In het dankwoord - het 'officieuze' gedeelte van dit werk - wil ik me dan ook eens iets meer laten gaan, en hoewel dit riskeert lang te worden, weet ik nu al dat dit nóg te kort is om alle steun te beschrijven die ik in de voorbije jaren heb gekregen. Bij deze mijn oprechte dank aan iedereen die ook maar op één of andere manier van betekenis is geweest bij de realisatie van deze thesis!

In de eerste plaats wil ik mijn promotor **Wim Vyverman** danken alsmede mijn co-promotoren **Koen Sabbe** en **Marc De Batist,** en mijn begeleider **Elie Verleyen**.

Wim, vooreerst heel erg bedankt om bij de start van mijn doctoraat in mij te geloven en mij aldus financiële steun te bieden! Het Holant project was zeer interessant, en hoewel paleo-cores niet altijd eenduidig te interpreteren zijn, vond ik de Beak-cores wel bijzondere exemplaren. Ook bedankt voor het doornemen van mijn teksten, voor de raadgevingen, alsook het persoonlijk begrip op enkele moeilijke momenten tijdens de eerste jaren. Verder dank ik je voor het bieden van de mogelijkheid tot veldwerk in Chili: dat was, net zoals dit hele doctoraat, een leerrijke ervaring.

Koen, jij hebt me binnengeloodsd in het labo en me, samen met Elie en Wim, begeleid bij mijn beursaanvragen. Bedankt hiervoor, alsook voor het aanvragen van projecten, de hulp bij het publiceren van de Marcacocha-paper, het doornemen van de andere papers, en naar het einde toe voor de 'grove borstel' bij Hoofdstukken 4 en 5 van deze thesis. Ook bedankt voor het respect, en voor de juiste knik en interesse op het juiste moment, vooral tijdens de laatste maanden van vorig jaar.

Marc, allereerst bedankt omdat ik op ENSO-Chile mocht werken, en meer bepaald op hét orakel van Puyehue. Ook bedankt omdat ik steeds bij je terecht kon met gelijk welke vragen of problemen, om er samen antwoorden of oplossingen voor te zoeken, voor je raad en morele opstekers. Een zeer grote merci ook voor het overnemen van de financiering van de laatste maanden van mijn doctoraat.

Elie, vooreerst ook merci voor het schrijven (samen met Wim en Koen) van projectaanvragen en het editen van de projectrapporten. Voor de begeleiding, vooral bij Hoofdstukken 2, 6 en 7 in dit doctoraat, het interpreteren van de pigment-chromatogrammen, het aanreiking van literatuur en de tips en babbels in onze bureau. Ook bedankt om mij te betrekken bij de biogeografie-papers, waarbij ik mijn geografenhart nog eens kon ophalen, ik vond het zeer interessant!

I would like to express my appreciation for the other members of the jury, **Holger Cremer, Dominic Hodgson, Dirk Verschuren** and **Dominique Adriaens**, for the in-depth review of the thesis and their presence during the private and public defence.

At the British Antarctic Survey, I met **Dominic Hodgson** and **Steve Roberts,** who I gratefully acknowledge for the scientific discussions, the dating and sedimentological data from the Beak Island cores and the help in writing the Beak-papers (Chapters 6 and 7). Dom, many thanks for providing the context of this research, of which I felt very honoured to be involved in. Steve: thanks for the hospitality whenever I was at BAS; for the bikes, food & good care. Thanks as well for your help during the fieldwork campaign, for learning me how to take a core and for doing most of the heavy coring work. **Andrea Balbo**, thank you for your kindness and your help with subsampling!
Viv Jones: many thanks for providing the original slides, counting sheets and pictures from the diatom surface dataset from Livingston & Signy Islands; for kindly taking the time to go through my pictures and species together, and for answering my questions via e-mail.
Sebastien Bertrand, thanks a lot for the good collaboration on the Puyehue C/N paper (Chapter 3), the fruitful discussions and the very fast responses to all my questions. Thanks as well for the hospitality when I went for subsampling the Puyehue cores in Liège. Credits also go to **Nathalie Fagel**, who, together with Marc and the whole Puyehue team in Liège created the opportunity for me to work together on this Chilean core.
Bart Van de Vijver: heel erg bedankt voor de hulp, het meermaals samen doornemen van mijn diatomeeën-fotoboeken, het beschrijven van de nieuwe soorten in Hoofdstuk 5, en het kritisch doornemen van Hoofdstuk 4, alsook voor je aanstekelijke diatomeeën-enthousiasme!

Renaat Dasseville: bedankt voor de hulp bij vele pigment-analyses en de uitleg bij de SEM, het bestellen van materiaal en je vele andere 'onzichtbare' maar nodige labo-taken!
Dirk Verschuren voor de Holivar-uitnodiging (Kastanienbaum, 2004), de interesse en het verlenen van tijdschriften en informatie; dank u wel!
Alex Chepstow-Lusty: although Marcacocha is not a part of this thesis, you were there at the beginning of my Msc and PhD period, and your enthusiasm and positivism made it a joy to communicate with you. I hope I will ever meet you in real life so we can finally have that pint you still owe me ☺!
Carolina Diaz, **Patricio Moreno, Rodrigo Villa** and the staff of **CONAF** are thanked for their help during the fieldwork campaign. **Mario Pino** and the students are thanked for the great atmosphere and stimulating discussions during our visit in Valdivia.

Melianie Raymond, Rhian Salmon and **all APECS-EOC members**, thanks for your enthusiasm about the poles, for making progress as a group and for the positive atmosphere. An extra thanks to Melianie for her energy-boosting e-mails, which kept me going in the final months!

Thesisstudenten **Veerle De Bock, Wim Van Nieuwenhuyze, Frauke Van de Moortel, Margo Eeckhout, Griet Terryn, Isabelle Van Landeghem, Melina Kyametis, Krista Bonny** en **Frederique Lagae**: bedankt voor jullie inzet. Jullie data zijn uiteindelijk niet rechtstreeks gebruikt in deze thesis, maar jullie enthousiasme was fijn en het was telkens leerrijk om jullie te begeleiden.

De groep collega's binnen PAE wil ik bedanken voor de fijne momenten, de grappen en de grollen. Naast Wim, Koen en Elie wil ik graag nog enkele mensen specifiek vernoemen, omdat hun hulp en steun voor mij van onschatbare waarde zijn geweest.

Lena De Groot: zonder jou zou het labo vierkant draaien, bedankt voor alle administratieve zaken die jij in orde brengt, er is je nooit iets te veel gevraagd. Bedankt ook voor de soms hilarische momenten, en voor de vele vrouwen-onder-elkaar- babbels!
Griet Casteleyn: merci voor de grappige momenten, en voor je luisterend oor, gedurende die vijf jaar heb je me er dikwijls bovenop geholpen als ik de zaken niet (en soms ook wel) in het juiste perspectief zag. Ook als je zelf in de stress zat heb je nog tijd vrijgemaakt; ik zal nooit vergeten dat je in december spontaan aan mijn deur stond met raad én daad, heel erg bedankt!
Caroline Souffreau: bedankt om samen "Pujeeweee" onveilig te maken, maar nog véél meer dank voor je ondersteunende mails, vele smsjes en telefoontjes tijdens de eindspurt!
Jeroen Gillard en **Bart Vanelslander**: bedankt voor de babbels en het begrip, en ook omdat jullie steeds objectief probeerden te zijn en jullie mening durfden zeggen, omdat ik op jullie kon vertrouwen!
Marie Lionard: merci de ta chaleur et de ton amitié dans le labo, pour tes mails supportifs et pour les moments de Skype quand tu étais au Canada! **Ineke** dankjewel voor het samen stressen in de eindperiode, de raad en je rustige uitstraling**. Katleen** dank voor je hulpvaardigheid, CD's en boeken.
Sophie, Els, Ann-Eline en **Ines**: voor jullie mails, smsjes en succeswensen, en ook het geduld tijdens de laatste loodjes-maanden. **Aaike, Maria, Pieter** voor de Bailey's ☺**, Nicolas, Dries, Katrijn, Olga, Victor, Jeroen, Hara, Annelies, Julie, Sofie, Koenraad, Sylvie, Christine, Ester, Antonyia, Annick** en **Ilse** bedankt voor de sfeer, babbels en interesse.

Collega's van de Algologie: bedankt voor de sfeer! **Christelle**: voor je aanstekelijke lach en voor alle praktische hulp. **Cathy, Eric, Henry, Enrico, Tom, Ana, Ellen, Olivier, Heroen** en vooral **Frederik** en **Klaas**: een grote merci!

De ploeg van de Limnologie heeft me altijd een zeer welkom gevoel gegeven, bedankt daar allemaal!
En in het bijzonder: **Hilde** en **Leen** voor de e-mails en raad in de laatste maanden, een hele grote MERCI !
Angelica, Vanessa en **Kay**: bedankt voor de interesse!

Collega's van het RCMG: bedankt voor de goeie sfeer; toch nog even vernoemen: **Francois, Mieke, Veerle, Anneleen** en alle anderen. Een speciaal woord van dank ook aan **Katrien**; bedankt voor de steun tijdens het veldwerk en om mijn gebrekkige Spaans daar aan te vullen met jouw Italio-Spaanse tongval, het samen negotiëren met de eigenaar van L. Pato, de leuke autoritten en vlotte sampling. Ook voor je vriendschap ná de staalnameperiode, en aanmoedigingen aan het einde van de rit, bel me zeker op als jij in die 'fase' komt!

Nathalie Van der Putten, Sarah Deprez, Karine, Peter, Dennis en andere collega's van de Geografie, bedankt voor de interesse, goede intenties, succeswensen!

Tenslotte wil ik ook nog familie en vrienden bedanken.

Elke en **Tom**, ik weet niet hoe ik jullie kan bedanken, dus ik schrijf het hier alvast neer: dank voor alles! Jullie deur stond steeds voor me open, bedankt voor de raad, het luisterend oor, de vele etentjes, attenties, smsjes, telefoontjes. Een extra dank voor de hulp in de laatste weken, en voor het nalezen van mijn teksten. **Tobytje**, jij bent de perfecte remedie tegen stress en zorgen, je deed me er meermaals aan herinneren dat er in het leven ook andere dingen zijn dan alleen S8, ik kijk er al naar uit om je weer wat meer te zien binnenkort!
Zus **Veerle**, je bent wellicht de grootste enthousiasteling en meest meelevende persoon geweest wat mijn werk betreft. In Chili kreeg ik bijna dagelijks een wat-ben-je-daar-aan-het-doen-en-hoe-is-het-daar- mail, en ook nadien kreeg ik af en toe een wees-toch-trots-je-doet-iets-sjiek boodschap. Bedankt voor je extra steun en hulp in de laatste weken, omdat je zoveel geduld en begrip voor me had en gewoon omdat je me echt graag ziet.
Bart, Trui, **Lander** en **Anneleentje**, bedankt voor de verstrooiing in Schelderode. Altijd fijn om Anneleentje te zien lachen, en Lander te zien spelen. Bart ook bedankt voor de tips op werkvlak telkens als ik een vraag had.

Emily, we hebben de eindspurt elk apart gemaakt, sorry dat ik jouw doctoraatsverdediging hierdoor gemist heb. Een grote dank u voor de steun via telefoon, sms, uitstapjes, ... je herkenbare verhalen, en je vertikale foto's ☺.
Maureen, merci voor alle toffe momenten! Voor je vetmesterij-partijen, de babbels in het labo, voor je Chili-overlevingspakket en de slingers aan mijn deur toen ik terug kwam, kortom voor de vele kleine en grotere attenties. Ook nog een extra merci aan je ouders voor dat ene belangrijke gesprek in eerdere tijden van twijfel.
Leen-en-Kenneth, bedankt voor de vriendschap en vooral -Leen- om me zeer goed te begrijpen.
Goele: merci voor het vele luisteren naar mijn verhalen, de interesse en je attentheid, en ook voor het keuren van mijn knappe mannelijke collega's ☺.
Ilse, Lore, Michèle, het (virtueel) samen joggen deed me deugd, maar vooral ook de spacy etentjes, die me uiteraard inspiratie brachten bij het interpreteren van mijn data. Bedankt voor de babbels en vele ondersteunende smsjes, en ook voor meneer pinguin uit het bompakket, hij staat naast mijn computer!
Senilitas-vrienden: **Liesbeth** en **Koen**, **Dieter** en **Johan, Willem**: bedankt voor de interesse, smsjes en facebook-berichtjes, vooral in de laatste fase van mijn doctoraat! **Karen, Wim, Wim** & **Sofie, Nathalie** & **Els, Willem, Maya** & **Rob** en alle anderen voor de feestjes en ontspanning. **Eveline Pringels** en **Dieter Collier**: bedankt voor de raad, interesse en de morele steun!
Wim Uyttenhove, voor je aanmoedigingen bij elk telefoontje en je immer optimisme.
Veerle en **Brenda**: bedankt voor de fijne gesprekken en voor jullie extra steun in de laatste maand!
Bioloog-vriendjes: **An** & **Klaas, Wouter, Mathias, Sarah DB, Martine** & **Gert, Griet** & **Pieter, Hadewich:** heel erg bedankt voor de ontspannende momenten samen. **Veronica:** thanks for your inspiring talks.

Graag wil ik ook twee mensen vernoemen die ons tot spijt onlangs hebben verlaten, maar die ik er zeer graag had bij gehad omdat ze veel voor mij hebben betekend:

Kirsten, je volgde de eerste jaren van thesissen en beursaanvragen van dichtbij, en je wist hoe belangrijk dit voor me was. Bedankt voor je kaartjes, sms-jes, je vrolijke 'Hey Mie' en vooral voor jouw typerende '*Alegria'*, ik probeer er voor altijd een stukje van te bewaren.

Margriet, bedankt voor alles wat je voor Veerle en mij hebt gedaan; niet alleen voor de lieve attenties tijdens mijn studie- en doctoraatsperiode, maar ook voor al je zorgen in die 28 jaar. Enorm bedankt dat ik je mocht kennen.

Tot slot wil ik bovenal mijn ouders bedanken:

Mama en **papa**, dit klinkt wellicht een beetje melig, maar het is welgemeend en iedereen mag het weten: bedankt dat jullie mijn ouders zijn. Mama, je wijsheid, zachtaardigheid, geduld en onvoorwaardelijke steun zijn van onschatbare waarde. Papa, ik heb bewondering voor je sterke doorzettingsvermogen, zin voor detail en juistheid. Een extra dank voor de motivatie en raad in de laatste maanden en ook na de voorverdediging.
Jullie hebben me deze hele periode door dik en dun gesteund, en niet alleen voor dit, maar ook gewoon voor alles: heel, heel erg bedankt!!

Chapter 1

Introduction

The Earth's climate is currently experiencing many changes (IPCC, 2007), necessating the development of reliable models to better quantify the Earth's climate system and to predict future climate changes. One way to test these models is to assess their ability to reproduce the spatial and temporal patterns of natural climate variability (Hodgson et al., 2007). The basic data for such validation exercises needs to come from a global network of accurately dated paleoclimatic records.

The International Geosphere Biosphere Programme (IGBP) has recognized this need for a global network of climate histories through its core project PAGES (Past Global Changes), which aims to coordinate and support paleoenvironmental research on a global scale. One of the first[1] foci of PAGES was the establishment of three latitudinal continental transects of paleoclimate study sites (Pole-Equator-Pole or PEP 1, 2 and 3; respectively the Americas, Africa and Australasia), which have significantly advanced our understanding of past climate change on a global basis (Shulmeister et al., 2006). However, in the Southern Hemisphere these transects end at c. 52°S, with the exception of the PEP-1 transect spanning the Americas, which is now being extended towards 54°S (e.g. Huber et al., 2004).

In the early decades of paleoclimatic research, Late Quaternary climate reconstructions mainly focused on the Northern Hemisphere. At millennial time-scales, this was justified by the recognition of the dominant role of the North Atlantic region in modulating climate change (Kershaw & Chappellaz, 2007). However, the increasing amount of Antarctic climate records has enabled comparisons between Arctic and Antarctic climate modes, and has enabled the development of models, which have indicated that during the last deglaciation rapid climate oscillations in the Northern Hemisphere might have been triggered by gradual changes in the Southern high latitudes, through a bipolar seesaw mechanism (Knorr & Lohman, 2003; Weaver et al., 2003). As a results of these findings, scientific focus has recently shifted to the Southern Hemispheric high latitudes.

[1] The original science structure of PAGES has been redefined in 2005, leading to the definition of four new foci. Although former Focus 1 (i.e. the project "Paleoclimates of the Northern and Southern Hemisphere", (PANASH) through which the PEP-transects were established) has been concluded, related activities are now included in the new Focus 2 (Modes of Climate Variability) and Focus 3 (Earth System Dynamics) (see http://www.pages-igbp.org/science/index.html).

Similarly, the (mainly Pacific) tropics have been recognized as playing a larger role in global climate modulation than previously thought (Beaufort et al., 2001). An increasing number of satellite observations and instrumental climate records has shed light on interannual to decadal tropical oscillations (such as El Niño), and their teleconnections with high-latitude and other climate modes. Moreover, recent proxy evidence from the tropical Pacific has suggested significant long-term changes in frequency and/or amplitude of these oscillations (Cane, 2005), which may thus have interacted with centennial and millennial scale climate changes across the world (Shulmeister et al., 2006; Pena & Cacho, 2009).

One of the main scientific challenges today is to elucidate the connection between past climate changes in the Southern Hemispheric high latitudes, and the tropics and mid-latitudes. More specifically, reconstructions of the strength and position of the Westerly Winds (now at 50°S) are of primary importance. This is because (1) the Southern Westerlies (and the associated Antarctic Circumpolar Current, ACC) are the only tropospheric wind belts encircling the globe without major topographic disturbances, thereby isolating Antarctica and its climate from the rest of the world, (2) the Westerlies are currently influenced by both Antarctic and tropical oscillations, since they are 'physically connected' with both the polar and midlatitudinal atmospheric circulation cells, and (3) due to their physical linkage with the upper tropospheric polar jet, they have an influence on transmitting climate anomalies towards other parts of the world.

The very southerly extending position of South America, and the northern position of the Antarctic Peninsula makes the Americas PEP-I transect the most suitable of the three transects to construct a well-covered latitudinal transect of paleoclimate records to investigate the nature and strength of these teleconnections.

Apart from the link between low- and high-latitude climate changes at different time scales, many other questions remain about climate evolution in both South America and the Antarctic Peninsula. In southern South America there is still controversy about the exact timing of deglaciation, and about the existence, timing and extent of a climate cooling between c. 15 and 11 ka BP (Bennett et al., 2000; Hajdas et al., 2003). In the Antarctic Peninsula there are some apparent inconsistencies concerning the Early Holocene optimum (11-9.5 ka BP, as recorded in ice core records from inland Antarctica; Masson-Delmotte et al., 2006), and many unknowns remain about the exact timing and duration of Holocene warm and cold periods in different regions of the Antarctic Peninsula (see Bentley et al., 2009 for a review). The number of well-dated paleo-environmental records is still too scarce

in the Antarctic Peninsula, to make good comparisons of Holocene climate in different parts of the Peninsula, and especially between the eastern and western sides of the Peninsula.

In the context of recent global climate change there is an urgent need for a better understanding of past natural climatic variability. This is particularly true for the Antarctic Peninsula, where the recent temperature increase is six times the global mean warming (Vaughan et al., 2003), and where large scale ice shelf break-up, glacier retreat and environmental changes along the coastlines occur (e.g. Scambos et al., 2003; De Angelis & Skvarca, 2003).

1.1. Research methodologies

One way to reconstruct past climate variability is to analyze sediments that accumulate at the bottom of lakes. Because lakes can be affected by climate in several ways (e.g. through changes in water supply, ice cover, temperature and wind, or indirectly through changes in the catchment area), it is possible to combine different sedimentological, biological and geochemical proxies into detailed paleo-environmental or paleoclimatic reconstructions. Some of the key methods used in the study of lake histories (paleolimnology), and in particular those methods used in this thesis, are described below.

1.1.1. Physical properties of lake sediments

Magnetic susceptibility (MS) measures the ease with which sediments can be magnetised, and thus monitor the concentration of iron-bearing minerals in sediments (Nowaczyk, 2001). MS can be regarded as a proxy for minerogenic contribution to the sediment, since iron-bearing minerals are common in many rock types and their weathering products (Zolitschka et al., 2001). The MS measurements are fast and non-destructive, which makes them standard methods applied on stratigraphic sections and sediment cores. In this context, they often reflect changes of the bulk composition of the sediments, and the obtained logs can be used for cross-correllation of sediment cores from different sites and depths (Nowaczyk, 2001).

1.1.2. Geochemical proxies

The amount of organic matter is one of the most widely used geochemical proxies in paleolimnology, and can be used to infer past primary production in the lake and/or its

catchment, if (a) sedimentation rates are known, (b) changes in influx of allochtonous organic matter can be detected or assumed to be constant and (c) decay rates of the organic matter can be assumed to be constant through time (the latter being influenced by e.g. oxic/anoxic conditions in the sediment pore waters; Meyers & Teranes, 2001). It is most commonly determined by the Loss on Ignition (LOI_{550}) technique, in which the relative loss of weight of a dried sample is determined after ashing it at 550°C for two (Dean, 1974) to four (Heiri et al., 2001) hours in an oven. The fraction of organic material determined by this method is on average twice the Total Organic Carbon (TOC) percentage of the sample. However, due to the loss of volatile compounds during burning the LOI_{550} is slightly less reliable than TOC measurements, but it is a very fast and cheap method for determining the organic content of samples (Heiri et al., 2001).

The amount of carbonates can be determined by burning the remaining LOI_{550} fraction at 950°C for two hours (Dean, 1974). This proxy is often interpreted in terms of the precipitation-evaporation balance of closed lakes, but can also be biotically influenced (e.g. Dittrich et al., 2004).

The bulk organic C/N ratio is often used for identifying the autochtonous and the allochtonous (i.e. coming from the catchment) fraction of the organic material. This is based on the fact that algae generally have C/N atomic ratios between 4 and 10, whereas vascular land plants, which are cellulose-rich and protein-poor, produce organic matter that has C/N atomic ratios higher than 20 (Meyers and Teranes, 2001). The fraction autochtonous versus allochtonous organic matter is then calculated by means of a "mixing equation" where these values, and the organic C/N ratio of the fossil sample are used as parameters or "end-members".

Stable carbon isotopes ($d^{13}C$) of lacustrine organic matter is generally used for assessing organic matter sources and for reconstructing past algal productivity and changes in the availability of nutrients in surface waters (Meyers & Teranes, 2001). In most lake systems, the combination of increased accumulation rates of organic matter and increased $d^{13}C$ values are interpreted in terms of increased lake productivity, as phytoplankton preferentially consumes dissolved $^{12}CO_2$, thereby increasing the $d^{13}C$ of the remaining dissolved inorganic carbon (DIC) in the lake, causing a subsequent rise in organic matter $d^{13}C$ when the DIC supplies become more depleted (Meyers & Teranes, 2001).

Stable nitrogen isotopes ($d^{15}N$) are less widely used as a paleolimnological proxy than carbon isotopes, but can similarly help to distinguish the sources of organic matter, and to reconstruct past changes in the availability of nutrients to aquatic producers (Talbot, 2001) and thus productivity rates (Meyers & Teranes, 2001). The dynamics of

nitrogen cycling are, however, more complicated, making the interpretations of sedimentary $d^{15}N$ records more difficult (Meyers & Teranes (2001) and references therein).

Chlorophylls, carotenoids and their derivatives can be extracted from aquatic sediments, and can reveal information on the structure and composition of former aquatic communities. Often, pigments from certain algae, phototrophic bacteria and higher plants preserve long after all morphological structures have disappeared (Leavitt & Hodgson, 2001). Fossil pigments have also be used to infer past food-web interactions, lake acidification, past UV radiation environments (Leavitt & Hogdson, 2001; Hodgson et al., 2005). New methods using High Performance Liquid Stratigraphy (HPLC) enable relatively rapid analyses of sediment samples (Leavitt & Hodgson, 2001).

1.1.3. Microfossils

Fossil diatom species are one of the most commonly used proxies in paleolimnology because of the good preservation of their silica cell walls, which permits rapid identification to species level, and because they are known to respond rapidly to many different environmental changes. Diatoms (Bacillariophyta) are unicellular algae, living in wet habitats, ranging from freshwater to hypersaline lakes, to rivers and oceans, and in wet terrestrial habitats. In (sub-) Antarctic regions, they are often one of the most common algal groups (Van de Vijver & Mataloni 2008; Jones 1996; Sabbe et al., 2003).

In order to reconstruct past environmental conditions in a lake based on diatom species assemblages in the sediments, the relation between species and their ecology needs to be assessed. This is often done in a qualitative way, but species' optima and tolerances to an environmental variable of interest can also be quantitatively determined by use of modern calibration datasets, containing a large number of lake surface sediment samples, covering a broad (often climatically related) ecological gradient. The calculation of the species-environment relationships (called transfer-functions) involves multiple regression and calibration techniques, and can subsequently be applied to fossil diatom assemblages, in order to estimate past values of the chosen variable.

Until recently, Antarctic diatoms have often been identified with reference to European and North-American diatom floras. However, recent research has focused on the taxonomy of (sub-) Antarctic diatoms, leading to the description of many new species that were previously often force-fitted within well-known species complexes (e.g. Van de Vijver et al., 2006; Van de Vijver, 2008; Van de Vijver & Mataloni, 2008). This has led to an increased number of endems identified in the Antarctic, supporting the recent view

that many diatoms have a restricted biogeography (Vyverman et al., 2007; Verleyen et al., in press). For both (paleo)ecological and biogeographical research, a growing number of diatom datasets are being combined. In such cases it is crucial that these are correctly intercalibrated, and hence it is helpful to supplement systematic studies with detailed illustrations, containing the complete morphological variability of all taxa found in the study regions.

1.2. Aims and outline of this thesis

This thesis aims to contribute to the extension of the PEP 1 transect through reconstructions of postglacial climate changes from southwestern South America to the Antarctic Peninsula. To this end, lake sediments were analyzed for biological, sedimentological and geochemical proxies, in order to infer past climatic changes at key sites along a latitudinal transect from southern South America (40°S) through the Antarctic Peninsula (68°S). More specific, the aims are to reduce uncertainties about (1) the timing of deglaciation in north Patagonia, (2) the existence, duration and extent of a late-glacial climate cooling in southern South America, (3) Holocene climate variability in southern Chile, that may be related to long-term changes in tropical Pacific climate oscillations, (4) the existence and exact timing of warm and/or moist periods shortly before and during the Holocene (e.g. the Early Holocene optimum and the Mid-Holocene hypsithermal; see Chapter 8) in the Antarctic Peninsula.

Two main study sites, located at 40°S (Lago Puyehue, Chile) and 63°S (Lakes Beak-1 and -2), respectively (Fig. 1), are brought into focus.

Lake sediment cores from Lago Puyehue were collected in the framework of the SSTC project “A continuous Holocene record of ENSO variability in Southern Chile” (ENSO-Chile, EV/12/10B). The cores from Beak Island were taken in the framework of the Belgian SSTC project “Holocene climate variability and ecosystem change in coastal East and Maritime Antarctica” (HOLANT, SD/CA/01A, 2005-2009) and are part of the British Antarctic Survey project “Climate and Chemistry” (CACHE), of which the project “CACHE-PEP” forms the branch connecting Antarctic research to the PEP-transects, through a program of collaborative fieldwork collecting ice cores, and marine and lake sediment core data (Hodgson et al., 2007). Our cores from Lake Puyehue (ENSO-CHILE; Fig. 1) and from the lakes on Beak Island (HOLANT; Fig. 1) will contribute to international efforts of obtaining a global synthesis of climate changes in the

past, together with lake sediment cores from Annenkov Island (South Georgia; HOLANT), Pourquoi-Pas and Horseshoe Island (Marguerite Bay region; HOLANT), Syowa Oasis (HOLANT) and southern Patagonia (Bilateral cooperation program between Flanders and Chile; HOLANT) (see Fig. 1 and Chapter 8).

In particular, the CACHE-PEP and HOLANT projects aim at studying (1) the timing, duration and magnitude of Holocene climate anomalies in the abovementioned regions and their relationships with existing climate records of Antarctic inland sites (ice cores), (2) the interaction between Holocene climate changes and ice sheet/glacier dynamics, and (3) the interaction between Holocene climate changes and the diversity of primary producers in Antarctic lakes.

This research further fits within the different former and current foci of PAGES (Past Global Changes; see PAGES, 2008), and especially within the second focus 'regional climate change', which aims at contributing towards a global coverage of high-resolution,

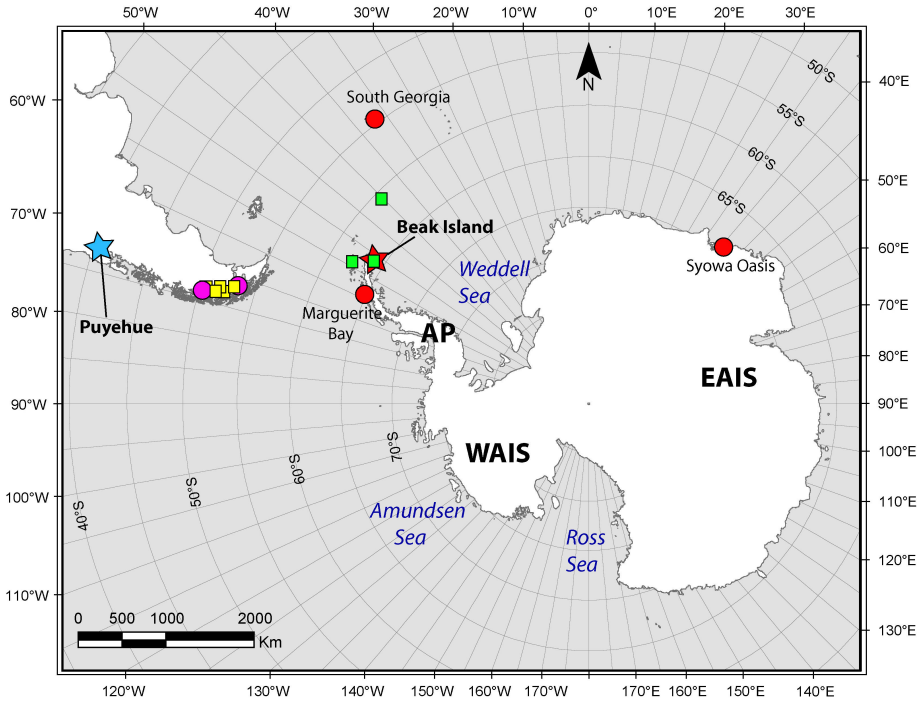

Figure 1: Location of relevant lake sediment cores taken in the framework of ENSO-Chile (blue symbols), HOLANT (red symbols), and the Bilateral cooperation program between Flanders and Chile (pink and yellow symbols). Location of the sampling areas for building a surface dataset are indicated by green and yellow squares. The two study sites of this thesis (Lago Puyehue and Beak Island) are indicated by a star. EAIS: East Antarctic Ice Sheet. WAIS: West Antarctic Ice Sheet. AP: Antarctic Peninsula.

well-dated paleoclimatic data, reconstructions of past climate-state parameters (e.g. temperature, precipitation, atmospheric pressure fields), and a better understanding of past modes of climate variability and teleconnections. The main questions addressed in this programme are: (1) How have regional climates and the Earth's natural environment changed in the past? (2) What are the main patterns and modes of climate variability on sub-decadal to orbital timescales? (3) How does climate variability relate to the mean state of the climate system? (4) How do large-scale changes in the climate system control regional climate and environmental change, and how do regional environmental changes feedback on/in to the global climate system? (PAGES, 2008).

The first two chapters of this thesis are dedicated to a reconstruction of the postglacial paleoenvironmental and related paleoclimatic changes at mid-latitudes in South America, inferred from an 11.22 m sediment core from Lake Puyehue (Chilean Lake District, 40°S), located at the northern boundary of the Southern Hemisphere Westerly Wind belt.

In **Chapter 2**, we use fossil diatom assemblages from the Puyehue sediment record in order to reconstruct past changes in the lake environment, and interpret them in terms of past changes in temperature and rainfall, which may be related to the position and/or strength of the Southern Westerlies.

In **Chapter 3** we use C/N analyses on the Puyehue core, in order to detect changes in the main source (terrestrial versus aquatic) of organic matter through time, and compare this with the pollen and diatom concentrations in the core. In order to infer the fraction of terrestrial organic matter (f_T), the ratio C/N is measured in different terrestrial and aquatic sources, and is incorporated (as N/C; Perdue & Koprivnjak, 2007) in a mixing equation. We reconstruct the pathways and reworking of organic matter in the watershed of Lake Puyehue, in order to find the best parameters for this equation, and compare the geochemical data with those from previous analyses (e.g. diatoms (Chapter 2) and pollen data; Vargas-Ramirez et al., 2008).

Chapters 4 to 7 are dedicated to the Antarctic Peninsula, where we first study in detail the contemporary diatom communities in Maritime Antarctica and Beak Island, in order to better constrain the ecological preferences of the diatoms found in fossil assemblages from Beak Island.

For this, we first investigate the diatom communities in 75 surface sediment samples from Livingston, Signy and Beak Island (**Chapter 4**). We revised species identifications and taxonomy of an existing database of 69 samples from Signy and Livingston Islands (Jones et al., 1993; Jones & Juggins, 1995) and extended it with six surface samples from Beak Island. In this chapter, we provide an illustrated checklist of freshwater diatoms, with an updated nomenclature and remarks on the ecology and systematics of some selected taxa.

In **Chapter 5**, we describe five new species, belonging to the genera *Chamaepinnularia, Craticula, Diadesmis* and *Navicula*.

In **Chapter 6**, we explore the diatom species composition in our intercalibrated dataset and compare the diatom compositions from Beak Island with those from Livingston and Signy Islands. After comparing the performance of different inference models, we generate a transfer function for ammonium (NH_4^+) concentrations, and employ it in a sediment core from a shallow coastal lake on Beak Island (Beak-2).

In **Chapter 7**, we reconstruct changes in glacial extent, sea-ice, climate and relative sea level using well-dated sediment cores collected from an isolation basin on Beak Island. This island is located at the (north)eastern side of the Antarctic Peninsula, an area that is - in contrast to the northwestern side - virtually unexplored in terms of paleolimnology. Moreover, the marine section of the sediment core provides one of the rare shallow marine sediment records from the Peninsula. A minimum age for deglaciation, and changes in sea-ice duration can be deduced from the marine sediment section of the core. In the freshwater section of Beak-1, which spans the last 6000 years, fluctuations in diatom productivity and pigment concentrations are linked to climatic optima.

References:

Beaufort L., de Garidel-Thoron T., Mix A.C., Pisias N.G. 2001. ENSO-like forcing on oceanic primary production during the Late Pleistocene. Science. 293: 2440-2444.

Bennett K.D., Haberle S.G., Lumley S.H. 2000. The last glacial-Holocene transition in Southern Chile. Science. 290: 325-328.

Bentley M.J., Hodgson D.A., Smith J.A., Ó Cofaigh C., Domack E.W., Larter R.D., Roberts S.J., Brachfeld S., Leventer A., Hjort C., Hillenbrand C-D., Evans J. 2009. Mechanisms of Holocene palaeoenvironmental change in the Antarctic Peninsula region. The Holocene. 19: 51-69.

Cane M.A. 2005. The evolution of El Niño, past and future. Earth and Planetary Science Letters. 230: 227-240.

Dean W.E. 1974. Determination of Carbonate and Organic-Matter in Calcareous Sediments and Sedimentary-Rocks by Loss on Ignition - Comparison With Other Methods. Journal of Sedimentary Petrology. 44: 242-248.

De Angelis H., Skvarca P. 2003. Glacier Surge After Ice Shelf Collapse. Science. 299: 1560-1562.

Dittrich M., Kurz P., Wehrli B. 2004. The Role of Autotrophic Picocyanobacteria in Calcite Precipitation in an Oligotrophic Lake. Geomicrobiology Journal. 21: 45-53.

Hajdas I., Bonani G., Moreno P.I. and Ariztegui D. 2003. Precise radiocarbon dating of Late-Glacial cooling in mid-latitude South America. Quaternary Research. 59: 70-78.

Heiri O., Lotter A.F., Lemcke G. 2001. Loss on ignition as a method for estimating organic and carbonate content in sediments: reproductibility and comparability of results. Journal of Paleolimnology. 25: 101-110.

Hodgson D.A., Vyverman W., Verleyen E., Leavitt P.R., Sabbe K., Squier A.H., Keely B.J. 2005. Late Pleistocene record of elevated UV radiation in an Antarctic lake. Earth and Planetary Science Letters. 236. 765-772.

Hodgson D.A., Wolff E., Mulvaney R., Allen C. 2007. Extending the Americas paleoclimate transect through the Antarctic Peninsula to the Pole. PAGES News. 15 (1): 6-7.

Huber U., Markgraf V., Schäblitz F. 2004. Geographical and temporal trends in Late Quaternary fire histories of Fuego-Patagonia, South America. Quaternary Science Reviews. 23: 1079-1097.

IPCC. 2007. Climate Change 2007: Synthesis report. Contribution of Working Groups I, II and III to the Fourth Assessment Report of the Intergovernmental Panel on Climate Change [Core Writing Team, Pachauri, R.K. and Resinger, A. (eds.)]. IPCC, Geneva, Switzerland, 104 pp.

Jones V. 1996. The diversity, distribution and ecology of diatoms from Antarctic inland waters. Biodiversity and Conservation. 5: 1433-1449.

Jones V., Juggins S., Ellis-Evans J.C. 1993. The relationship between water chemistry and surface sediment diatom assemblages in maritime Antarctic lakes. Antarctic Science. 5 (4): 339-348.

Jones V. & Juggins S. 1995. The construction of a diatom-based chlorophyll a transfer function and its application at three lakes on Signy Island (maritime Antarctic) subject to differing degrees of nutrient enrichment. Freshwater biology. 34: 433-445.

Kershaw P. & Chappellaz J. 2007. Editorial: Developments in Southern Hemisphere paleoclimate research. PAGES news. 15 (2): 2-2.

Knorr G. & Lohmann G. 2003. Southern Ocean origin for the resumption of Atlantic thermohaline circulation during deglaciation. Nature. 424: 532-536.

Leavitt P.R. & Hodgson D.A. 2001. Sedimentary pigments. In Smol JP & Last WS (Eds): Developments in palaeoenvironmental research, v. 3: Tracking environmental changes using lake sediments, biological techniques and indicators. Kluwer: 295-325.

Masson-Delmotte V., Kageyama M., Braconnot P., Charbit S., Krinner G., Ritz C., Guilyardi E., Jouzel J., Abe-Ouchi A., Crucifix M., Gladstone R.M., Hewitt C.D., Kitoh A., Le Grande A., Marti O., Merkel U., Motoi T., Ohgaito R., Otto-Bliesner B., Peltier W.R., Ross I., Valdes P.J., Vettoretti G., Weber S.L., Wolk F., Yu Y. 2006. Past and future polar amplification of climate change: climate model intercomparisons and ice-core constraints. Climate Dynamics. 26 (5): 513-529.

Meyers P.A. & Teranes J.L. 2001. Sediment Organic Matter. In: Last, W.M., Smol, J.P. (Eds), Tracking environmental changes using lake sediment - Vol. 2: Physical and geochemical methods. Kluwer Academic, Dordrecht, The Netherlands: 239-270.

Nowaczyk N.R. 2001. Logging of magnetic susceptibility. In: Last W.M. & Smol J.P. 2001. Tracking Environmental Change Using Lake Sediments. Vol. 1: Basin Analysis, Coring, and Chronological Techniques. Kluwer Academic Publishers, Dordrecht, The Netherlands.

PAGES. 2008. Past Global Changes, website http://www.pages-igbp.org/science/index.html

Pena L.D. & Cacho I. 2009. High-to low-latitude teleconnections during glacial terminations associated with ENSO-like variability. PAGES Newsletter. 17 (1): 5-7.

Perdue E.M. & Koprivnjak J.-F. 2007. Using the C/N ratio to estimate terrigenous inputs of organic matter to aquatic environments. Estuarine Coastal and Shelf Science. 73 (1–2): 65–72.

Sabbe K., Verleyen E., Hodgson D.A., Vanhoutte K., Vyverman W. 2003. Benthic diatom flora of freshwater and saline lakes in the Larsemann Hills and Rauer Islands, East Antarctica. Antarctic Science. 15 (2): 227-248.

Scambos T., Hulbe C., Fahnestock M. 2003. Climate-Induced Ice Shelf Disintegration in the Antarctic Peninsula. Antarctic Peninsula Climate Variability: Historical and Paleoenvironmental Perspectives, 79, 79-92. International Workshop on Antarctic Peninsula Climate Variability, Date: APR, 2002 Hamilton Coll Clinton NY.

Shulmeister J., Rodbell T., Gagan M.K., Seltzer G.O. 2006. Inter-hemispheric linkages in climate change: paleo-perspectives for future climate change. Climate of the Past Discussions. 2: 79-122.

Talbot M.R. 2001. Nitrogen isotopes in palaeolimnology. In: Last, W. M., Smol, J.P. (Eds.), Tracking Environmental Change Using Lake Sediments. Volume 2: Physical and Geochemical Techniques. Kluwer Academic Publishers, Dordrecht, The Netherlands: 401-439.

Van de Vijver B., Van Dam H., Beyens L. 2006. *Luticola higleri sp. nov.*, a new diatom species from King George Island (South Shetland Islands, Antarctica. Nova Hedwigia. 82(1-2): 69-79.

Van de Vijver B. 2008. *Pinnularia obaesa* sp. nov. and *P. australorabenhorstii* sp. nov., two new large *Pinnularia* (sect. *Distantes*) from the Antarctic King George Island (South Shetland Islands). Diatom Research. 23: 221-232.

Van de Vijver B. & Mataloni G. 2008. New and interesting species in the genus *Luticola* D.G. Mann (Bacillariophyta) from Deception Island (South Shetland Islands). Phycologia. 47: 451-467.

Vargas-Ramirez L., Roche E., Gerrienne P., Hooghiemstra H. 2008. A pollen-based record of late glacial-Holocene climatic variability in the southern lake district, Chile. Journal of Paleolimnology. 39: 197-217.

Vaughan D.G., Marshall G.J., Connolley W.M., Parkinson C., Mulvaney R., Hodgson D.A., King J.C., Pudsey C.J., Turner J. 2003. Recent Rapid Regional Climate Warming on the Antarctic Peninsula. Climatic Change. 60: 243-274.

Verleyen E., Vyverman W., Sterken M., Hodgson D.A., De Wever A., Juggins S., Van de Vijver B., Jones V.J., Vanormelingen P., Roberts D., Flower R., Kilroy C., Souffreau C., Sabbe K. In Press. The importance of dispersal related and local factors in shaping the taxonomic structure of diatom metacommunities. Oikos. DOI: 10.1111/j.1600-0706.2009.17575.x

Vyverman W., Verleyen E., Sabbe K., Vanhoutte K., Sterken M., Hodgson D.A., Mann D.G., Juggins S., Van de Vijver B., Jones V., Flower R., Roberts D., Chepurnov V.A., Kilroy C., Vanormelingen P., De Wever A. 2007. Historical processes constrain patterns in global diatom diversity. Ecology. 88 (8): 1924-1931.

Weaver A.J., Saenko O.A., Clark P.U., Mitrovica J.X. 2003. Meltwater Pulse 1A from Antarctica as a Trigger of the Bolling-Allerod Warm Interval. Science. 299 (5613): 1709-1713.

Zolitschka B., Mingram J., Van der Gaast S., Fred Jansen J.H., Naumann R. 2001. Sediment logging techniques. In: Last W.M. & Smol J.P. 2001. Tracking Environmental Change Using Lake Sediments. Vol. 1: Basin Analysis, Coring, and Chronological Techniques. Kluwer Academic Publishers, Dordrecht, The Netherlands.

Chapter 2

Late Quaternary climatic changes in southern Chile, as recorded in a diatom sequence of Lago Puyehue (40°40'S)

Mieke Sterken, Elie Verleyen, Koen Sabbe, Griet Terryn, Francois Charlet, Sébastien Bertrand, Xavier Boës, Nathalie Fagel, Marc De Batist and Wim Vyverman

Abstract

A late Quaternary diatom stratigraphy of Lago Puyehue (40°40'S, 72°28'W) was examined in order to infer past limnological and climatic changes in the South-Chilean Lake District. The diatom assemblages were well preserved in a 1,122 cm long, ^{14}C-dated sediment core spanning the last 17,900 years, and suggest an early deglaciation of Lago Puyehue. The presence of a short cold spell in South Chile, equivalent to the Younger Dryas event in the Northern Hemisphere, the Antarctic Cold Reversal in Antarctica, or the Huelmo-Mascardi event in southern South America, was not clearly evidenced in the diatom data, although some climate instability may have occurred between 13,400 and 11,700 cal. yr. BP. A relatively long period between 16,850 and 12,810 cal. yr. BP with low absolute abundances and biovolumes is tentatively interpreted as a period of low rainfall and/or temperatures. An increase in the moisture supply to the lake was tentatively inferred at 12,810 cal. yr. BP. After 9550 cal. yr. BP, inferred stronger and longer persisting summer stratification, may have been the result of the higher temperatures associated with an Early Holocene thermal optimum. The Mid-Holocene appeared to be characterized by a decrease in precipitation, culminating around 5000 cal. yr. BP, and rising again after 3000 cal. yr. BP, likely associated with a previously documented lowered frequency and amplitude of El Niño events. An increase in precipitation during the Late Holocene (3000 cal. yr. BP-present) is linked to subsequent increased frequency of El Niño occurrences, leading to drier summers and slightly moister winters in the region.

This chapter is an adapted version of

Sterken M., Verleyen E., Sabbe K., Terryn G., Charlet F., Bertrand S., Boës X., Fagel N., De Batist M., Vyverman W. (2008). Late Quaternary climatic changes in southern Chile, as recorded in a diatom sequence of Lago Puyehue (40° 40'S). *Journal of Paleolimnology*, 39, 219-235.

and:

Sterken M., Verleyen E., Sabbe K., De Batist M., Vyverman W. (unpublished manuscript). The effect of tephra depositions on diatom productivity and composition in Lago Puyehue, southern Chile.

The abovementioned manuscript of Sterken et al., (2008) is published as part of a special issue dedicated to the paleolimnological research on Lago Puyehue. This special issue contains papers on the sedimentology and age-depth modelling (Bertrand et al., 2008), the seismic stratigraphy (Charlet et al., 2008), the pollen analyses (Vargas-Ramirez et al., 2008) and high-resolution image (and varve) analyses (Boës and Fagel, 2008a; Boës and Fagel, 2008b; Fagel et al., 2008) on sediment cores from Lago Puyehue.

Contribution of the author: diatom microscopy, statistical analyses, interpretation and writing of largest part of the paper.

2.1. Introduction

Recent investigations have shown that the Southern Hemisphere plays a greater role in the regulation of global climate than previously thought (e.g. Ribbe, 2004; Knorr & Lohman, 2003). At high latitudes, sub-Antarctica plays a key role in the regulation of the global CO_2 balance, through the supply of nutrient-rich waters to the Sub-Antarctic Mode Water (SAMW), spreading throughout the Southern Hemisphere and North-Atlantic, and strongly influencing the distribution of photosynthetic micro-algae in the oceans (Sarmiento et al., 2004). At low latitudes the "West Pacific Warm Pool" (WPWP) is an important source of warm and moist air being transported towards the poles. Changes in temperature, size and position of the WPWP are strongly correlated to the El Niño Southern Oscillation (ENSO) and the Pacific Decadal Oscillation (PDO), implying that both oscillations significantly influence the flow of energy towards high latitudes (Gagan et al., 2004; Turney et al., 2004). At mid-latitudes, the Southern Westerlies (40-55°S) are influenced by both equatorial and polar atmospheric processes, and are therefore crucial in understanding interactions between low- and high-latitudinal climate variability, such as teleconnections between ENSO and the Antarctic Circumpolar Wave (ACW; White et al., 2002; Renwick &d Revell, 1999). In the global network of paleoclimatic studies however, reconstructions in the southern mid-latitudes are still sparse. Moreover, many uncertainties exist about the timing and extent of climatic events, both within and between East- and West-Pacific areas.

A first issue of debate is the exact timing and rate of deglaciation of the North-Patagonian ice sheet (e.g. Lowell et al., 1995; McCulloch & Davies, 2001; Bentley, 1997). Moreover, the northern part (i.e. north of 43°S) of the Patagonian ice sheet is very dynamic, and is represented with considerable uncertainty in recently developed ice sheet models (e.g. Hulton et al., 2002).

A second unknown is the occurrence of a Younger Dryas (YD) counterpart in the Southern Hemisphere, and more particularly in southern South America. Some studies support a cold spell in Patagonia, coincident with the northern hemispheric YD (Heusser et al., 1995; Denton et al., 1999), while others report a cooling phase (the Huelmo-Mascardi event) starting before the YD (Ariztegui et al., 1997; Hajdas et al., 2003; Moreno & Léon, 2003). More southwards (51°S and 53°S), a glacial stage coinciding with the Antarctic Cold Reversal was inferred from geomorphologic evidence (Fogwill & Kubik, 2005; Sugden et al., 2005). In contrast, many peat and marine sediment cores between 40° and 47°S showed no clear reversal or stagnation in air temperature nor Sea-

Surface Temperature (SST) trends during the deglaciation period (Lamy et al., 2004; Bennett et al., 2000; Haberle and Bennett, 2004).

A third uncertainty concerns the past evolution of ENSO-related climate variability and its influence on regional climate dynamics. Throughout the Holocene, the timing of the onset and duration of these changes seems to differ between study sites both close to (e.g. Rodbell et al., 1999; Sandweiss et al., 1996; Keefer et al., 2003), and remote from, each other (e.g. Rodbell et al., 1999 vs. Haug et al., 2001; Lamy et al., 2001 vs. Jenny et al., 2002; 2003). Recent studies have additionally indicated that the influence of ENSO on regional climates depends upon the study area and the period considered (Shulmeister et al., 2006; Jorgetti et al., 2006). In particular, the relationship between El Niño and the position and strength of the Southern Westerlies is still unsufficiently known, both for the Australian sector (e.g. Shulmeister et al., 2004) and in southern South America (e.g. Lamy et al., 1999; Moreno 2004).

One way to address these issues is to examine continental records of climate change along a transect encompassing the latitudinal range of Westerly Wind activity. Continuous lacustrine sediment cores can provide much of this detailed environmental and climatological information, at a high temporal resolution (e.g. Smol et al., 2001). In this paper we aim to infer past limnological and climatological changes in the Chilean Lake District, based on a post-glacial diatom stratigraphy from Lago Puyehue (40°S), situated at the northern boundary of the Westerly Wind belt. This will contribute to the growing network of paleoclimate studies in southern South America (e.g. Moreno et al., 1999; Denton et al., 1999; Bennett et al., 2000; Lowell et al., 1995; Lamy et al., 2004; Haberzettl et al., 2005; Bracco et al., 2005) and to the discussion regarding (a) the deglaciation of parts of the North-Patagonian ice sheet, (b) the occurrence of a YD counterpart in southern Chile and (c) the Holocene evolution of ENSO-related climate events.

2.2. Study area

Lago Puyehue is situated in the south (40°40’S, 72°28’W, 184 m a.s.l.) of the Araucanian Lake District (North Patagonia, Chile), which is a subsiding, sediment trapping depression between the Andes (E) and the Coastal Cordillera (W) (Fig. 1; Clapperton 1993). The lake has a maximum length of 23 km, a maximum depth of 123 m and a mean

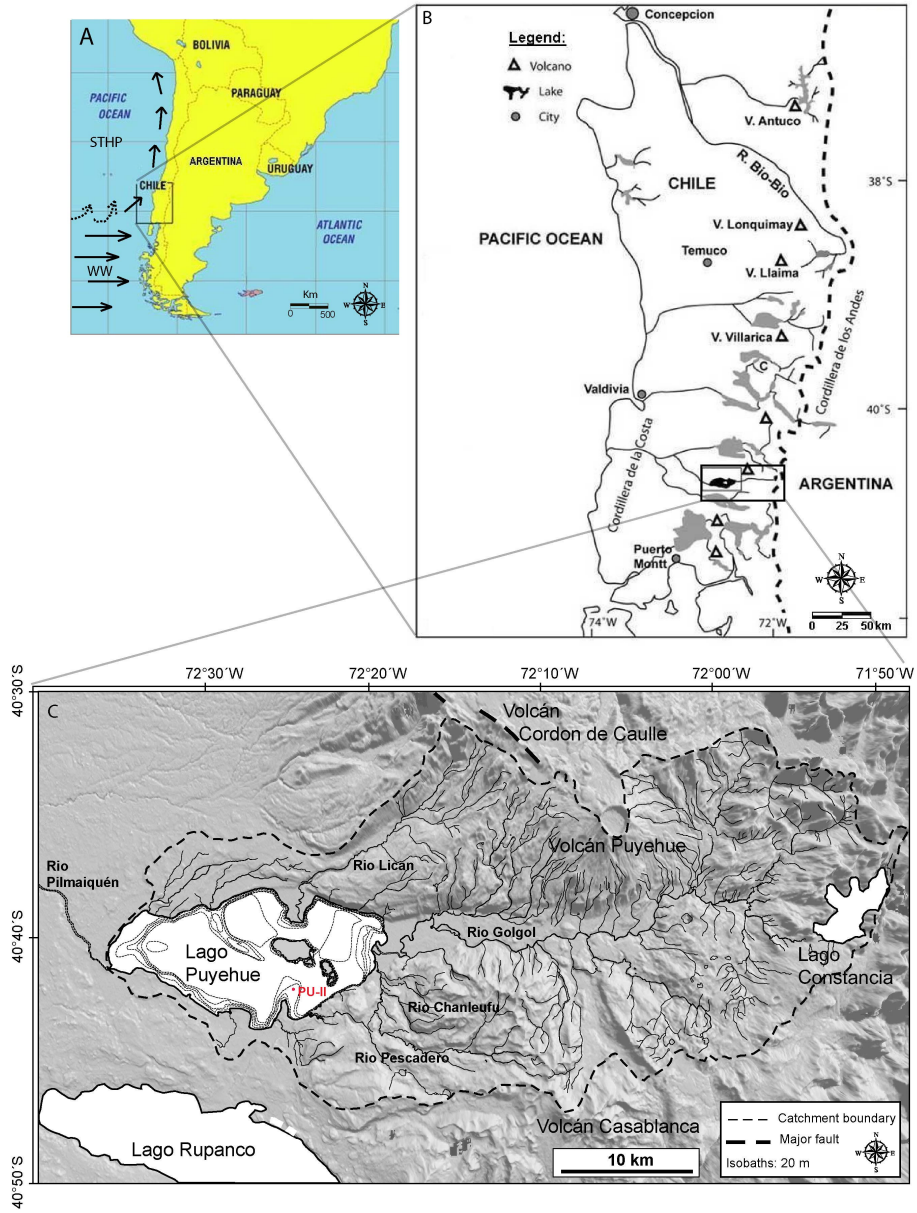

Figure 1 (previous page): Map of the study area showing (A) the location of the Chilean Lake District in South America, with representation of the main wind patterns (solid arrows), the mean position of the Westerly Wind drift (WW), the Subtropical High Pressure Cell (STHP), and the Subantarctic Mode Water pathway (SAMW; dotted arrows); (B) the location of Lago Puyehue in the Lake District; and (C) the catchment of Lago Puyehue with its rivers and volcanoes, the bathymetry of Lago Puyehue (based on Campos et al., 1989) and the location of the coring site (PU-II) in Lago Puyehue. Map C is redrawn from Charlet et al. (2008).

depth of 76.3 m (Campos et al., 1989). The surface area is 165.4 km^2, and its volume is 12.6 km^3.

The stratification regime of Lago Puyehue is temperate monomictic, with winter circulation from July to September, and thermal stratification from December to March. Winter homothermy is at about 9º-10ºC, while summer surface temperatures reach up to 13º-19ºC, with a thermocline depth between 16 and 22 m (Campos et al., 1989). The oligotrophic and mainly P-limited lake has a mean Secchi depth of 10.7 m. Si-levels are high; the mean concentration of SiO_2 is 15 mg/l (Campos et al., 1989). The phyto- and zooplankton communities of Lago Puyehue are described by Thomasson (1963) and Campos et al. (1989). Phytoplankton biomass and abundance is maximal in summer, with a pronounced dominance of Cyanobacteria (mainly *Anabaena espiroide* Bory). Diatoms, mainly composed of centric taxa, dominate the phytoplankton in late autumn, winter and early spring, when N and P levels are high, the N/P ratio is decreased, and mixing prevents genera such as *Aulacoseira* Thwaites from sinking (Campos et al., 1989). The main inflows to Lago Puyehue are situated in the east of the lake (Rio Golgol, Rio Chanleufu, Rio Lican and Rio Pescadero). The main outflow is the Rio Pilmaiquén in the west. Further details on the physical, chemical and biological properties of the lake and its inflows are described in Campos et al. (1989).

The catchment area of Lago Puyehue covers 1510 km^2, and extends far to the east of the lake. It is composed of Quaternary volcanic, mainly andesitic and basaltic rocks (Bertrand, 2002). The upperflows of the Rio Golgol drain an area with Lower-Cretaceous and Cenozoic granitic rocks, comprising 10 % of the surface area of the catchment. Quaternary fluvio-glacial deposits prevail in the immediate vicinity of the lake (Bertrand, 2002). The catchment area of Lago Puyehue consists almost entirely of 'Trumao'-soils. These well-drained volcanic ash soils consist of morainic parent material, covered by up to several metres of volcanic ashes (Langohr, 1971; 1974). The ash is of acidic to intermediate (andesitic) nature, and the soils are extremely porous (Langohr, 1971). Several conical volcanoes, belonging to the active Southern Volcanic Zone (SVZ) (33º S to 46º S), are situated in the vicinity of Lago Puyehue (Clapperton, 1993). Of immediate importance for the lake are the Casablanca volcano (22.7 km SE of the lake), the Puyehue volcano (29 km E of Lago Puyehue) and its fissural prolongation Cordon de Caulle.

Natural vegetation in the catchment area is well preserved, and consists mainly of Valdivian and North-Patagonian rainforests (Vargas-Ramirez et al., 2008); only the shores of Lago Puyehue have been strongly altered by humans, mostly for tourist purposes. A detailed description of the Puyehue National park, its vegetation as well as

the predominant soil types can be found in Schick (1980) and Vargas-Ramirez et al. (2008).

2.2.1. Climatic settings

The climate in the Chilean Lake District is transitional between the Chilean Mediterranean climate, with cool dry summers and moderate wet winters, and the southern Patagonian oceanic climate, with all year round precipitation (Laugénie, 1982). Mean annual air temperature ranges from 12°C at 40°S towards 5°C at 55°S (Hulton et al., 2002). Besides a north-south gradient, a strong east-west gradient exists in both precipitation and temperature, as the Andes form a physical barrier for the Westerlies, causing heavy orographic rains on their western slope, and air temperature declines with increasing height.

Mean annual air temperature in the catchment area of Lago Puyehue is between 6 and 9°C, with maxima of 20°C in January, and minima of 2°C in July (Schick, 1980). Freezing sometimes occurs at night in winter, but complete ice covering of the lakes has never been observed (Thomasson, 1963). Snow cover occurs from May to November, and the current Equilibrium Line Altitude lies at 1700-1600 m height (Laugénie, 1982; Hubbard, 1997). Mean annual precipitation reaches up to 2000 mm near the lake, and up to more than 3000 mm in the Puyehue catchment area (Laugénie, 1982). Monthly precipitation varies from 162-187 mm (January-February) to 450-520 mm in May and June respectively (Centro de Información Ambiental del Parque Nacional de Puyehue, CONAF, pers. comm.). Precipitation is determined by the strength and position of the Westerly Winds, and is maximal at 50°S (> 7000 mm/yr), decreasing towards the north (2500 mm at 40°S) and south (1000 mm at 55°S) (Hulton et al., 2002).

The Lake District is strongly influenced by ENSO. According to Montecinos and Aceituno (2003) a negative correlation exists between summer precipitation at 38-40°S, and SST anomalies in the Niño-3.4 region (120°-170°W, 5°N-5°S). This is in contrast to an above average winter precipitation between 30 and 35°S, and an above-average late spring precipitation (October-November) between 35 and 38°S during El Niño as a result of strengthened Westerly flows in sub-tropical central Chile (Montecinos et al., 2000).

2.3. Materials and Methods

2.3.1. Core PU-II

The coring site (PU-II) was selected in the southeast (40º41.843'S, 72º25.341'W) of Lago Puyehue on the basis of seismic bathymetry (Fig. 2; Charlet et al., 2008). The core was taken in an interflow zone, at a water depth of 48.4 m (Figs. 1 and 2; De Batist et al., 2008). Coring operations were carried out with a UWITEC piston corer. The core is 1,122 cm long, and large parts of it are annually laminated.

Ten samples were analysed for bulk radiocarbon dating at the Poznan Radiocarbon Laboratory (Table 2; Czernik & Goslar, 2001). Radiocarbon dates were calibrated with Bcal using atmospheric data of Stuiver et al. (1998), and we used the weighted average of each calibrated date to construct the age-depth model (see 4.2. in this Chapter, and Bertrand et al., 2008). Additional ^{210}Pb and ^{137}Cs datings were performed (Arnaud et al., 2006) and were consistent with the age-depth model (Bertrand et al., 2008). Two tephra layers, dated by varve counting (Boës & Fagel, 2008a) and originating from historical volcanic eruptions (Puyehue and Cordon Caulle: 1921-1922 AD; Osorno: 1575 AD), were used as chronostratigraphic markers in the upper part of the core (Fig. 3; Bertrand et al., 2008).

2.3.2. Diatom and loss on ignition analysis

Sub-samples of approximately 0.5 cm^3 were taken from the PU-II core at intervals of 20 cm. The samples were weighed, dried at 60°C for 24 hours, and weighed again to calculate the water content. Samples for diatom analyses were diluted in distilled water, without oxidation treatment, and were spiked with polystyrene microspheres (concentration: 4.92 x 10^6 l^{-1}) to allow for quantitative analysis (Battarbee & Kneen, 1982). Frustules were mounted in Naphrax® medium. Transects were scanned at a magnification of 10 x 100 x with a Leitz Diaplan and a Zeiss Axioplan II light microscope. A minimum of 200 valves was counted per sample. Diatoms were identified to generic or specific level, according to Round et al. (1990), Rumrich et al. (2000), Round & Bukhtiyarova (1996) and Frenguelli (1942). The genus *Naviculadicta* was applied following Rumrich et al. (2000), although we acknowledge this genus still needs to be taxonomically revised. Total diatom biovolume calculations were based on size measurements of all taxa having a mean abundance greater than 1 % in the core. A minimum of 25 valves was measured for each taxon. All measured taxa comprised on average 96 % of the total diatom abundances in the core.

The biovolumes are expressed in μm^3 (Table 1), and are calculated as

$$B = \pi \left(\frac{D}{2}\right)^2 d \quad \text{for centric species,}$$

and as $$B = \pi \left(\frac{L\,W}{4}\right) d \quad \text{for pennate species, with:}$$

B = biovolume, D = diameter valve; d = valve depth; L = valve length; W = valve width.

***Table 1*:** List of species measured for diatom biovolume calculation. The diameter (D) was measured for centric species, the Length and Width (L & W) were measured for pennate species. The valve depth (d) was measured as half the distance between two valves in one frustule seen in girdle view. N refers to the number of valves measured, % is the average percentage of occurrence in the whole core, and the calculated volume is given in μm^3.

Species name	Diameter (D)	Depth(d)	Length (L)	Width (W)	N (L,W)	N (d)	%	volume (μm^3)
Cyclotella stelligera	5.2	0.9	-	-	294	23	61.4	19.1
Aulacoseira granulata	14.9	19.4	19.4	-	291	291	14.5	3404.4
Gomphonema	-	3.3	24.2	5.2	42	13	2.1	323.0
Nitzschia	-	1.1	14.2	2.3	43	2	3.7	29.1
Staurosira	-	2.5	7.7	2.9	51	50	9.5	44.0
Fragilaria	-	1.2	21.8	2.8	25	8	1.4	54.8
Melosira	21.6	18.1	18.1	-	30	1	1.4	6665.2
Cyclostephanos	29.2	8.5	-	-	81	1	1.7	5699.7

LOI_{550} values were measured every 10 cm, after heating dried sediment samples of 1 g for 4 h at 550°C in order to estimate the organic matter content and inorganic C, following the method of Heiri et al. (2001), and were interpreted according to Santisteban et al. (2004) and Bertrand et al. (2008).

2.3.3. Tephra-associated diatom analyses

The close proximity of active volcanoes in the catchment of Lago Puyehue (see 2.2. and Fig. 1) calls for the need to assess the potential impact of tephra depositions (see 2.4.1. and Fig. 3) on the diatom communities in the lake, as to detect/discern any interference between past volcanic and climate-related ecological changes in the lake. For this, we compared fossil diatom communities from immediately below, in and above five selected tephra layers (see 2.4.1.) from core PU-II. A minimum of five successive subsamples (each 0.5 cm^3 volume) was taken below and above each tephra layer. Sample preparation

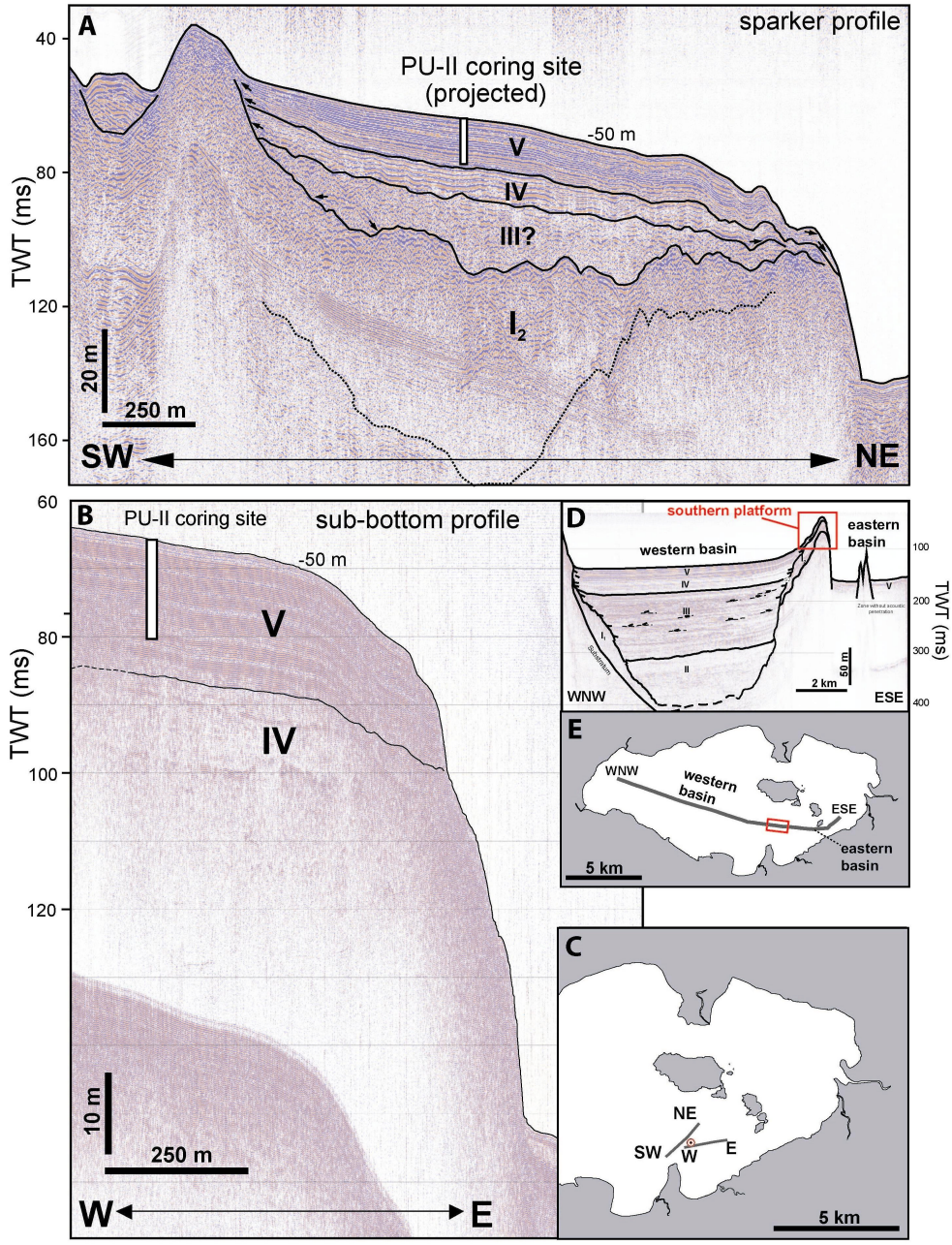
A
sparker profile
PU-II coring site
(projected)
-50 m
V
IV
III?
I2
20 m
250 m
SW
NE
TWT (ms)
40
80
120
160
B
PU-II coring site
sub-bottom profile
-50 m
V
IV
10 m
250 m
W
E
TWT (ms)
60
80
100
120
D
southern platform
western basin
eastern basin
WNW
ESE
2 km
50 m
TWT (ms)
100
200
300
400
E
WNW
western basin
ESE
eastern basin
5 km
C
NE
SW
W
E
5 km

Figure 2 (opposite page): (A) Seismic stratigraphy across a southwest-northeast section through the southern platform (see insets (C) and (D-E) for locating the transect and the platform). (B) Seismic stratigraphy along a west-east transect shown in inset (C). (D) Seismic profile crossing the whole lake from west to east (see inset (E)), showing the western sub-basin, the southern platform, and the easter sub-basin. Figures redrawn from Charlet et al. (2008). TWT stands for two-way travel time of the seismic signal. The symbols I to V represent different stratigraphical units (from old to young) as described in Charlet et al. (2008). These units were interpreted as (I) moraine, ice-contact or outwash deposits, (II) glaciolacustrine sediments deposited in a pro- or subglacial lake at the onset of deglaciation, (III) lacustrine fan deposits fed by sediment-laden meltwater streams in a proglacial lake, (IV) distal deposits of fluvially derived sediment in an open postglacial lake, and (V) predominantly authigenic lacustrine sediments (mainly of biogenic origin), accumulated in an open, postglacial lake (Charlet et al., 2008).

and diatom analysis occurred as described in 2.3.2. Tephra layers were detected by macroscopical description, magnetic susceptibility and grain size analyses (Bertrand et al., 2008; Boës & Fagel, 2008b; Juvigné et al., unpubl. data). The tephra layers were selected to have positions as distant as possbile from nearby tephra layers in the core.

2.3.4. Numerical analysis

Cluster analysis, constrained by sample depth, was performed on the relative diatom abundances using the programs CONISS (Grimm, 1987) and Tilia 2.0b4 (Grimm, 1991). Graphs were plotted using Tilia Graph and TG View 1.1.1.1. (Grimm, 2001). For grouping samples according to their taxonomic composition without sample depth constraints, an ordination was done on the relative abundance data of all samples. An initial Detrended Correspondence Analysis (DCA) with detrending by segments and downweighting of rare species was applied on the log (x+1) transformed data. The results show that the length of gradient of the first axis was short (1.56 standard deviation units), indicating that Principal Components Analysis (PCA) should be applied (cf. ter Braak & Prentice, 1988). Ordinations were carried out using the program CANOCO 4.5 (ter Braak & Smilauer, 2002).

2.4. Results

2.4.1. Lithology of core PU-II and selection of tephra layers

Core PU-II consists of finely laminated to homogeneous brown to brown-grey clay/silt (Fig. 3). Three turbidite layers were macroscopically observed at 379.5-381 cm, 396.5-397.25 cm and 956-971 cm depth (Bertrand et al. (2008); green bars in Fig. 3). Seventy-eight tephra layers with a mean thickness of 0.7 ± 1.1 cm and a total thickness of 52.3 cm were visually recognised (Bertrand et al., 2008). Twelve tephra layers were larger than 1 cm and are plotted on Fig. 3 (blue 'T100' and 'T500' bars and all red bars). The five tephra layers with the largest distance to the most proximal tephras (blue bars in Fig. 3) were observed at 102.3-109.8 cm (T100), 417.6-417.8/418.1-419.1 cm (T400), 497.4-502.9 cm (T500), 875-875.2 cm (T800) and 1078-1078.5 cm (T1000).

LOI_{550} ranged between 2.35 and 10.23 % (mean value: 5.73 ± 7.8 %), starting with low values between 1120 and 810 cm (mean value: 3.65 ± 0.4 %). A major shift towards higher values is observed at 810 cm. Between 805 and 50 cm values are around 6.33 %, with the exception of some minima between 3-5 % at 182, 250, 360, 391, 491, 610 and 711 cm depth. From 50 cm towards the top of the core an increasing trend in LOI_{550} values is observed, respectively from 8.62 to 10.23 % (Fig. 5; Bertrand et al., 2008).

2.4.2. Chronology

We constructed a discontinuous age-depth model based on nine AMS radiocarbon dates (Table 2; Fig. 3). One radiocarbon date (at 1119 cm) was omitted from the age-depth model as it showed an inversion with the date at 1012 cm (Table 2; Bertrand et al., 2008). This choice was corroborated by the very low carbon content of this sample (0.4 mg), making the result less reliable (Bertrand et al., 2008). Continuous sedimentation rates were assumed at 0-56.6 cm (sedimentation rate SR: 1.58 mm yr^{-1}), between 56.6 and 152.5 cm (SR: 0.36 mm yr^{-1}), and between 152.5 and 640.4 cm (SR: 0.87 mm yr^{-1}). The sedimentation rate between 640.4 and 1012 cm was 0.51 mm yr^{-1} and was assumed to be constant up to 1122 cm, resulting in an extrapolated basal age of 17,915 cal. yr. BP (Bertrand et al., 2008). All interpolations were corrected for instantaneous deposits (i.e. 78 tephra layers and three turbidites). The overall mean accumulation rate was 0.63 mm yr^{-1} (Bertrand et al., 2008). The diatom sampling resolution of c. 20 cm therefore resulted in a mean temporal resolution between 128 and 630 years (average: 324 years).

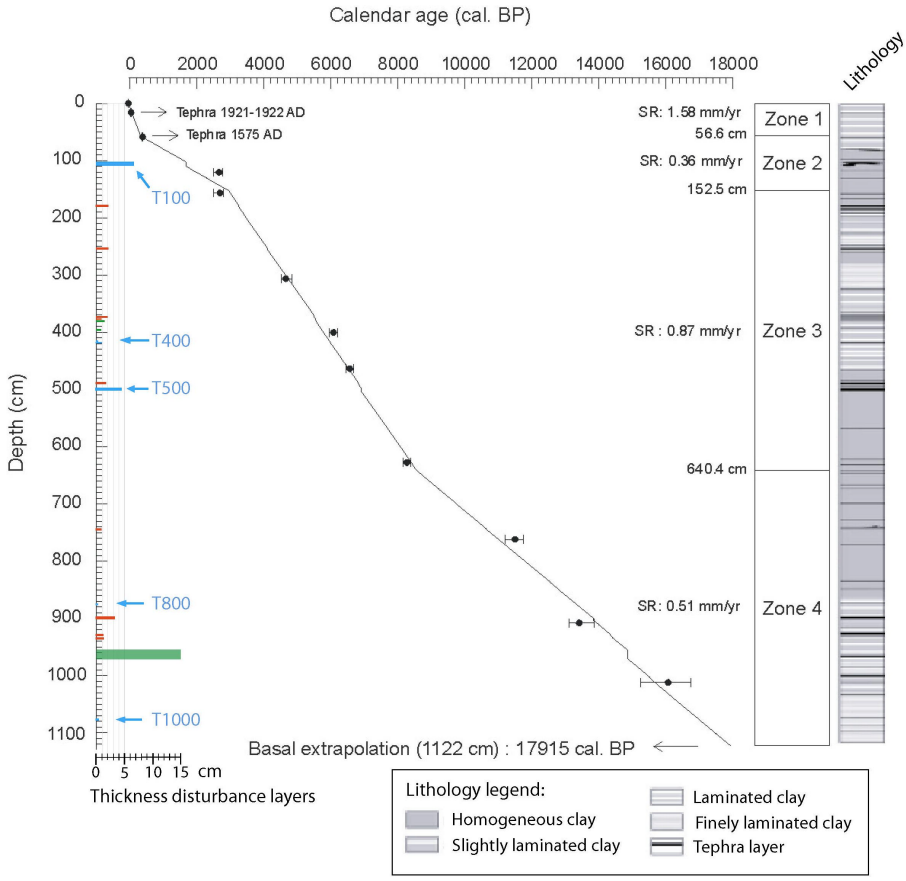

Figure 3: Age-depth model from Lago Puyehue sediment core PU-II. Mean weighted average calibrated ages are plotted, with error bars representing the full range of calibrated radiocarbon ages. Linear regressions are performed by use of Psimpoll software (Bennett 1994). Figure redrawn from Bertrand et al. (2008). Major disturbance layers are indicated at their respective depths (left vertical axis), with green bars representing turbidites, red bars representing tephra layers larger than 1 cm, and blue bars (T100-T1000) representing the five tephra layers studied in this chapter. The lithology of the core is based on macroscopic descriptions, from Bertrand et al. (2008).

Table 2: Bulk radiocarbon dates from the PU-II sediment core. The symbol (*****) marks the date excluded from the age depth model. The range of calendar ages is calculated with OxCal v3.9 (Bronk Ramsey 2001). The calibrated age is calculated as a weighted average, by use of Bcal, and is used for the final age-depth model (Bertrand et al., 2008).

Depth (cm)	Laboratory Reference	^{14}C age ± σ (yr BP)	Calibrated age (cal. yr. BP)	2s error rang of calibrated age
120.5	Poz-5922	2570 ± 35	2655	2490-2770
156.5	Poz-1406	2590 ± 40	2681	2490-2790
306.5	Poz-7660	4110 ± 40	4648	4510-4830
400.5	Poz-2201	5300 ± 40	6074	5940-6200
463.75	Poz-5923	5760 ± 40	6560	6440-6670
627.75	Poz-5925	7450 ± 50	8262	8160-8390
762	Poz-1405	10010 ± 60	11494	11200-11750
908	Poz-7661	11440 ± 80	13407	13100-13850
1012	Poz-2215	13410 ± 100	16063	15250-16750
(*)1119	Poz-7662	12880 ± 90	15355	14350-15950

2.4.3. Impact of tephra deposition on diatom communities

All of our diatom sequences, each representing time intervals between 59 and 153 years, show an in-tephra dilution of the total diatom concentrations, but further only reveal a slight decrease or minor rise in total diatom concentrations after tephra deposition (Fig. 4). Similarly, diatom taxon compositions did not shift significantly, although some small local changes could be seen (Fig. 4), like the very short-lived change in *Nitzschia* (T100, T1000) and minor increase in *Staurosira* s.l. (T100, T500, T1000), and a small in-tephra increase of *Aulacoseira granulata* percentages in T1000 and T400. These changes are, however, smaller than the overall diatom community changes observed throughout the core (Fig. 4).

2.4.4. Long-term diatom analysis

Three main biostratigraphical zones (Puyehue Diatom Zones; PDZ) could be observed (Fig. 5); i.e. between 17,900 and 9550 cal. yr. BP (1120-690 cm; PDZ 1), between 9550 cal. yr. BP and 4760 cal. yr. BP (690-310 cm; PDZ 2) and from 4760 cal. yr. BP until present (310-0.5 cm; PDZ 3). On the PCA biplot (Fig. 6) these three groups of samples, as defined by cluster analysis, were clearly separated from each other, indicating that diatom composition changed over time without reversal to previous compositions. In

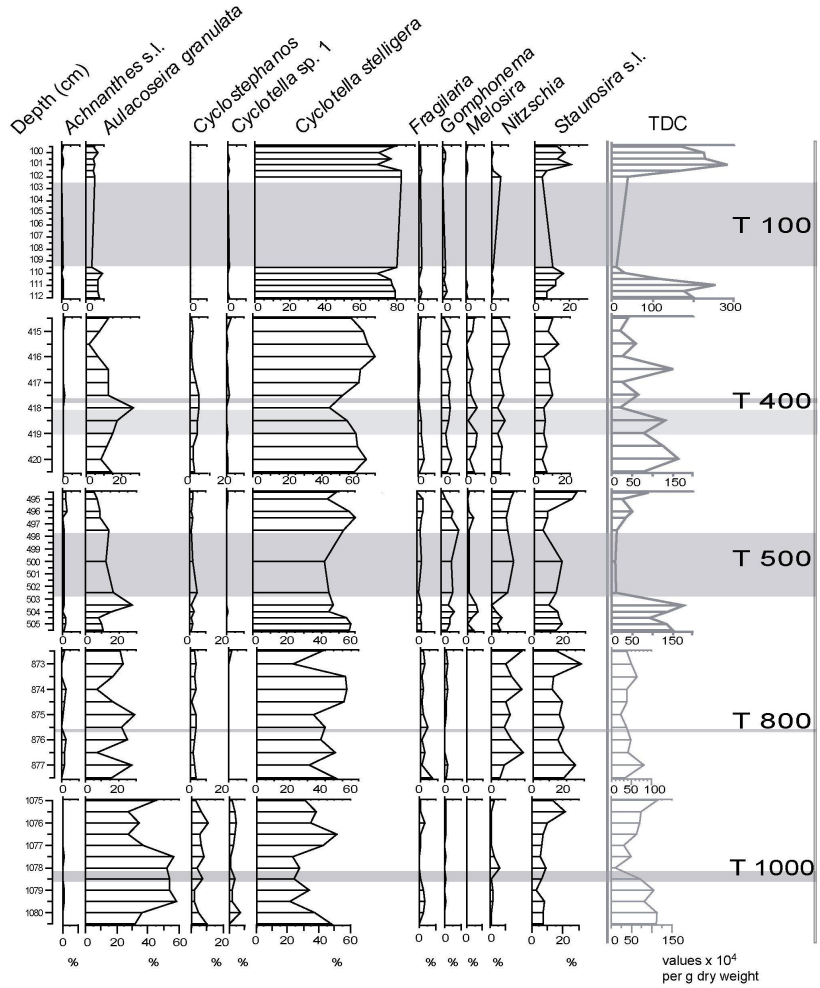

Figure 4: Diatom relative abundances (%) in the five selected sediment sequences in the PU-II core. Only the taxa with an average relative abundance of more than 0.5 % are shown. TDC represents the total diatom concentration (in 10^4 valves per g dry weight). The horizontal gray bars indicate the position of the tephra layers as observed in the core.

general, large eutrophic species (PDZ 1) were followed by high abundances of epiphytic taxa (PDZ 2), and finally by more oligotrophic indicator species (PDZ 3). A list of taxa and their environmental interpretations is given in Table 3, and the CONISS sub-divisions of each diatom zone are illustrated in Fig. 5, and described below.

* *PDZ 1 (1120-690 cm; 17,900-9550 cal. yr. BP)*

PDZ 1 is characterized by a high mean abundance of *Aulacoseira cf. granulata* (21.6 % versus 10.5 and 7.3 % in PDZ 2 and PDZ 3 respectively). *Aulacoseira* is a planktonic genus (Round et al., 1990), although some species, such as *A. granulata* and *A. distans*, are often also mentioned as being tychoplanktonic (e.g. Jenny et al., 2002). *A. granulata* favours well-mixed waters, with a high Si:P ratio (Cox, 1996; Blinn et al., 1994; Kilham et al., 1986). Both PDZ 1 and PDZ 2 contain relatively high abundances of tychoplanktonic (i.e. *Nitzschia* and *Staurosira*) (Round et al., 1990; Patrick & Reimer, 1966) and planktonic taxa that thrive well in nutrient enriched, turbid waters (e.g. *Cyclostephanos*) (Håkansson, 2002; Cholnoky, 1968).

PDZ 1 can be further divided into three subzones and starts with a remarkable peak in both total and relative diatom abundances at 1080 cm depth (PDZ 1a, 1120-1070 cm; 17,900-16,850 cal. yr. BP). The two samples in this zone are primarily characterized by low percentages of *Nitzschia* (1.3 %) and *Staurosira* (6.6 %). Both *Cyclostephanos* and *Cyclotella* sp. 1 are relatively abundant (5.6 and 4.2 % respectively), and some epiphytic taxa, characterizing zones PDZ 1c and PDZ 2, also appear in this zone. Absolute diatom abundances rise from 444 x 10^3 valves per g dry weight (at 1100 cm depth) to 1,504 x 10^3 valves per g dry weight at 1080 cm. This shift is accompanied by a decline in *Cyclotella stelligera* (from 54.6 to 36.0 % respectively), and a rise in *Aulacoseira* cf. *granulata* (25.2 to 36.0 %). As the volume of *A.* cf. *granulata* is approximately 178 times larger than that of *C. stelligera*, the former species is more likely to drive total diatom biovolume (Fig. 5), which peaks at 1080 cm depth.

PDZ 1b (1070-850 cm; 16,850-12,810 cal. yr. BP) is less variable in taxonomic composition (Fig. 5). This zone contains slightly lower percentages of *Aulacoseira cf. granulata* (14.9 %) and higher percentages of *Cyclotella stelligera* (51.9 %). Increased but more variable abundances of *Nitzschia* and *Staurosira* (on average 7.2 % and 15.8 % respectively) are observed in this zone. Sub-dominant taxa are *Cyclostephanos* (3.4 %), *Cyclotella* sp. 1 (0.8 %) and *Fragilaria* (1.0 %). Diatom biovolume and total abundance are low through this zone (330 x 10^3 valves per g dry weight, Fig. 5).

PDZ 1c (850-690 cm, 12,810-9550 cal. yr. BP) is marked by the appearance of the epiphytic taxa *Gomphonema* (0.6 %) and *Melosira* (0.04 %). Total diatom abundances rise towards a mean value of 516 x 10^3 valves per g dry weight, which is largely due to an increase in *Aulacoseira* cf. *granulata* (from 14.9 % in PDZ 1b to 28.6 % in PDZ 1c), resulting in an even stronger increase in diatom biovolume.

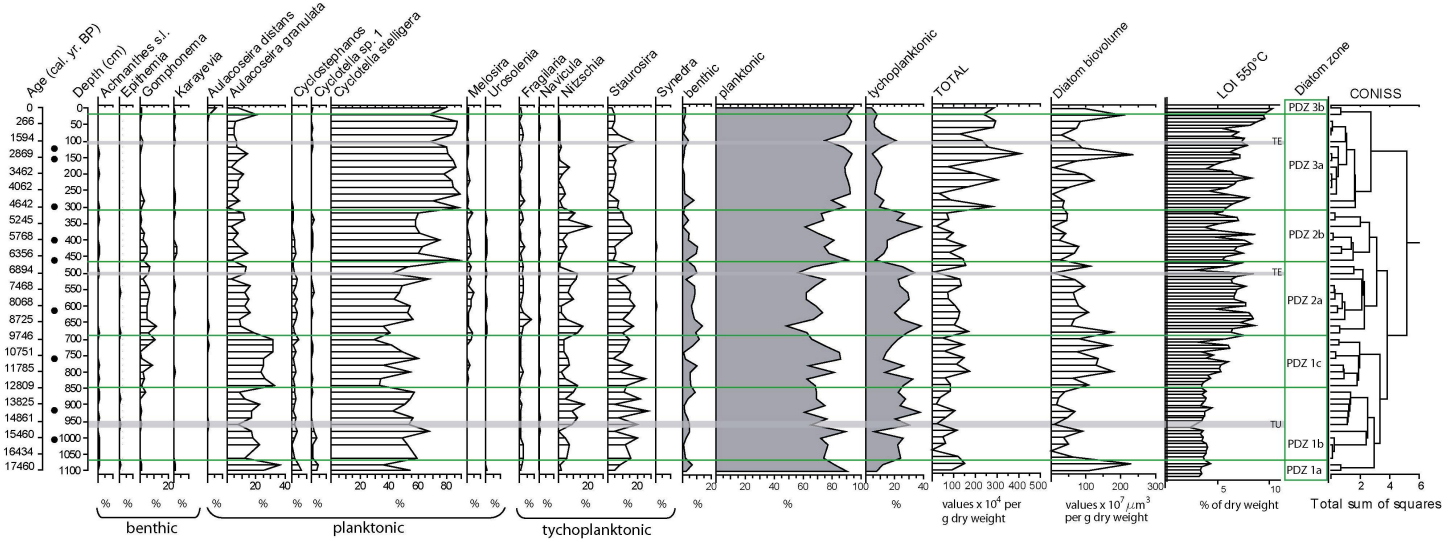

Figure 5: Diatom stratigraphy and CONISS cluster analysis of core PU-II, plotted against core depth (cm). Interpolated calibrated ages are given on the first axis, and the depths of the ^{14}C-dated samples are indicated by black dots (see Table 2 and Fig. 3 for the dates). Relative abundances (%) of taxa with an average relative abundance of more than 0.5 % are shown. The relative abundances of all benthic, planktonic and tychoplanktonic taxa together are given, as well as the total diatom concentration (in valves per g dry weight) and calculated diatom biovolumes (in µm^3 per g dry weight). LOI_{550} is plotted as % of dry weight (Bertrand et al., 2008). The grey shaded lines represent instantaneous deposits larger than 5 cm, and are indicated by TE for tephra's and TU for the turbidite layer between 956 and 971 cm depth.

* *PDZ 2 (690-310 cm; 9550-4760 cal. yr. BP)*

Zone PDZ 2 is generally characterized by increased numbers of epiphytic taxa (*Gomphonema*, *Melosira*, *Naviculadicta* and *Fragilaria*), and mesotrophic genera, such as *Synedra* and *Urosolenia* (Diaz et al., 1998). The benthic/epiphytic taxa account for 6.4 % of the diatoms in PDZ 2, instead of 1.7 % in PDZ 3, and 4.3 % in PDZ 1. *Cyclostephanos*, a planktonic genus favouring higher nutrient concentrations is present in the same relative amounts as in PDZ 1 (0.4 %), as well as *Cyclotella sp. 1* (i.e. 1.8 %). A gradual increase in the relative abundance of *C. stelligera* is observed in PDZ 2, with maximum values around 380-400 cm (60-74 %), coinciding with declines in *Nitzschia* and *Staurosira* relative abundances.

Zone PDZ 2 can be further divided into two subzones, which are characterized by decreasing *Aulacoseira* cf. *granulata* abundances of 12.4 % for PDZ 2a (690-470 cm; 9550-6600 cal. yr. BP) and 7.8 % for PDZ 2b (470-310 cm; 6600-4760 cal. yr. BP). In PDZ 2b total diatom abundances decline towards 94 x 10^3 valves per g dry weight (at 360 cm depth).

* *PDZ 3 (310-0.5 cm; 4760 cal. yr. BP- present)*

The diatom communities in PDZ 3 (310-0.5 cm; 4760 cal. yr. BP-present) are very distinct from those in PDZ 1 and PDZ 2, and show a lower variability in taxonomic composition (Fig. 5). Zone PDZ 3 is characterized by very high abundances of *Cyclotella stelligera* (respectively 82.1 and 73.3 %), and by the absence of *Cyclostephanos* and *Cyclotella* sp. 1. The upper diatom zone can be further divided into two sub-zones due to a last shift in diatom taxonomic composition near 30 cm. The relative abundances of *Aulacoseira cf. granulata*, *Nitzschia* and *Staurosira* are low (respectively 6.3 %, 1.7 % and 5.7 % for PDZ 3a). Epiphytic diatoms, as well as *Synedra* and *Urosolenia* are rare. Absolute diatom abundances rise in this zone from 166 x 10^3 valves per g dry weight at 260 cm depth towards 2,316 x 10^3 valves per g at 100 cm depth. This increase is observed in most diatom taxa, including *A.* cf. *granulata* and most epiphytic taxa, and is most pronounced in *C. stelligera*. Likewise, total diatom biovolume increases to a maximum at 150-100 cm depth (Fig. 5), as it is mostly driven by *A.* cf. *granulata*.

In PDZ 3b (30-0.5 cm; 500 cal. yr. BP – present) only contains two samples, of which the sample at 20 cm contained an increased percentage of *Aulacoseira* cf. *granulata* (i.e. 20.9 %). Both samples where devoid of *Nitzschia*, and contained low amounts of *Staurosira* (2.4 and 4.7 %). A remarkable maximum of *A. distans* (6.1 % or 88 x 10^3 valves per g dry weight) occurred at 0.5 cm depth.

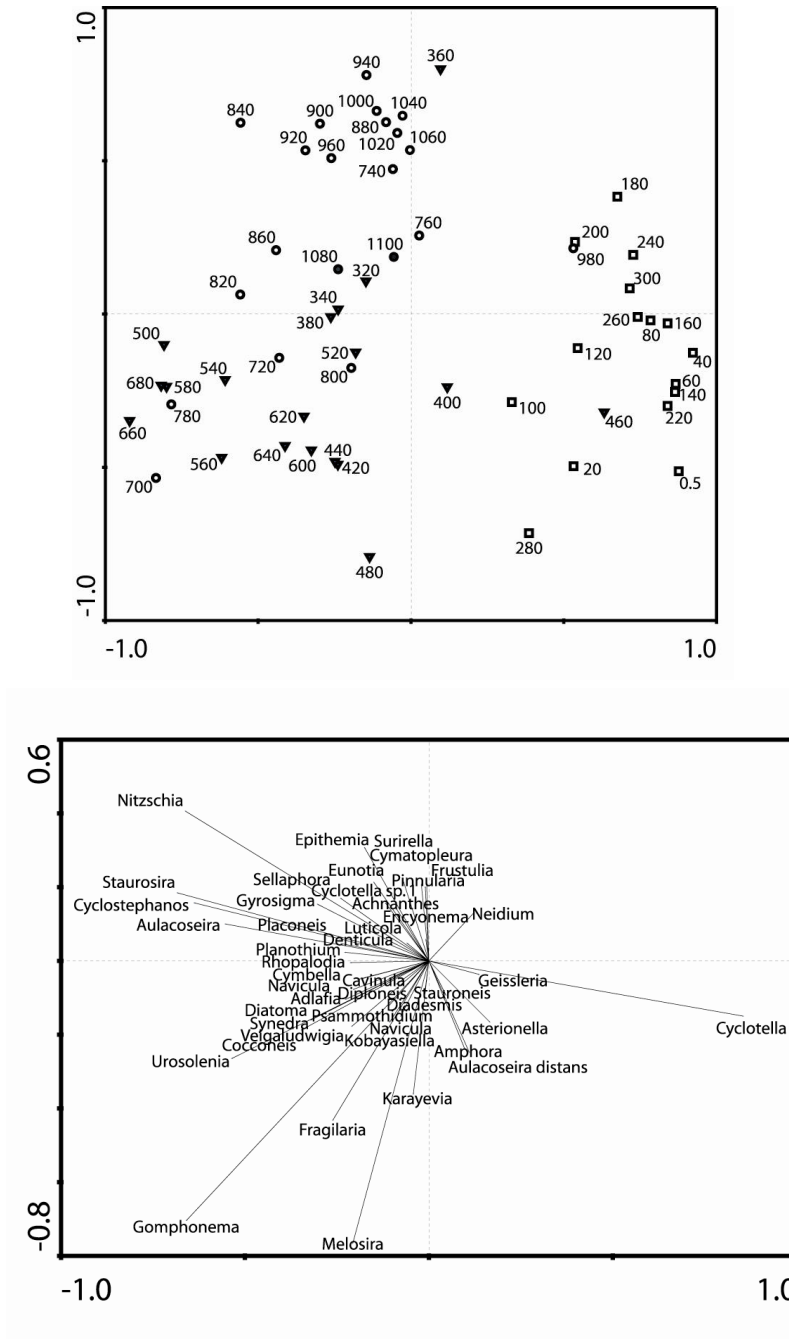

Figure 6: Principal Component Analysis sample and species plot of the diatom assemblages in core PU-II (axes 1 and 2). Hollow squares are samples from diatom zone P3, filled triangles: zone P2, hollow circles: zones P1b and P1C, and filled circles: zone P1a.

2.5. Discussion

A clear long-term evolution in the diatom composition of Lago Puyehue over the last 17,900 years is evidenced by the clear separation of different diatom zones in the ordination analysis (Fig. 6), suggesting that diatom composition changed over time without reversal to previous compositions, and thus pointing to a progressive evolution of the lake's ecology. Comparison between fossil diatom communities below and above five selected tephra layers (Fig. 4), of which one (T100) was the thickest in the core, revealed no consistent, significant effects of tephra deposition on the diatom generic composition neither on total diatom concentrations. This is in contrast to other studies which reported a positive effect of tephra deposition on diatom productivity, and/or more pronounced changes in diatom compositions (e.g. Telford et al., 2004; Lotter et al., 1995), and may be explained by the large volume, the high silica concentrations (15 mg/l; Campos et al., 1989) and the nutrient balance of Lago Puyehue and its catchment. The observed absence of large shifts in post-tephra diatom community compositions and abundances in the PU-II core diminishes possible volcanic-related misinterpretations of the long-term diatom record.

The diatom community of Lago Puyehue starts with predominantly eutrophic indicator taxa in PDZ 1 (e.g. *Cyclostephanos* and large *Aulacoseira* species), followed by an increase in epiphytic and more meso- and oligotrophic indicator taxa (PDZ 2), and finally culminating in diatom communities dominated by *Cyclotella stelligera*, a common planktonic, oligotrophic species (PDZ 3, Fig. 5). Shorter-term changes in diatom community structure are superimposed on this slow but steady evolution of the lake. Both kinds of changes probably reflect strong local and regional climate variation, which might include both direct (e.g. changing temperature, precipitation and wind speed) and indirect impacts (e.g. climate-induced catchment changes).

2.5.1. The deglaciation phase

Analyses of the basal sediments of the core support an early retreat of the Puyehue glacier from the lake, before 17,900 cal. yr. BP. These results narrow down previous age ranges of the lake's deglaciation, which was placed between 19,500 ^{14}C yr. BP (moraines PIIa and PIIb in Fig. 7) and 12,230 ^{14}C yr. BP (moraine PV in Fig. 7; Bentley 1997). Our data extend the timing of minimum deglaciation to somewhat before 17,900 cal. yr. BP, as total diatom abundances are high in the basal sediments, and as the common occurrence of *Aulacoseira cf. granulata* in these layers points to sufficiently high mixing

levels in the lake (Kilham et al., 1986), which is unlikely to have occurred in a glaciated or ice-covered lake. In addition, no coarse debris bearing sediments were observed in the lower part of the PU-II core, which would have been present when the glacier retreated from the basin (e.g. Smith et al., 2006; Hendy et al., 2000). This interpretation corresponds well with the findings based on the seismic stratigraphy of the lake (Charlet et al., 2008), indicating that the PU-II core reached three quarters of the depth of seismic unit V (Fig. 2; Charlet et al., 2008), which was interpreted as a unit of sediments deposited in a postglacial lake (Charlet et al., 2008).

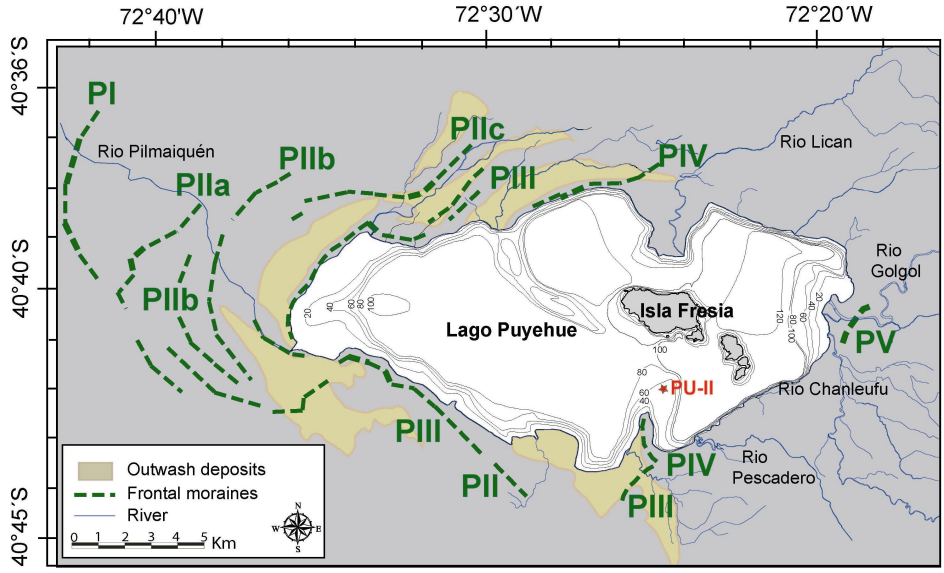

Figure 7: Bathymetric map of Lago Puyehue, showing the location of the coring site (PU-II), the main rivers, and the moraine ridges mapped by Bentley (1997). The indication of outwash deposits is based on Charlet et al., (2008).

These data are important for the debate over the timing of regional deglaciation of northern Patagonia. According to McCulloch et al. (2000) the deglaciation of Patagonia started synchronously over 16° of latitude between 14,600 and 14,300 ^{14}C yr. BP (17,500-17,150 cal. yr. BP). The discrepancy between our data and the studies mentioned by McCulloch et al. (2000) (e.g. Denton et al., 1999) may reflect the heterogeneity of glacier responses to climatic changes in Patagonia (Bennett et al., 2000). In the Chilean Lake District, glacier responses seem to be highly dependent on the geomorphology of the glacial basins (Bentley, 1997; Hubbard, 1997). Differences in glacier response time to climate change can be in the order of 1000 years (e.g. Hubbard, 1997). Further, a

modeling study of the Patagonian Ice Sheet revealed that the northern part of the ice sheet is difficult to model as a result of the higher temperatures in the Chilean Lake District, which implies that the North-Patagonian Ice Sheet is highly sensitive to precipitation changes (Hulton et al., 2002). It is also believed that 50 % of the ice sheet (mainly in the north) melted in a short time window after the start of the deglaciation phase (Hulton et al., 2002). It is thus possible that the Puyehue glacier, as a part of this unstable continental ice mass, started to retreat earlier and faster than previously believed, implying an enhanced deglaciation of the Puyehue catchment area between 17,050 and 16,650 cal. yr. BP.

Between 17,900 and 17,050 cal. yr. BP high percentages of *Aulacoseira cf. granulata* and *Cyclostephanos* are observed. Large *Aulacoseira* and *Cyclostephanos* species are known to favour well-mixed, nutrient-rich waters; in comparison to smaller, oligotrophic indicator species, they can also thrive better in lower light environments (Kilham et al., 1986). Their high abundances can thus be explained by high mixing levels and consequently by high nutrient levels in the lake, maintained by suppressed temperatures and high levels of direct precipitation and wind stress. This is confirmed by the pollen record, which revealed a predominance of cold-resistant and hygrophilous vegetation during this period (Vargas-Ramirez et al., 2008).

At 17,050 cal. yr. BP (1080 cm depth) a peak in diatom biovolume and percentage of *Aulacoseira* cf. *granulata* was observed (Fig. 5), which coincided with an increase in loss on ignition (LOI_{550}) and biogenic silica (BSi) content (Bertrand et al., 2008). We carefully interpret this change in terms of phytoplankton and diatom productivity, respectively, assuming constant sedimentation rates (Fig. 3) and assuming that there were no major changes in terrestrial organic matter influx. This increased productivity can be tentatively interpreted as a short warming pulse between 17,460 and 17,050 cal. yr. BP, as temperature can limit algal growth (Reynolds 1973; 1984).

The possible occurrence of a warming step between 17,460 and 17,050 cal. yr. BP would coincide with the main warming pulse which is believed to have pulled the ice sheet out of the LGM between 17,500 and 17,150 cal. yr. BP (Hulton et al., 2002; McCulloch et al., 2000). This may evenly corroborate glacier recessions further south (Seno Reloncavi; 41°30'S; and the south of Isla Grande de Chiloé; 42°30'-43°00'; Lowell et al., 1995) which are dated at about 13,900-13,000 ^{14}C yr. BP, and which may lag the change in our record as a result of the progressive southward movement of the Southern Westerlies. The warming trend similarly corroborates marine records (ODP site 1233) near the coast of the Chilean Lake District, which showed a warming step of 2-3°C at 19,200-17,400 cal. yr. BP in the alkenone SST record (Lamy et al., 2004).

2.5.2. Late-glacial climate – Termination I

A pronounced, short cooling event or neoglaciation similar to the northern hemispheric Younger Dryas (YD) chronozone (12,890 and 11,650 cal. yr. BP; Stuiver et al., 1995), the Antarctic Cold Reversal (ACR; 14,000-12,500 cal. yr. BP; Jouzel et al., 2001) or the Huelmo-Mascardi event (HM; approx. 11,400-10,200 ^{14}C yr. BP; Hajdas et al., 2003) was difficult to observe in the diatom stratigraphy. Instead, the entire period between 16,850 cal. yr. BP and 12,810 cal. yr. BP was generally characterized by low absolute diatom abundances and biovolumes, with only minor fluctuations in the diatom community composition (Fig. 5). During this period of generally lower diatom productivity, two local minima in total diatom abundances and *A. cf. granulata* percentages were observed, namely at ca. 14,860 cal. yr. BP (960 cm) and between ca. 13,830 and 12,600 cal. yr. BP (900-840 cm), the former being explained by the presence of a turbidite between 956-971 cm depth (Bertrand et al., 2008). The low diatom abundances between 16,850 and 12,810 cal. yr. BP could be interpreted as a dry and perhaps cold period, in which diatom productivity was suppressed by low levels of incoming nutrients (either through direct precipitation or by diminished river discharges), by low temperatures, or by a combination of both factors. Interestingly, a smectite type of clay (probably vermiculite, Bertrand et al., 2008) is present between 17,900 and ca. 11,500 cal. yr. BP in core PU-II, and could have had an additional impact on the diatom productivity and the virtual absence of epiphytes in Lago Puyehue. Some types of suspended clays decrease the light penetration in lakes, thereby reducing the depth of the photic zone, and thus potentially influencing the phytoplankton community structure and productivity (Cuker et al., 1990). Still we acknowledge this could not explain the higher diatom total abundances and biovolumes at 17,900-17,050 cal. yr. BP and 12,800-11,500 cal. yr. BP, where similarly high clay densities are measured (Bertrand et al., 2008).

A relatively dry and cold period between 16,850 and 12,810 cal. yr. BP, as cautiously inferred from our diatom data, is in agreement with pollen analyses at 41° and 43°S, pointing to cold-temperate climate conditions between 15,000 and 11,000 cal. yr. BP, and between 16,700 and 11,550 cal. yr. BP respectively (Moreno 2004, Abarzua et al., 2004). However, our interpretation conflicts with the rather humid conditions as inferred by the same pollen analyses (Moreno, 2004; Abarzua et al., 2004), although moraine dating studies in southern Patagonia (46-55°S) revealed a 'Magellan late-glacial ice advance' between 15,500 and 12,000 cal. yr. BP (Sugden et al., 2005), which was explained by a southward shift of the Westerlies, causing drier conditions in the north (Sugden et al., 2005).

The global character and timing of the YD is still a subject of debate (Rodbell, 2000) and a lot of inconsistencies remain, especially in the mid-latitudes of the Southern Hemisphere. In New Zealand, a late Glacial Reversal (NZLGR) in temperature was derived from oxygen isotope ratios in speleothems from northwestern South Island between 13,530 and 11,140 cal. yr. BP. The carbon isotope ratios from the same sequences however did not show any cooling (Williams et al., 2005). Similarly, former observations of neoglacial advances at the timing of the YD were recently linked to changes in Westerly Wind activity, instead of only temperature changes (e.g. Singer et al. (1998), see also Shulmeister et al. (2004) for an overview).

In tropical South America the growth of an ice sheet, caused by a temperature decline of 3°C, was reported by Clapperton et al. (1997) between 11,000 and 10,000 ^{14}C yr. BP, while the ice cores of Sajama (Bolivia) and Huascaran (Peru) showed a decrease in $\delta^{18}O_{ice}$ values around 14,000 BP, constituting the start of a deglaciation climatic reversal (DCR) (Thompson et al., 1998). In northern Bolivia, glacier advances culminated shortly before 10,700 and 9,700 ^{14}C BP (Abbott et al., 1997), and in Peru glaciers reached their maximum extent at 11,280-10,990 ^{14}C yr. BP (Central-Peru), and at 11,500 to 10,900 ^{14}C yr. BP; (South Peru; Rodbell and Seltzer, 2000). These advances are said to be mainly driven by moisture changes (Kull et al., 2003) instead of regional climate cooling.

According to many terrestrial records in southern South America (41-42°S; Ariztegui et al., 1997; Moreno, 2004; Moreno et al., 1999; 2001; Denton et al., 1999; Heusser et al., 1995), a cooling trend or neoglaciation was observed at 11,400-10,200 ^{14}C yr. BP (Ariztegui et al., 1997) or at 12,200 ^{14}C yr. BP (Denton et al., 1999), while further south (between 44 and 47°S), recent pollen analyses have not revealed any pause or reversal in vegetation development during this period (Bennett et al., 2000, Haberle & Bennett, 2004). Based on marine sediment cores, however, Lamy et al. (2004) did not find evidence an extensive SST cooling in the SE-Pacific (41°S) during the YD, instead, a rapid rise of about 2°C was observed between 12,700 and 12,100 cal. yr. BP.

None of the events described above is fully resolved in the Lago Puyehue diatom record, however, in Chapter 3, additional geochemical analyses support the hypothesis of a moister and perhaps warming climate at the beginning of the Younger Dryas.

2.5.3. Glacial-Holocene transition

The period between 12,810 and 9550 cal. yr. BP (zone PDZ 1c) is a major transitional zone in the core and represents the transition from the last deglaciation towards the Holocene. This period is globally recognized as an era of rapid climate change.

At 12,810 cal. yr. BP (850 cm depth), the Lago Puyehue diatom record shows a rise in *Aulacoseira cf. granulata* percentages and diatom total abundances, together with the appearance of epiphytic and riverine taxa (*Gomphonema, Karayevia, Melosira*) (Fig. 5). These taxa are possibly derived from littoral and riverine environments, and could, together with *Aulacoseira cf. granulata*, indicate higher supplies of fluvial water to the lake. This could result from higher amounts of either meltwater or precipitation.

Higher moisture availability could be the result of a rise in SST, as observed around 12,700 cal. yr. BP (41°S; Lamy et al., 2004), and the subsequent supply of moister air to the Andes, causing higher amounts of direct rainfall near the lake and probably elevated annual snow accumulation in the mountains and resulting in higher river (meltwater) discharges during winter, spring and early summer. This, however, is in disagreement with the pollen record of PU-II (Vargas-Ramirez et al., 2008), evidencing semi-dry conditions between 10,010 and 7450 ^{14}C BP (11,000 - 8000 cal. yr. BP), and with similar pollen records nearby (e.g. Moreno, 2004) that point to warm and dry conditions between 11,000 and 7600 cal. yr. BP. This apparent discrepancy calls for further study and discussions about the paleoclimate in southern Chile at the boundary between the Last Glaciation and the Holocene.

2.5.4. The Holocene

Higher interglacial temperatures, which characterize the Holocene, are generally mirrored in the diatom stratigraphy of Lago Puyehue through high relative abundances of *Cyclotella stelligera* and low percentages of *Aulacoseira cf. granulata* (Figs. 2 and 3). *Cyclotella* is a planktonic genus that requires more light and less nutrients than many other diatom genera, implying that it is often found in low energy environments (Reynolds, 1997). Higher air and surface-water temperatures could have lead to an increase in *Cyclotella* abundances through an increased strength and duration of summer stratification.

Towards the Mid-Holocene, a decrease in diatom total abundances, biovolumes and *Aulacoseira cf. granulata* percentages could be tentatively interpreted as a result of decreasing wind and precipitation levels and/or increasing temperatures. This is supported by a drop in eutrophic indicator *Cyclostephanos* abundances (Round et al., 1990; Kilham et al., 1986), and a short-lived disappearance of epiphytic taxa between ca.

4750 and 3000 cal. yr. BP (ca. 300-150 cm depth; Fig. 5). It is however difficult to distinguish whether this would result from stronger and longer summer stratification periods, from lowered winter precipitation, or both.

According to Lamy et al. (2001, 2004) the Westerlies shifted southward from 41°S between 7700 and 4000 cal. yr. BP, implying lower precipitation values at 41°S. These findings were supported by the presence of enhanced inferred Westerly Wind activity at 49°S around 6800 cal. yr. BP (Gilli et al., 2005), and by a glacial advance around 6200 cal. yr. BP at 46°S (Douglass et al., 2005). In contrast, Moreno (2004) derived a cool and wet phase between 7600 and 4100 cal. yr. BP from pollen records at 41°S, which is confirmed by the presence of humid indicator taxa in the pollen record of Lago Puyehue (Vargas-Ramirez et al., 2008).

The Late Holocene (from 3000 cal. yr. BP onwards (zone PDZ 3a)) was characterized by an increase in diatom total abundances, increased *Cyclotella stelligera* percentages, and a re-appearance of some epiphytic taxa (*Gomphonema*, *Karayevia*) (Fig. 5). This could reflect an enhanced seasonality with increased winter precipitation levels, and drier summers, perhaps both accompanied by higher temperatures. Although the percentages of epiphytic and eutrophic indicator taxa stayed suppressed due to the larger increase in *Cyclotella stelligera* abundances, their absolute abundances increased during the late-Holocene, together with LOI_{550} values, which might point to higher river discharges combined with elevated temperatures. The high relative abundances of *Cyclotella* could have resulted from an earlier start of stratification in spring, and drier than normal summers; *Cyclotella* requires lower nutrient levels than most *Chlorophyceae* and *Cyanophyceae* (Reynolds, 1997), and could thus have replaced their niches during late summer, when P and N availabilities were minimal.

Our speculation of enhanced seasonality would support the increased occurrence of El Niño in the late-Holocene as reported from studies in tropical South America (e.g. Moy et al., 2002), and could be related to the enhanced insolation seasonality in the Late Holocene (Berger 1978). During summer, El Niño is known to be associated with drier than normal summers at 38-41°S (Renwick & Revell, 1999; Renwick, 1998; Montecinos & Aceituno, 2003), which is in accordance with the very high percentages of *Cyclotella stelligera* in the late-Holocene (Fig. 5).

In general, besides the growing importance of *Cyclotella stelligera*, an increased centennial to millennial variability of the total diatom abundances was observed towards the late-Holocene. This co-varied with other proxies, such as diatom biovolumes, loss on ignition (Fig. 5), biogenic silica content and grain size distribution (Bertrand et al., 2008). A higher Late Holocene climate variability is in agreement with several paleoclimatic

reconstructions in both tropical and mid-latitude Pacific regions, and is often mentioned together with increased frequencies and amplitudes of El Niño in the Late Holocene. In almost all South-Chilean records, a warm and often dry period has been observed in the Early Holocene (e.g. Moreno & León, 2003; Moreno, 2004; Haberle & Bennett, 2004), which was followed by warmer and wetter conditions in the late-Holocene (i.e. from 3200-2000 cal. yr. BP to present). These observations are in agreement with a larger seasonal or inter-annual meridional shift of the Westerlies during the late-Holocene.

Many tropical records similarly confirm a lowered frequency and amplitude of El Niño occurrences in the early- to Mid-Holocene, as modeled by Clement et al. (2000). The timing of the end of the ENSO suppression is still a matter of debate, and ranges from ca. 7000-5000 ^{14}C yr. BP (Rodbell et al., 1999), 5800-5400 ^{14}C yr. BP (Haug et al., 2001; Sandweiss et al., 1996) and 5400-5300 cal. yr. BP (McGregor & Gagan, 2004; Keefer et al., 2003). All records show, however, a strong increase in frequency of El Niño-related climate events and variability somewhere after 3800 cal. yr. BP (e.g. Haug et al., 2001; Rodbell et al., 1999 ; Moy et al., 2002).

2.6. Conclusions

The diatom data in the sediment core from Lago Puyehue support an early deglaciation of the lake (i.e. earlier than 17,900 cal. yr. BP). We have evidence of a sudden rise in productivity probably caused by a warming pulse at ca. 17,300 cal. yr. BP. This is coincident with a warming step which is believed to have triggered the rapid deglaciation of the Patagonian Ice Sheet (McCulloch et al., 2000; Chapters 3 and 8). At 12,810-11,800 cal. yr. BP the start of a moister period could be tentatively inferred. The Lago Puyehue diatom record shows no clear evidence for a rapid and short lived late-glacial cooling event at the time of the Antarctic Cold Reversal, the Huelmo-Mascardi event, or the northern hemispheric Younger Dryas cold episode, although a period of low productivity was recognised between 16,850 and 12,810 cal. yr. BP, and some climate instability may have occurred between 13,400 and 11,700 cal. yr. BP. The interpretation of low productivity during this interval is supported by geochemical data presented in Chapter 3. The Holocene is characterized by high abundances of oligotrophic indicator species, which could be attributed to (a) enhanced summer stratification, caused by warmer temperatures, and (b) stabilization of the catchment vegetation. Towards the Mid-Holocene lower precipitation values were tentatively inferred from the lowered diatom total abundances and a temporal disappearance of epiphytic taxa in the core. The late-

Holocene was characterized by high centennial to millennial variability in both diatom total abundances and sedimentological proxies (Bertrand et al., 2008). This variability probably reflected enhanced climate variability, as was also observed in records elsewhere in South America. From 3000 cal. yr. BP drier summers and slightly wetter winters may be related to a change in El Niño properties as reported from Holocene paleoclimatic studies in the tropical Pacific. Our results indicate that gaps remain in our knowledge regarding the strength and position of the Southern Westerlies during the Holocene. In order to resolve this, more continuous high-resolution multi-proxy records are needed for southern South America.

Acknowledgements

This research is supported by the Belgian SSTC project EV/12/10B "A continuous Holocene record of ENSO variability in southern Chile". C. Beck, M. Tardy, F. Arnaud, V. Lignier, X. Boës, S. Bertrand, F. Charlet, F. Devleeschouwer, L. Vargas Ramirez, W. San Martin and A. Peña have done the coring fieldwork. Valuable assistence for the fieldwork (2001-2002) was provided by M. Pino, M. Mardones and R. Urrutia.

Table 3: Key diatom taxa and their ecological preferences. Taxa with an average relative abundance exceeding 0.5 % are shown in bold. Ecological information from: Campos et al. (1989), Cholnoky (1968), Cox (1996), Patrick and Reimer (1966), Round et al. (1990), Rühland et al. (2003) and Schmidt et al. (2004).

Genus/species name	Life form	Ecological charactertistics
Achnanthes s.l. Bory	**Benthic**	
Adlafia Moser	Benthic	
Amphora Ehrenberg ex. Kützing	Benthic	
Asterionella Hassall	Planktonic	
Aulacoseira distans Ehrenberg (Simonsen)	**Planktonic (also cited as tychoplanktonic)**	
Aulacoseira granulata (Ehrenberg (Simonsen)	**Planktonic (also cited as tychoplanktonic)**	**nutrient rich, well mixed waters**
Brachysira Kützing	Benthic	
Caloneis Cleve	Benthic	
Cavinula Mann & Stickle	Benthic	
Cocconeis Ehrenberg	Benthic (epiphytic)	
Cyclostephanos Round ex. Theriot	**Planktonic**	**nutrient rich, turbid waters**
Cyclotella sp. 1	**Planktonic**	**nutrient rich, turbid waters**
Cyclotella stelligera Ehrenberg (Cleve & Grunow)	**Planktonic**	**oligotrophic, deep, low energy environments**
Cymatopleura Smith	Benthic	
Cymbella Agardh	Benthic	
Denticula Kützing	Benthic	
Diadesmis Kützing	Benthic	damp surfaces
Diatoma Bory	Tychoplanktonic	
Diploneis Ehrenberg	Benthic (epipelic)	
Encyonema Kützing	Benthic	
Epithemia Brébisson	**Benthic**	**oligotrophic, acid environments, shallow waters**
Eucocconeis Cleve	Benthic	
Eunotia Ehrenberg	Benthic	oligotrophic / dystrophic environments
Fragilaria Lyngbye	**Tychoplanktonic**	
Frustulia Rabenhorst	Benthic	acidic environments (often found in bogs and/or on aerated surfaces)
Geissleria Lange-Bertalot & Metzeltin	Planktonic	
Gomphonema Ehrenberg	**Benthic (epiphytic)**	
Gyrosigma Hassall	Benthic	
Hantzschia Grunow	Benthic	*H. amphioxis* is typical for soils or aerated surfaces, many *Hantzschia* species can survive osmotic pressure changes
Hippodonta Lange-Bertalot	Benthic	
Karayevia Round a Bukhtiyarova	**Benthic**	
Kobayasiella Lange-Bertalot	Benthic	
Lecohuia Lange-Bertalot ex. Rumrich et al.	Benthic	

Table 3 *(continued)*

Genus/species name	Life form	Ecological charactertistics
Luticola Mann ex. Round et al.	Benthic	supralittoral places, aerated surfaces
Melosira Agardh	**Planktonic**	
Navicula Bory	**Benthic**	**many species are found in slightly brackish environments**
Naviculadicta Lange-Bertalot ex. Rumrich et al.	Benthic	
Neidium Pfitzer	Benthic	oligotrophic, freshwater environments
Nitzschia Hassall	**Tychoplanktonic**	
Pinnularia Ehrenberg	Benthic	acidic environments, damp surfaces, peat bogs
Placoneis Mereschowsky	Benthic	
Planothidium Round & Bukhtiyarova	Benthic	
Psammothidium Bukhtiyarova & Round	Benthic	
Rhopalodia Müller	Benthic	
Sellaphora Mereschowsky	Benthic	
Stauroneis Ehrenberg	Benthic	damp surfaces, environments with changes in osmotic pressure, *Stauroneis* contains many brackish water species
Staurosira (Ehrenberg) Williams & Round	**Tychoplanktonic**	**disturbed environments, can survive osmotic and nutrient changes *S. brevistriata* is often found in oxygen-poor environments**
Surirella Turpin	Benthic	some species marine, other brackish, some species can stand osmotic pressure changes
Synedra Ehrenberg	**Tychoplanktonic**	
Urosolenia Round & Crawford ex. Round et al.	**Planktonic**	
Veigaludwigia Lange-Bertalot & Rumrich ex. Rumrich et al.	Benthic	

References

Abarzúa A.M., Villagrán C., Moreno P. 2004. Deglacial and postglacial climate history in east-central Isla Grande de Chiloé, southern Chile (43°S). Quaternary Research. 62: 49-59.

Abbott M.B., Seltzer G.O., Kelts K.R., Southon J. 1997. Holocene paleohydrology of the tropical Andes from lake records. Quaternary Research. 47: 70-80.

Ariztegui D., Bianchi M.M., Masaferro J., Lafargue E., Niessen F. 1997. Interhemispheric synchony of late-glacial climatic instability as recorded in proglacial Lake Mascardi, Argentina. Journal of Quaternary Science. 12: 333-338.

Arnaud F., Magand O., Chapron E., Bertrand S., Boës X., Mélières M.A. (2006). Radionuclide dating (^{210}Pb, ^{137}Cs, ^{241}Am) of recent lake sediments in a highly active geodynamic settings (Lakes Puyehue and Icalma - Chilean Lake District). Science of the Total Environment. 366: 837-850.

Battarbee R.W., Kneen M. 1982. The use of electronically counted microspheres in absolute diatom analysis. Limnology and Oceanography. 27: 184-188.

Bennett K.D. 1994. 'Psimpoll' version 2.23: A C program for analysing pollen data and plotting pollen diagrams. INQUA Working Group on Data Handling Methods Newsletter. 11: 4-6.

Bennett K.D., Haberle S.G., Lumley S.H. 2000. The last glacial-Holocene transition in Southern Chile. Science. 290: 325-328.

Bentley M.J. 1997. Relative and radiocarbon chronology of two former glaciers in the Chilean Lake District. Journal of Quaternary Science. 12: 25-33.

Berger A.L. 1978. Long-term variations of daily insolation and Quaternary climatic changes. Journal of Atmospherical Sciences. 35 (12), 2362-2367.

Bertrand S. 2002. Caractérisation des apports sédimentaires lacustres de la region des lacs, Chili Méridional (Exemple des lacs Icalma et Puyehue). Unpublished Msc. Thesis. Department of Geology, University of Liège, 51 pp.

Bertrand S., Charlet F., Charlier B., Renson V., Fagel, N. 2008. Climate variability of southern Chile since the Last Glacial Maximum: a continuous sedimentological record from Lago Puyehue (40°S). Journal of Paleolimnology. 39 (2): 179-195.

Boës X., Fagel N. 2008a. Relationships between southern Chilean varved lake sediments, precipitation and ENSO for the last 600 years. Journal of Paleolimnology. 39 (2): 237-252.

Boës X., Fagel N. 2008b. Timing of the late glacial and Younger Dryas cold reversal in southern Chile varved sediments. Journal of Paleolimnology. 39 (2): 267-281.

Blinn D.W., Hevly R.H., Davis O.K. 1994. Continuous Holocene record of diatom stratigraphy, paleohydrology, and anthropogenic activity in a spring-mound in southwestern United-States. Quaternary Research. 42: 197-205.

Bracco R., Inda H., del Puerto L., Castiñera C., Sprechmann P., Garcia-Rodríguez F. 2005. Relationships between Holocene sea-level variations, trophic development, and climatic change in Negra Lagoon, Southern Uruguay. Journal of Paleolimnology. 33: 253-263.

Bronk Ramsey C. 2001. Development of the Radiocarbon program OxCal. Radiocarbon. 43 (2A): 355-363.

Campos H., Steffen W., Agüero G., Parra O., Zúñiga L. 1989. Estudios limnologicos en el Lago Puyehue (Chile): Morfometria, factores fisicos y quimicos, plancton y productividad primaria. Medio Ambiente. 10: 36-53.

Charlet F., De Batist M., Chapron E., Bertrand S., Pino M., Urrutia R. 2008. Seismic-stratigraphy of Lago Puyehue (Chilean Lake District): new views on its deglacial and Holocene evolution. Journal of Paleolimnology. 39 (2): 163-177.

Cholnoky B.J. 1968. Die Ökologie der Diatomeen in Binnengewassern. J. Cramer, Lehre, 699pp.

Clapperton C.M. 1993. Quaternary Geology and Geomorphology of South America. Elsevier Science b.v., Amsterdam. 800 pp.

Clapperton C.M., Hall M., Mothes P., Hole M.J., Still J.W., Helmens K.F., Kuhry P., Gemmel A.M.D. 1997. A Younger Dryas Icecap in the Equatorial Andes. Quaternary Research. 47: 13-28.

Clement A.C., Seager R., Cane M.A. 2000. Suppression of El Niño during the Mid-Holocene by changes in the Earth's orbit. Paleoceanography. 15: 731-737.

Cox E.J. 1996. Identification of freshwater diatoms from live material. Chapman and Hall, London, 158 pp.

Cuker B.E., Gama P.T., Burkholder J.M. 1990. Type of suspended clay influences lake productivity and phytoplankton community response to phosphorus loading. Limnology and Oceanography. 35 (4): 830-839.

Czernik T. & Goslar T. 2001. Preparation of graphite targets in the Gwilice radiocarbon laboratory for AMS 14C dating. Radiocarbon. 43: 283-291.

De Batist M., Fagel N., Loutre M.F., Chapron E. 2008. A 17,900 year multi-proxy lacustrine record of Lago Puyehue (Chilean Lake District): Introduction. Journal of Paleolimnology. 39: 151-161.

Denton G.H., Lowell T.V., Heusser C.J., Schlüchter C., Andersen B.G., Heusser L.E., Moreno P.I., Marchant D.R. 1999. Geomorphology, stratigraphy, and radiocarbon chronology of Llanquihue drift in the area of the Southern Lake District, Seno Reloncaví, and Isla Grande de Chiloé, Chile. Geografiska Annaler. A 81: 167-229.

Diaz M.M., Pedrozo F.L., Temporetti P.F. 1998. Phytoplankton of two Araucanian lakes of differing trophic status (Argentina). Hydrobiologia. 369-370: 45-57.

Douglass D.C., Singer B.S., Kaplan M.R., Ackert R.P., Mickelson D.M., Caffee M.W. 2005. Evidence of early Holocene glacial advances in southern South America from cosmogenic surface-exposure dating. Geology. 33 (3): 237-240.

Fagel N., Boës X., Loutre M.F. 2008. Climate oscillations evidenced by spectral analysis of Southern Chilean lacustrine sediments: the assessment of ENSO over the last 600 years. Journal of Paleolimnology. 39 (2): 253-266.

Fogwill C.J. & Kubik P.W. 2005. A glacial stage spanning the Antarctic Cold Reversal in Torres del Paine (51°S), Chile, based on preliminary cosmogenic exposure ages. Geografiska Annaler. A 87: 403-408.

Frenguelli J. 1942. Diatomeas del Neuquen (Patagonia). Revista del Museo de la Plata Sección Botanica. 5: 73-219.

Gagan M.K., Hendy E.J., Haberle S.G., Hantoro W.S. 2004. Post-glacial evolution of the Indo-Pacific Warm Pool and El Niño-Southern oscillation. Quaternary International. 118-119: 127-143.

Gilli A., Ariztegui D., Anselmetti F.S., McKenzie J.A., Markgraf V., Hajdas I., McCulloch R.D. 2005. Mid-Holocene strengthening of the Southern Westerlies in South America – Sedimentological evidences from Lago Cardiel, Argentina (49°S). Global and Planetary Change. 49: 75-93.

Grimm E.C. 1987. CONISS, a FORTRAN-77 program for stratigraphically constrained cluster analysis by the method of incremental sum of squares. Computers and Geosciences - UK. 13: 13-15.

Grimm E.C. 1991. Tilia version 2.0b4. Springfield: Illinois State Museum, Illinois.

Grimm E.G. 2001. TGView version 1.1.1.1. Springfield: Illinois State Museum, Illinois.

Haberle S.G. & Bennett K.D. 2004. Postglacial formation and dynamics of North Patagonian Rainforest in the Chonos Archipelago, Southern Chile. Quaternary Science Reviews. 23: 2433-2452.

Haberzettl T., Fey M., Luecke A., Maidana N., Mayr C., Ohlendorf C., Schaebitz F., Schleser G.H., Wille M., Zolitschka B. 2005. Climatically induced lake level changes during the last two millennia as reflected in sediments of Laguna Potrok Aike, southern Patagonia (Santa Cruz, Argentina). Journal of Paleolimnology. 33: 283-302.

Hajdas I., Bonani G., Moreno P.I. and Ariztegui D. 2003. Precise radiocarbon dating of Late-Glacial cooling in mid-latitude South America. Quaternary Research. 59: 70-78.

Håkansson H. 2002. A compilation and evaluation of species in the general Stephanodiscus, Cyclostephanos and Cyclotella with a new genus in the family Stephanodiscaceae. Diatom Research. 17: 1-139.

Haug G.H., Hughen K.A., Sigman D.M., Peterson L.C., Röhl U. 2001. Southward migration of the Intertropical Convergence Zone through the Holocene. Science. 293: 1304-1308.

Heiri O., Lotter A.F., Lemcke G. 2001. Loss on ignition as a method for estimating organic and carbonate content in sediments: reproductibility and comparability of results. Journal of Paleolimnology. 25: 101-110.

Hendy C.H., Sadler A.J., Denton G.H., Hall B.L. 2000. Proglacial lake-ice conveyors: a new mechanism for deposition of drift in polar environments. Geografiska Annaler. A 82: 249-270.

Heusser C.J., Denton G.H., Hauser A., Andersen B.G., Lowell T.V. 1995. Quaternary pollen records from the archipelago de Chiloe in the context of glaciation and climate. Revista Geologica de Chile. 22: 25-46.

Hubbard A.L. 1997. Modelling climate, topography and palaeoglacier fluctuations in the Chilean Andes. Earth Surface Processes and Landforms. 22, 79-92.

Hulton N.R.J., Purves R.S., McCulloch R.D., Sudgen D.E., Bentley M.J. 2002. The Last Glacial Maximum and deglaciation in southern South America. Quaternary Science Reviews. 21: 233-241.

Jenny B., Valero-Garcés B.L., Villa-Martínez R., Urrutia R., Geyh M., Veit H. 2002. Early to Mid-Holocene Aridity in Central Chile and the Southern Westerlies: The Laguna Aculeo Record (34°S). Quaternary Research. 58: 160-170.

Jenny B., Wilhelm D., Valero-Garcés B.L. 2003. The Southern Westerlies in Central Chile: Holocene precipitation estimates based on a water balance model for Laguna Aculeo (33°50'S). Climate Dynamics. 20: 269-280.

Jorgetti T., Silva Dias P.L., Braconnot P. 2006. Review of: El Niño over South America during the mid-Holocene. Advances in Geosciences. 6: 279-282.

Jouzel J., Masson V., Cattani O., Falourd S., Stievenard M., Stenni B., Longinelli A. Johnsen S.J., Steffensen J.P., Petit J.-R., Schwander J., Souchez R. and Barkov N.I. 2001. A new 27 ky high resolution East Antarctic climate record. Geophysical Research Letters. 28: 3199-3202.

Keefer D.K., Moseley M.E., deFrance S.D. 2003. A 38000-year record of floods and debris flows in the Ilo region of southern Peru and its relation to El Niño events and great earthquakes. Palaeogeography, Palaeoclimatology, Palaeoecology. 194: 41-77.

Kilham P., Kilham S.S., Hecky R.E. 1986. Hypothesized resource relationships among African planktonic diatoms. Limnology and Oceanography. 31: 1169-1181.

Knorr G. & Lohman G. 2003. Southern Ocean origin for the resumption of Atlantic thermohaline circulation during deglaciation. Nature. 424: 532-536.

Kull C., Hanni F., Grosjean M., Veit H. 2003. Evidence of an LGM cooling in NW-Argentina (22 degrees S) derived from a glacier climate model. Quaternary International. 108: 3-11.

Lamy F., Hebbeln D., Röhl U., Wefer G. 2001. Holocene rainfall variability in southern Chile: a marine record of latitudinal shifts of the Southern Westerlies. Earth and Planetary Science Letters. 185: 369-382.

Lamy F., Hebbeln D., Wefer G. 1999. High-resolution marine record of climatic change in mid-latitude Chile during the last 28,000 years based on terrigenous sediment parameters. Quaternary Research. 51: 83-93.

Lamy F., Kaiser J., Ninnemann U., Hebbeln D., Arz H.W., Stoner J. 2004. Antarctic timing of surface water changes off Chile and Patagonian Ice Sheet response. Science. 304: 1959-1962.

Langohr R. 1971. The volcanic ash soils of the Central valley of Central Chile I. Deposition and origin of the parent materials of the Trumae soils within the Itata River basin. Pédologie. 11: 259-293.

Langohr R. 1974. The volcanic ash soils of the Central valley of central Chile II. The parent materials of the Trumae and Nadi soils of the Lake District in relation with the geomorphology and quaternary geology. Pédologie. 14: 238-255.

Laugénie C. 1982. La région des lacs, Chili Méridional, recherches sur l'evolution géomorphologique d'un piémont glaciaire quaternaire andin. Unpublished PhD thesis, University of Bordeaux III, France, 822 p.

Lotter A.F., Birks H.J.B. and Zolitschka B. 1995. Late-glacial pollen and diatom changes in response to two different environmental perturbations: volcanic eruption and Younger Dryas cooling. J. Paleolimnol. 14: 23-47.

Lowell T.V., Heusser C.J., Andersen B.G., Moreno P.I., Hauser A., Heusser L.E., Schluchter C., Marchant D.R., Denton G.H. 1995. Interhemispheric correlation of late Pleistocene glacial events. Science. 269: 1541-1549.

McCulloch R.D. & Davies S.J. 2001. Late-glacial and Holocene palaeoenvironmental change in the central Strait of Magellan, southern Patagonia. Palaeogeography, Palaeoclimatology, Palaeoecology. 173: 143-173.

McCulloch R.D., Bentley M.J., Purves R.S., Hulton N.R.J., Sudgen D.E., Clapperton C.M. 2000. Climatic inferences from glacial and palaeoecological evidence at the last glacial termination, southern South America. Journal of Quaternary Science. 15: 409-417.

McGregor H.V., Gagan M.K. 2004. Western Pacific coral $\delta^{18}O$ records of anomalous Holocene variability in the El Niño-Southern Oscillation, Geophysical Research Letters. 31. L11204, doi: 10.1029/2004GL019972: 1-4.

Montecinos A. & Aceituno P. 2003. Seasonality of the ENSO-related rainfall variability in central Chile and associated circulation anomalies. Journal of Climate. 16: 281- 296.

Montecinos A., Diaz A., Aceituno P. 2000. Seasonal diagnostic and predictability of rainfall in subtropical South America based on tropical Pacific SST. Journal of Climate. 13: 746-758.

Moreno P.I. 2004. Millennial-scale climate variability in Northwest Patagonia over the last 15 000 yr. Journal of Quaternary Science. 19: 35-47.

Moreno P.I. & Léon A.L. 2003. Abrupt vegetation changes during the last glacial to Holocene transition in mid-latitude South America. Journal of Quaternary Science. 18: 787-800.

Moreno P.I., Jacobson G.L., Lowell T.V., Denton G.M. 2001. Interhemispheric climate links revealed by a late-glacial cooling episode in southern Chile. Nature. 409: 804-808.

Moreno P.I., Lowell T.V., Jacobson G.L., Denton G.H. 1999. Abrupt vegetation and climate changes during the last glacial maximum and last termination in the Chilean Lake District: a case study from Canal de la Puntilla (41°S). Geografiska Annaler A. 81: 285-311.

Moy C.M., Seltzer G.O., Rodbell D.T., Anderson D.M. 2002. Variability of El Niño/Southern Oscillation activity at millennial timescales during the Holocene epoch. Nature. 420: 162-165.

Patrick R. & Reimer C.W. 1966. The diatoms of the United States, exclusive of Alaska and Hawaii. Volume 1. Academy of Natural Sciences of Philadelphia, Philadelphia, 688 pp.

Renwick J.A. 1998. ENSO-related variability in the frequency of South Pacific Blocking. Monthly Weather Reviews. 126: 3117-3123.

Renwick J.A. & Revell M.J. 1999. Blocking over the South Pacific and Rossby Wave Propagation. Monthly Weather Reviews. 127: 2233-2247.

Reynolds C.S. 1973. The seasonal periodicity of planktonic diatoms in a shallow eutrophic lake. Freshwater biology. 3: 89-110.

Reynolds C.S. 1984. The ecology of freshwater phytoplankton. Cambridge University Press, Cambridge, UK, 384 pp.

Reynolds C.S. 1997. Vegetation processes in the pelagic: a model for ecosustem theory. In: Kinne O. (Ed.): Excellence in Ecology 9. Ecology Institute, Oldendorf/Luhe, 371pp.

Ribbe J. 2004. The southern supplier. Nature. 427: 23-24.

Rodbell D.T. 2000. The Younger Dryas: Cold, cold everywhere? Science. 290: 285-286.

Rodbell D.T. & Seltzer G.O. 2000. Rapid ice margin fluctuations during the Younger Dryas in the tropical Andes. Quaternary Research. 54: 328-338.

Rodbell D.T., Seltzer G.O., Anderson D.M., Abbott M.B., Enfield D.B. and Newman J.H. 1999. An ~15,000-year record of El Niño-driven alleviation in southwestern Ecuador. Science. 283: 516-520.

Round F.E. & Bukhtiyarova L. 1996. Four new genera based on *Achnanthes* (*Achnanthidium*) together with a re-definition of *Achnanthidium.* Diatom Research. 11: 345-361.

Round F.E., Crawford R.M., Mann D.G. 1990. The diatoms: biology and morphology of the genera. Cambridge University Press, Campbridge, 747 pp.

Rühland K.M., Smol J.P., Pienitz R. 2003. Ecology and spatial distributions of surface-sediment diatoms from 77 lakes in the subarctic Canadian treeline region. Canadian Journal of Botany. 81: 57-73.

Rumrich U., Lange-Bertalot H. and Rumrich M., 2000. Diatoms of the Andes, from Venezuela to Patagonia/Tierra del Fuego, and two additional contributions. ARG Gartner Verlag KG, Koningstein, 673 pp.

Sandweiss D.H., Richardson J.B., Reitz E.J., Rollins H.B., Maasch K.A. 1996. Geoarchaeological evidence from Peru for a 5000 years BP onset of El Niño. Science 273: 1531-1533.

Santisteban J.I., Mediavilla R., López-Pamo E., Dabrio C.J., Blanca Ruiz Zapata M., José Gil Garcia M., Castaño S., Martínez-Alfaro P.E. 2004. Loss on ignition: a qualitative or quantitative method for organic matter and carbonate mineral content in sediments? Journal of Paleolimnology. 32: 287-299.

Sarmiento J.L., Gruber N., Brzezinski M.A., Dunne J.P. 2004. High-latitude controls of thermocline nutrients and low latitude biological productivity. Nature. 427: 56-60.

Schick M. 1980. Flora del parque nacional Puyehue. Universitaria, Santiago, 557p.

Schmidt R., Kamenik C., Lange-Bertalot H., Klee R. 2004. Fragilaria and Staurosira (Bacillariophyceae) from sediment surfaces of 40 lakes in the Austrian Alps in relation to environmental variables, and their potential for palaeoclimatology. Journal of Limnology. 63 (2), 171-189.

Shulmeister J., Rodbell D.T., Gagan M.K., Seltzer G.O. 2006. Inter-hemispheric linkages in climate change: paleo-perspectives for future climate change. Climate of the Past Discussions. 2: 79-122.

Shulmeister J., Goodwin I., Renwick J., Harle K., Armand L., McGlone M.S., Cook E.,
Dodson J., Hesse P.P., Mayewski P., Curran M. 2004. The Southern Hemisphere westerlies in the Australasian sector over the last glacial cycle: a synthesis. Quaternary International. 118-119: 23-53.

Singer C., Shulmeister J., McLea B. 1998. Evidence against a significant Younger Dryas cooling event in New Zealand. Science. 281: 812-814.

Smith J.A., Hodgson D.A., Bentley M.J., Verleyen E., Leng M.J., Roberts S.J. 2006. Limnology of two Antarctic epishelf lakes and their potential to record periods of ice shelf loss. Journal of Paleolimnology. 35: 373-394.

Smol J.P., Birks H.J.B., Last W.M. (Eds.) 2001. Tracking environmental change using lake sediments volume 3: terrestrial, algal, and siliceous indicators. Kluwer Academic Publishers, Dordrecht, 371 pp.

Stuiver M., Grootes P.M., Braziunas T.F. 1995. The GISP2 $\delta^{18}O$ climate record of the past 16,500 years and the role of the sun, ocean, and volcanoes. Quaternary Research. 44: 341-354.

Stuiver M., Reimer P.J., Bard E., Beck J.W., Burr G.S., Hughen K.A., Kromer B., McCormac G., van der Plicht J., Spurk M. 1998. Intcal98 radiocarbon age calibration, 24,000-0 cal. BP. Radiocarbon. 40: 1041-1083.

Sugden D.E., Bentley M.J., Fogwill C.J., Hulton N.R.J., McCulloch R.D., Purves R.S. 2005. Late-glacial glacier events in southernmost South America: a blend of 'northern' and 'southern' hemispheric climatic signals? Geografiska Annaler A. 87A: 273-288.

Telford R.J., Barker P., Metcalfe S., Newton A., 2004. Lacustrine responses to tephra deposition: examples from Mexico. Quaternary Sci. Rev. 23: 2337-2353.

ter Braak C.J.F. & Smilauer P. 2002. CANOCO for Windows 4.5., Biometris – Plant Research International, Wageningen, The Netherlands.

ter Braak C.J.F. & Prentice I.C. 1988. A theory of gradient analysis. Advances in Ecological Research. 18: 271-317.

Thomasson K. 1963. Araucanian Lakes, plankton studies in North Patagonia with notes on terrestrial vegetation. Almqvist & Wiksells Boktryckeri A.B., Uppsala, 139 pp.

Thompson L.G., Davis M.E., Mosley-Thompson E., Sowers T.A., Henderson K.A., Zagorodnov V.S., Lin P.N., Mikhalenko V.N., Campen R.L., Bolzan J.F., Cole-Dai J., Francou B. 1998. A 25,000-year tropical climate history from Bilivian ice cores. Science. 282: 1858-1864.

Turney C.S.M., Kershaw. A.P., Clemens S.C., Branch N., Moss P.T., Fifield L.K. 2004. Millennial and orbital variations of El Niño/Southern Oscillation and high-latitude climate in the last glacial period. Nature. 428: 306-310.

Vargas-Ramirez L., Roche E., Gerrienne P., Hooghiemstra, H. 2008. Pollen-based record of Lateglacial-Holocene climatic variability on southern Lake District, Chile. Journal of Paleolimnology. 39 (2): 197-217.

White W.B., Chen S.C., Allan R.J., Stone R.C. 2002. Positive feedbacks between the Antarctic Circumpolar Wave and the global El Nino-Southern Oscillation Wave. Journal of Geophysical Research - Oceans. 107: 1-17.

Williams P.W., King D.N.T., Zhao J.-X., Collerson K.D. 2005. Late Pleistocene to Holocene composite speleothem ^{18}O and ^{13}C chronologies from South Island, New Zealand - did a global Younger Dryas really exist? Earth and Planetary Science Letters. 230: 301-317.

Chapter 3

Bulk organic geochemistry of sediments from Puyehue Lake and its watershed (Chile, 40°S): Implications for paleoenvironmental reconstructions

Sébastien Bertrand, Mieke Sterken, Lourdes Vargas-Ramirez, Marc De Batist, Wim Vyverman, Gilles Lepoint, and Nathalie Fagel

Abstract

Paleoclimate data from the mid-latitudes of the Southern Hemisphere yield conflicting evidence of interhemispheric synchrony/asynchrony in the climate system. In order to improve our understanding of past climate changes in southern South America, we investigated the sedimentary record of Puyehue Lake, at the northern boundary of the Southern Westerly Wind belt in south-central Chile (40°S). We analyzed the elemental (C, N) and stable isotopic ($d^{13}C$, $d^{15}N$) composition of the sedimentary organic matter preserved in the lake and its watershed to estimate the relative changes in the sources of sedimentary organic carbon through space and time. The geochemical signature of the aquatic (N/C: 0.130) and terrestrial (N/C: 0.069) end-members was determined on samples of lake particulate organic matter and Holocene paleosols, respectively. A simple mixing equation based on the N/C ratio of these end-members was then used to estimate the fraction of terrestrial carbon (f_T) preserved in the lake sediments. Our approach was validated using surface sediment samples, which show a strong relation between f_T and distance to the main rivers and to the shore. We further applied this equation to an 11.22 m long sediment core to reconstruct paleoenvironmental changes in Puyehue Lake and its watershed during the last 17.9 kyr. Our data provide evidence for a first warming pulse at 17.3 cal. ka BP, which triggered a rapid increase in lake diatom productivity, lagging the start of a similar increase in sea surface temperature (SST) off Chile by 1500 years. This delay is best explained by the presence of a large glacier in the lake watershed, which delayed the response of the terrestrial proxies and limited concomitant expansion of the vegetation in the lake watershed (low f_T). A second warming pulse at 12.8 cal. ka BP is inferred from a substantial increase in lake productivity and a major expansion of the vegetation in the lake watershed, demonstrating that the Puyehue glacier had considerably retreated from the watershed. This second warming pulse is synchronous

with a 2°C increase in SST and corresponds to the beginning of the Younger Dryas chronozone. These results may contribute to the mounting evidence that the climate in the mid-latitudes of the southern Hemisphere was warming during the Younger Dryas chronozone, in agreement with the bipolar see-saw hypothesis.

This chapter is an adapted version of

Bertrand S., Sterken M., Vargas-Ramirez L., De Batist M., Vyverman W., Lepoint G., Fagel N. (In Press). Bulk organic geochemistry of sediments from Puyehue Lake and it's watershed (Chile, 40°S): Implications for paleoenvironmental reconstructions. *Palaeogeography, Palaeoclimatology, Palaeoecology*.

Contribution of the author: diatom microscopy and index calculation, interpretation, writing parts of the paper.

3.1. Introduction

The geochemistry of lake sedimentary organic matter generally provides important information that can be used to reconstruct paleoenvironmental changes in lakes and their watersheds. Total organic matter is comprised of material derived from both terrestrial and aquatic sources, and it is necessary to constrain these sources as well as possible for improving the interpretation of paleoenvironmental and paleoclimate records. An accurate understanding of the nature of the bulk sedimentary organic matter can also provide clues to interpret age models based on radiocarbon measurement of bulk sediment samples (Colman et al., 1996). It is now commonplace to assess the origin of lake sedimentary organic matter using C/N ratios and carbon stable isotopes. However, to accurately reconstruct the relative contribution of each of the sources, it is essential to accurately characterize these sources and to look at the evolution of the geochemical properties of the organic matter during transport and sedimentation. This is however rarely done in paleoclimate and paleoenvironmental reconstructions.

Lake sedimentary organic matter is generally described as a binary mixture of terrestrial and aquatic end members that can be distinguished by their geochemical properties. Fresh organic matter from phytoplankton generally has C/N atomic ratios between 4 and 10; whereas terrestrial plants, which are cellulose-rich and protein-poor, produce organic matter that has C/N atomic ratios higher than 20 (Fig. 3; Meyers and Teranes, 2001). Similarly, the carbon ($d^{13}C$) and nitrogen ($d^{15}N$) isotopic compositions of sedimentary organic matter have successfully been used to estimate the content of terrestrial and aquatic sources (Lazerte, 1983). In freshwater environments, however, the use of carbon and nitrogen stable isotopes is relatively limited because of the similar isotopic values for both the terrestrial and aquatic organic sources if the catchment vegetation mainly consists of C3 plants. The carbon and nitrogen isotopic composition of organic matter in lake sediments can however provide important clues to assess past productivity rates and changes in the availability of nutrients in surface waters (Meyers and Teranes, 2001).

One of the main questions in present-day paleoclimate research concerns the role of the Southern Hemisphere in the initiation of abrupt and global climate changes during the Late Quaternary. Several studies have indeed demonstrated that climate records from Antarctic ice cores are clearly asynchronous with the rapid changes of the Northern Hemisphere, and suggest that abrupt paleoclimate changes are initiated in the Southern Hemisphere (Sowers and Bender, 1995; Blunier and Brook, 2001; EPICA Community Members, 2006).

Most paleoceanographic records available for the Southern Hemisphere follow a similar pattern, with sea surface temperatures of the Southern Pacific increasing in phase with Antarctic ice core records (Lamy et al., 2004, 2007; Kaiser et al., 2005; Stott et al., 2007). What remains very controversial is the nature and timing of abrupt climate changes in the mid-latitudes of the Southern Hemisphere, especially in terrestrial environments (Barrows et al., 2007). In South America, currently available terrestrial records indicate either interhemispheric synchrony (Lowell et al., 1995; Denton et al., 1999; Moreno et al., 2001), asynchrony (Bennett et al., 2000) or intermediate patterns (Hajdas et al., 2003).

Here, we present an integrated bulk organic geochemical study of the Puyehue lake-watershed system (Chile, 40ºS) to better understand the paleoenvironmental changes associated with climate variability in the mid-latitudes of South America. We investigate the bulk elemental and isotopic composition of sedimentary organic matter deposited in the lake and its watershed to determine the sources of sedimentary organic matter and estimate their relative contribution through time. These data are then used to reconstruct paleoenvironmental changes in South-Central Chile during the last 17.9 kyr.

3.2. Location and setting

Puyehue Lake (40°40’S, 72°28’W) is one of several large glacial, moraine-dammed piedmont lakes that constitute the Lake District in South-Central Chile (38-43°S; Campos et al., 1989). It is located at the western foothills of the Cordillera de Los Andes (Fig. 1) at an elevation of 185 m a.s.l. The lake has a maximum length of 23 km, a maximum depth of 123 m and a mean depth of 76.3 m (Campos et al., 1989). It covers 165.4 km² and is characterized by a complex bathymetry, with three sub-basins and a series of small bedrock islands in its centre (Charlet et al., 2008; Fig. 1). The largest sub-basin occupies the western side of the lake (WSB) and is almost completely isolated from the northern and eastern sub-basins by a lake-crossing ridge, which is interpreted as the continuation of an onshore moraine (Bentley, 1997). The deepest sub-basin is located in the eastern side of the lake (ESB), although this part of the lake receives large amounts of sediment through the Golgol and Lican rivers. The northern sub-basin (NSB) is locked between the bathymetric ridge and the delta of Lican River.

Puyehue Lake is oligotrophic and mainly P-limited (Campos et al., 1989). It has a high transparency (mean Secchi depth: 10.7 m) and its high silica concentration (15 mg/l; Campos et al., 1989) is characteristic for lakes located in volcanic environments.

Phytoplankton biomass is maximal in summer, with a pronounced dominance of Cyanobacteria (Campos et al., 1989). Diatoms dominate the phytoplankton in late autumn, winter and early spring, when the N and P levels are high (Campos et al., 1989). The bottom of the lake is oxic year-round and the lake is temperature stratified during the summer, with the depth of the thermocline varying between 15 and 20 m depth (Campos et al., 1989).

The region of Puyehue has been shaped by a complex interaction between Quaternary glaciations, volcanism, tectonics, and seismic activity. The lake is believed to occupy a glacial valley over-deepened by Quaternary glacial advances (Laugenie, 1982) and is dammed to the West by several moraine ridges (Bentley, 1997). Its catchment covers 1510 km² and extends far to the east of the lake. It is surrounded by several active volcanoes (e.g. Puyehue-Cordon de Caulle, Antillanca), which have a strong influence on the inorganic composition of the lake and watershed sediments (Bertrand et al., 2008; Bertrand and Fagel, 2008). The lake catchment is essentially composed of Quaternary volcanic rocks covered by several metres of post-glacial andosols, which frequently overly organic-poor glacial or fluvio-glacial deposits (Bertrand and Fagel, 2008). The main tributaries to the lake are the Golgol River, which drains more than 60 % of the lake watershed and the Lican River, which drains the western part of the Puyehue-Cordon de Caulle volcanic complex (Fig. 1). These two rivers are the main sources of detrital input to the lake. They mainly supply particles to the eastern and northern sub-basins. Of secondary importance are Chanleufu River and Pescadero River (Fig. 1). The lake is also fed from the north-west and south by a series of smaller rivers that contribute relatively little to the detrital supply, because of the small size and relatively flat morphology of their drainage basins (Fig. 1). For this reason, the detrital supply to the WSB is very limited and the particles deposited in the WSB are primarily of autochtonous origin (Bertrand et al., 2005). The outflow of Puyehue Lake (Pilmaiquen River) is located to the west. It cross-cuts several moraine ridges (Laugenie, 1982; Bentley, 1997), merges with Bueno River and flows westward into the Pacific.

The region of Puyehue has a humid temperate climate with Mediterranean influences. It is linked to the global climate via the Southern Westerlies, which, combined with the rough topography of the Andes, are responsible for high precipitation in the area. Around the lake, the annual rainfall averages 2000 mm/yr. It increases with elevation, and reaches up to 5000 mm/yr on top of regional volcanoes (Parada, 1973; Muñoz, 1980). At Aguas Calientes, located in the watershed of Puyehue Lake at ~ 5 km to the south-east of the lake, precipitation varies from 162 mm/month in summer to

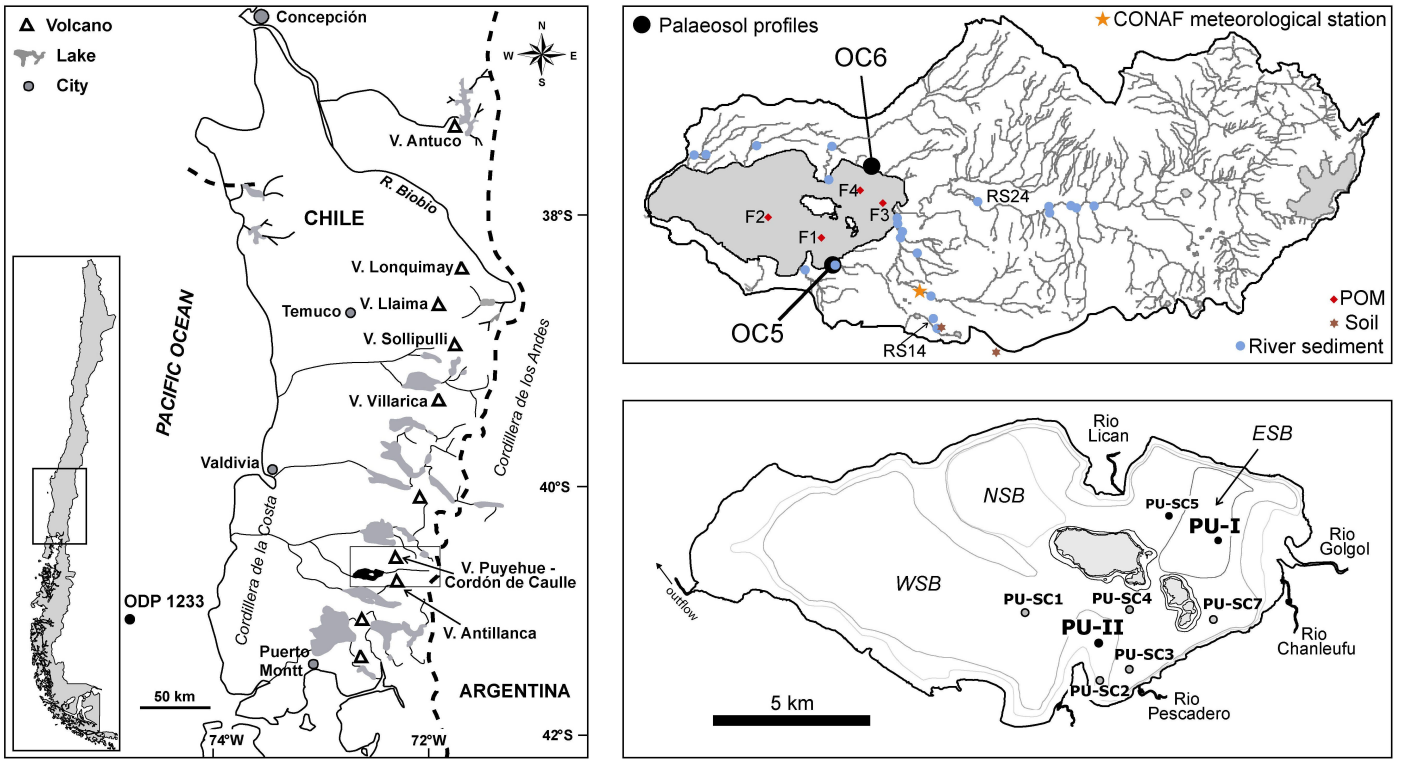
Volcano
Lake
City
Concepción
V. Antuco
R. Biobio
CHILE
38°S
V. Lonquimay
Temuco
V. Llaima
V. Sollipulli
V. Villarica
PACIFIC OCEAN
Cordillera de los Andes
Valdivia
40°S
Cordillera de la Costa
V. Puyehue - Cordón de Caulle
ODP 1233
V. Antillanca
Puerto Montt
50 km
ARGENTINA
74°W
72°W
42°S
N
W
E
S
Palaeosol profiles
CONAF meteorological station
OC6
F4
F2
F3
F1
RS24
OC5
RS14
POM
Soil
River sediment
Rio Lican
ESB
NSB
PU-SC5
PU-I
Rio Golgol
WSB
outflow
PU-SC1
PU-SC4
PU-SC7
PU-II
PU-SC3
PU-SC2
Rio Chanleufu
Rio Pescadero
5 km

Figure 1 *(opposite page):* Location of Puyehue Lake in South-Central Chile. The position of the coring sites (PU-SC1-5, PU-SC7, PU-I and PU-II; see 3.3.2.) is located on the bathymetric map of Campos et al. (1989). WSB, NSB, and ESB refer to the western, northern and eastern sub-basins of the lake, as described by Charlet et al. (2008). The position of river samples RS14 and RS24 is indicated, as these two samples have the highest (15.6) and lowest (9.6) C/N values, respectively.

524 mm/month in winter (Centro de Información Ambiental del Parque Nacional de Puyehue, CONAF, pers. comm.; Fig. 1). Seasonality in rainfall is caused by variations in the intensity and latitudinal position of the Southern Westerly Wind belt, which is presently centered at around 50°S in summer, and moves northward during winter. The mean annual air temperature is 6 to 9°C, with maxima reaching 20°C in January and minima of 2°C in July (Muñoz, 1980). Freezing sometimes occurs at night in winter, but complete ice covering of the lake has never been observed (Thomasson, 1963). Snow cover occurs in the catchment from May to November (Laugenie, 1982). This humid and temperate climate is responsible for the development of a dense temperate rainforest in the major part of the lake catchment (e.g. Moreno and Léon, 2003; Moreno, 2004).

3.3. Materials and methods

3.3.1. Terrestrial and aquatic sediment sources

In order to constrain the terrestrial sources of sedimentary organic matter deposited in Puyehue Lake, we conducted a sampling campaign in the watershed of the lake in January-February 2002. Samples of living vegetation (V), soils (SP), paleosols (OC) and river sediment (RS) were collected at representative locations in the lake watershed.

Vegetation samples (V1 to V6) representing the six most abundant taxa were picked by hand from living plants and air dried in the field. The selection of these taxa was based on an extensive botanical study of the lake watershed (Vargas-Ramirez et al., 2008): *Podocarpus nubigena* (V1), Myrtaceae (V2), *Nothofagus dombeyi* (V3), Compositae (V4), Gramineae (V5) and *Tristerix corymbosus* (V6). Before analysis, the vegetation samples were oven dried at 40ºC for 48h, ground and homogenized using an agate mortar.

River sediment samples (RS) were collected at 21 locations selected in the main rivers flowing into Puyehue Lake (Fig. 1). Samples were collected using a trowel and avoiding coarse particles. The sediment samples were stored in air-tight Whirl-Pak plastic bags and freeze-dried in the lab.

Twelve samples of paleosol were collected from two vertical profiles (outcrops) located at the southern (OC5) and northern (OC6) shores of the lake (Fig. 1). The outcrops are composed of fluvioglacial deposits overlain by several meters of brown silty loams, transformed into andosols by weathering and pedogenetic processes (Bertrand and Fagel, 2008). The brown silty loams are composed of volcanic ashes continuously deposited throughout the Holocene and therefore contain various levels of degraded organic matter.

In addition, we also collected two surface soil samples (SP) in the southern part of the lake watershed, which is covered by the typical temperate rainforest. These samples contain recently degraded organic matter and are therefore expected to be intermediate between the OC and V types. The OC and SP samples were collected using a trowel and stored in air-tight Whirl-Pak plastic bags. They were freeze-dried before final preparation for analysis.

To constrain the aquatic source of sedimentary organic matter in Puyehue Lake, we collected particulate organic matter (POM) at four stations across the lake (Fig. 1). Samples were collected in summer (December) 2004, i.e. when productivity is the highest (Campos et al., 1989), from the surface water in the Western (F2) and Eastern (F3 and F4) sub-basins, as well as on top of the sublacustrine moraine ridge (PU-II site, F1). POM was collected on pre-combusted fibreglass filters (Whatman GF/C) by filtering water samples until saturation. Between 4.8 and 6.2 liters of lake water were filtered for each sample and the filters were air-dried immediately after filtration. Samples were oven-dried at 40ºC for 24 hours before analysis.

3.3.2. Sedimentary organic matter

In order to reconstruct temporal changes in the source and composition of sedimentary organic matter, we sampled an 11.22m long sediment core from the southern part of the lake. The coring site (PU-II: 40º41.843' S, 72º25.341 W, Fig. 1) was selected after a preliminary seismic investigation (see Fig. 2 in Chapter 2 of this thesis; Charlet et al., 2008). It is located on a plateau at a water depth of 48.4 m, and is ideally isolated from the direct influence of underflow currents (De Batist et al., 2008). Coring operations were performed in February 2002 with an Uwitec piston corer operated from an anchored Uwitec platform.

The age model of core PU-II is based on nine radiocarbon dates obtained on bulk sediment and two tephra layers related to historical eruptions (Fig. 4). Details concerning the age-model construction are given in Bertrand et al. (2008) and in Chapter 2.

In spring/summer 2002, the working half of the composite PU-II core was continuously sub-sampled in 1 cm thick slices. Samples were placed in plastic bags and stored at a constant temperature of 4ºC. For the present study, we selected samples every 10 cm from 0 to 750 cm, and every 5 cm below 750 cm. This represents a temporal sampling resolution of 60 - 300 years during the Holocene, and ~100 years during the last deglaciation. Samples were carefully selected avoiding sediment containing macroscopically visible tephra layers. Samples below tephra layers were preferred in order to discard a possible influence of tephras on vegetation and/or plankton, which may alter the sedimentary organic geochemical record. Before analysis samples were freeze-dried, ground and homogenized using an agate mortar.

Finally, in order to test the validity of sedimentary organic matter geochemistry as a source proxy, we sampled surficial (core-top) sediments at eight locations more or less influenced by direct detrital supply (PU-SC1-5, PU-SC7 and PU-I and PU-II; Fig. 1). Samples were taken in the 2 main sub-basins of the lake (ESB and WSB), as well as on the elevated platform located in the southern part of the lake. The samples with prefix PU-SC were collected using a short Uwitec gravity coring device (Bertrand et al., 2005). Core PU-I was taken with an Uwitec piston corer operated from an anchored Uwitec platform. For the present study, we selected the 0-1 cm samples only. These samples were freeze-dried and ground and homogenized using an agate mortar.

In order to assess the relationship between the fraction of terrestrial organic carbon in these core-top sediments, and their potential susceptibility to terrestrial sediment supply, a ‘distance to river and shore index’ was calculated. This distance index was calculated as $D = \log(a) + 0.5 \log(b) + 0.5 \log(c)$, with (a) = distance to the nearest main river, (b) = distance to the nearest shore, and (c) = distance to the nearest secondary river (all distances in m). The main rivers are Rio Golgol and Rio Lican, and the secondary rivers are Rio Pescadero and Rio Chanleufu (Fig. 1). Distances to secondary rivers and shores were given half weighting because of their smaller contribution to the total sediment supply compared to major rivers. We used the logarithms of the distances, in order to account for the generally known exponential decrease of sediment accumulation rate with increasing distance to the source (Schiefer, 2006). Local variations might be explained by differences in basin shape, height of the water column and water circulation patterns.

3.3.3. Sample preparation

Before analysis, the freeze-dried samples from soils (SP), paleosols (OC), and river sediment (RS) were sieved at 106 µm to discard the coarse particles that do not represent the fraction of sediment reaching the coring site. In order to estimate the organic content

of the samples, three grams of sediment for each terrestrial and lake sediment sample was separated for loss-on-ignition (LOI) measurements. LOI was measured after 24h at 105°C (LOI_{105}), after an additional 4h at 550°C (LOI_{550}) and after an additional 2h at 950°C to estimate water content, organic matter content and inorganic carbonate content, respectively (Heiri et al., 2001). Because LOI_{550} is dependent on the sample weight (Heiri et al., 2001), we always used 1g of dry samples (0.98 ± 0.09 g). For the PU-II long core, we used the LOI_{550} data of Bertrand et al. (2008). The LOI_{550} data were used to estimate the optimal sample weight for carbon and nitrogen elemental and isotopic analysis (between 15 and 75 mg for PU-II long core).

3.3.4. Carbon and nitrogen elemental and isotopic analysis

After freeze-drying and either grinding and homogenization in an agate mortar (lake sediments) or sieving at 106 µm (SP, OC, RS), sediment samples were packed in tin capsules, treated with 1N sulphurous acid to remove eventual carbonates (Verardo et al., 1990) and analyzed at the UCDavis Stable Isotope Facility (USA). Total Organic Carbon (TOC), Total Organic Nitrogen (TON) and stable isotope ratios of sedimentary carbon and nitrogen were measured by continuous flow isotope ratio mass spectrometry (CF-IRMS; 20-20 SERCON mass spectrometer) after sample combustion to CO_2 and N_2 at 1000°C in an on-line elemental analyzer (PDZEuropa ANCA-GSL). Before introduction to the IRMS the gases were separated on a SUPELCO Carbosieve G column. Sample isotope ratios were compared to those of pure cylinder gases injected directly into the IRMS before and after the sample peaks and provisional $d^{15}N$ (AIR) and $d^{13}C$ (PDB) values were calculated. Provisional isotope values were adjusted to bring the mean values of working standard samples distributed at intervals in each analytical run to the correct values of the working standards. The working standards are a mixture of ammonium sulfate and sucrose with $d^{15}N$ vs. Air = 1.33 ‰ and $d^{13}C$ vs. PDB = -24.44 ‰. These standards are periodically calibrated against international isotope standards (IAEA N1, N3; IAEA CH7, NBS22). Total C and N are calculated from the integrated total beam energy of the sample in the mass spectrometer compared to a calibration curve derived from standard samples of known C and N content. The precision, calculated by replicate analysis of the internal standard (mixture of ammonium sulfate and sucrose), is 0.09 ‰ for $d^{13}C$ and 0.14 ‰ for $d^{15}N$.

For the POM (F1 to F4) and living vegetation (V1 to V6) samples, TOC, TON and $d^{13}C$ were measured on a FISONS NA 1500 NC elemental analyzer coupled with an Optima mass spectrometer (VG IR-MS) at the Oceanology Laboratory, University of Liège, Belgium. For $\delta^{13}C$ routine measurements are precise within 0.3 ‰. Vegetation

samples were measured twice (low and high mass) to optimize the signal for C and N, respectively.

Isotopic measurements are expressed relative to VPDB ($\delta^{13}C$) and AIR ($\delta^{15}N$) standards. For C/N ratios, we always use the atomic C/N values (C/N weight ratio multiplied by 1.167), as opposed to weight ratios, because they reflect the biogeochemical stoichiometry (Meyers and Teranes, 2001). Carbonate has never been detected in our samples. Since our samples are characterized by relatively high TOC, the residual inorganic nitrogen is negligible, and the measured C/N ratios accurately reflect the organic matter sources (Meyers and Teranes, 2001).

3.3.5. Calculation of the fractions of terrestrial and aquatic organic carbon

In order to estimate the proportion of aquatic and terrestrially-derived organic carbon in the sediments of Puyehue Lake, we use a simple mixing equation based on the proportions of C and N measured in both aquatic (A) and terrestrial (T) end-members.
The mixing model is based on the following equation (Perdue & Koprivnjak, 2007):

$$\frac{N}{C} = f_T \left(\frac{N}{C}\right)_T + f_A \left(\frac{N}{C}\right)_A \quad (1)$$

where f_T and f_A are the fractions of terrestrial and aquatic organic carbon, respectively. The N and the C in the lake sediment samples are both derived from the two end members, so the N/C of the lake sediment samples can be rewritten as equation (2):

$$\frac{N}{C} = \frac{(N_T + N_A)}{(C_T + C_A)} \quad (2)$$

Substituting $N_T=(N/C)_T C_T$ and $N_A=(N/C)_A C_A$ in equation (2), results in:

$$\frac{N}{C} = \frac{((N/C)_T C_T + (N/C)_A C_A)}{(C_T + C_A)} \quad (3)$$

Which can be rewritten into:

$$\frac{N}{C} = \left(\frac{C_T}{C_T + C_A}\right)\left(\frac{N}{C}\right)_T + \left(\frac{C_A}{C_T + C_A}\right)\left(\frac{N}{C}\right)_A \quad (4)$$

With the assumption that $f_T + f_A = 1$, we can calculate the fraction of terrestrial organic carbon as:

$$f_T = \frac{(N/C) - (N/C)_A}{(N/C)_T - (N/C)_A} \quad (5)$$

Previously, many authors used the C/N ratios of these end-members to calculate the terrestrial fraction of organic material, assuming that this also represents the terrestrial fraction of organic carbon. However, Perdue and Koprivnjak (2007) demonstrated that mixing equations based on C/N data always underestimate the terrestrial fraction of organic carbon, because terrestrial organic matter is relatively depleted in nitrogen, and these C/N based mixing equations calculate the fraction of terrestrial vs. aquatic organic nitrogen (as $f_T = N_T/(N_T+N_A)$ and $f_A = N_A/(N_T+N_A)$) instead of carbon. This results in curved instead of linear C/N mixing lines (i.e. the predicted C/N as a function of f_T) (Perdue & Koprivnjak, 2007).

Apart from the terrestrial organic matter as a fraction (f_T) of total organic matter (TOC), the concentration of aquatic organic carbon (aqOC) was also calculated (in % of sedimentary dry weight), by multiplying the TOC values with f_A, or thus: aqOC = TOC * (1-f_T). A biogenic silica index, (bioSi/aqOC) was calculated as the ratio of the biogenic silica content (bioSi) from Bertrand et al. (2008) and the aquatic organic carbon content (aqOC) of the samples. Although this (unit-less) index does not represent the diatoms as a 'true' fraction of the total aquatic community, it may give useful indications of their relative importance in past aquatic productivity changes.

3.4. Results

3.4.1. Particulate organic matter

The four lacustrine POM samples display C/N atomic ratios varying between 7.7 and 9.6 (8.5 ± 0.8) (average ± 1 s; Table 2, Fig. 2). The highest value is observed for sample F3, which is located near the mouth of the Golgol River, the main tributary and main source of detrital particles to the lake (Fig. 1). The lowest value is associated with sample F2, collected in the western sub-basin, and therefore protected from the direct influence of any river input. The $d^{13}C$ values average -28.0 ‰ (± 2.0). The most negative value (-29.9 ‰) is associated with sample F3. The $d^{15}N$ values vary between 0.7 and 3.6 ‰ (2.3 ± 1.5 ‰).

3.4.2. Living vegetation

The C/N atomic ratios of the six analyzed living vegetation samples are high and highly variable (55.1 ± 21.8) (Fig. 2). The carbon isotopic values are less variable and they average -29.7 ‰ (± 1.5). Interestingly, sample V5 (Gramineae) has the lowest atomic C/N ratio (28.1) and the least negative $d^{13}C$ (-27.5 ‰). $d^{15}N$ has not been measured.

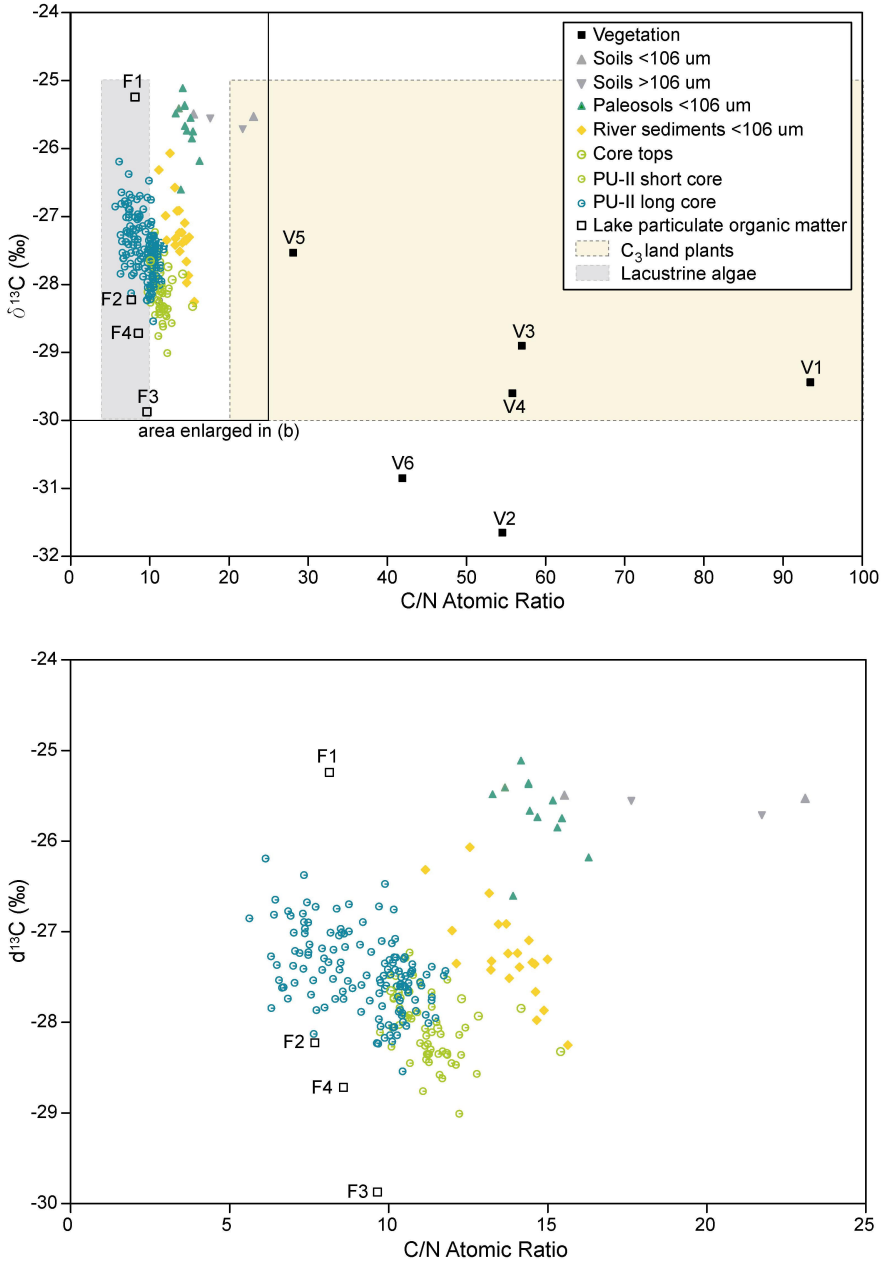

Figure 2: C/N vs. $d^{13}C$ biplots of the aquatic, terrestrial and sediment samples. The vegetation samples represent the most common regional species (1: *Podocarpus nubigena*; 2: Myrtaceae; 3: *Nothofagus dombeyi*; 4: Compositae; 5: Gramineae; 6: *Tristerix corymbosus*). For PU-II long core, the data from 971 to 935 cm were not included because of their association with a major turbidite. The ranges of C/N and $d^{13}C$ values for C3 plants and lacustrine algae, indicated in grey and yellow respectively, are generalised values from Meyers & Teranes (2001).

These values are in the range of values expected for terrestrial plants, and are in good agreement with the data obtained by Sepúlveda (2005) on living vegetation samples from Northern Patagonia (C/N: 35.2 ± 13.6; $d^{13}C$: -30.3 ‰ ± 2.3). The wide range of C/N values found in fresh vegetation represents the variety of species analyzed and reflects the natural variation in biochemical composition of land plants (Meyers, 2003).

Table 2: Average and standard deviation (± 1s) of the bulk organic geochemical data obtained on Puyehue Lake and watershed sediment samples. The values obtained on the lake particulate organic matter (POM) and living vegetation are also indicated. n refers to the number of analyzed samples. [a] not measured on F3, [b] also includes PU-I-P5 and PU-II-P5, [c] from Bertrand et al. (2005).

Sample type	n	TOC (%)	C/N	N/C	$d^{13}C$ (‰)	$d^{15}N$ (‰)
Living vegetation (V1-6)	6	46.0 ± 3.6	55.1 ± 21.8	0.021 ± 0.008	-29.7 ± 1.5	--
Particulate organic matter (F1-4)	4	28.5 ± 7.6	8.5 ± 0.8	0.118 ± 0.011	-28.0 ± 2.0	2.3 ± 1.5[a]
Paleosols (OC5-6)	12	4.0 ± 1.6	14.6 ± 0.8	0.069 ± 0.004	-25.7 ± 0.4	6.8 ± 1.5
Present-day soils (SP2-3)	2	3.3 ± 3.6	19.3 ± 5.4	0.054 ± 0.015	-25.5 ± 0.0	2.4 ± 4.5
River sediment (RS14-34)	21	3.4 ± 2.3	13.7 ± 1.1	0.073 ± 0.006	-27.2 ± 0.5	2.0 ± 1.6
Surface sediment samples (SC1-7)[b]	8	3.2 ± 0.4	12.4 ± 1.7	0.082 ± 0.011	-28.0 ± 0.3	0.7 ± 0.4
PU-II short core (0-53 cm)[c]	53	2.5 ± 0.6	11.1 ± 0.7	0.091 ± 0.006	-28.1 ± 0.4	--
PU-II long core (0-1122 cm)	146	1.2 ± 0.7	9.0 ± 1.8	0.117 ± 0.036	-27.4 ± 0.5	-0.3 ± 0.6

3.4.3. Watershed sediment samples

The C/N atomic ratio of the samples collected in the two paleosol profiles (OC) shows an average of 14.6 (± 0.8). The two profiles are not significantly different from each other. The only difference is the trend of C/N from the bottom to the top of the profiles, which is increasing in OC5 and decreasing in OC6 (Fig. 3). Regarding the $d^{13}C$, the 2 outcrops are not significantly different either, and the values average -25.7 ± 0.4 ‰. Both outcrops show a slightly decreasing upward trend. The $d^{15}N$ values are highly variable and differ significantly between OC5 (7.5 ± 0.7 ‰) and OC6 (6.0 ± 1.7 ‰).

The two soil samples (SP) show C/N atomic ratios of 15.5 and 23.1, and the isotopic values are -25.5 ± 0.0 ‰ and 2.4 ± 4.5 ‰ for $d^{13}C$ and $d^{15}N$, respectively. The coarser than 106 um fraction has been analyzed separately and shows slightly different C/N ratios (17.6 and 21.8). The $d^{13}C$ values are not significantly different. Our C/N data are slightly lower than the results obtained by Godoy et al. (2001) on soil samples from the Puyehue National Park (atomic C/N: 24.5-25.5).

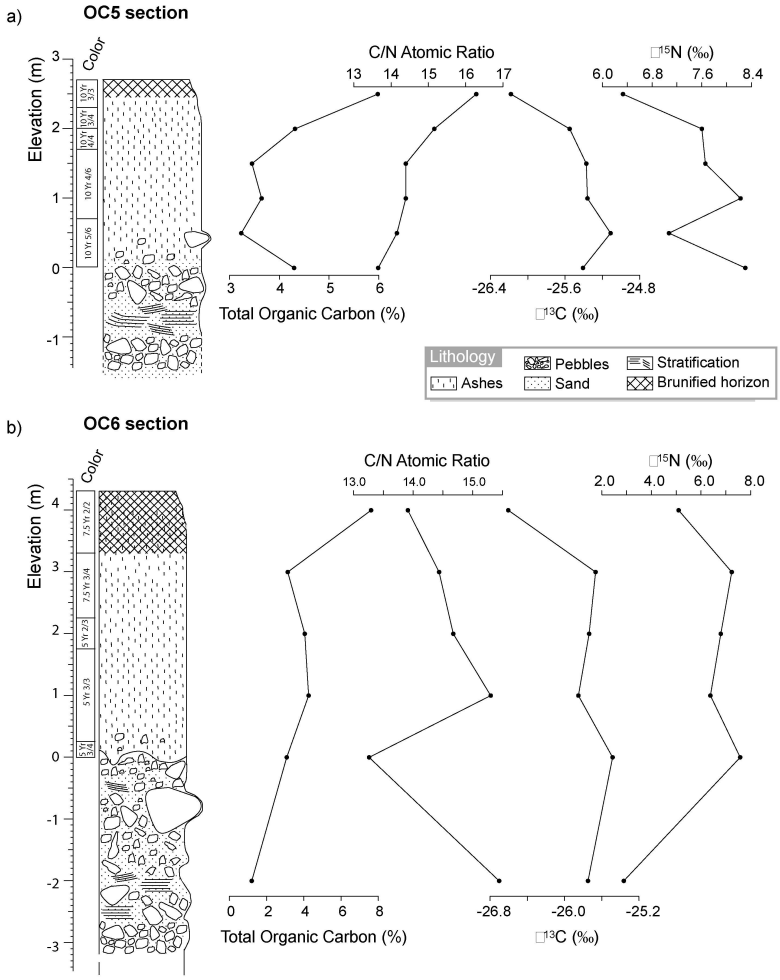

Figure 3: Bulk organic geochemical data (TOC, atomic C/N, $d^{13}C$, $d^{15}N$) obtained on two paleosol outcrops occurring at the southern (OC5) and northern (OC6) shores of Puyehue Lake. For location, see Fig. 1. The profiles are essentially composed of volcanic ashes deposited continuously during the Holocene (Bertrand and Fagel, 2008). The base of the outcrops (< 0 m) is believed to date from the last deglaciation.

The C/N atomic ratio of the river sediment samples (RS14 to 34) averages 13.7 (± 1.1), with the highest value for RS14 (15.6) and the lowest for RS24 (9.6). These values are not clustered by river, nor correlated with the distance to/from the river mouth. It seems, however, that samples collected in the southern part of the watershed have slightly higher C/N ratios. The stable carbon isotopes display values ranging from -26.1 ‰ to -28.3 ‰ (-27.2 ± 0.5 ‰). Samples with higher C/N ratios tend to have a more negative $d^{13}C$ (r^2 = 0.53). The $d^{15}N$ values average 2.0 (± 1.6) ‰ and show no correlation with either C/N or $d^{13}C$.

3.4.4. Surface lake sediment samples

The TOC of the surface lake sediment samples varies from 2.70 to 3.68 %. The average C/N atomic ratio is 12.4 (± 1.7), with extreme values of 15.4 for PU-SC3 (southern shore) and 10.1 for PU-SC1 (western sub-basin) (Fig. 1). The surface sediment samples are characterized by a rather constant $d^{13}C$ of -28.0 ± 0.3 ‰, and by $d^{15}N$ of 0.7 ± 0.4 ‰.

3.4.5. Downcore record

The PU-II sediment core covers the last 17.9 kyr and the radiocarbon dates are given in Table 1. Details concerning the age-model construction are given in Bertrand et al. (2008). The radiocarbon age-model is consistent with accumulation rates calculated from ^{210}Pb and ^{137}Cs concentrations (Arnaud et al., 2006), as well as with the varve-counting data of Boës and Fagel (2008), and the tephrochronological model of Bertrand et al. (in press).

In general, the sediments in the core are composed of finely laminated to homogeneous brown silty particles (Bertrand et al., 2008) and contain seventy-eight tephra layers, generally less than 1 cm thick and well distributed throughout the core (Bertrand et al., in press) (Fig. 4). Grain-size data have shown that the sediment of PU-II core contains 3 turbidites, at 379.5-381, 396.5-397.25 and 956-971 cm (Bertrand et al., 2008).

The downcore record of TOC, C/N atomic ratios and $d^{13}C$ is illustrated in Fig. 4. The $d^{15}N$ data are not represented because they show no variation with depth (average: -0.3 ± 0.6 ‰). The TOC varies from 0.3 to 3.0 % (average[2]: 1.2 ± 0.7 %), with the lowest values being located under 830 cm (average: 0.5 ± 0.1 %). The overall C/N trend is similar to that of TOC, with the lowest values occurring under 830 cm. The only exception to this trend are the high (10.9 to 12.9) C/N atomic ratios within the turbidite

[2] Averages are calculated with exclusion of the values registered in the turbidite layer of 956-971 cm depth.

layer at 956-971 cm. The presence of this turbidite also seems to affect the overlying values (between 956 to 935 cm), which are all very low (as low as 2.9) and appear as "outliers" compared to the general trend. Concerning the $d^{13}C$, the values vary between -25.0 and -28.5 ‰ (average: -27.4 ± 0.5 ‰), with the highest values occurring in the lower part of the core (Fig. 4), except for a more negative excursion between 870 and 1000 cm.

Table 1: AMS radiocarbon dates obtained on bulk sediment samples of PU-II long core. Calendar ages have been calculated using the Intcal98 calibration curve. For more details regarding the radiocarbon dates and age-model, see Bertrand et al. (2008).

Depth (mblf)	Laboratory n°	^{14}C age ± 1s (yr BP)	2s error range calibrated ages (OxCal) (cal yr. BP)	Weighted Average (BCal) (cal yr. BP)
120.5 cm	Poz-5922	2570 ± 35	2490 - 2770 (95.4 %)	2655
156.5 cm	Poz-1406	2590 ± 40	2490 - 2790 (95.4 %)	2681
306.5 cm	Poz-7660	4110 ± 40	4510 - 4830 (92.7 %)	4648
400.5 cm	Poz-2201	5300 ± 40	5940 - 6200 (95.4 %)	6074
463.75 cm	Poz-5923	5760 ± 40	6440 - 6670 (95.4 %)	6560
627.75 cm	Poz-5925	7450 ± 50	8160 - 8390 (93.9 %)	8262
762 cm	Poz-1405	10,010 ± 60	11,200 – 11,750 (91.0 %)	11,494
908 cm	Poz-7661	11,440 ± 80	13,100 – 13,850 (95.4 %)	13,407
1012 cm	Poz-2215	13,410 ± 100	15,250 – 16,750 (95.4 %)	16,063

The calculated fraction of terrestrial organic matter (f_T) and the aquatic organic carbon content (aqOC), as well as the biogenic silica index (bioSi/aqOC) are shown in Fig. 7. The f_T values range between 22.0 % and 67.4 %, (average: 34.5 ± 23.2 %); they are lowest between 1122 and 830 cm (c. 17.9-12.4 cal. kyr BP; average 5.6 ± 5.4 %) and increase rapidly to an average of 49.6 ± 11.7 % between 830 and 0 cm depth. Two local minima are observed at 481.5 (c. 6740 cal. yr. BP) and 320.5 cm depth (c. 4890 cal. yr. BP). The aqOC ranges between 0.3 and 1.2 % (average: 0.7 ± 0.2 %), and undergoes a more gradual increase towards maximum values at 670.5 (c. 9150 cal. yr. BP) and 431.5 cm depth (c. 6130 cal. yr. BP). The biogenic silica index ranges between 5 and 45, and

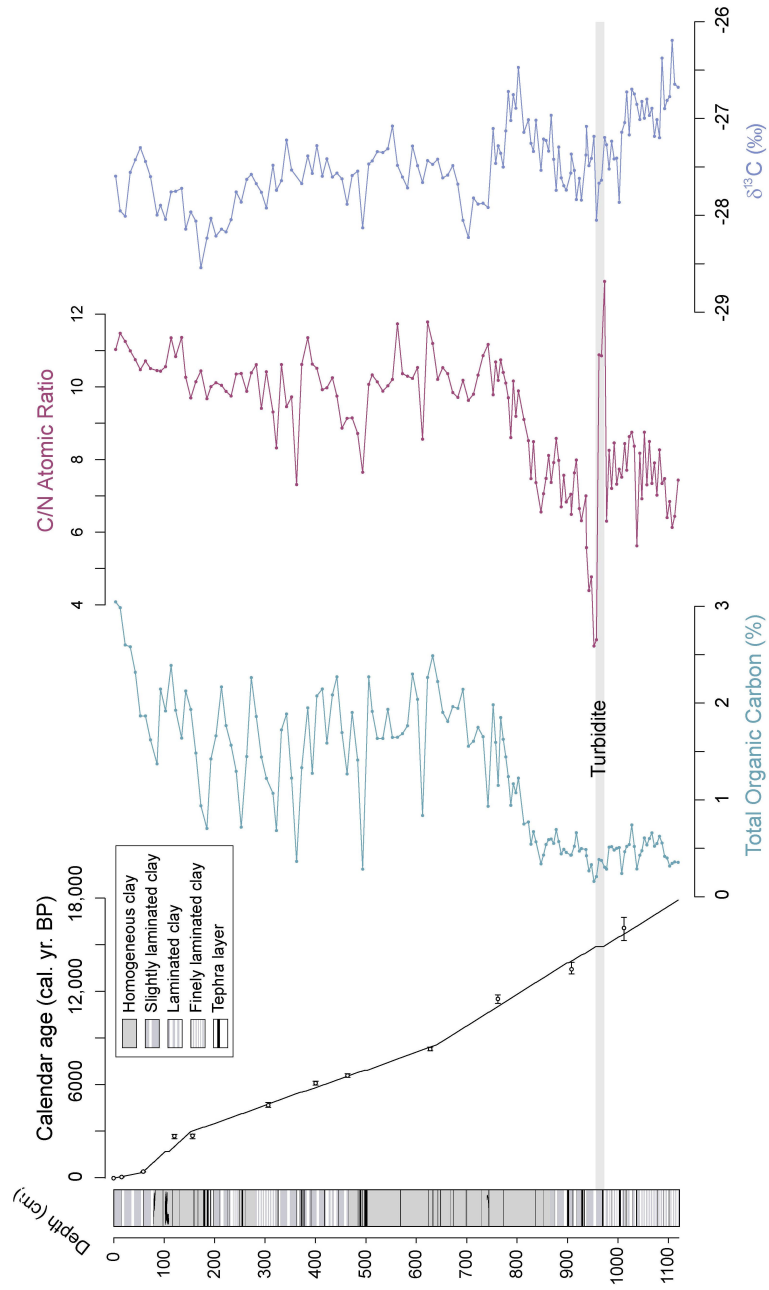

Figure 4: Bulk organic geochemical data obtained on sediment core PU-II. Note the presence of a turbidite at 956-971 cm. The lithology and age-model are represented according to Bertrand et al. (2008). The AMS radiocarbon results are given in Table 1.

mainly follows the patterns observed in the 'detrital vs. biogenic index'(see Bertrand et al., 2008; and Fig. 7). It is high at the bottom of the core, and decreases steadily towards c. 850 cm (~12.8 cal. ka BP), after which it rapidly increases to a maximum at 780 cm (c. 11.4 cal. ka BP). After a gradual decline values remain low in the top most part of the core, with the exception of a sharp maximum at the top (20 cm depth; c. 80 cal. yr. BP; Fig. 7).

3.5. Discussion

3.5.1. Sources of sedimentary organic matter

The interpretation of organic geochemical records of lake sediments requires an accurate understanding of the sources of organic matter. In lake systems, organic matter is generally a mixture of aquatic and terrestrial end-members in varying proportions (Meyers and Teranes 2001). These two groups can generally be distinguished by their C/N ratio because lacustrine algae are characterized by C/N values ranging from 6 to 12, while vascular land plants create organic matter that usually has C/N ratios higher than 20 (Meyers and Teranes, 2001). Generally, stable carbon and nitrogen isotopes can also help identify the sources of sedimentary organic matter (Lazerte, 1983). However, lake-derived organic matter that is produced by phytoplankton (C3 algae) using dissolved CO_2 is usually in equilibrium with the atmosphere and is therefore isotopically indistinguishable from organic matter produced by C3 plants in the surrounding watershed (Meyers and Teranes, 2001; Sifeddine et al., 2004). Therefore, if the catchment vegetation mainly consists of C3 plants, carbon and nitrogen isotopes are of limited use to quantify organic matter sources in lake systems, but they can provide important information regarding the productivity rates and sources of nutrients.

3.5.1.1. Aquatic end-member

The stoichiometry of lake plankton is generally different from the Redfield ratio, as defined for marine plankton. The C/N ratio of lake plankton is generally around 10, but varies with nutrient availability and with species-specific characteristics (Sterner and Elser, 2002). One of the problems that arises in the determination of lake plankton stoichiometry is that samples, generally collected by filtration of lake water, may contain terrestrial particles. Although several studies provide evidence that the terrestrial contamination is negligible (Hecky et al., 1993), others attempt to correct for detrital contribution by regression analysis, assuming a constant element/chlorophyll ratio for

lake organic matter. This correction is very approximate because it has been shown that the element/chlorophyll ratio varies largely with nutrient stress and light limitation (Healy and Hendzel, 1980). Therefore, correcting for detrital supply is generally not recommended, except for samples collected in small and shallow lakes, where detrital material is easily resuspended (Hecky et al., 1993). It has not been applied here.

The carbon stable isotopic values of lake plankton generally average -27‰ but vary significantly among taxonomic groups (Vuorio et al., 2006), with low values for chrysophytes and diatoms (-34.4 to -26.6 ‰) and high values for cyanobacteria (-32.4 ‰ to -5.9 ‰), which dominate the plankton of Puyehue Lake (Campos et al., 1989). Similarly, the $d^{15}N$ values of lake plankton range from -2 to 13 ‰, with high values for chrysophytes, dinophytes and diatoms, and low values for cyanobacteria (Vuorio et al., 2006). In addition to inter-specific variability, carbon stable isotopes also vary with lake productivity. This relationship is based on the observation that, during photosynthesis, phytoplankton preferentially consume dissolved $^{12}CO_2$, which results in the production of ^{13}C-poor organic matter and removal of ^{12}C from surface water dissolved inorganic carbon (DIC). As the supplies of DIC become depleted, the $d^{13}C$ values of the remaining inorganic carbon increase and produce a subsequent increase in the $d^{13}C$ values of newly produced organic matter (Meyers and Teranes, 2001). Therefore, increased productivity yields an increase in $d^{13}C$ of organic matter that is produced in the lake and is available for sedimentation. $d^{15}N$ on the other hand, is essentially used to identify past changes in availability of nitrogen to aquatic producers (Talbot, 2001).

The four POM samples from Puyehue Lake were collected in summer, i.e. when precipitation is minimal. We therefore consider that the detrital influence is small and that our samples mostly represent the aquatic source of organic matter. Moreover, the samples were collected in the upper meter of the water column, which is only affected by virtually particle-free overflow currents.

The C/N atomic ratios of the 4 POM samples decrease with increasing distance to major river mouths. Samples collected in the eastern part of the lake probably contain a small fraction of terrestrial organic matter, as evidenced by their higher C/N ratios. The best example is sample F3 (C/N: 9.6) that is directly influenced by the supply of terrestrial particles from the Golgol River. This interpretation is supported by the low TOC value of this sample (19.6 %) compared to the other POM samples (Table 2). The sample collected in the western side of the lake (F2) is protected from any direct river input of terrestrial organic carbon, and is therefore used to determine the aquatic end-member (C/N: 7.7). This value is close to the average C/N of the POM samples (8.5 ± 0.8) but better represents the pure autochtonous organism fraction. This relatively high value

is in agreement with a low to moderate deficiency of Puyehue Lake in nitrogen, especially in summer when the productivity is high (Healey and Hendzel, 1980; Campos et al., 1989).

The $d^{13}C$ and $d^{15}N$ values average -28.0 ‰ and 2.3 ‰, respectively (Table 2), which is in agreement with the values observed for diatoms, and to a lesser extent, cyanobacteria in Finnish lakes (Vuorio et al., 2006). Interestingly, the most negative $d^{13}C$ value (-29.9 ‰) is associated to sample F3, which presumably contains a significant fraction of terrestrial organic matter. This might indicate that terrestrial carbon has low $d^{13}C$ values compared to the lake plankton.

3.5.1.2. Terrestrial end-member

Terrestrial organic matter originates from organisms living in the lake watershed. Before reaching lake systems, it generally gets exposed to various processes (e.g. degradation and remineralization by incorporation into soils, transportation by rivers etc.) that alter its geochemical signature. In the literature, geochemical data obtained on living vegetation, soil, and river sediment samples have inconsistently been used to characterize the terrestrial end-member of sedimentary organic carbon (e.g. Colman et al., 1996; Baier et al., 2004; Sepúlveda, 2005), reflecting the difficulty of assigning a single geochemical value to the terrestrial end-member. Although Kendall et al. (2001) recognize that senescent leaves probably better represent the terrestrial end-member than fresh leaves, very few authors have looked at the geochemical transformations that occur during transport of organic matter from terrestrial environments to lake systems. In order to select the best terrestrial end-member for the sedimentary organic matter of Puyehue Lake, the geochemical composition of the possible sources of terrestrial sedimentary organic matter has been analyzed and is described below.

a. Living vegetation

Terrestrial vegetation is characterized by C-rich, cellulose-rich and protein-poor structural material, resulting in typically high C/N ratios, with reported averages of 36 ± 23 (Elser et al., 2000) or 43 (McGroddy et al., 2004) for foliage and 67 for litter (McGroddy et al., 2004). Values as low as 7.5 and as high as 225 have been documented (Sterner and Elser, 2002). Within a single large plant, leaves, stems and roots have highly contrasting elemental composition, with leaves containing more nitrogen than any other plant material (Sterner and Elser, 2002). Elemental variations are also linked to many other variables, including growth conditions (nutrients, light, temperature, etc.), biogeography (latitude), and phylogenetic affiliation (Sterner and

Elser, 2002). Some authors argue that the stoichiometry of terrestrial plants can be grouped by biomes (McGroddy et al., 2004). For temperate broadleaves, for example, values of 35 ± 4 for foliage and 58 ± 4 for litter are to be expected (McGroddy et al., 2004). Therefore, a single average C/N ratio does not accurately represent the natural vegetation of a complete watershed.

The living vegetation samples collected in the watershed of Puyehue Lake show typical C/N values of 55.1 ± 21.8, with large species-specific differences (Fig. 2). Although some of the samples contained stems, most of our samples are composed of leaves, as they represent the major fraction of organic matter reaching the lake.

The $d^{13}C$ of terrestrial vegetation is more constant than its C/N ratio, despite potential differences caused by the growing stage of plants (i.e. 'juvenile effect'; Francey & Farquhar, 1982) and moisture stress in plants (Buhay et al., 2008). It generally averages -28 ‰, with extreme values of -25 and -29 ‰ for C3 plants (O'Leary, 1988) or -23 to -31 ‰ (Meyers and Teranes, 2001). This relative constancy is due to the continuous equilibrium exchange reactions that occur between vegetation and atmospheric CO_2. Similarly, $d^{15}N$ of terrestrial vegetation generally varies between 2 and -6 ‰ (Fry, 1991).

The carbon isotopic composition of the six terrestrial taxa analyzed in the watershed of Puyehue Lake ($d^{13}C$: -29.7 ± 1.5 ‰; Fig. 2) agrees with values generally accepted for terrestrial vegetation, although on the low side. Our isotopic data are in perfect agreement with data obtained on fresh vegetation samples from Northern Patagonia (-30.3 ± 2.3 ‰) by Sepúlveda (2005).

b. Organic matter in soils and paleosols

Organic matter in soils originates from terrestrial organisms living at the surface of soil profiles. It is in a constant state of decomposition (Post et al., 1985). The elemental and isotopic geochemical composition of soil organic matter consequently reflects the types of plant that they host, minus the effect of biological degradation (Kendall et al., 2001). Even after burial of the paleosol soil organic matter (SOM) frequently decomposes further, resulting in significant variations of its geochemical composition (Wynn, 2007). C/N ratios typically decrease with depth (e.g. Boström et al., 2007; Nierop et al., 2007) due to the microbial immobilization of nitrogenous material accompanied by the remineralization of carbon (Meyers and Ishiwatari, 1993). Therefore, litter has a higher C/N ratio than the humus derived from it, which has in turn a higher C/N ratio than the organic matter incorporated in soil profiles (Post et al., 1985).

The $d^{13}C$ of SOM commonly increases with depth by 1 to 6 ‰ relative to the isotopic composition of the original biomass (Boström et al., 2007; Wynn, 2007). The mechanisms behind this process are still unclear but involve preferential decomposition of certain components, variable mobility of sorption of dissolved organic carbon with variable isotopic values, kinetic discrimination against ^{13}C during respiration and microbes as precursors of stable organic matter (Boström et al., 2007). The $d^{15}N$ of soil organic matter similarly increases up to 10‰ with depth (Nadelhoffer and Fry, 1988). Most of these changes generally occur in the upper cm of soil profiles, resulting in a strong decrease of C/N ratios and increase in $d^{13}C$ and $d^{15}N$ values in the first ~20 cm and stabilisation of these values deeper in the profiles (Boström et al., 2007; Nierop et al., 2007).

In the two soil samples analyzed in the watershed of Puyehue Lake, the C/N of SOM (19.3) is significantly lower than for living plants (55.1 ± 21.8). Similarly, we observe a significant increase in $d^{13}C$ from -29.7 ‰ for terrestrial plants (V) to -25.6 ‰ for soil organic matter (SP) (+ 4.1 ‰; Table 2). Compared to the soil samples (SP), the upper paleosol samples (OC) show a significant decrease in C/N (from 19.3 to 14.6) but no significant change in $d^{13}C$ (from -25.5 to -25.7 ± 0.4 ‰; Figs. 3, 4, Table 2). These relatively high C/N values are typical for soils developed in humid and cold areas (Post et al., 1985, Brady, 1990).

In the paleosol profile OC5, we observe a significant downward decrease in C/N, and a slight increase in $d^{13}C$ and $d^{15}N$ (Fig. 3). The downward changes are less clear in profile OC6 (Fig. 3). We observe generally constant C/N, $d^{13}C$ and $d^{15}N$ values, except for the uppermost sample. In both profiles, the downward changes are lower than expected, providing evidence that most of the geochemical changes occur during early soil burial. The points representing the OC5 and OC6 samples are clearly grouped in the $d^{13}C$ versus C/N diagram (Fig. 2), and are therefore easy to distinguish from other types of organic matter. The only difference compared to the present-day soils is the decrease in C/N (Fig. 2). Compared to the living terrestrial vegetation, there is a clear decrease in both C/N and $d^{13}C$ (Fig. 2).

c. River sediments

Although the organic matter transported by rivers is primarily of terrestrial origin (Prahl et al., 1994), river plankton and macroorganisms can also contribute significantly to the total budget (Kendall et al., 2001; Wissel et al., 2005). The terrestrial organic matter transported by rivers is a mixture of relatively fresh organic matter from local vegetation and organic matter previously incorporated in soils and

paleosols, with their typical C/N and $d^{13}C$ values (Fig. 2, Table 2). The C/N values of river plankton and microorganisms are generally lower than 10 (Rostad et al., 1997; Kendall et al., 2001). Therefore, the C/N composition of river POM and river sedimentary OM is generally between 8 and 15, depending on the relative contribution of the autochtonous (river) and terrestrial sources, respectively (Kendall et al., 2001). The difference in $d^{13}C$ between terrestrial and aquatic (river) organic matter is generally not significant enough to discriminate between the two sources of river organic matter (Kendall et al., 2001).

Our data show that the C/N values of the river sediment samples are slightly lower than for the soils and paleosols (13.7 ± 1.1; Fig. 2). This is probably due to the combined incorporation of (1) fresh vegetation, (2) degraded organic matter from soils and paleosols and (3) river plankton. The low C/N ratios suggest a low contribution of fresh terrestrial organic matter. In addition, the influence of river plankton on the C/N data seems particularly important in Golgol River, where the 3 lowest C/N values have been measured. This is in agreement with the relatively large size of this river, where the aquatic productivity tends to contribute significantly to the total organic carbon content (Vannote et al., 1980). If we assume that the river plankton has $d^{13}C$ values relatively similar to the present-day vegetation (-29.7 ‰), the $d^{13}C$ values of the river sediment samples (-27.2 ± 0.5 ‰) are also indicative of a mixture between river plankton and soils and paleosols (-25.5 ± 0.0 ‰ and -25.7 ± 0.4 ‰, respectively).

3.5.1.3. Selection of geochemical values for the aquatic and terrestrial end-members

The data obtained on the watershed samples show a constant decrease of the C/N ratio during degradation of terrestrial organic matter by incorporation into soils and transport to Puyehue Lake (Fig. 2; Table 2). Although the river sediments represent most of the material transported from the catchment to the lake, the geochemical values of these samples are also affected by aquatic organic matter produced within the rivers, and can therefore not be used to characterize the pure terrestrial end-member. Because the contribution of fresh vegetation to the organic matter contained in river sediments seems relatively small, we argue that the degraded organic matter contained in paleosols best represent the terrestrial end-member. The C/N value used to define the terrestrial end-member is therefore 14.6 ± 0.8. Although the $d^{13}C$ values of the different sources of organic matter are not very distinct, we use the $d^{13}C$ of the paleosols (-25.7 ± 0.4 ‰) to

characterize the terrestrial end-member. The $d^{15}N$ values of the various sources of organic matter are too similar to define end-members and use them in mixing equations.

For the aquatic end-member, we use the geochemical values of the sample of lake particulate organic matter the least influenced by terrestrial particles (F2, C/N: 7.7 and $d^{13}C$: -28.2 ‰).

During the selection of the terrestrial and aquatic end-members we have shown that living vegetation samples cannot be used to define the geochemical signature of the terrestrial end-member. Studies that do so (e.g. Colman et al., 1996; Sepúlveda, 2005) don't take into account the evolution of the geochemical properties of the organic matter during incorporation into soils and transport by rivers. These papers therefore overestimate the contribution of terrestrial organic matter to sedimentary environments.

3.5.2. Mixing equation

In the previous paragraph, we demonstrated that C/N ratios can be used to distinguish between the aquatic and terrestrial sources of organic matter. These end-members can then be used in a mixing equation to estimate the relative contribution of each source of organic matter to lake sediments. Although Fig. 2 shows that the $d^{13}C$ data of Puyehue Lake sediments roughly occur between the terrestrial and aquatic $d^{13}C$ values, the difference in $d^{13}C$ between the two end-members is too small to allow a precise quantification. Moreover, in lake systems, the $d^{13}C$ signature of sedimentary organic matter is significantly driven by changes in productivity, altering the source signal.

Here, we use the N/C values of the aquatic and terrestrial end-members in a mixing equation to estimate the proportion of terrestrially-derived organic carbon in the sediments of Puyehue Lake. The use of such equations has recently been reviewed by Perdue and Koprivnjak (2007), who demonstrated that it is better to use N/C ratios than C/N in the mixing equation (see 3.3.5.). Besides for mathematical reasons (see 3.3.5.; Perdue & Koprivnjak, 2007), the use of N/C ratios also has the advantage of providing similar ranges of variation for both the terrestrial (0.021 ± 0.008) and aquatic (0.118 ± 0.011) end-members and, as such, simplifying graphical representations (Fig. 5). This equation can be applied to any sample of sedimentary organic matter from Puyehue Lake, by using 0.130 for the aquatic end-member ($(N/C)_A$) and 0.069 for the terrestrial end-member ($(N/C)_T$). We plotted the C/N ratios in Figs. 2 and 3 in order to allow for intercomparison with other studies, as the C/N based mixing equations have been widely used in other sedimentary organic matter studies (Perdue & Koprivnjak, 2007).

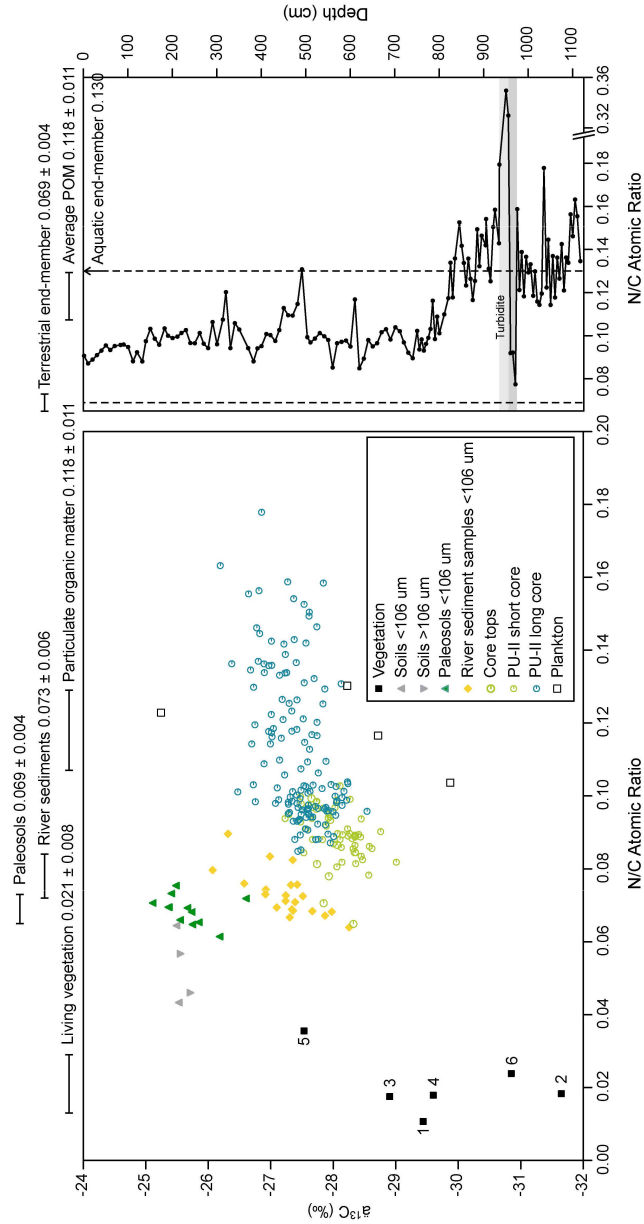

Figure 5: N/C vs. $d^{13}C$ biplot of terrestrial, aquatic and lake sediment samples. The N/C average and standard deviation (1s) of the main groups of samples are also shown. The downcore evolution of the N/C ratio is represented, with indication of the N/C values selected for the terrestrial (0.069) and aquatic (0.130) end-members. A comparison with Fig. 2 clearly shows the adequacy of using N/C instead of C/N for graphical representation of aquatic, terrestrial and sedimentary data. For PU-II long core, the samples located within and immediately above the turbidite are shown by the dark and light grey shaded areas, respectively.

3.5.3. Surface variability

The proportion of terrestrial organic carbon contained in the eight surface sediment samples has been estimated from their bulk C/N data, using the mixing equation described in 3.3.5. The results show a clear relationship between the fraction of terrestrial organic carbon and the distance to the main lake tributaries and to the shore (Fig. 6).The fraction of terrestrial carbon is the lowest (50 %) at site PU-SC1 (western sub-basin), which is protected from any direct river input (Fig. 1). It is the highest (100 and 97 %) at sites PU-SC3 and PU-SC7, respectively. These two sites are close to the southern shore of the lake and probably receive direct inputs of terrestrial organic matter during the rainy season (Figs. 1, 6). In addition, site PU-SC3 is directly influenced by the plume of Pescadero River, which explains the very high fraction of terrestrial organic carbon at this site (Fig. 1). The surface sample of site PU-II is intermediate (67 %).

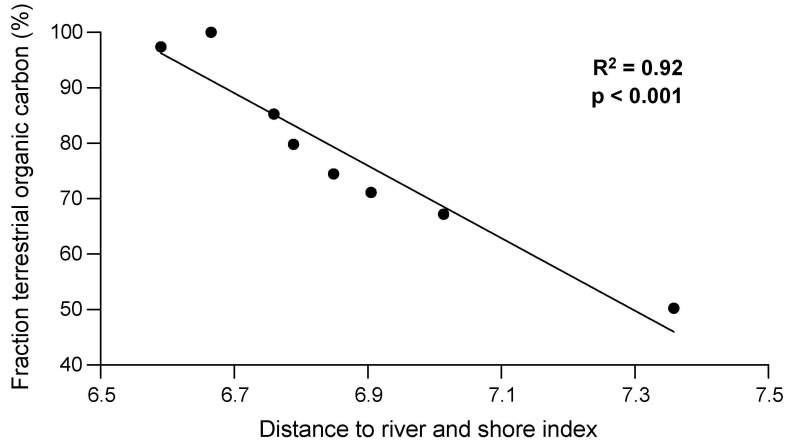

Figure 6: Relation between the fraction of terrestrial carbon contained in the surface sediment samples of Puyehue Lake and the distance to river and shore index (D = log (a) + 0.5 log (b) + 0.5 log (c). The main (bigger) rivers are Rio Golgol and Rio Lican, and the secondary rivers are Rio Pescadero and Rio Chanleufu. Distances to secondary river and shore were given half weighting to account for their smaller contribution to the total sediment supply compared to major rivers.

3.5.4. Downcore variability

Similarly to the surface samples, we applied Equation (2) to the C/N data from the PU-II long core to estimate the proportion of terrestrial carbon preserved in the sediments of Puyehue Lake since the end of the Last Glacial Maximum. Although organic carbon concentrations generally decrease by a factor of 10 during sinking and early diagenesis,

the initial C/N and carbon isotopic ratios remain relatively unchanged and can therefore be used to reconstruct past changes in organic carbon sources (Meyers and Ishiwatari, 1993; Meyers, 2003).

Before interpreting any data in terms of paleoenvironmental and/or paleoclimate changes, it is essential to carefully inspect the results and withdraw data associated to non-continuously deposited with sedimentary units (e.g. tephra layers, turbidites, etc). For PU-II long core, samples were carefully selected to avoid the tephra layers, but some of the analyzed samples were collected within a turbidite at 971-956 cm. These samples show anomalously high C/N values (10-12), and the samples located immediately above the turbidite (956-935 cm) present extremely low C/N values (Fig. 4). The high C/N values between 971 and 956 cm probably reflect the terrestrial origin of the sediment particles composing the turbidite. Above the turbidite (956-935 cm), the low C/N values most likely reflect the increase in nutrients (N, P) associated to the high supply of terrestrial material by the turbidite-triggering event. Therefore, the geochemical data associated with the deposition of this turbidite have been removed from the database used for paleoenvironmental and paleoclimate interpretations.

As shown in Fig. 5, the N/C ratio of PU-II long core above 830 cm typically oscillates between the aquatic and terrestrial end-members. Below 830 cm, however, the N/C values are frequently higher than 0.130, reflecting the high nitrogen content of these samples. These high N/C ratios cannot be explained by a simple mixing between the present-day aquatic and terrestrial end-members, but are probably due to a combination of various factors, such as (1) degradation of sedimentary organic matter during early diagenesis (loss of C), (2) high nitrogen supply at the time of sedimentation, (3) different plankton communities below 830 cm (Sterken et al., 2008) characterized by different stoichiometries, or (4) seasonality of the primary plankton communities: our POM samples were taken during summer and might therefore contain less diatoms relative to cyano- and chlorophytes, which could make a difference in the stoichiometry of the aquatic end-member (e.g. Arrigo, 2005). For these samples, the application of equation (2) provides negative f_T values that were modelled to 0.

The resulting f_T plot is represented in Fig. 7. The fraction of terrestrial carbon strikingly follows the total organic carbon ($r^2 = 0.72$, $p < 0.0001$), providing evidence that most of the changes in TOC are due to changes in terrestrial organic matter. Before 12.8 cal. ka BP the results show an extremely low fraction of terrestrial carbon, demonstrating that the main source of organic matter during the last deglaciation was aquatic. At 12.8 cal. ka BP, the TOC and f_T concomitantly increase, evidencing an increased supply in terrestrial organic matter, most likely linked to the development of

the vegetation in the lake watershed. This increase seems to occur progressively between 12.8 and 11.2 cal. ka BP. After 11.2 cal. ka BP, the TOC and f_T remain generally high, with secondary decreases at 6.9-6.1 and 5.45 - 4.55 cal. ka BP. It is noteworthy that the $d^{13}C$ signal does not follow the changes in f_T, and therefore probably reflects changes in lake productivity instead of changes in the origin of the sedimentary organic matter. In addition, minor increases in $d^{13}C$ might be due to the development of C4 plants in the lake watershed, which was however relatively limited since plants using the C4 pathway are characteristic of dry and warm environments, such as tropical grasslands and savannah (Osborne and Beerling, 2006).

3.5.5. Implication for bulk radiocarbon ages

The important changes in the source of organic carbon through time have a direct influence on the interpretation of the bulk radiocarbon ages and on the construction of the age-depth model of PU-II long core. By using bulk samples for radiocarbon dating, Bertrand et al. (2008) assumed that the radiocarbon dates represent the age of sediment deposition. However, since bulk samples contain a mixture of aquatic (syndepositional) and terrestrial (aged) organic matter, some of the dates might be older than the true age of deposition.

As the two radiocarbon samples at 908 and 1012 cm (13,100-13,850 and 15,250-16,750 cal. yr. BP, respectively) do not contain any significant amount of terrestrial carbon (Fig. 7), they probably reflect a more correct age of deposition. For the samples younger than 12.8 cal. yr. BP, the fraction of terrestrial organic carbon is significant, making the bulk radiocarbon ages older than the age of sediment deposition since residence times of terrestrial organic matter in lake watersheds is typically in the order of several hundred years (e.g. Drenzek et al., 2009). This interpretation is in agreement with the tephrochronological model of Bertrand et al. (in press), who show that the radiocarbon dates of bulk samples encompassing the AD 1907 tephra are 500-600 years older than expected. Since these samples contain a significant amount (~60 %) of terrestrial carbon, we can assume that the terrestrial carbon reaching the lake is aged (~1000 years old), which justifies the use of the paleosol geochemical values to define the terrestrial end-member. Our findings that the two lowermost radiocarbon dates are not affected by incorporation of old radiocarbon, increase the reliability of the chronology of the lower part of the core (> 12.8 cal. ka BP), which is a crucial point when discussing changes associated with the deglaciation/Holocene transition.

3.5.6. Paleoenvironmental and paleoclimate interpretation and comparison with other proxies

In Fig. 7, the TOC and f_T data of PU-II long core are compared to sedimentological and paleoecological (pollen, diatoms) data previously obtained on the same sediment core (Bertrand et al., 2008; Sterken et al., 2008; Vargas-Ramirez et al., 2008).

Sedimentological and diatom biovolume data show that the biogenic silica productivity of Puyehue Lake quickly increases at 17.3 ka (Fig. 7). This increase has been interpreted as the first warming pulse initiating the main phase of the deglaciation in South-Central Chile (Bertrand et al., 2008; Sterken et al., 2008). The organic record of Puyehue Lake shows a small but significant concomitant increase in TOC, and only a minor shift in f_T.

Most of the increase in TOC between 17.3–16.3 cal. ka BP is probably linked to the increased lake diatom productivity, as seen in the biogenic silica index and diatom biovolume records (Fig. 7). The minor increase in f_T that follows the warming pulse most likely reflects the very limited expansion of the vegetation cover in the lake watershed in response to the first warming pulse, in agreement with palynological data (Vargas-Ramirez et al., 2008). At ODP site 1233, which is located immediately off the coast of Chile at the same latitude than Puyehue (Fig. 1), Lamy et al. (2007) demonstrated a

Figure 7 *(opposite page)*: Comparison of geochemical, paleoecological and sedimentological data obtained on PU-II long core. The results are plotted versus time, according to the age-depth model of Bertrand et al. (2008). The fraction of terrestrial carbon (f_T) is calculated using the N/C mixing equation (equation 5), with N/C values of 0.130 for the aquatic end-member and 0.069 for the terrestrial end-member. Negative values (mainly below 830 cm) have been set to zero. The data from 971 to 935 cm were not included because of their association with a major turbidite. The aquatic organic carbon data (aqOC) were calculated as TOC * (1 - f_T). The biogenic silica index is used to indicate the relative importance of diatoms in the total aquatic community (unitless). The pollen concentration data are from Vargas-Ramirez et al. (2008). Two data points (159-160 cm and 179-180 cm) have been removed from the original database because of the presence of a tephra layer in these samples, leading to extremely low pollen concentrations. The detrital *vs.* biogenic index is issued from Bertrand et al. (2008). Positive values indicate high terrestrial content (driven by the sediment content in Ti, Al and magnetic susceptibility), and low values indicate a high biogenic content of the sediment (driven by biogenic silica, LOI_{550}, LOI_{105}, and grain-size; Bertrand et al., 2008). The diatom biovolume data are from Sterken et al. (2008). The tephra thickness (horizontal bars in the right column) of the most important tephras (≥ 10 mm thick) is drawn according to Bertrand et al. (in press). The TOC, aqOC, f_T, $d^{13}C$, biogenic silica index and detrital *vs.* biogenic index data are all given as three points running averages. The original pollen concentrations and diatom biovolumes data have a lower temporal resolution (20 cm) and have therefore not been smoothed. Grey horizontal bars and dotted lines indicate periods and events that were discussed in the paper.

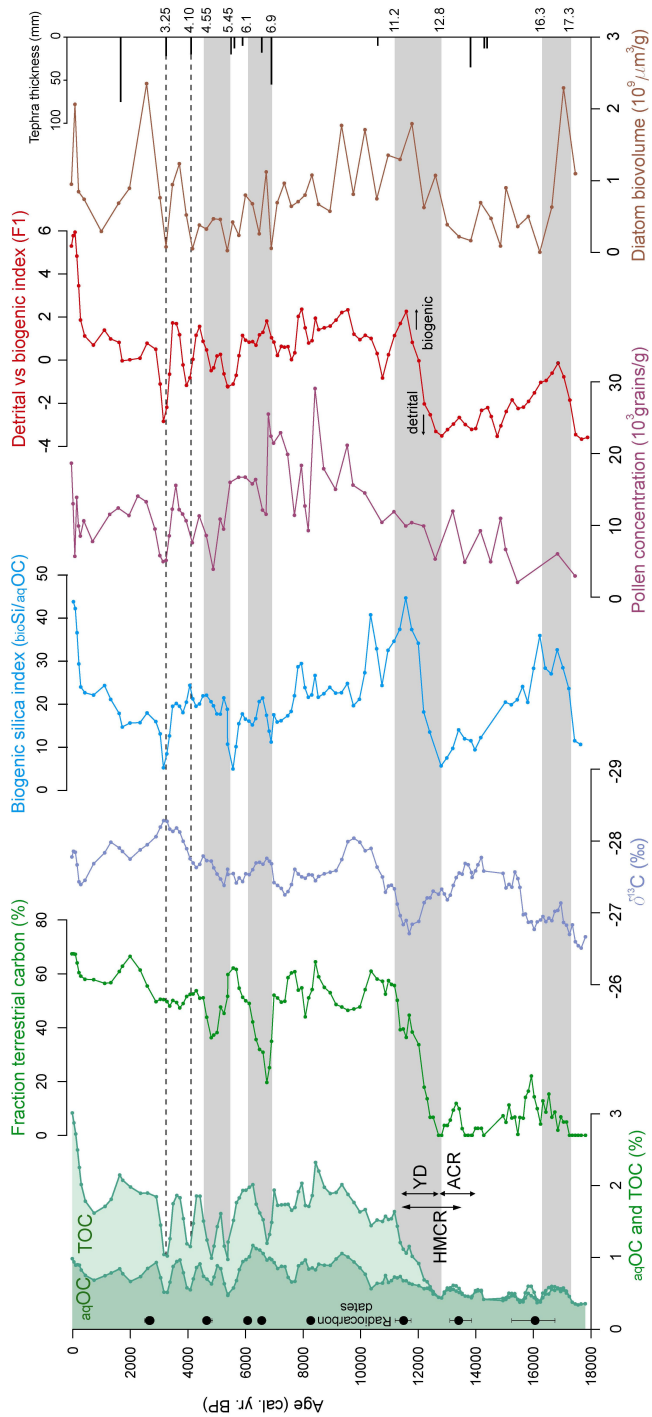
Age (cal. yr. BP)
aqOC and TOC (%)
δ13C (‰)
Fraction terrestrial carbon (%)
Biogenic silica index (bioSi/aqOC)
Pollen concentration (10³grains/g)
Detrital vs biogenic index (F1)
Diatom biovolume (10⁹/µm³/g)
Tephra thickness (mm)
aqOC
TOC
Radiocarbon dates
YD
ACR
HMCR
detrital
biogenic
3.25
4.10
4.55
5.45
6.1
6.9
11.2
12.8
16.3
17.3

gradual increase of sea surface temperature of nearly 5°C between 18.8 and 16.7 cal. ka BP (Fig. 8). The comparison of the two records shows a 1500 years delay in the increase of Puyehue Lake productivity compared to the start of the SST increase (Fig. 8), at least if the biogenic silica values in our core represent a true minimum at c. 17.9 cal. ka BP. This likely lagging response can be explained by the presence of a large glacier in the watershed of Puyehue Lake, which delayed the increase in lake temperature, decreased light availability through the influx of glacial melt water and clays, and largely limited the expansion of the vegetation around the lake. The presence of such a glacier in the watershed of Puyehue Lake is supported by geomorphological observations (Bentley, 1997), and the observed response time seems typical for glaciers in the Chilean Andes (Hubbard, 1997; Lamy et al., 2004). The rapid retreat of Andean glaciers after approx. 17.5 cal. ka BP is also supported by geomorphological and palynological evidences of several sites between 40 and 42°S (Denton et al., 1999), and by the salinity record of ODP Site 1233, showing a strong meltwater influence between ~17.8 and 15.8 cal. ka BP (Lamy et al., 2004).

The period between 17.3 and 12.8 cal. ka BP in the PU-II record is characterized by a constantly low f_T, a moderately low TOC, and a decrease in the biogenic silica index, which might indicate an increased replacement of diatoms by other types of aquatic organisms (cyanobacteria, chlorophytes) during parts of the year. This relative decrease in biogenic silica might have been caused by low nutrient supplies, low temperature, and/or reduced lake mixing (Bertrand et al, 2008; Sterken et al., 2008), resulting from a southward shift of the Westerlies, as was deduced by a concomitant ice advance in the region of Magellan (Sudgen et al., 2005). It is supported by the $d^{13}C$ data, which show lower values between 15.5 and 13.5 cal. ka BP, arguing for a decreased lake productivity. The low but significant pollen concentration values during this period probably represent pollen grains originating from the Coastal Cordillera and Central Depression and transported by the Westerlies, since the fraction of terrestrial carbon originating from the lake watershed remains extremely low.

Interestingly, this period corresponds to nearly constant sea surface temperatures at site ODP 1233 (Lamy et al., 2007; Fig. 8). The presence of a cold reversal during the deglaciation is not clearly expressed in our organic geochemical data, but the low biogenic silica values observed at around 13.2-12.7 cal. ka BP (Fig. 7) may possibly be interpreted in terms of a (Huelmo-Mascardi) cold reversal, as was argued by Bertrand et al. (2008).

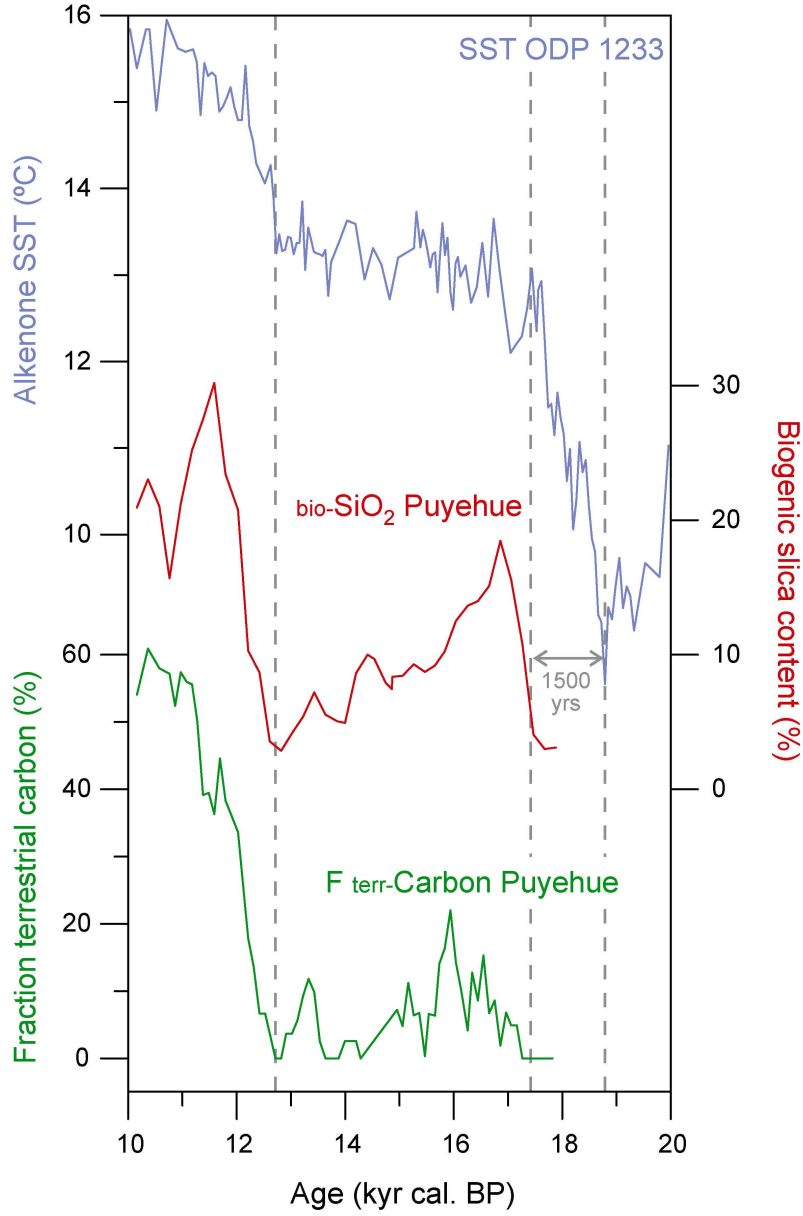

Figure 8: Sea surface temperature of ODP Site 1233 compared to two paleoenvironmental records from Puyehue Lake. (A) Alkenone sea-surface temperature from ODP site 1233 (Lamy et al., 2007); (B) Biogenic silica content of sediment core PU-II (Bertrand et al., 2008); (C) Fraction of terrestrial carbon in sediment core PU-II (this study).

The period between 12.8 and 11.8 cal. ka BP corresponds to major changes in the core and represents the transition from the last deglaciation to the Holocene (Figs. 7, 8). We observe simultaneous increases in TOC, f_T, biogenic silica, and secondarily $d^{13}C$, most likely reflecting a second major warming pulse. This important warming triggered an increase of lake (mainly diatom) productivity and a subsequent rapid expansion and development of the vegetation in the lake watershed (Fig. 7). The timing of this 2nd warming pulse in the sediment of Puyehue Lake (12.8 cal. ka BP) falls into the first half of the Younger Dryas chronozone (Fig. 7) and therefore contributes to the mounting evidence that the mid-latitudes of the Southern Hemisphere were warming during the Younger Dryas chronozone, in agreement with the bipolar see-saw hypothesis of Stocker (1998). These important changes in the limnology of Puyehue Lake and in the vegetation cover in the catchment strikingly correspond to a 2°C increase in the sea surface temperature of ODP site 1233 (Fig. 8). The synchronicity of these abrupt changes in Puyehue and at ODP site 1233 probably demonstrate that the glacier had nearly totally retreated from the lake watershed by that time and did not delay the response time of the different terrestrial proxies.

During the Holocene, the TOC and f_T data are generally high, especially between 11.2 cal. ka BP and 6.9 cal. ka BP. These high values at the beginning of the Holocene indicate a luxuriant development of the terrestrial vegetation in the catchment area, most probably indicating high temperatures (Moreno, 2004; Vargas-Ramirez et al., 2008). After 6.9 cal. ka BP, we observe a slight decrease in lake productivity and in the density of the vegetation cover, with several major decreases in terrestrial organic carbon at 6.90-6.10 and 5.45-4.55 cal. ka BP, as well as 4.10 and 3.25 cal. ka BP. These changes are not clearly expressed in the other proxies (Fig. 7) but they might reflect periods of stronger volcanic activity, affecting the terrestrial vegetation in the lake watershed (at 6.9-6.1 and 5.45-4.55 cal. ka BP), or affecting/diluting directly all sediments in the lake (at 4.10 and 3.25 cal. ka BP). This interpretation is supported by tephrochronological data, which suggest a high volcanic activity between 7.0 and 5.5 cal. ka BP (Fig. 7; Bertrand et al., in press). In particular, three thick tephra layers (55, 5, and 18 mm) occur between 6.9 and 6.8 cal. ka BP, and two other ones (13 and 5 mm) at 5500 cal. yr. BP, corresponding to the onset of the low TOC and f_T values. The two relatively less important decreases in TOC at 4.10 and 3.25 cal. ka BP are not reflected in the f_T data but stand out in the detrital vs. biogenic index and diatom biovolume data. These two peaks occur immediately above two major tephra layers (20 and 22 mm thick) that might have caused

a decrease in lake productivity (but see Chapter 2) or more probably an overall dilution of the sediments located in between the visually distinct (registered) tephra layers.

3.6. Conclusions

The bulk organic geochemistry of sediments from Puyehue Lake and its watershed provides important information about the sources of sedimentary organic matter and changes in their relative contribution through space and time. We demonstrated that the C/N ratio of the potential sources of terrestrial organic matter in the lake watershed constantly decreases during incorporation into soils and transport to sedimentary environments. Therefore, the organic matter contained in paleosols best represents the terrestrial end-member. After careful selection of the terrestrial and aquatic end-members, their N/C ratios were used in a simple mixing equation to estimate the fraction of terrestrial carbon preserved in lake sediments. For the recent sediments, we observe a direct relation between the fraction of terrestrial carbon and the distance to the main tributaries and to the lake shore. In addition, we showed that during the last 17.9 kyr, the TOC and the fraction of terrestrial carbon shift simultaneously and reflect the expansion of the vegetation in the lake watershed. During the last deglaciation, a first warming pulse at 17.3 cal. ka BP significantly increased the productivity of Puyehue Lake, but the presence of a glacier in the lake watershed limited the concomitant expansion of the terrestrial vegetation. Furthermore, the existence of the Puyehue glacier delayed the response time of the terrestrial proxies by ~1500 years compared to the increase in sea surface temperature. A second warming pulse is recorded in the sediments of Puyehue Lake at 12.8 cal. ka BP, and is synchronous with a 2°C increase in sea surface temperature, demonstrating that the Puyehue glacier had significantly retreated from the lake watershed during the first phase of the deglaciation. The timing of this second warming pulse corresponds to the beginning of the Younger Dryas chronozone, providing additional evidence for the absence of a Younger Dryas cooling in southern South America. Finally, the Holocene is characterized by an abundant vegetation cover probably linked to high temperatures between 11.2 and 6.9 cal. ka BP, and by several centennial-scale changes in lake plankton and terrestrial vegetation, possibly caused by increased volcanic activity. Our results may contribute to the mounting evidence that the climate in the mid-latitudes of the southern Hemisphere was warming during the Younger Dryas chronozone, in agreement with the bipolar see-saw hypothesis.

Acknowledgments

This research was partly supported by the Belgian OSTC project EV/12/10B "A continuous Holocene record of ENSO variability in southern Chile". We acknowledge François Charlet for the collection of the POM samples and Elie Verleyen for stimulating discussions. Sediment cores were collected with the help of Fabien Arnaud, Christian Beck (U. Savoie, France), Vincent Lignier (ENS Lyon, France), Xavier Boës (U. Liège, Belgium), Waldo San Martin, and Alejandro Peña (U. Concepción, Chile). The fieldwork in Chile has benefited from the logistic support of Roberto Urrutia (U. Concepción, Chile) and Mario Pino (U. Valdivia, Chile). S.B. is supported by a BAEF fellowship (Belgian American Educational Foundation), and by an EU Marie Curie Outgoing Fellowship under the FP6 programme.

References

Arnaud F., Magand O., Chapron E., Bertrand S., Boës X., Charlet F., Mélières M.A. 2006. Radionuclide profiles (^{210}Pb, ^{137}Cs, ^{241}Am) of recent lake sediments in highly active geodynamic settings (Lakes Puyehue and Icalma – Chilean Lake District). Science of the Total Environment. 366: 837-850.

Arrigo K. 2005. Marine microorganisms and global nutrient cycles. Nature. 437: 349-355.

Baier J., Lucke A., Negendank J.F.W., Schelser G.-H., Zolitschka B. 2004. Diatom and geochemical evidence of mid- to late Holocene climatic changes at Lake Holzmaar, West-Eifel (Germany). Quaternary International. 133 (1): 81-96.

Barrows T., Lehman S.J., Fifield L.K., De Deckker P. 2007. Absence of Cooling in New Zealand and the Adjacent Ocean During the Younger Dryas Chronozone. Science. 318: 86-89.

Bennett K.D., Haberle S.G., Lumley S.H. 2000. The last Glacial-Holocene transition in southern Chile. Science. 290: 325-328.

Bentley M.J. 1997. Relative and radiocarbon chronology of two former glaciers in the Chilean Lake District. Journal of Quaternary Science. 12: 25-33.

Bertrand S. & Fagel N. 2008. Nature, origin, transport and deposition of andosol parent material in south-central Chile (36-42ºS). Catena. 73 (1): 10-22.

Bertrand S., Boës X., Castiaux J., Charlet F., Urrutia R., Espinoza C., Charlier B., Lepoint G., Fagel N. 2005. Temporal evolution of sediment supply in Lago Puyehue (Southern Chile) during the last 600 years and its climatic significance. Quaternary Research. 64: 163-175.

Bertrand S., Charlet F., Charlier B., Renson V., Fagel N. 2008. Climate variability of Southern Chile since the Last Glacial Maximum: a continuous sedimentological record from Lago Puyehue (40°S). Journal of Paleolimnology. 39 (2): 179-195.

Bertrand S., Castiaux J., Juvigné E. In press. Tephrostratigraphy of the Late Glacial and Holocene sediments of Puyehue Lake (Southern Volcanic Zone, Chile, 40°S). Quaternary Research. In press.

Blunier T. & Brook E.J. 2001. Timing of millennial-scale climate change in Antarctica and Greenland during the last glacial period. Science. 291: 109–112.

Boës X. & Fagel N. 2008. Relationships between southern Chilean varved lake sediments, precipitation and ENSO for the last 600 years. Journal of Paleolimnology. 39 (2): 237-252.

Boström B., Comstedt D., Ekblad A. 2007. Isotope fractionation and 13C enrichment in soil profiles during the decomposition of soil organic matter. Oecologia. 153 (1): 89-98.

Brady N.C. 1990. The nature and properties of soils (10th edition). MacMillan Publishing Company, NewYork.

Buhay W.M., Timsic S., Blair D., Reynolds J., Jarvis S., Petrash D., Rempel M., Bailey D. 2008. Riparian influences on carbon isotopic composition of tree rings in the Slave River Delta, Northwest Territories, Canada. Chemical Geology. 252 (1-2): 9-20.

Campos H., Steffen W., Agüero G., Parra O., Zúñiga L. 1989. Estudios limnologicos en el Lago Puyehue (Chile): morfometria, factores fisicos y quimicos, plancton y productividad primaria. Medio Ambiente. 10: 36-53.

Charlet F., De Batist M., Chapron E., Bertrand S., Pino M., Urrutia R. 2008. Seismic stratigraphy of Lago Puyehue (Chilean Lake District): new views on its deglacial and Holocene evolution. Journal of Paleolimnology. 39 (2): 163-177.

Colman S.M., Jones G.A., Rubin M., King J.W., Peck J.A., Orem W.H. 1996. AMS radiocarbon analyses from Lake Baikal, Siberia: challenges of dating sediments from a large, oligotrophic lake. Quaternary Science Reviews. 15: 669–684.

De Batist M., Fagel N., Loutre M.-F., Chapron E. 2008. A 17,900-year multi-proxy lacustrine record of Lago Puyehue (Chilean Lake District): introduction. Journal of Paleolimnology. 39 (2): 151-161.

Denton G.H., Heusser C.J., Lowell T.V., Moreno P.I., Andersen B.G., Heusser L.E., Schlüter C., Marchant D.R. 1999. Geomorphology, stratigraphy, and radiocarbon chronology of Llanquihue drift in the area of the southern lake district, seno reloncaví, and isla grande de Chiloé, Chile. Geografiska Annaler. 81 A(2): 167-212.

Drenzek N.J., Hughen K.A., Montluçon D.B., Southon J.R., dos Santos G.M., Druffel E.R.M., Giosan L., Eglinton T.I. 2009. A new look at old carbon in active margin sediments. Geology. 37 (3): 239-242.

Elser J.J., Fagan W., Denno R.F., Dobberfuhl D.R., Folarin A., Huberty A., Interlandi S., Kilham S.S., McCauley E., Schulz K.L., Siemann E.H., Sterner R.W. 2000. Elemental analysis illuminates nutritional constraints on terrestrial and freshwater food webs. Nature. 408: 578-580.

EPICA Community Members. 2006. One-to-one coupling of glacial variability in Greenland and Antarctica. Nature. 444: 195-198.

Francey R.J., Farquhar B.D. 1982. An explanation of $^{13}C/^{12}C$ variations in tree rings. Nature. 297: 28-31.

Fry B. 1991. Stable isotope diagrams of freshwater food webs. Ecology. 72: 2293–2297.

Godoy R., Oyarzún C., Gerding V. 2001. Precipitation chemistry in deciduous and evergreen *Nothofagus* forest of southern Chile under a low- deposition climate. Basic and Applied Ecology. 2: 65-72.

Hajdas I., Bonani G., Moreno P., Aritzegui D. 2003. Precise radiocarbon dating of Late-Glacial cooling in mid-latitude South America. Quaternary Research. 59: 70-78.

Healey F.P. & Hendzel L.L. 1980. Physiological indicators of nutrient deficiency in lake phytoplankton. Canadian Journal of Fisheries and Aquatic Sciences. 37: 442-453.

Hecky R.E., Campbell P., Hendzel L.L. 1993. The stoichiometry of carbon, nitrogen, and phosphorous in particulate matter of lakes and oceans. Limnology and Oceanography. 38 (4): 709-724.

Heiri O., Lotter A.F., Lemcke G. 2001. Loss on ignition as a method for estimating organic and carbonate content in sediments: reproducibility and comparability of results. Journal of Paleolimnology. 25: 101-110.

Hubbard A. 1997. Modeling climate, topography and paleo-glacier fluctuations in the Chilean Andes, Earth Surface Processes and Landforms. 22 (1): 79-92.

Kaiser J., Lamy F., Hebbeln D. 2005. A 70-kyr sea surface temperature record off southern Chile (Ocean Drilling Program Site 1233). Paleoceanography. 20: doi:10.1029/2005PA001146

Kendall C., Silva S.R., Kelly V.J. 2001. Carbon and nitrogen isotopic compositions of particulate organic matter in four large river systems across the United States. Hydrological Processes. 15: 1301–1346.

Lamy F., Kaiser J., Ninnemann U., Hebbeln D., Arz H.W., Stoner J. 2004. Antarctic timing of surface water changes off Chile and Patagonian ice sheet response. Science. 304: 1959-1962.

Lamy F., Kaiser J., Arz H.W., Hebbeln D., Ninnemann U., Timm O., Timmermann A., Toggweiler J.R. 2007. Modulation of the bipolar seesaw in the Southeast Pacific during Termination 1. Earth and Planetary Science Letters. 259: 400-413.

Laugenie C. 1982. La région des lacs, Chili méridional. Unpublished PhD thesis, Université de Bordeaux III, 822 p.

Lazerte B.D. 1983. Stable carbon isotope ratios: implications for the source of sediment carbon and for phytoplankton carbon assimilation in Lake Memphremagog, Quebec. Canadian Journal of Fisheries and Aquatic Sciences. 40: 1658–1666.

Lowell T. V., Heusser C. J., Andersen B.G., Moreno P.I., Hauser A., Heusser L.E. Schüchter C., Marchant D.R., Denton G. H. 1995. Interhemispheric correlation of Late Pleistocene Glacial events. Science. 269: 1541–1549.

McGroddy M.E., Daufresne T., Hedin L.O. 2004. Scaling of C:N:P stoichiometry in forests worldwide: implications of terrestrial redfield-type ratios. Ecology. 85: 2390–2401.

Meyers P.A. 2003. Applications of organic geochemistry to paleolimnological reconstructions: a summary of examples from the Laurentian Great Lakes. Organic Geochemistry. 34 (2): 261–289.

Meyers P.A. & Ishiwatari R. 1993. Lacustrine organic geochemistry—an overview of indicators of organic matter sources and diagenesis in lake sediments. Organic Geochemistry. 20: 867–900.

Meyers P.A. & Teranes J.L. 2001. Sediment Organic Matter. In: Last, W.M., Smol, J.P. (Eds), Tracking environmental changes using lake sediment - Vol. 2: Physical and geochemical methods. Kluwer Academic, Dordrecht, The Netherlands, pp. 239-270.

Moreno P.I. 2004. Millenial-scale climate variability in northwest Patagonia over the last 15000 yr. Journal of Quaternary Science. 19: 35-47.

Moreno P.I., Leon A.L. 2003. Abrupt vegetation changes during the last glacial to Holocene transition in mid-latitude South America. Journal of Quaternary Science. 18: 1-14.

Moreno P.I., Jacobson G.L.J., Lowell T.V., Denton G.H. 2001. Interhemispheric climate links revealed by a late-glacial cooling episode in southern Chile. Nature. 409: 804-808.

Muñoz M. 1980. Flora del parque nacional Puyehue. Universitaria, Santiago, 557 p.

Nadelhoffer K.J. & Fry B. 1988. Controls on natural nitrogen-15 and carbon-13 abundances in forest soil organic matter. Soil Science Society of America Journal. 52: 1633–1640.

Nierop K.G.J., Tonneijck F.H., Jansen B., Verstraten J.M. 2007. Organic matter in volcanic ash soils under forest and Páramo along an Ecuadorian altitudinal transect. Soil Science Society of America Journal. 71: 1119–1127.

O'Leary M.H. 1988. Carbon isotopes in photosynthesis. Bioscience. 38: 328–336.

Osborne C.P. & Beerling D.J. 2006. Nature's green revolution: the remarkable evolutionary rise of C4 plants. Philosophical Transactions of the Royal Society, Series B. 361: 173-194.

Parada M.G. 1973. Pluviometria de Chile. Isoyetas de Valdivia-Puerto Montt. CORFO Departamento de Recursos hydraulicos, 73 p.

Perdue E.M. & Koprivnjak J.-F. 2007. Using the C/N ratio to estimate terrigenous inputs of organic matter to aquatic environments. Estuarine Coastal and Shelf Science. 73 (1–2): 65–72.

Post W.M., Pastor J., Zinke P.J., Stangenberger A.G. 1985. Global patterns of soil nitrogen storage. Nature. 317: 613-616.

Prahl F.G., Ertel J.R., Goni M.A., Sparrow M.A., Eversmeyer B. 1994. Terrestrial organic carbon contributions to sediments on the Washington margin. Geochimica Cosmochimcia Acta. 58: 3035–3048.

Rostad C.E., Leenheer J.A., Daniel S.R. 1997. Organic carbon and nitrogen content associated with colloids and suspended particulates from the Mississippi River and some of its tributaries. Environmental Science and Technology. 31: 3218–3225.

Schiefer E. 2006. Contemporary sedimentation rates and depositional structures in a Montane Lake, Coast Mountains, British Columbia, Canada. Earth Surface Processes and Landforms. 31: 1311-1324.

Sepúlveda J. 2005. Aporte de material terrigeno en fiordos de Patagonia del Norte: Evidencia geoquimica en sedimentos recientes y del Holoceno tardio. University of Concepción, Chile. Unpublished Master thesis.

Sifeddine A., Wirrmann D., Luiza A., Albuquerque S., Turcq B., Campello Cordeiro R., H.C. Gurgel M., Joao Abrao J. 2004. Bulk composition of sedimentary organic matter used in palaeoenvironmental reconstructions: examples from the tropical belt of South America and Africa. Palaeogeography, Palaeoclimatology, Palaeoecology. 214 (1-2): 41-53.

Sowers T. A. & Bender M. 1995. Climate records during the last deglaciation. Science. 269: 210-214.

Sterken M., Verleyen E., Sabbe K., Terryn G., Charlet F., Bertrand S., Boës X., Fagel X., De Batist M., Vyverman W. 2008. Late Quaternary climatic changes in Southern Chile, as recorded in a diatom sequence of Lago Puyehue (40°40'S). Journal of Paleolimnology. 39 (2): 219-235.

Sterner R.W. & Elser J.J. 2002. Ecological Stoichiometry: the Biology of Elements from Molecules to the Biosphere. Princeton University Press, Princeton.

Stocker T.F. 1998. The seesaw effect. Science. 282: 61–62.

Stott L., Timmermann A, Thunell R. 2007. Southern Hemisphere and Deep Sea Warming led deglacial Atmospheric CO2 rise and Tropical Warming. Science. 318: 435-438.

Sudgen E., Bentley M.J., Fogwill C.J., Hulton N.R.J., McCulloch R.D., Purves R.S. 2005. Late-glacial glacier events in southernmost south America: A blend of 'Northern' and 'Southern' hemispheric climatic signals? Geografiska Annaler, Series A: Physical Geography. 87 (2): 273–288.

Talbot M. R. 2001. Nitrogen isotopes in palaeolimnology. In: Last, W. M., Smol, J.P. (Eds.), Tracking Environmental Change Using Lake Sediments. Volume 2: Physical and Geochemical Techniques. Kluwer Academic Publishers, Dordrecht, The Netherlands, pp. 401-439.

Thomasson K. 1963. Araucanian Lakes. Acta Phytogeographica Sueca. 47: 1–139.

Vannote R.L., Minshall G.W., Cummins K.W., Sedell J.R., Cushing C.E. 1980. The river continuum concept. Canadian Journal of Fisheries and Aquatic Sciences. 37: 130-137.

Vargas-Ramirez L., Roche E., Gerrienne P., Hooghiemstra H. 2008. A pollen-based record of late glacial–Holocene climatic variability in the southern lake district, Chile. Journal of Paleolimnology. 39 (2): 197-217.

Verardo D.J., Froelich P.N., McIntyre A. 1990. Determination of organic carbon and nitrogen in sediments using the Carlo-Erba NA-1500 analyzer. Deep-Sea Research. 37: 157–165.

Vuorio K., Meili M., Sarvala J. 2006. Taxon-specific variation in the stable isotopic signatures ($d^{13}C$ and $d^{15}N$) of lake phytoplankton. Freshwater Biology. 51: 807-822.

Wissel B., Gace A., Fry B. 2005. Tracing river influences on phytoplankton dynamics in two Louisiana estuaries. Ecology. 86: 2751-2762.

Wynn J.G. 2007. Carbon isotope fractionation during decomposition of organic matter in soils and paleosols: Implications for paleoecological interpretations of paleosols, Palaeogeography, Palaeoclimatology, Palaeoecology. 251 (3-4): 437-448.

Chapter 4

An illustrated and annotated checklist of freshwater diatoms (Bacillariophyta) from Maritime Antarctica (Livingston, Signy and Beak Island)

Mieke Sterken, Bart Van de Vijver, Vivienne J. Jones, Elie Verleyen, Dominic A. Hodgson, Wim Vyverman & Koen Sabbe.

Abstract

One hundred and two diatom taxa, belonging to thirty-eight genera, were observed in recent, subfossil and fossil freshwater sediments of three islands in the proximity of the northern Antarctic Peninsula, viz. Signy Island (South Orkneys), Livingston Island (South Shetlands) and Beak Island (James Ross Island group). *Pinnularia* (9 taxa), *Chamaepinnularia*, *Nitzschia*, *Psammothidium* and *Stauroneis* (7 taxa), *Navicula* and *Planothidium* (6 taxa), and *Diadesmis* and *Luticola* (both 5 taxa) proved to be the most species-rich genera. Original morphometric data (including length, width and stria density) and illustrations are presented for all taxa observed. The exact taxonomic identity of about forty species remains uncertain and requires further study. Given the fact that most of these may turn out to be endemic to the region, and that fourteen positively identified species are hitherto only known from the Antarctic region, about half of all taxa are probably restricted to the Antarctic.

This chapter is a manuscript in preparation.

Contribution of the author: diatom photography, measurements, intercalibration and writing largest part of the paper.

4.1. Introduction

Diatoms are one of the most species-rich and omnipresent algal groups in sub-Antarctic and Antarctic freshwater environments, and are characterized by a high degree of endemism (Spaulding et al., in press and references therein). Because of the good fossilization potential of their siliceous cell wall and the fact that many species have distinct ecological optima and narrow amplitudes, they are commonly used as indicators for monitoring the ecological status of contemporary environments and reconstructing past environmental and climatic conditions (Smol and Stoermer in press). Especially in the ice-free regions of Antarctica, where higher vegetation is often absent, diatoms are of paramount importance for paleo-ecological research (e.g. Chapters 6 and 7; Verleyen et al., 2003).

Recent revisions of diatom systematics and biodiversity in the Antarctic (e.g. Van de Vijver & Mataloni, 2008) have shown that in the past many species have been wrongly identified, usually by force-fitting to known European or North-American species (see Sabbe et al., 2003 for a detailed discussion of this issue). This practice has had serious repercussions on our understanding of diatom biodiversity and biogeography in the Antarctic, and may also lead to incorrect inferences of present and past environmental conditions.

In this study we present a thoroughly revised and intercalibrated checklist of diatoms found in various freshwater environments from three islands in Maritime Antarctica (Livingston, Signy and Beak Island). All entries are annotated, illustrated and provided with original morphometric data. The checklist is based on a re-analysis of materials from Livingston & Signy Islands (cf. Jones et al., 1993; Jones & Juggins, 1995), supplemented with newly collected recent and fossil materials from lakes and ponds on Beak Island (NE-Antarctic Peninsula, Chapters 6 and 7).

4.2. Material and methods

4.2.1. Study area

Livingston Island (62°40'S, 61°00'W) is situated in the South Shetland Islands. Samples were obtained from lakes in the largest ice-free area (i.e. the Beyers Peninsula, 50 km^2), consisting of an inland, upper-level area (between 85 and 193 m a.s.l.) and a low-level coastal area (Jones et al., 1993).

Livingston Island experiences a maritime Antarctic climate strongly influenced by the Westerly Winds, which implies higher precipitation rates and milder temperatures than in continental Antarctica (Van de Vijver et al., 2006; see Chapter 6 for more details). The island's geology consists of Jurassic-Cretaceous shales, sandstones and volcanic rocks (Hobbs, 1968). The snow-free ground is usually barren and rocky with a sparse vegetation, mainly comprising lichens and mosses in inland sites, and a more extensive cover of lichens, mosses and two flowering plants in the coastal areas (Van de Vijver et al., 2006; Jones et al., 1993). Most of the lakes on Livingston Island are situated on the barren central plateau. In summer, all lakes are ice-free and well mixed by wind. The lakes are generally nutrient poor, except for the brackish coastal lakes, which are heavily influenced by sea spray and in some cases by large animal populations (Jones et al., 1993).

Signy Island (60°43'S, 45°38'W) is a low-lying (max. height 279 m) island located in the South Orkneys. Approximately 32 % of the island is covered with a thin, climate-sensitive ice-cap (Hodgson & Convey, 2005). Similarly to Livingston Island, Signy has a maritime Antarctic climate (Van de Vijver et al., 2006). The island mainly consists of metamorphic rocks (schists), and the soils are generally more acid than those on Livingston Island (Jones et al., 1993). The ice-free areas of Signy Island are well vegetated with patches of mosses, lichens, and some flowering plants (Smith, 1972), and the catchments of the lakes are generally more densely vegetated than those on Livingston Island (Jones et al., 1993). Signy Island lakes become ice-free and well mixed in summer, but experience a (several weeks) shorter period of ice cover than those on Livingston Island, due to the lower snow accumumation, which causes a lower albedo at the lake surfaces (Jones et al., 1993). Lakes on Signy Island are generally more nutrient rich than those on Livingston Island, which is mainly due to the influence of animals (birds, fur seals) in the Signy lake catchments (Jones et al., 1993).

A detailed description of the geology and vegetation of both Signy and Livingston islands, and the physical, chemical and biological characteristics of the study lakes are given in Jones et al. (1993), Jones & Juggins (1995), Heywood et al. (1979; 1980) and references in these papers. Except for Oppenheim (1994), who described and illustrated several *Achnanthes* (s.l.) species, none of the other limnological and/or diatom studies in the area have provided illustrations.

Beak Island (63°36'S, 57°20'S) is a small, ice-free island located in the northern Prince Gustav Channel, between Eagle Island and Tabarin Peninsula. The island is assumed to either have the same continental climate regime as James Ross Island (50 km SW of Beak, with mean monthly temperatures below 0°C (Björck et al., 1996) or a climate in between maritime and continental (Hawes & Brazier, 1991), as winter temperatures only occasionally fall below -20°C (data for nearby Seymour Island, Jones & Limbert, 1989). James Ross Island is influenced by the rain shadow effect of the mountains of the Antarctic Peninsula (AP), and is probably characterized by yearly maximum precipitation values of 100-200 mm yr^{-1} (Sugden, 1982). Beak Island is composed of Miocenic volcanic rocks (James Ross Volcanic Island group; Bibby, 1966). The island contains a few lakes and shallow ponds, which have small, barren catchments, partly vegetated by moss banks (see Chapters 6 and 7). Details about the lakes and their limnology can be found in Sterken et al. (Chapter 6).

4.2.2. Sampling and microscopic analyses

For details of sampling and sample preparation of the Livingston and Signy Island materials from subfossil surface sediments, see Jones & Juggins (1995) and Jones et al. (1993). Detailed information on the Beak Island materials (recent, subfossil and fossil samples) can be found in Chapter 6. Samples from Beak Island were oxidized using hydrogen peroxide (Renberg, 1990); oxidized materials were mounted in Naphrax. Original light microscope (LM) pictures of all materials were taken with an Olympus DP50 camera on an Olympus CX 41 microscope at 10x100x magnification. SEM pictures were taken by use of a JEOL JSM5600LV (JEOL, Tokyo, Japan). Morphometric data (L= length, W = width, D = diameter, S = stria density, F = fibula density, FD = frustule depth) are given as ranges and number of specimens measured (n). Measurements of stria densities (S) refer to the central area and the apex (alongside the raphe). RLV refers to the rapheless valve and RV to the raphe valve in monoraphid species.

For the distribution of the listed diatom taxa among the three islands we refer to Table 5 in Chapter 6.

4.3. Checklist

Achnanthes cf. *muelleri* Carlson

Figs. 1-5

L: 33.0-37.4 μm (n = 6); W: 10.1-13.8 μm (n = 6); S: 10-11 in 10 μm (n = 6)

Our specimens are identical to the smaller specimens illustrated in Van de Vijver et al. (2002, Figs 5-7), which are narrower (10-14 vs. 16-21 μm) than those illustrated in the type description in Carlson (1913). In our specimens the rectangular fascia reaches the valve margin; this is not the case in the type illustrations and the larger specimens illustrated in Van de Vijver et al. (2002). This species is similar to *Achnanthes taylorensis* (Kellogg et al., 1980) but has a narrower fascia and a more rhombic valve outline (cf. Sabbe et al., 2003, figs. 1-2 and 74-75).

Achnanthidium cf. *exiguum* (Grunow) Czarnecki

Figs. 35-36

L: 8.1-18.2 μm (n = 8); W: 5.3-7.6 μm (n = 8); S: 22-27 in 10 μm (n = 8)

Basionym of *A. exiguum* (Grunow) Czarnecki: *Achnanthes exigua* Grunow

Our specimens closely match the description of *Achnanthes exigua* sensu Krammer & Lange-Bertalot (1991b), but differ in the presence of a clear, narrow asymmetric fascia on the RLV, extending to the valve margins [in Krammer & Lange-Bertalot (1991b; p. 294 Figs. 1-19)] the RLV only has a minor interruption in stria pattern, often only on one side of the valve and not extending to the valve margin].

Achnanthidium minutissimum (Kützing) Czarnecki s.l.

Figs. 24-27

L: 8.5-16.7 μm (n = 33); W: 2.0-2.9 μm (n = 33); S: 25-32 in 10 μm (n = 26)

Basionym: *Achnanthes minutissima* Kützing

Our specimens match the description and pictures of *Achnanthidium minutissimum* Kützing described in Round & Bukhtiyarova (1996) and Van de Vijver et al. (2002). This is a very variable taxon. A detailed morphometric and electron microscopic study is required to study variability within this taxon s.l. in the Antarctic region.

Adlafia bryophila (Petersen) Lange-Bertalot

Figs. 22-23

L: 13.3-20.3 µm (n = 6); W: 3.1-4.8 µm (n = 6); S: 21-30 in 10 µm (n = 5)

Basionym: *Navicula bryophila* Petersen

Our specimens match those illustrated in Lange-Bertalot (2001) and Van de Vijver et al. (2002) but have a lower stria density (21-30 vs. 29-36 and 30-38 in 10 µm respectively). According to Lange-Bertalot (2001) *Adlafia bryophila* may be conspecific with *A. muscora* (Kociolek & Reviers) Lange-Bertalot (Moser et al., 1998).

Adlafia cf. *minuscula* (Grunow) Lange-Bertalot

Figs. 28-29

L: 9.9-12.4 µm (n = 4); W: 2.8-3.6 µm (n = 4); striae indistinct in LM

Basionym of *A. minuscula* (Grunow) Lange-Bertalot var. *minuscula: Navicula minuscula* Grunow (in Van Heurck)

Our specimens match the description of *Adlafia minuscula* (var. *minuscula*) in Lange-Bertalot (2001). However, our valves are slightly smaller and have a slightly higher L/W ratio (i.e. 3.2-3.6 vs. 2.9-3.3 in Lange-Bertalot 2001, n = 7). *Adlafia minuscula* specimens illustrated in Van de Vijver et al. (2002) are larger and more robust (L: 14-16 µm; W: 4.6-6 µm; S: 35-40 in 10 µm). Details of the raphe and striae should be checked by SEM.

Amphora cf. *oligotraphenta* Lange-Bertalot

Figs. 6-13

L: 20.7-30.5 µm (n = 18); W: 3.8-5.5 µm (n = 18); S: 19-28 in 10 µm (n = 17)

Our specimens closely resemble those illustrated in Lange-Bertalot & Metzeltin (1996) for *Amphora oligotraphenta*, which is mainly separated from *A. veneta* on the basis of its ecology, with *A. veneta* preferring higher elektrolyte values (Lange-Bertalot & Metzeltin, 1996). However, no size range or description was given in Lange-Bertalot & Metzeltin (1996). Our specimens also closely match the description of *Amphora veneta* Kützing and the figure of *Amphora veneta* var. *capitata* Kützing in Krammer & Lange-Bertalot (1986; p. 744 Fig. 8). The apices of our specimens seem to be slightly more rounded and less capitate than those of the specimens in Krammer & Lange-Bertalot (1986). *Amphora veneta* Kützing illustrated in Sabbe et al. (2003) and Cremer et al. (2004) have less

pronounced capitate apices which are bent to the ventral side. This is a very variable taxon (or group of taxa) which requires further study.

Aulacoseira sp. 1

Figs. 46-58

Diameter: 8.9-12 µm (n = 8); FD: 6.15-10 µm (n = 5)

This taxon, which most probably belongs to the genus *Aulacoseira*, is uniquely characterized by the areolation pattern of the valve face, with the areolae strongly decreasing in size from the centre of the valve to the valve margin. Six to seven rimoportulae appear to be present along the valve margin (Figs. 51, 57). SEM is needed to elucidate the identification of this species.

Brachysira minor (Krasske) Lange-Bertalot

Figs. 14-16

L: 8.3-16.3 µm (n = 7); W: 2.6-3.7 µm (n = 7); striae indistinct in LM

Basionym: *Anomoeoneis minor* Krasske

Our specimens closely match the lectotype specimens from Chile illustrated in Lange-Bertalot et al. (1996) but are slightly smaller and appear to be more delicate. They are also smaller, have more broadly rounded apices and have slightly more linear-elliptic not rhombic-lanceolate valves than those from Southern Chile illustrated in Lange-Bertalot & Moser (1994; Figs. 1-7). The specimen from the Antarctic Peninsula illustrated in Lange-Bertalot & Moser (1994; Fig. 8) fully matches our specimens.

Caloneis cf. *bacillum* (Grunow) Cleve sensu auct. nonnull. (non sensu Grunow)

Figs. 17-21

L: 13.5-27.6 µm (n = 8); W: 4.1-5.5 µm (n = 6); S: 20-24 in 10 µm (n = 8); FD: 4 µm (n = 2)

Basionym of *C. bacillum* (Grunow) Cleve: *Stauroneis bacillum* Grunow

Our specimens fall within the range of the description given by Kelly et al. (2005; L: 15-48 µm; W: 4-9 µm; S: 20-30 per 10 µm). Our specimens are also in accordance with *Caloneis bacillum* (Grunow) Cleve as described and illustrated in Krammer & Lange-Bertalot (1986; p. 390, Fig. 173: 9-20), although our larger specimens tend to have a

smaller L/W-ratio (2.9-6.2 vs. 3.0-3.8). Variability in valve outline also seems to be greater in Krammer & Lange-Bertalot (1986) with our specimens most closely resembling their more linear forms (figs. 14-16). Van de Vijver et al. (2002) described this species as *Caloneis* cf. *bacillum* from Possession Island (Crozet Archipelago), but his specimens were generally larger (L: 22-42 µm; W: 4-6 µm; S: 22-26 per 10 µm). While the original *C. bacillum* (Grunow) Cleve is a typical brackish-marine taxon, many freshwater forms are now associated with this name. The taxonomic status of the latter requires further study.

Cavinula pseudoscutiformis (Hustedt) Mann & Stickle

Figs. 44-45
L: 9.4-10.7 µm (n = 4); W: 8.4-10.1 µm (n = 4); S: 19-24 in 10 µm (n = 4)
Basionym: *Navicula pseudoscutiformis* Hustedt

Our specimens closely match the description of this species given by Riaux-Gobin & Compère (2004). *C. kerguelensis* Riaux-Gobin & Compère has a higher stria density [25.4 striae in 10 µm; and less roundish valves (L/W: 1.26 vs. 1.06-1.14 in our specimens) (Riaux-Gobin & Compère 2004)]. *C. kerguelensis* might be marine, while *C. pseudoscutiformis* is a freshwater species.

Chamaepinnularia aliena (Krasske) Van de Vijver & Le Cohu

Figs. 367-370
L: 13.3-13.9 µm (n = 4); W: 3.3-3.6 µm (n = 4); S: 24-28 in 10 µm (n = 4)
Basionym: *Navicula aliena* Krasske (in Lange-Bertalot)

This taxon agrees with *Chamaepinnularia aliena* (Krasske) Van de Vijver & Le Cohu (L: 11-12 µm; W: 3-3.5 µm; S: 24-26 per 10 µm in Van de Vijver et al., 2002). *C. aliena* closely ressembles *C. evanida* but can be distinguished by its longer more lanceolate outline.

Chamaepinnularia australomediocris (Lange-Bertalot & Schmidt) Van de Vijver

Figs. 37-39
L: 8.8-12.0 µm (n = 6); W: 2.7-3.0 µm (n = 6); S: 21-29 in 10 µm (n = 6)
Basionym: *Navicula australomediocris* Lange-Bertalot & Schmidt

SEM and LM observations on our specimens fully correspond with those illustrated in Van de Vijver et al. (2002).

Chamaepinnularia cymatopleura (West & West) Cavacini

Fig. 80
L: 18.4 μm (n = 1); W: 4.7 μm (n = 1); S: 22 in 10 μm (n = 1)
Basionym: *Navicula cymatopleura* West & West

Our specimen corresponds to the description and illustrations for this species in Sabbe et al. (2003), Cremer et al. (2004) and Cavacini et al. (2006)

Chamaepinnularia gerlachei Van de Vijver & Sterken

Figs. 59-66
L: 13.7-29.9 μm (n = 16); W: 3.5-4.9 μm (n = 16); S: 15-20 in 10 μm (n = 16)

Chamaepinnularia gerlachei is described and discussed in Chapter 5.

Chamaepinnularia krookiformis (Krammer) Lange-Bertalot & Krammer

Figs. 81-90
L: 13.4-23.4 μm (n = 18); W: 3.1-5.4 μm (n = 18); S: 18-28 in 10 μm (n = 18)
Basionym: *Pinnularia krookiformis* Krammer

Our specimens correspond to those of this species illustrated in Lange-Bertalot & Genkal (1999) and with the description in Cavacini et al. (2006) but are slightly narrower than those in Cavacini et al. (2006; W: 5-11 μm).

Chamaepinnularia krookii (Grunow) Lange-Bertalot & Krammer

Figs. 70-73
L: 11.7-18.3 μm (n = 9); W: 3.7-4.1 μm (n = 9); S: 18-20 in 10 μm (n = 9)
Basionym: *Navicula krookii* Grunow

Our specimens correspond with the pictures of *Chamaepinnularia krookii* (Grunow) Lange-Bertalot & Krammer illustrated in Lange-Bertalot & Genkal (1999), and with the

descriptions given for this species in Cavacini et al. (2006). Our specimens however are narrower than those in Cavacini et al. (2006; W: 4-7 µm).

Chamaepinnularia sp. 1

Figs. 40-43

L: 8.1-9.4 µm (n = 5); W: 3.2-4.0 µm (n = 5); S: 25-32 in 10 µm (n = 5).

Our specimens resemble *Navicula* (?) sp. 2 in Sabbe et al. (2003) but the specimens illustrated there are narrower (2.6-3.0 µm). They are also similar to *Chamaepinnularia evanida* (Hustedt) Lange-Bertalot (cf. Krammer & Lange-Bertalot, 1986) but are wider, have a slightly larger central area and on average higher stria density (*N. evanida*: L: 8-10 µm; W: 3 µm; S: 24 in 10 µm, in Hustedt, 1942; L: 6-10 µm; W: 2.5-3 µm; S: 24-28 in 10 µm, in Krammer & Lange-Bertalot, 1986; L: 7-10 µm; W: 2-3 µm; S: 23-25 per 10 µm, in Van de Vijver et al., 2002). *Chamaepinnularia* sp. 1 also resembles *Chamaepinnularia spec*. in Van de Vijver et al. (2002; Pl. 86, Figs 15-22, W: 2-3 µm; S: 23-26 per 10 µm) are these are narrower and generally less finely striated.

Cocconeis placentula var. *euglypta* (Ehrenberg) Grunow

Fig. 79

L: 18.4 µm (n = 1); W: 12.8 µm (n = 1); S: 22 in 10 µm (n = 1)

Basionym: *Cocconeis Euglypta* Ehrenberg

Our single specimen matches the description given in Kelly et al. (2005) and Krammer & Lange-Bertalot (1986).

Craticula subpampeana Van de Vijver & Sterken

Figs. 110-111

L: 79.9-102.6 µm (n = 3); W: 16.9-19.1 µm (n = 3); S: 15 in 10 µm (n = 3)

Craticula subpampeana is described and discussed in Chapter 5.

Craticula antarctica Van de Vijver & Sabbe

Figs. 67-69

L: 23.5-29.5 µm (n = 8); W: 6.2-7.3 µm (n = 9); S: 17-20 in 10 µm (n = 9)

Craticula antarctica is described and discussed in Chapter 5.

Diadesmis australis Van de Vijver & Sabbe

Figs. 123-129

L: 6.3-16.7 µm (n = 18); W: 2.0 - 4.6 µm (n = 15); S: nvLM; D: 3 µm (n = 3)

Diadesmis australis is described and discussed in Chapter 5.

Diadesmis cf. *langebertalotii* Le Cohu & Van de Vijver

Figs. 140-148

L: 8.4-15.2 µm (n = 4); W: 2.1-2.6 µm (n = 4); S: striae indistinct in LM.

Our specimens closely match the description and illustrations for *Diadesmis langebertalotii* Le Cohu & Van de Vijver (2002). However, the constrictions at the valve ends are less pronounced than those illustrated in Le Cohu & Van de Vijver (2002; p. 127 figs. 42-47). *D. langebertalotii* may be conspecific with *Navicula nienta* Carter, described from Tristan da Cunha (Carter, 1966).

Diadesmis cf. *tabellariaeformis* (Krasske) Lange-Bertalot & Wojtal

Figs. 378-382

L: 10.4-13.7 µm (n = 7); W: 4.3-4.8 µm (n = 6); D: 2.6 µm (n = 1); S: 24-28 in 10 µm (n = 7)

Basionym of *D. tabellariaeformis* (Krasske) Lange-Bertalot & Wojtal: *Navicula tabellariaeformis* Krasske

Our specimens agree well with the description of the type of this species in Lange-Bertalot et al. (1996), but they are slightly smaller and narrower (L: 14-17 µm and W: 5.5-6 µm in Lange-Bertalot et al., 1996).

Diadesmis sp. 1

Figs. 112-116

L: 6.1-8.2 µm (n = 19); W: 2.2-3.7 µm (n = 19); S: 31-36 in 10 µm (n = 2)

This species strongly resembles *Diadesmis* sp. 1 in Cremer et al. (2004). However, our valves tend to be slightly wider (2-2.5 µm in Cremer et al., 2004), and striae were

sometimes resolvable in LM (not so in Cremer et al., 2004). *D. inconspicua* in Kopalova et al. (in press), which appears to be very similar to *Diadesmis* sp. 1 of Cremer et al. (2004), has a much higher stria density (31-32 vs. 50-60 in 10 µm in Kopalova et al., in press). Due to its small size this species can easily be confused with *Diadesmis comperei* Le Cohu & Van de Vijver and *D. ingeae* Van de Vijver. However, *D. ingeae* Van de Vijver is narrower and longer (see e.g. picture 5 l-p in Cremer et al., 2004), and *D. comperei* has a lower stria density (30-34 in10 µm, Le Cohu & Van de Vijver, 2002). *Diadesmis gallica* Smith has similar dimensions but bears spines along its margin (Sabbe et al., 2003), which are absent in our taxon.

Diadesmis sp. 2

Figs. 117-122

L: 7.8-26.9 µm (n = 10); W: 3.0-4.9 µm (n = 10); S: 25-31 in 10 µm (n = 10)

Encyonema minutum (Hilse in Rabenhorst) Mann

Figs. 92-98

L: 10.0-22.9 µm (n = 16); W: 4.5-6.1 µm (n = 16); S: 14-20 in 10 µm (n = 16)

Basionym: *Cymbella minuta* Hilse (in Rabenhorst)

Our specimens fit *Encyonema minutum* as described in Krammer & Lange-Bertalot (1986) and Kelly et al. (2005), both with respect to valve characteristics and dimensions. Fig. 98 could be an initial cell.

Eolimna minima (Grunow) Lange-Bertalot

Figs. 104-109, 130-139

L: 6.8-9.9 µm (n = 25); W: 2.5-3.3 µm (n = 25); S: 25-32 in 10 µm (n = 11)

Basionym: *Navicula minima* Grunow (in Van Heurck)

Our specimens match the description and pictures shown in Van de Vijver et al. (2002) for *Eolimna minima* (Grunow) Lange-Bertalot. This appears to be a variable species [cf. dimensions in Krammer & Lange-Bertalot (1986): L: 5-18 µm, W: 2-4.5 µm, S: 25-30 per 10 µm)]. The specimens shown in Figs. 104-109 differ from the others in having a wider central fascia.

Fragilaria capucina var. *capucina* Desmazières s.l.

Figs. 154-162

L: 22.6-54.2 µm (n = 14); W: 2.3-3.7 µm (n = 14); S: 16-19 in 10 µm (n = 14); L/W ratio: 8.6-19.5 (n = 14)

These specimens (form 1) correspond well with the description of *Fragilaria capucina* morphotype 2 in Van de Vijver et al. (2002; p. 44, Plate 7, Figs. 19-31). Some of our longest specimens (e.g. Figs. 155 and 162) could also belong to morphotype 3 (Van de Vijver et al., 2002).

Figs. 163-168

L: 13.4-26.2 µm (n = 12); W: 3.0-4.4 µm (n = 11); S: 17-19 in 10 µm (n = 12); D: 3 µm (n = 1); L/W ratio: 3.8-7.1 (n = 11)

These specimens (form 2) have the same characteristics as *F. capucina* morphotype 1 described in Van de Vijver et al. (2002; p. 41, Plate 7, Figs. 1-13). As in Van de Vijver et al. (2002) no difference in stria density was found between the different *F. capucina* morphotypes.

Gomphonema Ehrenberg spp.

Figs. 169-226

L: 13.5-39.9 µm (n = 125); W: 3.8-8.0 µm (n = 114); S: 10-26 in 10 µm (n = 124)

Our specimens belong to the variable species complex around *Gomphonema angustatum* (Kützing) Rabenhorst and varieties (e.g. *G. angustatum var. productum*) and similar species such as *G. micropus* Kützing (Reichardt, 1999), *G. gracile* Ehrenberg and *G. parvulum* Kützing. They are particularly common in the Antarctic (e.g. Wasell & Håkansson, 1992; Sabbe et al., 2003). Some valves are very similar to *Gomphonema signyensis* (e.g. Figs. 169-174) described by Kociolek & Jones (1995). A detailed morphometric and SEM analysis is necessary to elucidate variation patterns in this complex.

The *Hantzschia amphioxys* species complex

As the above *Gomphonema*, the species complex around *H. amphioxys* in (Sub)Antarctica is characterized by a high degree of morphological variability (see e.g. Ko-bayashi 1965 for the variability in Antarctic populations) and is in need of revision [cf. Sabbe et al. (2003) for a more detailed discussion of this complex]. Because *Hantzschia* was rather rare in our materials, we have as yet been unable to perform SEM studies. On the basis of LM, the following three morphotypes were provisionally distinguished.

Hantzschia cf. *amphioxys* (Ehrenberg) Grunow

Figs. 263-265

L: 28.4-53.2 μm (n = 3); W: 4.8-6.2 μm (n = 3); S: 22-24 in 10 μm (n = 3); F: 6-9 in 10 μm (n = 3)

Basionym of *H. amphioxys* (Ehrenberg) Grunow: *Eunotia amphioxis* Ehrenberg

This form corresponds to *Hantzschia* cf. *amphioxys* illustrated in Cremer et al. (2004; Figs. 8 a, b) and Van de Vijver et al. (2002, Pl. 123 Figs. 11-16).

Hantzschia sp. 1

Fig. 262

L: 53.0 μm (n = 1); W: 9.3 μm (n = 1); S: 19 in 10 μm (n = 1)

Hantzschia sp. 2

Figs. 259-261

L: 76.4-88.3 μm (n = 3); W: 12.9-13.4 μm (n = 3); S: 20-23 in 10 μm (n = 3); F: 5-6 in 10 um (n = 3)

Hantzschia sp. 1 and sp. 2 appear to be related to *H. abundans* Lange-Bertalot (Lange-Bertalot, 1993) and the Arctic species *H. hyperborea* (Grunow) Lange-Bertalot. *Hantzschia* sp. 2 closely resembles *Hantzschia* cf. *amphioxys* from the Larsemann Hills (E-Antarctica) as illustrated in Sabbe et al. (2003) but our specimens are wider.

Hippodonta hungarica (Grunow) Lange-Bertalot, Metzeltin & Witkowski

Figs. 227-230

L: 12.7-29.3 µm (n = 11); W: 3.9-6.4 µm (n = 10); D: 6.0 µm (n = 1); S: 9-11 in 10 µm (n = 11)

Basionym: *Navicula hungarica* Grunow

Our specimens correspond with the descriptions of this species in Krammer & Lange-Bertalot (1986) and Van de Vijver et al. (2002).

Luticola cf. *australomutica* Van de Vijver

Fig. 234

L: 24.0 µm (n =1); W: 7.1 µm (n = 1); S: 21 in 10 µm (n = 1)

This single specimen closely resembles *Luticola australomutica* (Van de Vijver & Mataloni, 2008) but appears to have smaller areaolae and a less transapically elongate axial area.

Luticola cf*. cohnii* (Hilse) Mann D.G. in Round et al. 1990

Figs. 235-236, 238-239

L: 10.1-30.7 µm (n = 8); W: 5.9-10.5 µm (n = 8); S: 14-21 in 10 µm (n = 8)

Basionym: *Stauroneis cohnii* Hilse

Our smaller specimens (e.g. Fig. 237) closely match the description of *Luticola cohnii* (Hilse) Mann given in Van de Vijver & Mataloni (2008). The larger specimens, which are characterized by lower stria densities than *L. cohnii* sensu Van de Vijver & Mataloni (2008) may belong to a separate taxon.

The *Luticola muticopsis* species complex

The species complex around the Antarctic endemic species *L. muticopsis* has been discussed in detail by Van de Vijver & Mataloni (2008) who clarified the identity of the type of this species.

Luticola cf. *muticopsis* s.s. (Van Heurck) Mann

Figs. 240-253

L: 15.3-29.4 µm (n = 16); W: 7.3-11.0 µm (n = 17); S: 12-19 in 10 µm (n = 17)

Basionym of *L. muticopsis* (Van Heurck) Mann : *Navicula muticopsis* Van Heurck

Our specimens closely resemble the description of the type of *Luticola muticopsis* (Van de Vijver & Mataloni, 2008) and *L. muticopsis* sensu Sabbe et al. (2003). However, many of our specimens have more distinctly capitate endings (hence cf.). Our specimens differ from the recently described *Luticola truncata* (Kopalova et al., in press) in the presence of a typically convex and one straight margin, and slightly more deflected central and terminal raphe endings.

***Luticola muticopsis* f. *reducta* West & West and f. *evoluta* West & West**

Figs. 231-233

L: 11.0-16.0 µm (n = 3); W: 6.3-6.4 µm (n = 3); S: 18-21 in 10 µm (n = 3)

These small *Luticola* specimens match the smaller *L. muticopsis* forms depected in Van de Vijver & Mataloni (2008; Figs. 78-89). They lack the typical rostrate-capitate apices and are more elliptic to elliptic-lanceolate with subrostrate ends. In the past, these forms have been identified as *L. muticopsis* f. *reducta* and f. *evoluta* (West & West, 1911; Ko-Bayashi, 1965). Until more populations are investigated from other Antarctic locations, it remains doubtful whether these forms only represent smaller forms of *L. muticopsis* s.s. or whether they should be described as an independent taxa (Van de Vijver & Mataloni, 2008).

***Luticola higleri* Van de Vijver, Van Dam & Beyens**

Figs. 254-258

L: 15.4-29.1 µm (n = 10); W: 6.8-10.8 µm (n = 10); S: 12-16 in 10 µm (n = 10)

Our specimens match the description of *Luticola higleri* (Van de Vijver et al., 2006) described from King George Island (South Shetland Islands). This species has previously been reported from Livingston Island under the name *Achnanthes kolbei* (Temniskova-Topalova et al., 1996; plate VI figs. 10-11). The species can be distinguished from *L. ledeganckii* Van de Vijver (Van de Vijver et al., 2002) by the weakly deflected central raphe endings (instead of being double curved) and the lower stria density (17-19 per 10 µm in *L. ledeganckii*).

Mayamaea cf. *atomus* var. *permitis* (Hustedt) Lange-Bertalot

Figs. 266-269

L: 6.2-7.0 μm (n = 5); W: 2.7-3.1 μm (n = 5); S: indistinct, ± 34 in 10 μm (n = 1)

Basionym of *Mayamaea atomus* var. *permitis* (Hustedt) Lange-Bertalot: *Navicula permitis* Hustedt

Our specimens closely match the description of this species given by Lange-Bertalot (2001; p. 136, 444) except for a small difference in width (3-4 μm in Lange-Bertalot, 2001). As SEM is needed to differentiate this species from *M. lacunolaciniata* (Lange-Bertalot & Bonik) Lange-Bertalot (see Lange-Bertalot, 2001), we refrain from making a positive identification.

Microcostatus cf. *naumannii* (Hustedt) Lange-Bertalot & Genkal

Figs. 270-273

L: 10.5-14.0 μm (n = 5); W: 4.2-4.5 μm (n = 5); S: 22-25 in 10 μm (n = 5)

Basionym of *Microcostatus naumannii* (Hustedt) Lange-Bertalot & Genkal: *Navicula naumannii* Hustedt

Our specimens differ from the holotype of *M. naumannii* illustrated in Krammer & Lange-Bertalot (1986) and Simonsen (1987) in the shape of the axial and central arean which are respectively less elongate and wider than the holotype.

Figs. 274-276

L: 9.4-9.6 μm (n = 3); W: 4.1-4.6 μm (n = 3); S: 24-26 in 10 μm (n = 3).

It is unclear whether these forms belong to the above taxon or whether they constitute a distinct taxon.

Muelleria australoatlantica Van de Vijver & Spaulding

Figs. 509-510

L: 40.2-41.2 μm (n = 2); W: 8.3-9.4 μm (n = 2); S: 18-19 in 10 μm (n = 2).

Muelleria australoatlantica is currently being described by Van de Vijver, Stanish & Spaulding (submitted).

Muelleria aequistriata Van de Vijver & Spaulding

Fig. 511

L: 27.8 µm (n = 1); W: 7.7 µm (n = 1); S: 20 in 10 µm (n = 1).

Muelleria aequistriata is currently being described by Van de Vijver, Stanish & Spaulding (submitted).

Navicula australoshetlandica Van de Vijver & Sabbe

Figs. 371-377

L: 13.8-20.8 µm (n = 24); W: 4.2-5.0 µm (n = 24); S: 13-15 in 10 µm (n = 24)

Navicula australoshetlandica is described and discussed in Chapter 5.

Navicula bicephala Hustedt

Figs. 280-284

L: 20.7-23.9 µm (n = 8); W: 3.7-4.3 µm (n = 8); S: 14-17 in 10 µm (n = 8)

Our specimens largely correspond to *N. bicephala* in Van de Vijver et al. (2002) but are on average slightly narrower.

Navicula cincta (Ehrenberg) Ralfs in Pritchard

Figs. 385-387

L: 25.2-31.5 µm (n = 4); W: 6.4-6.7 µm (n = 4); S: 10-11 in 10 µm (n = 4)

Basionym: *Pinnularia cincta* Ehrenberg

This species matches the size and description of *N. cincta* sensu Lange-Bertalot (2001).

Navicula gregaria Donkin

Figs. 291-295

L: 23.4-27.8 µm (n = 10); W: 5.8-6.8 µm (n = 10); S: 17-20 in 10 µm (n = 10)

Our specimens fully match the descriptions given in Lange-Bertalot (2001) for *N. gregaria*. We note, however, that there was much less variability in the size of our specimens and in the outline of the protracted ends, being subcapitate only, and not rostrate. Size ranges in Lange-Bertalot (2001) are 13-44 µm (length), 5-10 µm (width)

and striae density (13)15-18(20) per 10 μm. On intraspecific level our specimens correspond best with the description and illustrations provided for '*Navicula gregaria* B' in Cox (1987), a widespread form with nearly similar dimensions [i.e. L: 18-26 μm; W: 5-6 μm; S: 18-22 per 10 μm; Cox (1987)], which could be conspecific with *Navicula gregalis* Cholnoky 1963 (Cox, 1987).

Navicula cf. *libonensis* Schoeman

Figs. 285-290
L: 26.0-31.1 μm (n = 17); W: 4.7-6.6 μm (n = 17); S: 13-16 in 10 μm (n = 16)

Our specimens correspond to *N. libonensis* as described by Lange-Bertalot (2001).

Navicula cf. *obsoleta* Hustedt

Figs. 317-324, 325-330
L: 7.3-13.4 μm (n = 24); W: 2.4-3.2 μm (n = 24); S: 18-25 in 10 μm (n = 24)

Two forms have been grouped together under this taxon. One (Figs. 317-324) has a finer striation, a more lanceolate valve outline and narrower valve apices, the other (Figs. 325-330) has a more elliptic valve outline with less protracted and more rounded valve apices. Both forms have been tentatively placed in *Navicula obsoleta* Hustedt (Krammer & Lange-Bertalot, 1986). They also resemble *N. vaucheriae* Petersen (Krammer & Lange-Bertalot, 1986), which may be conspecific with *N. obsoleta*.

'Naviculadicta' elorantana Lange-Bertalot

Figs. (301-303?), 304-308, (309-316?)
L: 8.0-14.3 μm (n = 23); W: 3.4-4.6 μm (n = 23); S: 18-24 in 10 μm (n = 23).

Our specimens closely resemble '*Naviculadicta' elorantana* as illustrated in Van de Vijver et al. (2002). It is not sure whether some smaller specimens (e.g. Figs. 309-310, 311-312, 315-316) also belong to this taxon as the central area is much smaller. Some of these smaller forms are hard to distinguish from smaller specimens belonging to *Sellaphora* or *Chamaepinnularia* cf. *krookiformis* (cf. Figs. 74-78, 91) and *Incertae sedis* - pennate diatom sp. 1 (Figs. 383-385). Our longest specimens (Figs. 301-303) are longer than those in Van de Vijver et al. (2002). '*Naviculadicta' elorantana* also resembles

‘*Naviculadicta’ seminulum* Grunow (Van de Vijver et al., 2002) but this taxon typically has elliptical valves with non-produced apices.

‘Naviculadicta’ seminulum (Grunow) Lange-Bertalot

Figs. 331-342, (343-348?)
L: 5.9-13.6 µm (n = 32); W: 2.4-4.2 µm (n = 32); S: 17-23 in 10 µm (n = 31)
Basionym: *Navicula seminulum* Grunow

Our specimens agree with the description of this taxon in Van de Vijver et al. (2002). This taxon probably belongs in the genus *Sellaphora* Mereschkowski (as *Sellaphora seminulum* (Grunow) Mann).

Nitzschia gracilis Hantzsch

Figs. 486-501
L: 26.0-42.7 µm (n = 15); W: 2.6-3.6 µm (n = 15); S: indistinct in LM; F: 14-19 in 10 µm (n = 15)

Our specimens resemble *Nitzschia gracilis* Hantzsch (cf. Krammer & Lange-Bertalot, 1988; Van de Vijver et al., 2002). Our valves are slightly smaller and have narrower and longer apices than those illustrated in Van de Vijver et al. (2002).

Nitzschia frustulum (Kützing) Grunow

Figs. 414-424
L: 8.7-18.0 µm (n = 54); W: 2.6-4.3 µm (n = 56); S: 23-30 in 10 µm (n = 55); F: 10-15 in 10 µm (n = 51)
Basionym: *Synedra frustulum* Kützing

Our specimens match the description of *N. frustulum* var. *frustulum* in Van de Vijver et al. (2002), although valve variability seems to be larger in our specimens. Most of our specimens also match the illustrations in Cremer et al. (2004), but some tend to have higher stria densities (S: 22-25 per 10 µm in Cremer et al., 2004). It is possible that small specimens of *N. acidoclinata* (see Van de Vijver et al., 2002) have been included here. According to these authors this species is usually identified as *N. frustulum*, and SEM studies are needed in order to differentiate the two. Van de Vijver et al. (2002) note that

N. frustulum var. *kerguelensis* (described by Bourrelly & Manguin, 1954) may in fact be identical to *N. acidoclinata*.

Nitzschia homburgiensis **Lange-Bertalot**

Figs. 502-504

L: 29.5-37.6 μm (n = 12); W: 4.0-5.1 μm (n = 12); S: 32-36-nvLM in 10 μm (n = 4); F: 10-16 in 10 μm (n = 12)

Our specimens correspond with *Nitzschia homburgiensis* Lange-Bertalot as illustrated in Krammer & Lange-Bertalot (1988).

Nitzschia inconspicua **Grunow**

Figs. 425-469

L: 7.6-19.3 μm (n = 13); W: 2.4-3.4 μm (n = 13); S: 25-32 in 10 μm (n = 13); F: 9.0-14.7 in 10 μm (n = 12)

Our specimens are similar to those illustrated in Van de Vijver et al. (2002). The exact taxonomical position of this taxon is still unclear - it is sometimes considered to be a variety of *N. frustulum* (Van de Vijver et al., 2002).

Nitzschia paleacea **Grunow**

Figs. 470-485

L: 17.9-41.7 μm (n = 20); W: 1.7-3.3 μm (n = 20); S: 27 in 10 μm (n = 1), usually indistinct in LM (n = 19); F: 14-18 in 10 μm (n = 20)

Our specimens correspond with those illustrated in Krammer and Lange-Bertalot (1988).

Nitzschia perminuta **(Grunow) Peragallo**

Figs. 388-413

L: 11.4-27.8 μm (n = 85); W: 2.1-3.5 μm (n = 80); S: 21-32 in 10 μm (n = 80); F: 5-10 in 10 μm (n = 84); FD: 2-3 μm (n = 5)

Basionym: *Nitzschia palea* var. *perminuta* Grunow (in Cleve & Grunow)

Some specimens show features typical of *N. acidoclinata* Lange-Bertalot and *Nitzschia liebetruthii* Rabenhorst var. *liebetruthii* (see Van de Vijver et al., 2002).

Nitzschia cf. *pusilla* Grunow

Figs. 505-508

L: 26.7-30.6 µm (n = 9); W: 4.0-4.6 µm (n = 9); S: nvLM; F: 18-23 in 10 µm (n = 9)

Our specimens are slightly wider and have less produced apices than those illustrated in Van de Vijver et al. (2002). *Nitzschia communis* Rabenhorst in Van de Vijver et al. (2002) has lower stria and fibula densities and longer valves.

Orthoseira roeseana (Rabenhorst) O'Meara

Figs. 30-34

D: 15.3-30.3 µm (n = 4); mantle depth: 9 µm (n = 1).

Basionym: *Melosira roeseana* Rabenhorst

Orthoseira roeseana from Crozet has a valve diameter of 10-45 µm and a mantle depth of 5-10 µm (Van de Vijver et al., 2002). Diameter was 8-70 µm and mantle depth of 6-13 µm in Krammer et al. (1991a; p. 250, Tafel 10 Figs. 1-11, p. 252, Tafel 11 Figs. 1-2). Linking spines were not observed in our specimens.

Pinnularia borealis Ehrenberg 1843

Figs. 544-545

L: 26.8-41.1 µm (n = 4); W: 7.6-10.6 µm (n = 4); S: 5-6 in 10 µm (n = 4)

Our specimens match *P. borealis* of the Larsemann Hills (Sabbe et al., 2003). Similar valves have been placed in *P. borealis* var. *scalaris* (Ehrenberg) Rabenhorst by Van de Vijver et al. (2002), which is regarded as a synonym of *P. borealis* var. *rectangularis* Carlson 1913 (Krammer, 1992). As Van de Vijver et al. (2002) state, it is difficult to distinguish the different varieties of *P. borealis*.

Pinnularia cf. *divergens* var. *linearis* Oestrup 1910

Figs. 552-554

L: 94.5-111.5 µm (n = 3); W: 17.6-20.4 µm (n = 3); S: 10 in 10 µm (n = 3)

Our specimens closely resemble this taxon as illustrated in Krammer (1992; 2000) but are wider than those in Krammer (1992; 2000; 13-17 and 12-16 µm respectively).

Pinnularia gemella Van de Vijver

Figs. 540-543

L: 40.1-57.8 µm (n = 5); W: 6.9-8.5 µm (n = 5); S: 10-11 in 10 µm (n = 5)

This species is currently being described by Van de Vijver et al. (in prep., pers. comm.).

Pinnularia cf. *kolbei* Manguin

Figs. 681-683

L: 23.4-38.6 µm (n = 3); W: 8.6-11.0 µm (n = 3); S: 13-15 in 10 µm (n = 3), L/W: 3.0-3.8 (n = 3)

Our specimens resemble *P. kolbei* in Bourrelly & Manguin (1954) but have a raphe that is less bended, a narrower axial area and a distinctly bow-tie shaped central area.

Pinnularia microstauron (Ehrenberg) Cleve s.l.

Figs. 516-522

L: 32.9-54.0 µm (n = 14); W: 6.6-9.8 µm (n = 12); S: 12-15 in 10 µm (n = 14); FD: 8-10 µm (n = 2)

Basionym: *Stauroptera microstauron* Ehrenberg

Our specimens agree with the concept of this species of Krammer (1992; 2000) and Van de Vijver et al. (2002). Different varieties and morphotypes (cf. Krammer 1992; 2000) have been described within this taxon (see also below) which is in need of revision.

Pinnularia cf. *microstauron* (Ehrenberg) Cleve var. *nonfasciata* Krammer

Figs. 512-515, 523-529

L: 37.0-55.4 µm (n = 11); W: 8.0-12.3 µm (n = 11); S: 11-13 in 10 µm (n = 11)

Similar specimens belonging to this species illustrated in Krammer (2000) are slightly wider (13.4-14 µm). Our specimens match the illustrations of the type specimens of *P. krasskei* var. *ventricosa* Hustedt in Simonsen (1987) from South Georgia.

Pinnularia cf. *obscura* Krasske

Figs. 546-547

L: 25.1-25.6 µm (n = 3); W: 5.8-6.1 µm (n = 3); S: 9-11 in 10 µm (n = 3)

Our specimens look similar to *Pinnularia obscura* Krasske as illustrated in Van de Vijver et al. (2002) but have a slightly lower stria density. The lectotype of *P. obscura* (Lange-Bertalot et al., 1996) is narrower and has a higher stria density (15 striae in per 10 µm). In Krammer (1992) and Krammer & Lange-Bertalot (1986) *P. obscura* has a width of 3-6.5 µm and a stria density of 11-15 in 10 µm. Our specimens also need to be further compared to *P. intermedia* (Lagerstedt) Cleve (Krammer & Lange-Bertalot, 1986) and *P. schoenfelderi* Krammer (Krammer, 1992). *P. schoenfelderi* and *P. obscura* have often been confused in the past (Krammer, 2000).

Pinnularia cf. *splendida* Hustedt

Fig. 555

L: 65.2-90.3 µm (n = 2); W: 19.8-23.0 µm (n = 2); S: 4-5 in 10 µm (n = 2)

Our specimens match the description and illustrations for this species in Krammer (2000; p. 21, Fig. 4: 2-6).

Pinnularia subantarctica var. *elongata* (Manguin) Van de Vijver & Le Cohu

Figs. 548-551

L: 28.5-40.1 µm (n = 8); W: 6.0-7.0 µm (n = 8); S: 14-16 in 10 µm (n = 8)

Basionym: *Pinnularia microstauron* var. *elongata* Manguin

Our specimens match the descriptions and pictures in Van de Vijver et al. (2002; p. 96).

Placoneis cf. *elginensis* (Gregory) Cox s.l.

Figs. 296-300

L: 22.5-24.9 µm (n = 5); W: 6.6-8.2 µm (n = 5); S: 14-15 in 10 µm (n = 5).

Basionym of *P. elginensis* (Gregory) Cox: *Navicula elginensis* Gregory

Our valves show similarities with the species complex around *Placoneis elginensis* s.l. (see Cox, 2003). However, it was difficult to assign them to either *P. elginensis* (Gregory) Cox, *P. anglica* (Ralfs) Cox, *P. pseudoanglica* (Lange-Bertalot) Cox or *P.*

paraelginensis Lange-Bertalot. Our specimens have higher stria densities than any of these species (all between 10-12 striae in 10 μm) (Cox 2003). In addition, many specimens display a combination of features typical for different *Placoneis* species. For example, the specimen in Fig. 296 has a linear valve outline (like *P. elginensis* and *P. paraelginensis*) but has a small, elliptic central area (like in *P. pseudoanglica*).

Planothidium delicatulum (Kützing) Round & Bukhtiyarova s.l.

Figs. 577-581
L: 15.0-25.9 μm (n = 13); W: 5.7-8.6 μm (n = 13); S: 13-18 in 10 μm (n = 13).
Basionym: *Achnanthidium delicatulum* Kützing

Our specimens correspond to the description in Round & Bukhtiyarova (1996), although our stria densities are on average slightly higher.

Planothidium frequentissimum (Lange-Bertalot) Round & Bukhtiyarova

Figs. 556-560, 572-573?
L: 12.4-18.0 μm (n = 14); W: 4.3-5.7 μm (n = 14); S: 13-17 in 10 μm (n = 14).
Basionym: *Achanthes lanceolata* var. *dubia* f. *minuta* Grunow (in Van Heurck)

Our specimens generally match the description of this taxon in Krammer et al. (1991b; *Achnanthes lanceolata* spp. *frequentissima* Lange-Bertalot) and are characterized by a typical "double arched" structure in the centre of the valve, caused by the presence of an internal capped structure. However, most specimens have a more elongate valve outline and more produced, almost rostrate apices than those illustrated in Krammer et al. (1991b); only a few smaller valves were more elliptical. The morphological variability in this taxon needs to be further investigated; the elongate, lanceolate form (Figs. 556-557, 560, 572) was dominant in our samples.

Planothidium lanceolatum (Brébisson) Round & Bukhtiyarova s.l.

Figs. 566-571, 574-576
L: 10.9-28.8 μm (n = 20); W: 4.6-8.1 μm (n = 20); S: 13-16 in 10 μm (n = 20).
Basionym: *Achnanthidium lanceolata* (Brébisson) Grunow (in Cleve & Grunow)

We refer to our specimens as *P. lanceolatum* s.l. because the species complex around *P. lanceolatum* is not clearly resolved, with many existing varieties which are in need of revision (Oppenheim 1994; cf. also the two taxa above which were originally described

as varieties of *P. lanceolatum*). The illustrations in Oppenheim (1994; as *Achnanthes lanceolata* (Brébisson) Grunow) agree with our specimens, both in valve morphology and dimensions. The main distinguishing feature of this taxon is the distinct sinus being a simple depression not a "double arched" structure (see *P. frequentissimum*). The elliptic forms with rounded endings were most often found on Signy Island, while the larger, elliptic-lanceolate forms with produced apices were dominant on Livingston Island. In our samples from Beak Island no clear dominant morphology was observed.

***Planothidium quadripunctatum* (Oppenheim) Sabbe**

Figs. 582-587

L: 7.3-9.2 μm (n = 15); W: 2.7-4.7 μm (n = 15); S: 15-21 in 10 μm (n = 15).

Basionym: *Achnanthes quadripunctata* Oppenheim

Our specimens correspond well to those described in Oppenheim (1994), Van de Vijver et al. (2002) and Sabbe et al. (2003). For a detailed description of this species, see there. It is often difficult to distinguish this species from *Planothidium renei* (see below), which has a higher stria density (viz. 20-24 in 10 μm) and a different ultrastructure (terminal raphe endings are deflected in the same direction in *P. quadripunctatum* and in opposite directions in *P. renei*, and the striae are composed of 3-4 instead of 2 transapical rows of areolae in the latter). Preliminary SEM investigations have shown that some populations which were assigned to *P. quadripunctatum* on the basis of valve dimensions displayed ultrastructural features typical of *P. renei* in SEM. There also appears to be an overlap in stria densities in some populations. Further SEM and morphometric analyses are needed to resolve the relationship between these two species.

***Planothidium renei* (Lange-Bertalot & Schmidt) Van de Vijver**

Figs. 588-592

Recent materials (Livingston, Signy, Beak): L: 6.9-9.7 μm (n = 15); W: 3.7-4.2 μm (n = 15); S: 18-27 in 10 μm (n = 14).

Subfossil and fossil (core Lake Beak-1, cf. Chapters 6 and 7): L: 7.6-9.4 μm (n = 76); W: 3.8-4.6 μm (n = 76); S: 17-24 in 10 μm (n = 76)

Basionym: *Achnanthes renei* Lange-Bertalot & Schmidt (in Schmidt et al.)

Our specimens closely resemble *P. renei* as described in Van de Vijver et al. (2002), but stria densities were significantly more variable in our specimens (cf. 20-24 per 10 μm in

Van de Vijver et al., 2002). *P. renei* is sometimes difficult to distinguish from *P. quadripunctatum* (cf. above).

Planothidium sp. 1

Figs. 561-565

L: 17.4-23.7 µm (n = 12); W: 4.0-5.6 µm (n = 11); S: 14-17 in 10 µm (n = 12); D: 3 µm (n = 1).

The taxon closely resembles *Planothidium haynaldii* (Schaarschmidt) Lange-Bertalot & Genkal illustrated in Patrick & Reimer (1966) but differs in having an asymmetrical central area. *Achnanthes semifasciata* (Østrup) Foged sensu Foged (1974) has an asymmetrical central area but the original description in Østrup (1918) shows a more rhombical species. The Antarctic specimens probably represent a new species.

Psammothidium abundans (Manguin) Bukhtiyarova & Round

Figs. 599-605

L: 8.0-13.1 µm (n = 34); W: 3.2-4.7 µm (n = 34); S: 25-32 (often indistinct in LM) in 10 µm (n = 23).

Basionym: *Achnanthes abundans* Manguin (in Bourelly & Manguin)

Our specimens generally agree well with the extensive descriptions given by Bukhtiyarova & Round (1996), Sabbe et al. (2003) and Van de Vijver et al. (2008b, includes type material) but our specimens tend to be smaller and narrower. Further details on this species can be found in Bourrelly & Manguin (1954), Le Cohu & Maillard (1983) and Oppenheim (1994). This species was identified as *Achnanthes mollis* Krasske in Jones & Juggins (1995).

Psammothidium germainii (Manguin) Sabbe

Figs. 635-637 (form 1), 625-634 (form 2)

Dimensions form 1: L: 11.2-21.2 µm (n = 6); W: 6.5-8.8 µm (n = 6); S: 17-19 in 10 µm (n = 6)

Dimensions form 2: L: 13.2-18.3 µm (n = 13); W: 5.6-8.9 µm (n = 13); S: 21-28 in 10 µm (n = 13).

Basionym: *Achnanthes germainii* Manguin (in Bourelly & Manguin)

Form 1 has produced, almost rostrate apices and corresponds to the type specimens of this species shown in Bourelly & Manguin (1954). Similar forms were found in Oppenheim (1994) and Sabbe et al. (2003; except for their higher stria density of 20-21 in 10 μm). Form 2 is more lanceolate, lacks the produced apices and appears to have higher stria densities. Similar forms were illustrated by Van de Vijver et al. (2002) from Crozet. These forms need further investigation.

Psammothidium incognitum (Krasske) Van de Vijver

Figs. 593-598

L: 10.4-15.5 μm (n = 16); W: 4.5-5.6 μm (n = 16); S: 29-35 in 10 μm (n = 7).

Basionym: *Achnanthes incognita* Krasske (in Krasske)

Our specimens agree with those illustrated in Van de Vijver et al. (2002). *P. incognitum* (as *Achnanthes incognita* Krasske, 1939) was previously reported from Signy Island (Moss Lake, Khyber Lakes) by Oppenheim (1994). *P. incognitum* closely resembles *P. stauroneioides* (Manguin) Bukhtiyarova in shape, size and stria density, but differs in the shape of the central area on the rapheless valve, which is large and distinctly rhombic in the latter, not small and circular [cf. Van de Vijver et al. (2002) and Sabbe et al. (2003)], and possibly also the absence of an external terminal pore in the axial area of the rapheless valve [Oppenheim (1994); note that this pore is also not always present in *P. stauroneioides*, cf. Van de Vijver et al. (2002)].

Psammothidium cf. *investians* (Carter) Bukhtiyarova

Figs. 610-612

L: 13.4-14.9 μm (n = 3); W: 5.7-6.0 μm (n = 3); S: 26-31 in 10 μm (n = 3)

Basionym of *P. investians* (Carter) Bukhtiyarova: *Achnanthes investians* Carter

Our specimens resemble those shown in Van de Vijver et al. (2002) and those in Lange-Bertalot & Krammer (1989), which are based on the type material (BM 77587) from Tristan da Cunha (Carter, 1966). However, as they have a more lanceolate-rhombic valve outline (not elliptic) and the central area is larger than in the type illustrations, we as yet refrain from making a positive identification. This taxon should also be compared with *Achnanthes atlanta* Carter, *Achnanthes ninkei* Guermeer & Manguin and *A. laevis* Østrup.

Psammothidium manguinii (Hustedt) Van de Vijver

Figs. 606-609

L: 12.9-15.2 µm (n = 3); W: 5.9-6.4 µm (n = 3); S: 20-24 in 10 µm (n = 3)

Basionym: *Achnanthes manguinii* Hustedt

Our specimens are on average smaller and have a higher stria density than those illustrated in Oppenheim (1994; L: 15-22 µm, W: 6-9 µm, S: 15-20 per 10 µm (n =5)) but correspond well with the description of this species given by Bourrelly & Manguin (1954) and Van de Vijver et al. (2002).

Psammothidium metakryophilum (Lange Bertalot & Schmidt) Sabbe

Figs. 613-618

L: 8.3-15.4 µm (n = 36); W: 3.5-5.9 µm (n = 36); S: 24-33 in 10 µm (n = 33)

Basionym: *Achnanthes metakryophila* Lange-Bertalot & Schmidt (in Schmidt et al.)

Our specimens match those illustrated in Cremer et al. (2004) and Sabbe et al. (2003) but have a broader range in stria density. A detailed description of this species, comparison with similar species and notes on synonymy and biogeography are given in Sabbe et al. (2003).

Psammothidium subatomoides (Hustedt) Bukhtiyarova & Round

Figs. 619-624

L: 7.7 - 10.5 µm (n = 21); W: 4.5 - 5.4 µm (n = 21); S: 29 - 41 in 10 µm (n = 15)

Basionym: *Navicula subatomoides* Hustedt (in Schmidt)

Our specimens agree with those illustrated in Bukhtiyarova & Round (1996). Oppenheim (1994) found this species (as *Achnanthes subatomoides* (Hustedt) Lange-Bertalot & Archibald) in Heywood Lake (Signy Island).

Sellaphora sp. 1

Figs. 349-355

L: 17.2-18.9 µm (n = 6); W: 4.2-4.6 µm (n = 6); S: 28-33 in 10 µm (n = 2), often indistinct in LM.

Most of our specimens (especially the larger forms, Figs. 349-356) have valve outlines very similar to '*Naviculadicta' nana* (Hustedt) Lange-Bertalot (Lange-Bertalot, 1996). The holotype of this taxon however is relatively short with less protracted apices and has a stria density of about 40 striae in 10 μm (Lange-Bertalot, 1996).

***Stauroforma inermis* Flower, Jones & Round**

Figs. 638-640

L: 8.8-21.9 μm (n = 15); W: 3.2-4.4 μm (n = 15); S: 19-23 in 10 μm (n = 15)

Our specimens correspond with the descriptions and dimensions of this species in Van de Vijver et al. (2002). SEM observations (not shown) however, while revealing the absence of spines along the valve margin, did not reveal an apical pore field. The closely similar species *S. exiguiformis* (Lange-Bertalot) Flower, Jones & Round would have spines but no apical pore field. However, as in our specimens, the diagnositic features do not always match (cf. discussion in Van de Vijver et al. (2002) and Sabbe et al., 2003). Further research is necessary to assess whether we are deadling with two different species or not.

***Stauroneis* aff. *acidoclinata* Lange-Bertalot & Werum**

Figs. 669-674

L: 40.4-71.3 μm (n = 20); W: 10.0-13.2 μm (n = 20); S: 20-25 in 10 μm (n = 20)

This taxon resembles *S.* aff. *acidoclinata* illustrated in Van de Vijver et al. (2004a), but our specimens are narrower and have an on average higher stria density (W: 8.5-10 μm and S: 21-22 per 10 μm in *S.* aff. *Acidoclinata*; Van de Vijver et al., 2004).

***Stauroneis husvikensis* Van de Vijver & Lange Bertalot**

Fig. 687

L: 35.0 μm (n = 1); W: 6.5 μm (n = 1); S: 24 in 10 μm (n = 1)

The valve morphology of our single specimen matches the description of *S. husvikensis* from Husvik, South Georgia in Van de Vijver et al. (2004a).

***Stauroneis latistauros* Van de Vijver & Lange-Bertalot**

Figs. 667-668, 675-680

L: 30.9-58.3 μm (n = 16); W: 7.4-10.2 μm (n = 16); S: 18-22 in 10 μm (n = 16)

Our specimens match the description of *Stauroneis latistauros* in Van de Vijver et al. (2004a) and Sabbe et al. (2003; as *S. anceps* Ehrenberg; note that these have a higher stria density, viz. 22.5-25.5 in 10 µm).

The *Stauroneis* cf. *subgracilior* Lange-Bertalot et al. species complex

Several morphotypes could be distinguished within this taxon. Further research is needed to assess whether we are dealing with different entities of a single species.

Stauroneis cf. *subgracilior* Lange-Bertalot et al. form 1

Fig. 655

L: 39.3-51.8 µm; W: 7.5-8.5 µm; S: 22-26 per 10 µm; L/W: 5.0-6.1 (n = 8)

This form closely resembles *Stauroneis bryocola* Van de Vijver & Lange-Bertalot as described in Van de Vijver et al. (2004a). *Stauroneis sofia* Van de Vijver & Lange-Bertalot is also very similar, but is slightly larger and wider and has a slightly higher stria density (L: 47-82 µm, W: 8-10.5 µm, S: 25-26 per 10 µm; Van de Vijver et al., 2004a), and has a hyaline area around the central fascia and a ridge alongside the raphe.

Stauroneis cf. *subgracilior* Lange-Bertalot et al. form 2

Figs. 656-662, 664

L: 21.7-51.4 µm; W: 5.4-7.7 µm; S: 21-25 per 10 µm

This form resembles *Stauroneis subgracilior* 'Peninsula' Van de Vijver (2004a; manuscript name, Plate 69). However, our specimens have a lower stria density (26-28 in 10 µm in Van de Vijver et al., 2004a). Figs. 661-662 possibly represent resting stages. Interestingly, Figs. 660 and 661 represent two valves of the same frustules.

Stauroneis cf. *subgracilior* Lange-Bertalot et al. form 3

Fig. 663

L: 36.6 µm; W: 8.2 µm; S: 23 per 10 µm.

This specimen possibly belongs to *S.* cf. *subgracilior* Lange-Bertalot et al. form 2, but is provisionally separated on the basis of its narrower and very rectangular stauros. As stated above, more research on this group is needed.

Stauroneis cf. *subgracilior* Lange-Bertalot et al. form 4

Figs. 665-666

L: 41.7-42.8 µm; W: 9.1-9.7 µm; S: about 25 in 10 µm, indistinct

The valves of this group have a more rhombic outline and a narrower stauros than the other forms. These valves were found in one sample from Signy Island (SG-10).

Staurosira cf. *venter* (Ehrenberg) Cleve & Möller

Figs. 645-647

L: 8.6-13.4 µm (n = 7); W: 3.8-4.5 µm (n = 7); S: 13-14 in 10 µm (n = 7)

Synonym: *Fragilaria venter* Ehrenberg

Our specimens differ from the *Staurosira venter* depicted in Cremer et al. (2004) and Van de Vijver et al. (2002) in valve shape (not elliptical or lanceolate but more rhombic with produced, rounded apices) and lower stria density [cf. 16 and 20 in 10 µm in Cremer et al. (2004) and Van de Vijver et al. (2002) respectively)]. This taxon should also be compared with *Staurosira aventralis* in Rumrich et al. (2000).

Staurosira alpestris (Krasske) Van de Vijver

Figs. 149-153

L: 12.3-22.1 µm (n = 15); W: 2.7-5.2 µm (n = 14); S: 12-18 in 10 µm (n = 15); D: 3-5 µm (n = 3)

Basionym: *Fragilaria alpestris* Krasske (in Hustedt)

Our specimens agree with *S. alpestris* illustrated in Van de Vijver et al. (2002).

Staurosira *cf.* circula *Van de Vijver & Beyens*

Figs. 99-103

L: 5.3-6.7 µm (n =11); W: 5.5-7.0 µm (n = 8); D: 4.4-6.7 (n = 3); S: ± 18 in 10 µm (n = 11)

In LM, our specimens resemble *Staurosira circula* (Van de Vijver et al., 2002) and *Nanofrustulum shiloi* (Lee, Reimer & McEnery) Round, Hallsteinsen & Paasche (cf. Sabbe et al., 2003). Small representatives of *Staurosira* and related genera are notoriously difficult to identify and require SEM.

Staurosirella pinnata (Ehrenberg) Williams & Round

Figs. 641-644

L: 8.9-14.3 µm (n = 5); W: 2.8-4.3 µm (n = 5); S: 8-10 in 10 µm (n = 5)

Basionym: *Fragilaria pinnata* Ehrenberg

Our specimens closely ressemble the valve shown in Cremer et al. (2004) but they have a lower stria density (15 striae in 10 µm in Cremer et al., 2004). This is a difficult species (probably a species complex) in need of revision (cf. Rumrich et al., 2000, Paull et al., 2008).

Surirella sp. 1

Fig. 684-685

L: 41.6-51.9 µm (n = 4); W: 15.4-17.0 µm (n = 4); S: 22-26 in 10 µm (n = 4)

This unknown *Surirella* needs further investigation.

Incertae sedis – pennate diatom sp. 1

Figs. 74-78, 91, 383-385

L: 12.2-14.9 µm (n = 5); W: 4.2-4.8 µm (n = 5); S: 20-22 in 10 µm (n = 5)

Unidentified forms

The following forms remain as yet unidentified due to the rarity of the material: *Amphipleura* sp. (Figs 651-652), *Eunotia* spp. (Figs. 653 and 654), *Gomphonemopsis* sp. (Figs. 648-650), *Pinnularia* spp. (Figs. 530-539) and Incertae sedis (Figs. 356-366, 686a,b).

4.4. Summary

This paper presents the results of a detailed taxonomic intercalibration of freshwater diatom materials from three islands in the vicinity of the Antarctic Peninsula, viz. Signy Island (South Orkneys), Livingston Island (South Shetlands) and Beak Island (James Ross Island group). The materials from Signy and Livingston Islands have previously been examined and used for the construction of diatom transfer functions (Jones et al., 1993; Jones & Juggins, 1995) but a taxonomic survey was never published. As during the

recent decade numerous new studies on the taxonomy of (Sub)Antarctic diatoms have been published, a re-analysis and intercalibration of these materials was timely. The results of this intercalibration form the basis for transfer functions for the reconstruction of NH_4^+ concentrations, which are described in Chapter 6, and which are for the first time applied for the analyses of cores from Beak Island.

A total of 102 diatom taxa (including varieties and undescribed forms) belonging to at least 38 different genera was observed in recent/subfossil and fossil sediments from 66 lakes in these islands. The most species-rich genera were *Pinnularia* (9 taxa) *Chamaepinnularia*, *Nitzschia*, *Psammothidium* and *Stauroneis* (7 taxa), *Navicula* and *Planothidium* (6 taxa), *Diadesmis* and *Luticola* (both 5 taxa).

About sixty species could be positively identified. Significantly, 14 of these have been described very recently (since 2000) from the Antarctic region, testifying the recent renewed interest in diatom taxonomy and biogeography of this region (Spaulding et al. in press and references therein). The exact identity of many taxa however (in total about 40) is as yet uncertain. About 8 species appear to be new to science (e.g. the very distinct *Aulacoseira* species). Of the remainder, a considerable number closely resembles (hence 'cf.') known species or varieties but displays slight, possibly significant, differences with the type and/or other populations. Other taxa (e.g. *Hantzschia* cf. *amphioxys*, *Luticola muticopsis*, *Stauroneis* cf. *subgracilior*) appear to display a considerable degree of intraspecific variation (which has also been noted in other studies) which requires further study. Given the fact that recent diatom studies have revealed extensive semicryptic diversity in many established diatom taxa (e.g. Behnke et al., 2004; Beszteri et al., 2007; see Mann (1999) for a review), each case needs to be carefully studied (at least including morphometry of different populations and SEM analyses, and if at all possible, molecular analyses) to assess its true identity.

As the exact taxonomic identity of about 40 species remains uncertain, and hypothesizing that most of these may turn out to be endemic to the region, and that 14 positively identified species are hitherto only known from the Antarctic region, about half of all taxa are probably restricted to the Antarctic.

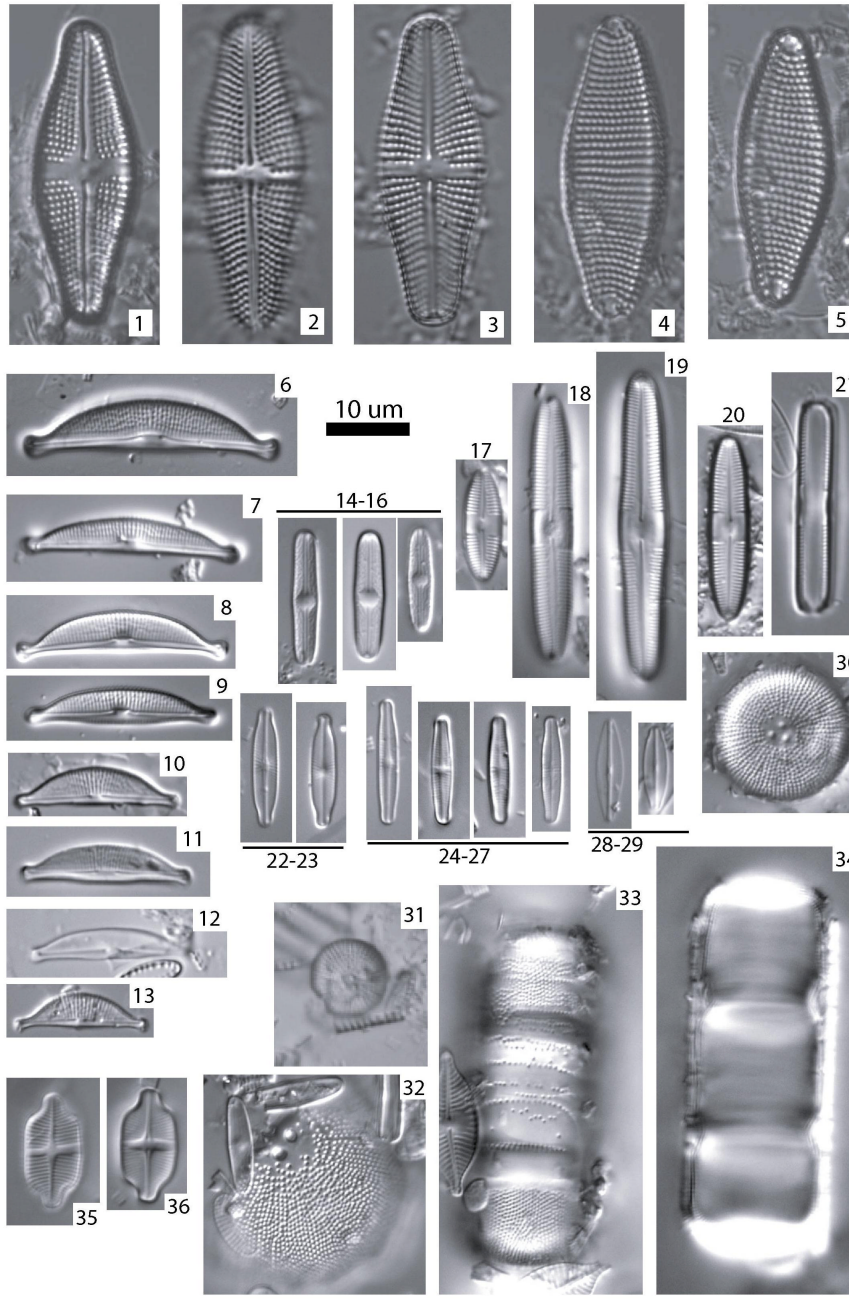

Plate 1: Figs. 1-5: *Achnanthes* cf. *muelleri*, Figs. 6-13: *Amphora* cf. *oligotraphenta*, Figs. 14-16: *Brachysira minor*, Figs. 17-21: *Caloneis* cf. *bacillum*, Figs. 22-23: *Adlafia bryophila*, Figs. 24-27: *Achnanthidium minutissimum* s.l., Figs. 28-29: *Adlafia* cf. *minuscula*, Figs. 30-34: *Orthoseira roeseana*, Figs. 35-36: *Achnanthidium* cf. *exiguum*

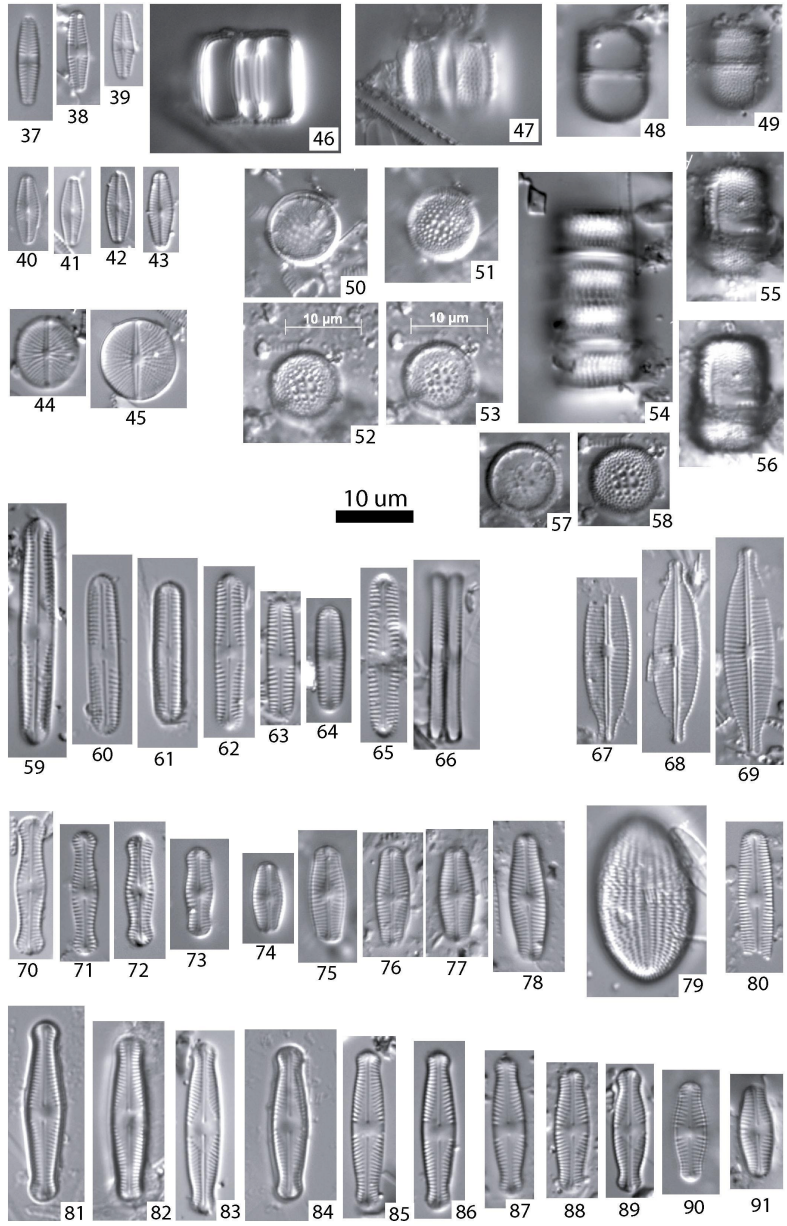

Plate 2: Figs. 37-39: *Chamaepinnularia australomediocris*, Figs. 40-43: *Chamaepinnularia* sp. 1, Figs. 44-45: *Cavinula pseudoscutiformis*, Figs. 46-58: *Aulacoseira* sp. 1, Figs. 59-66: *Chamaepinnularia gerlachei*, Figs. 67-69: *Craticula antarctica*, Figs. 70-73: *Chamaepinnularia krookii*, Figs. 74-78: Incertae sedis – pennate diatom sp. 1, Fig. 79: *Cocconeis placentula* var. *euglypta*, Fig. 80: *Chamaepinnularia cymatopleura*, Figs. 81-90: *Chamaepinnularia krookiformis*, Fig. 91: Incertae sedis – pennate diatom sp. 1

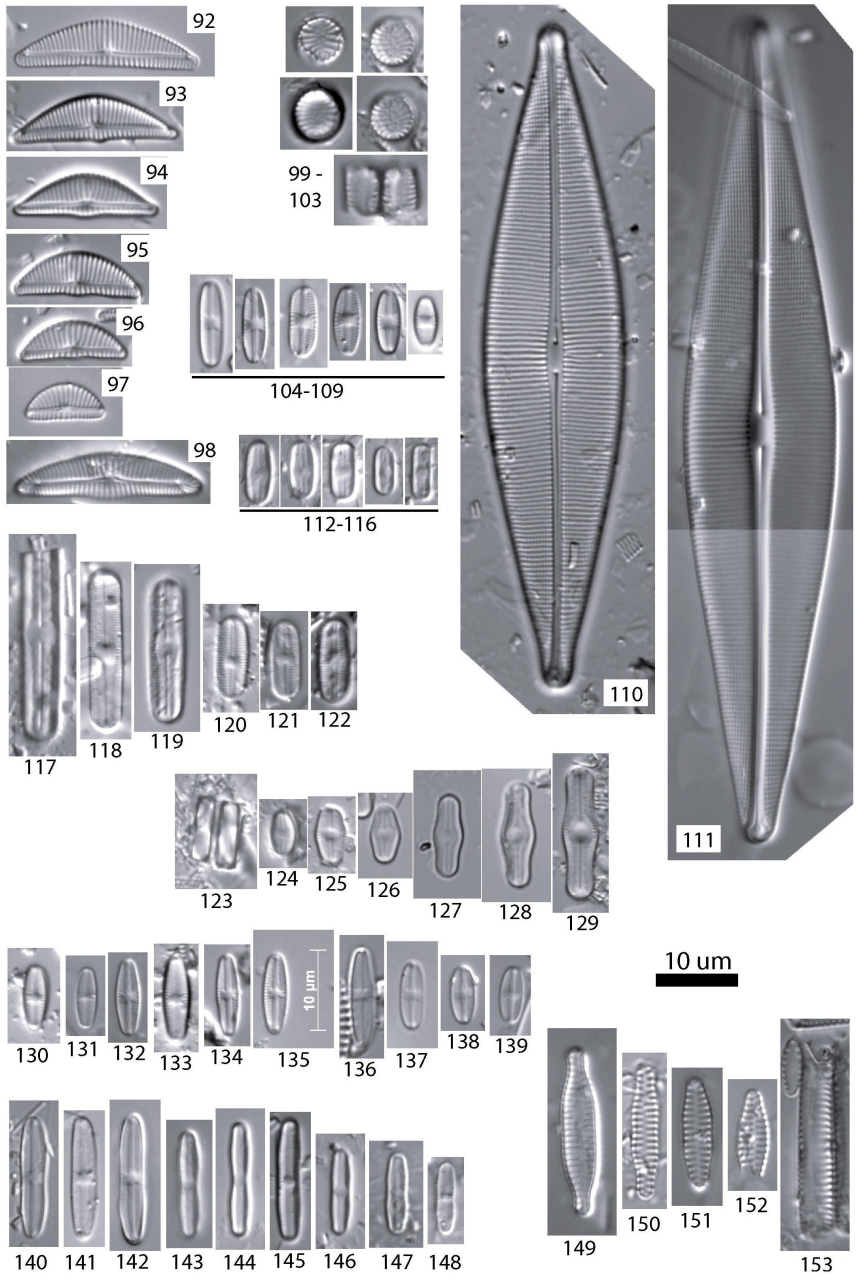

Plate 3: Figs. 92-98: *Encyonema minutum*, Figs. 99-103: *Staurosira* cf. *circula*, Figs. 104-109: *Eolimna minima*, Figs. 110-111: *Craticula subpampeana*, Figs. 112-116: *Diadesmis* sp. 1, Figs. 117-122: *Diadesmis* sp. 2, Figs. 123-129: *Diadesmis australis*, Figs. 130-139: *Eolimna minima*, Figs. 140-148: *Diadesmis* cf. *langebertalotii*, Figs. 149-153: *Staurosira alpestris*

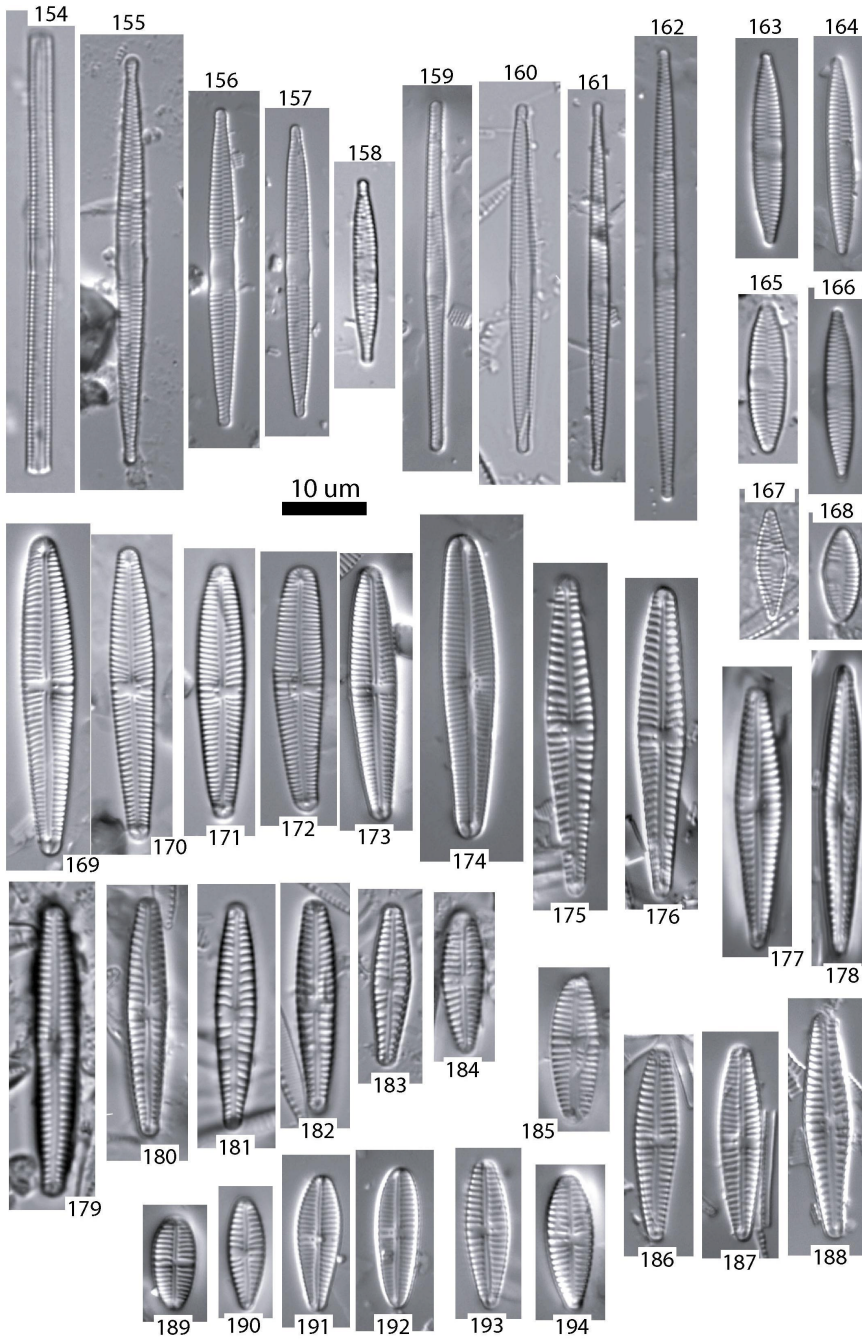

Plate 4: Figs. 154-162: *Fragilaria capucina* var. *capucina* form 1, Figs. 163-168: *Fragilaria capucina* var. *Capucina* form 2, Figs. 169-194: *Gomphonema* spp.

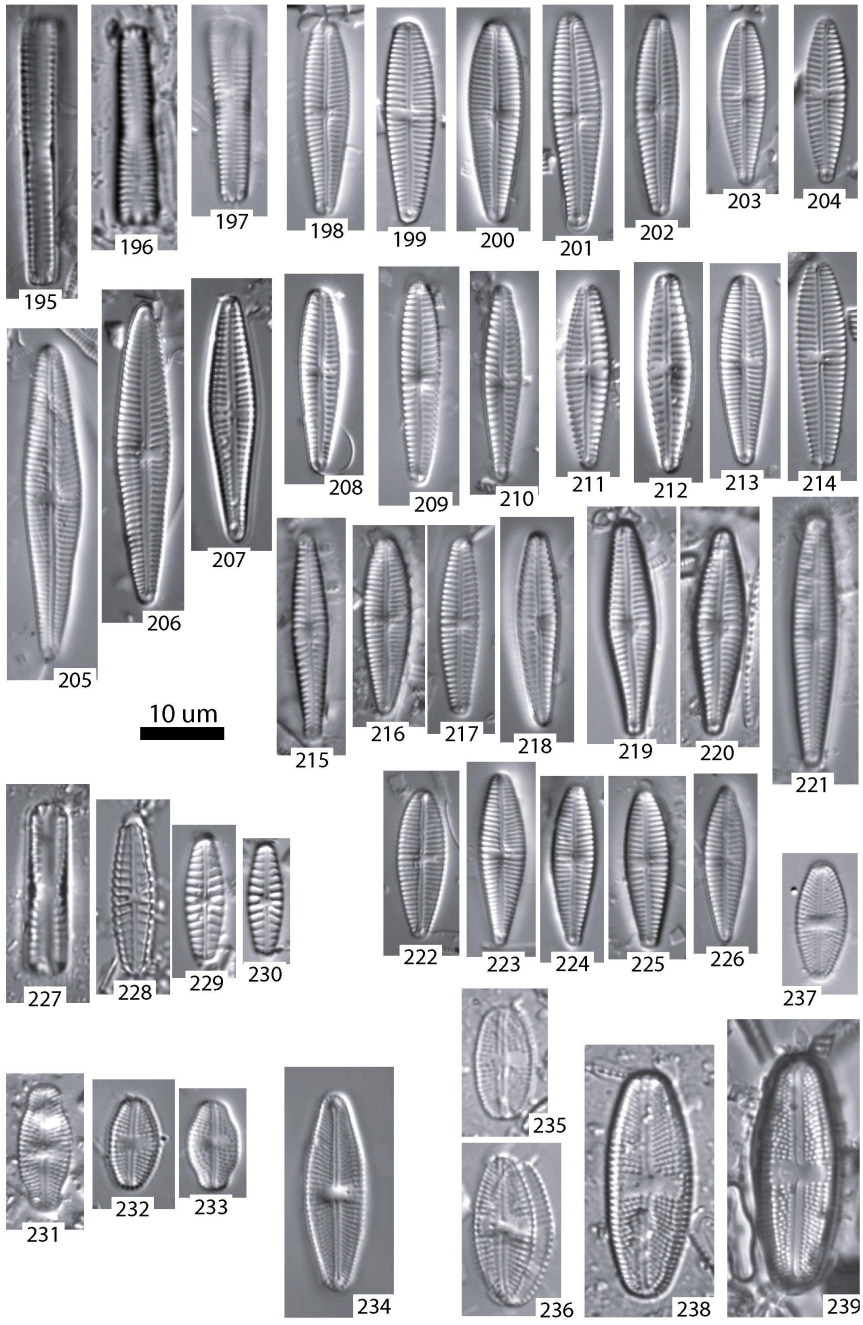

Plate 5: Figs. 195-226: *Gomphonema* spp., Figs. 227-230: *Hippodonta hungarica*, Figs. 231-233: *Luticola muticopsis* f. *reducta/evoluta*, Fig. 234: *Luticola* cf. *australomutica*, Figs. 235-236: *Luticola* cf. *cohnii*, Fig. 237: *Luticola* sp., Figs. 238-239: *Luticola* cf. *cohnii*

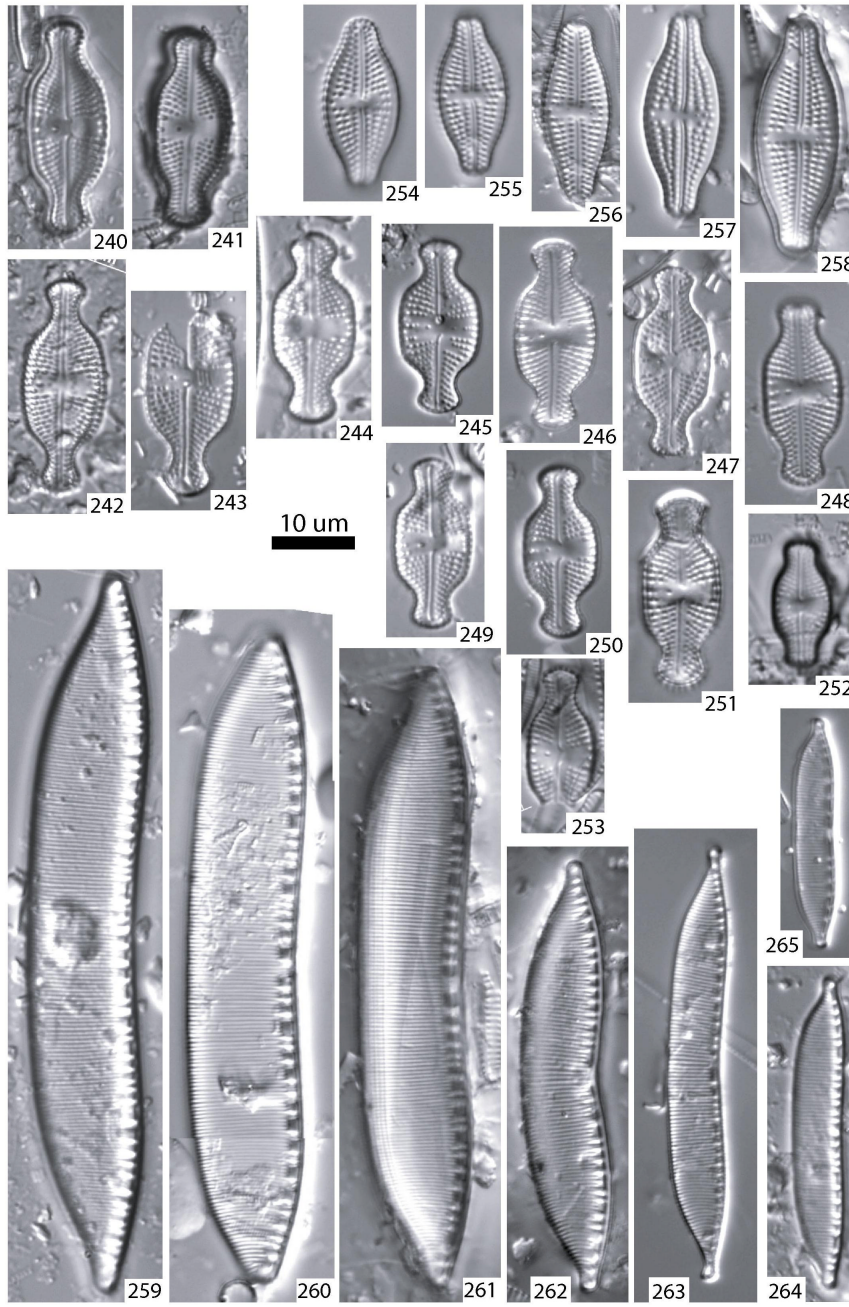

Plate 6: Figs. 240-253: *Luticola* cf. *muticopsis*, Figs. 254-258: *Luticola higleri*, Figs. 259-261: *Hantzschia* sp. 2, Fig. 262: *Hantzschia* sp. 1, Figs. 263-265: *Hantzschia* cf. *amphioxys*

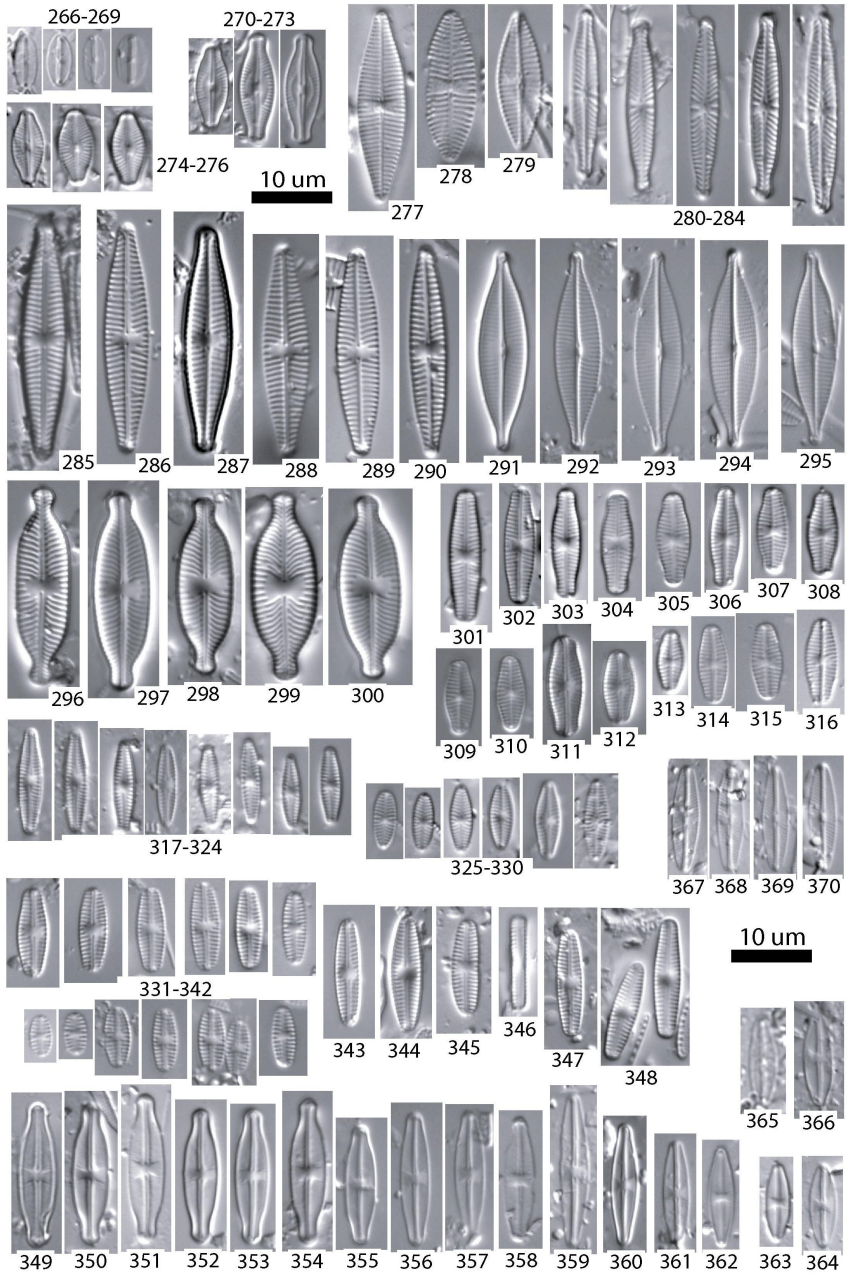

Plate 7: Figs. 266-269: *Mayamaea* cf. *atomus* var. *permitis*, Figs. 270-276: *Microcostatus* cf. *naumanni*, Figs. 277-279: *Navicula glaciei*, Figs. 280-284: *Navicula bicephala*, Figs. 285-290: *Navicula* cf. *libonensis*, Figs. 291-295: *Navicula gregaria*, Figs. 296-300: *Placoneis* cf. *elginensis*, Figs. 301-316: '*Naviculadicta' elorantana*, Figs. 317-330: *Navicula* cf. *obsoleta*, Figs. 331-348: '*Naviculadicta' seminulum*, Figs. 349-355: *Sellaphora* sp. 1, Figs. 356-366: Incertae sedis

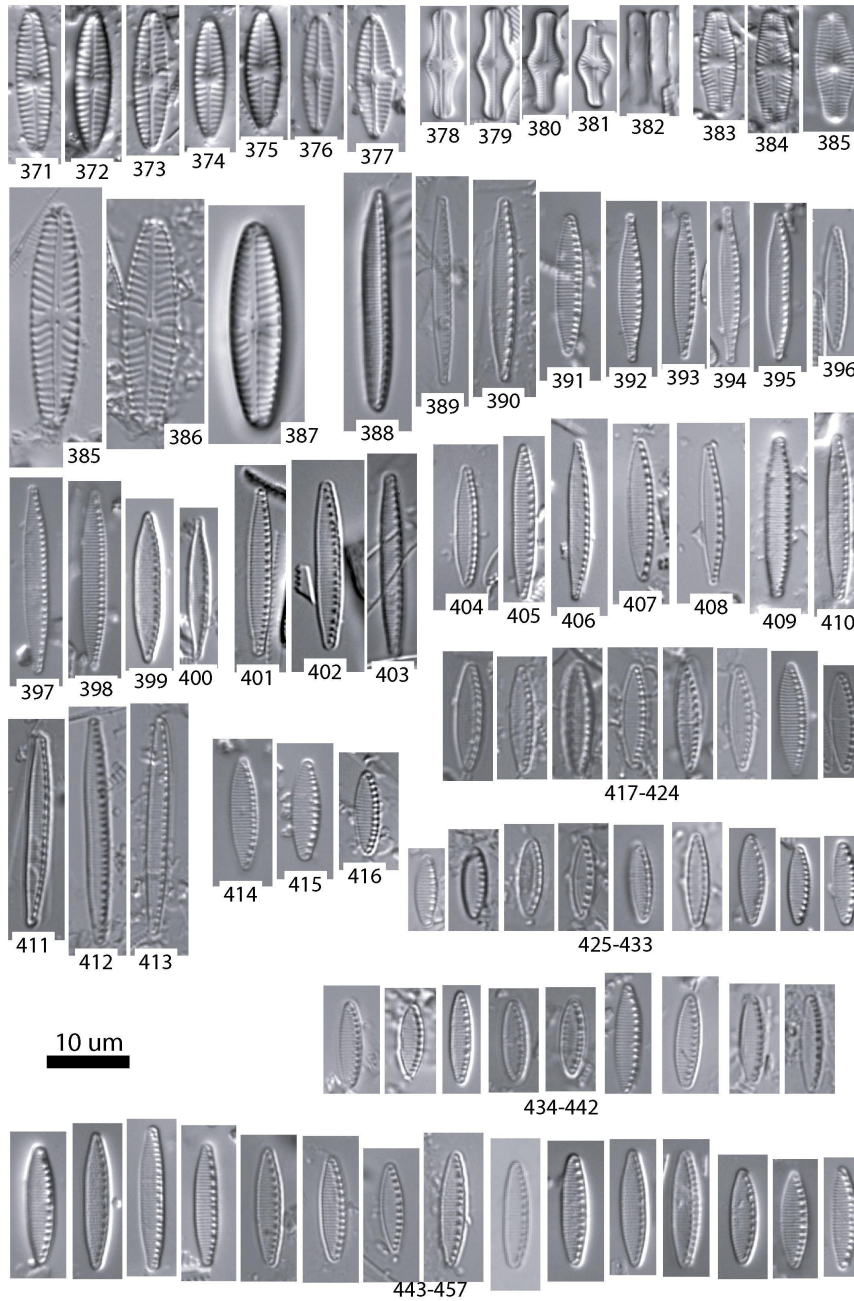

Plate 8: Figs. 371-377: *Navicula australoshetlandica*, Figs. 378-382: *Diadesmis* cf. *tabellariaeformis*, Figs. 383-385: Incertae sedis – pennate diatom sp. 1, Figs. 385-387: *Navicula cincta*, Figs. 388-413: *Nitzschia perminuta*, Figs. 414-424: *Nitzschia frustulum*, Figs. 425-457: *Nitzschia inconspicua*

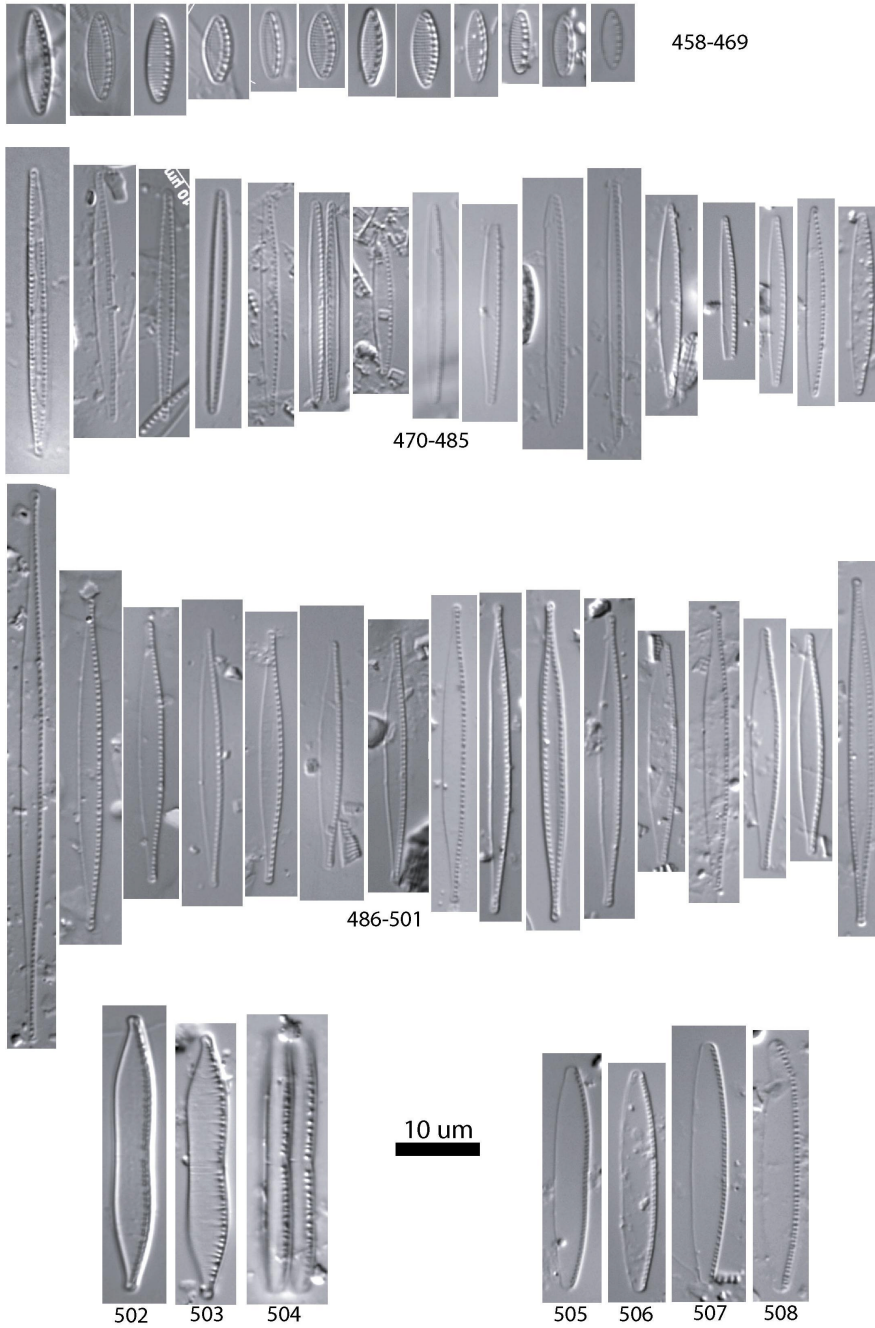

Plate 9: Figs. 458-469: *Nitzschia inconspicua*, Figs. 470-485: *Nitzschia paleacea*, Figs. 486-501: *Nitzschia gracilis*, Figs. 502-504: *Nitzschia homburgiensis*, Figs. 505-508: *Nitzschia* cf. *pusilla*

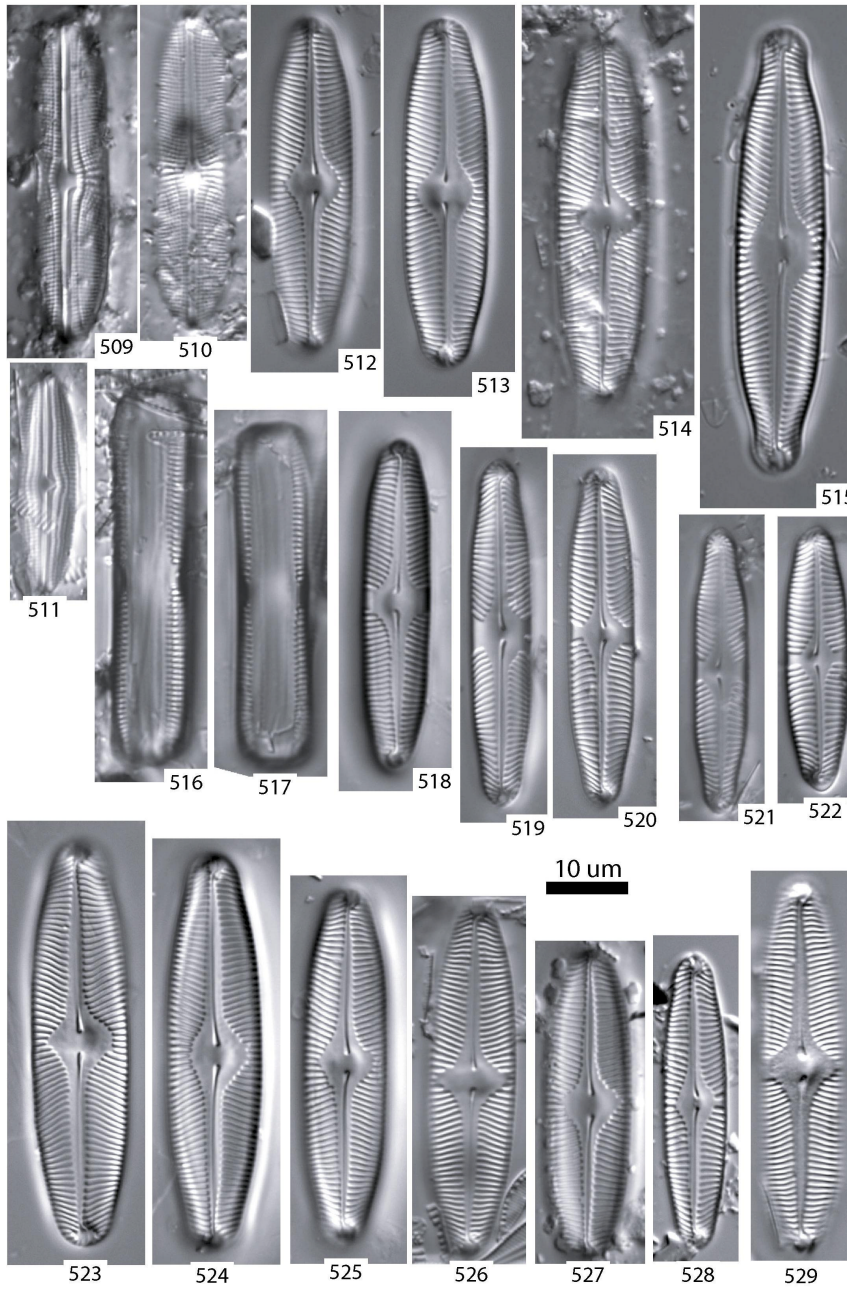

Plate 10: Figs. 509-510: *Muelleria australoatlantica*, Fig. 511: *Muelleria aequistriata*, Figs. 512-515: *Pinnularia* cf. *microstauron* var. *nonfasciata*, Figs. 516-522: *Pinnularia microstauron*, Figs. 523-529: *Pinnularia* cf. *microstauron* var. *nonfasciata*

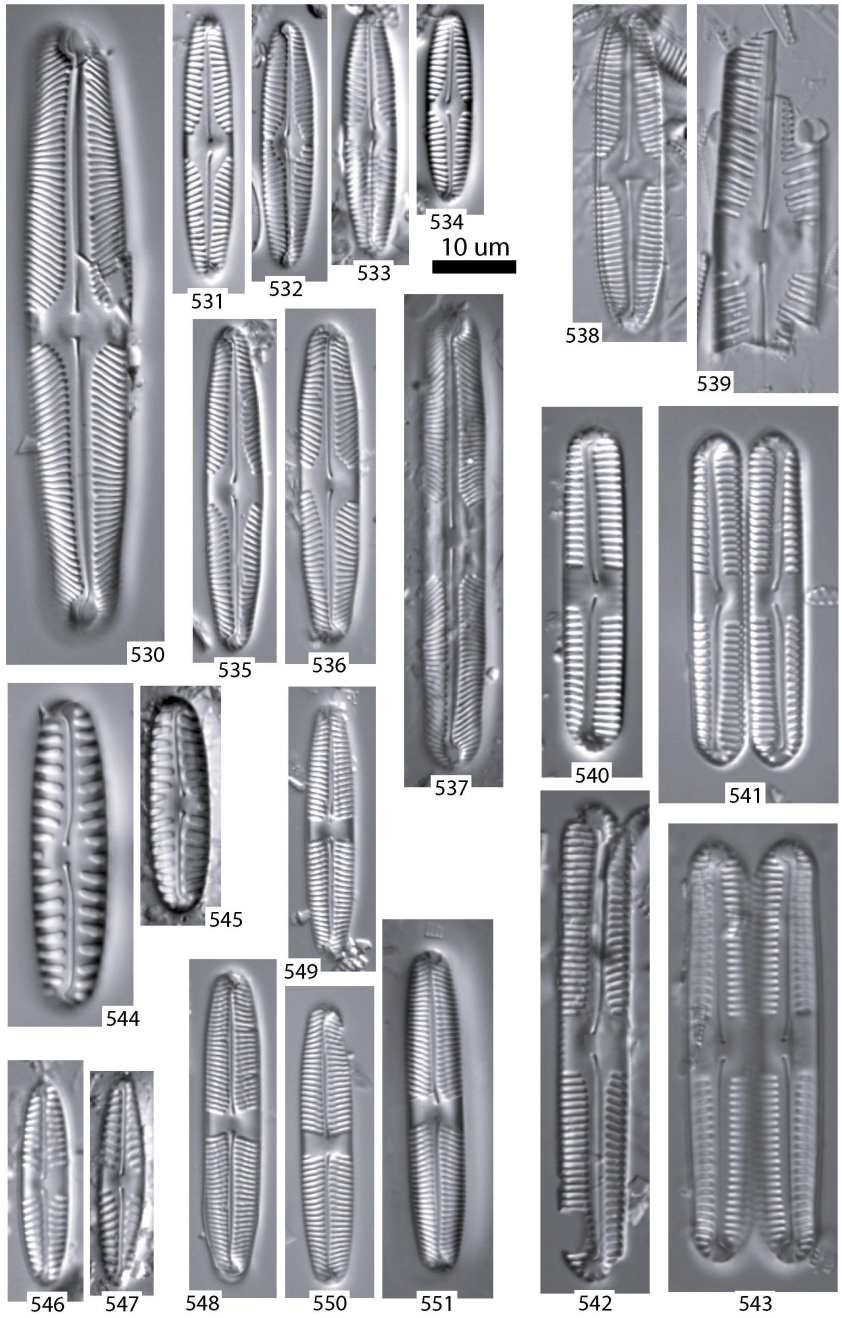

Plate 11: Figs. 530-539: unidentified *Pinnularia* spp., Figs. 540-543: *Pinnularia gemella*, Figs. 544-545: *Pinnularia borealis*, Figs. 546-547: *Pinnularia* cf. *obscura*, Figs. 548-551: *Pinnularia subantarctica* var. *elongata*

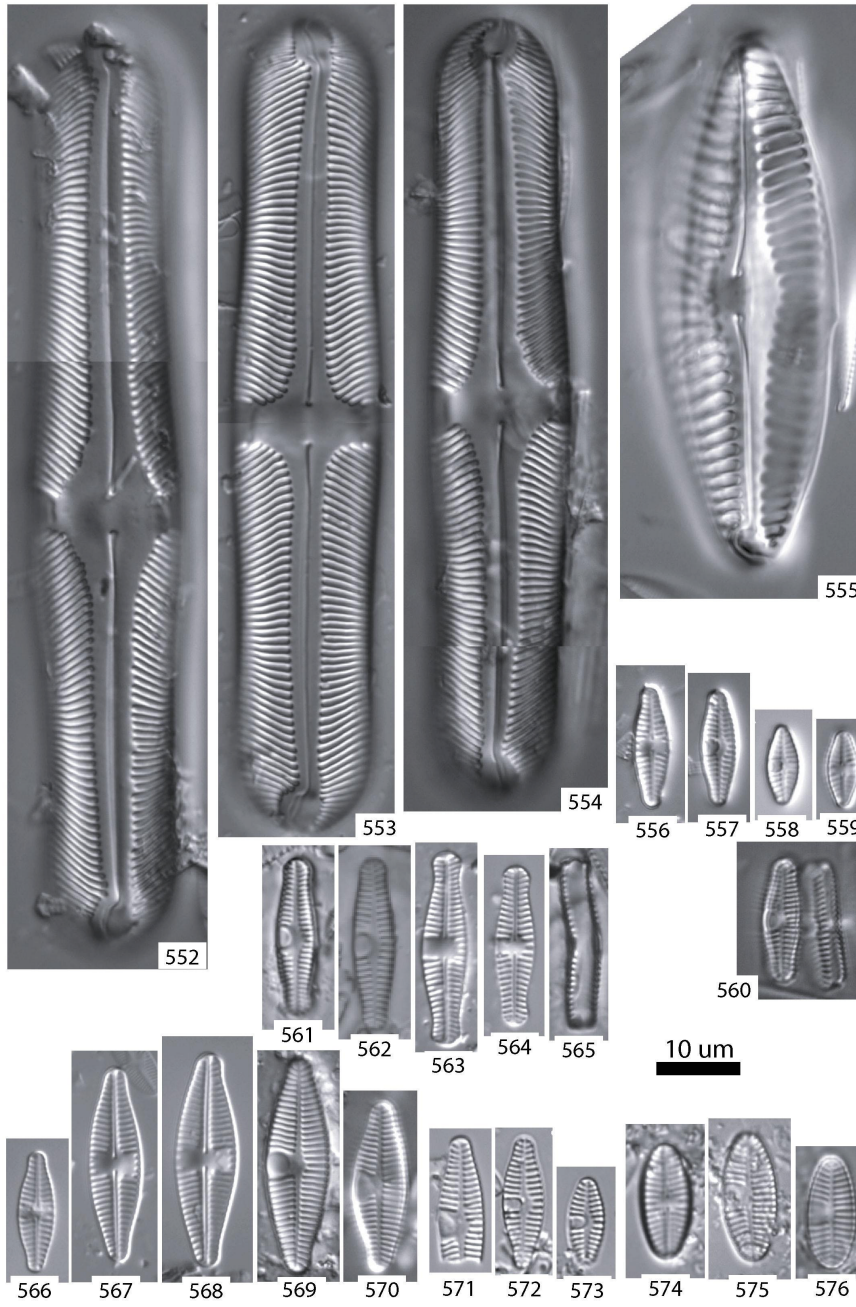

Plate 12: Figs. 552-554: *Pinnularia* cf. *divergens* var. *linearis*, Fig. 555: *Pinnularia* cf. *splendida*, Figs. 556-560: *Planothidium frequentissimum*, Figs. 561-565: *Planothidium* sp. 1, Figs. 566-571, 574-576: *Planothidium lanceolatum*, Figs. 572-573: *Planothidium frequentissimum*?

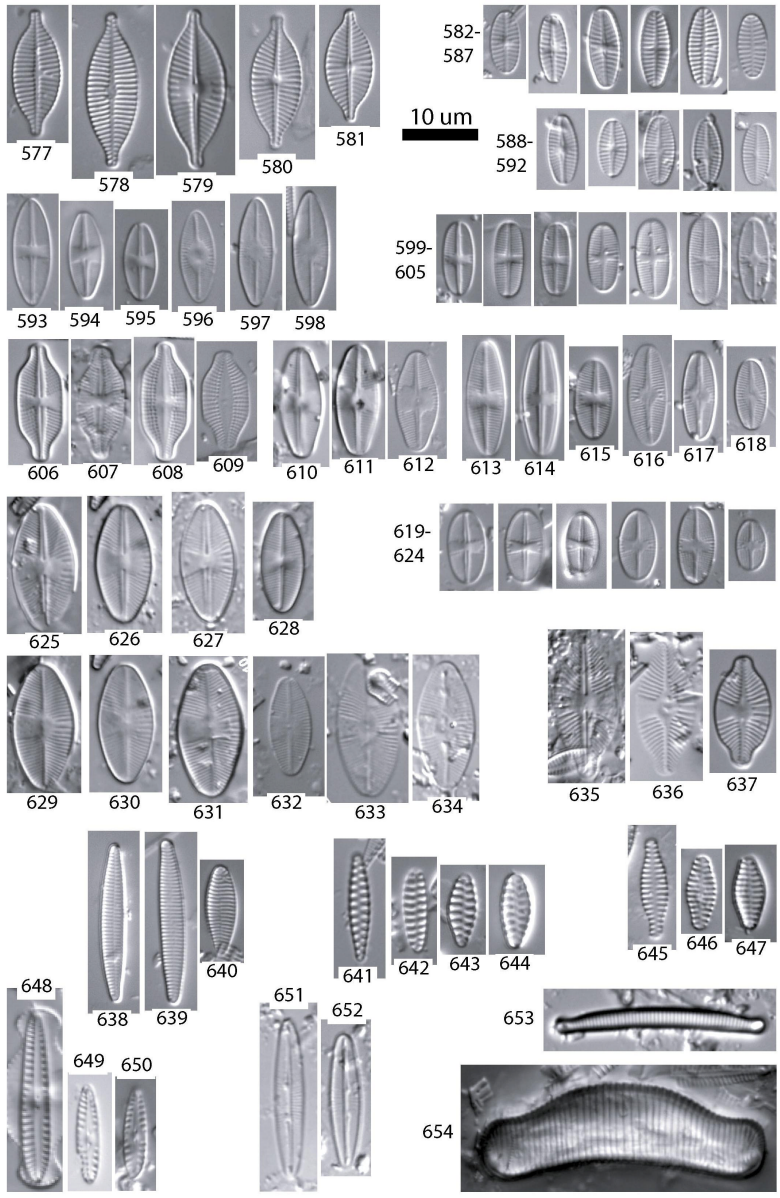

Plate 13: Figs. 577-581: *Planothidium delicatulum*, Figs. 582-587: *Planothidium quadripunctatum*, Figs. 588-592: *Planothidium renei*, Figs. 593-598: *Psammothidium incognitum*, Figs. 599-605: *Psammothidium abundans*, Figs. 606-609: *Psammothidium manguinii*, Figs. 610-612: *Psammothidium* cf. *investians*, Figs. 613-618: *Psammothidium metakryophilum*, Figs. 619-624: *Psammothidium subatomoides*, Figs. 625-634: *Psammothidium germainii* form 2, Figs. 635-637: *Psammothidium germainii* form 1, Figs. 638-640: *Stauroforma inermis*, Figs. 641-644: *Staurosirella pinnata*, Figs. 645-647: *Staurosira* cf. *venter*, Figs. 648-650: *Gomphonemopsis* sp., Figs. 651-652: *Amphipleura* sp., Fig. 653-654: *Eunotia* spp.

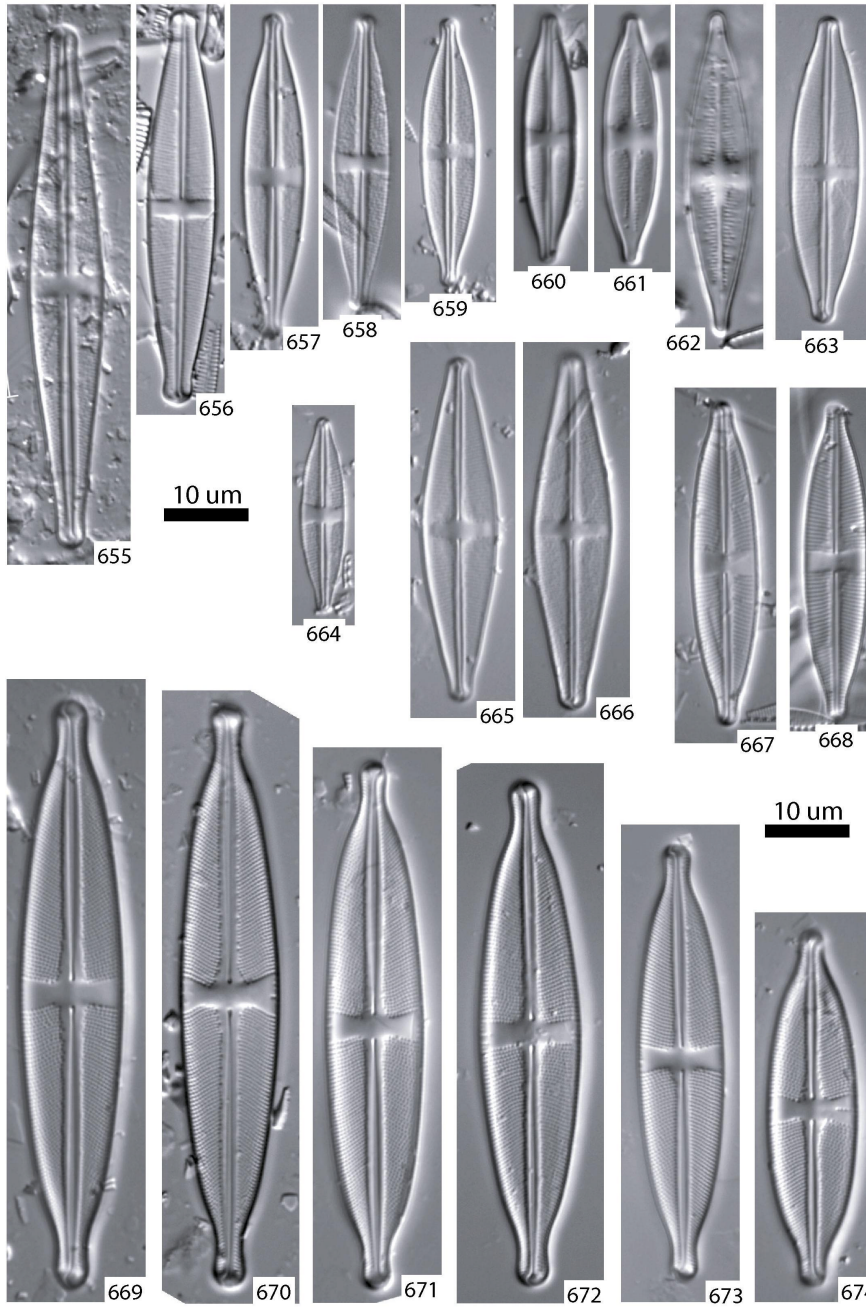

Plate 14: Figs. 655: *Stauroneis* cf. *subgracilior* form 1, Figs. 656-662, 664: *Stauroneis* cf. *subgracilior* form 2, Fig. 663: *Stauroneis* cf. *subgracilior* form 3, Figs. 665-666: *Stauroneis* cf. *subgracilior* form 4, Figs. 667-668: *Stauroneis latistauros*, Figs. 669-674: *Stauroneis* cf. *acidoclinata*

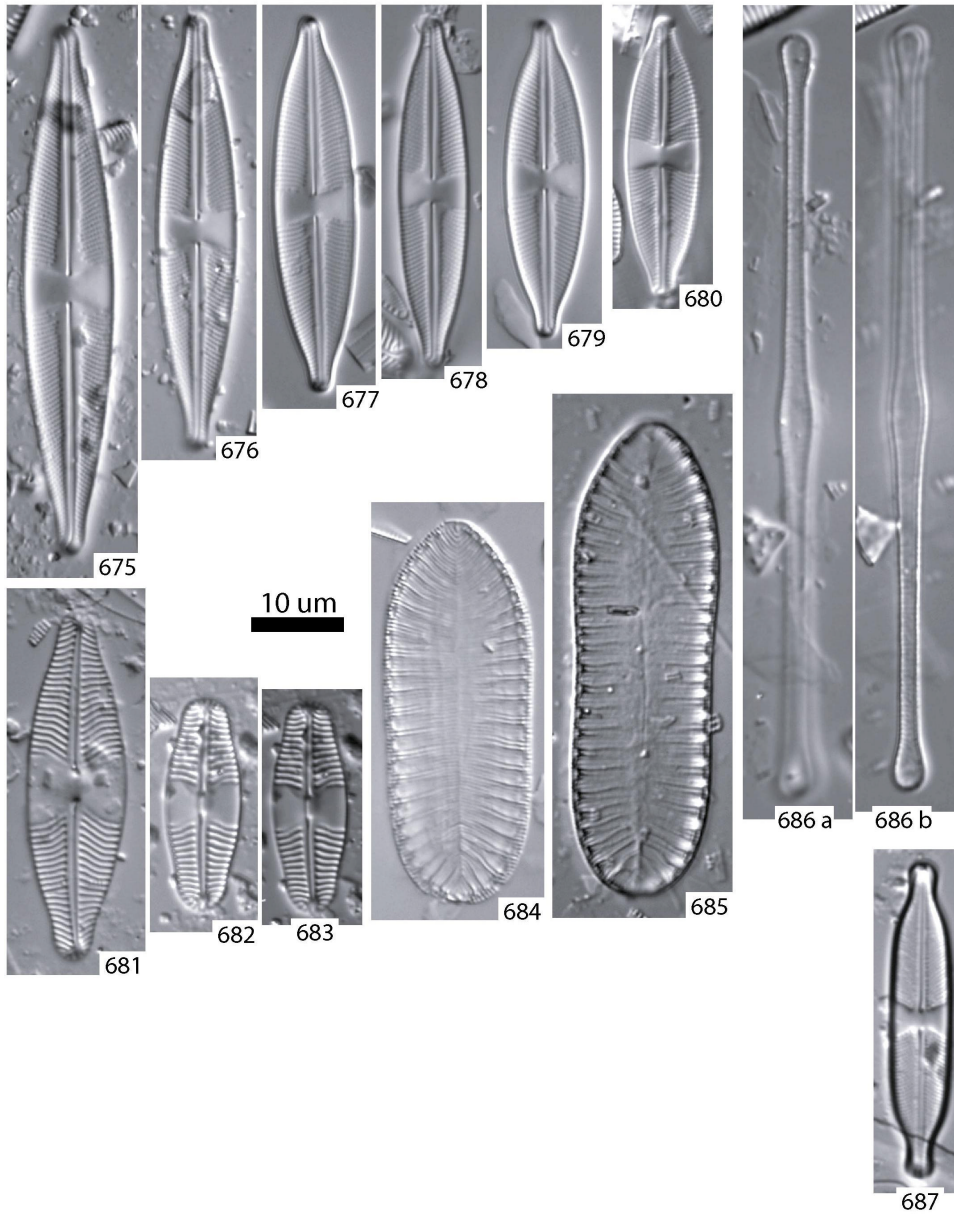

Plate 15: Figs. 675-680: *Stauroneis latistauros*, Figs. 681-683: *Pinnularia* cf. *kolbei*, Figs. 684-685: *Surirella* sp. 1, Figs. 686a-b: Incertae sedis, Fig. 687: *Stauroneis husvikensis*

References

Behnke A., Friedl T., Chepurnov V.A., Mann D.G. 2004. Reproductive compatibility and rDNA sequence analyses in the *Sellaphora pupula* species complex (Bacillariophyta). Journal of Phycology. 40 : 193-208.

Beszteri B., John U., Medlin L.K. 2007. An assessment of cryptic genetic diversity within the *Cyclotella meneghiniana* species complex (Bacillariophyta) based on nuclear and plastid genes, and amplified fragment length polymorphisms. European Journal of Phycology. 42 : 47-60.

Bibby J.S. 1966. The stratigraphy of part of north-east Graham Land and the James Ross Island Group. British Antarctic Survey, Scientific Reports. 53: 1-37.

Björck S., Olsson S., Ellis-Evans C., Håkansson H., Humlum O., de Lirio J.M. 1996. Late Holocene palaeoclimatic records from lake sediments on James Ross Island, Antarctica. Palaeogeography, Palaeoclimatology, Palaeoecology. 121: 195-220.

Bourrelly P., Manguin E. 1954. Mémoires de l'institut scientifique de Madagascar. Série B. Tome V: 8-58.

Bukhtiyarova L., Round F.E. 1996. Revision of the genus *Achnanthes* sensu lato. *Psammothidium*, a new genus based on *A. marginulatum.* Diatom Research. 11 (1): 1-30.

Carlson G.W.F. 1913. Süsswasseralgen aus der Antarktis, Süd-Georgien und den Falkland Inseln. In: Dr. Otto Nordenskjöld Wissenschaftliche Ergebnisse deer Schwedischen Südpolar Expedition 1901-1903, Band IV, 94 pp.

Carter JR. 1966. Some freshwater diatoms from Tristan da Cunha and Gough Island. Nova Hedwigia. 11: 443-481.

Cavacini P., Tagliaventi N., Fumanti B. 2006. Morphology, ecology and distribution of an endemic Antarctic lacustrine diatom: *Chamaepinnularia cymatopleura* comb. nov. Diatom Research. 21 (1): 57-70.

Cox E.J. 1987. Studies on the diatom genus Navicula Bory. VI. The identity, structure and ecology of some freshwater species. Diatom Research. 2 (2): 159-174.

Cox E.J. 1995. Studies on the diatom genus *Navicula* Bory. VII. The identity and typification of *Navicula gregaria* Donkin, *N. cryptocephala* Kützing and related taxa. Diatom Research. 10 (1): 91-111.

Cox E.J. 2003. *Placoneis* Mereschkowsky (Bacillariophyta) revisited: resolution of several typification and nomenclatural problems, including the generitype. Botanical Journal of the Linnean Society. 141 (1): p. 53-83.

Crawford R.M., Likhoshway Y. 1999. The frustule structure of original material of *Aulacoseira distans* (Ehrenberg) Simonsen. Diatom research. 14: 239-250.

Cremer H., Gore D., Hultzsch N., Melles M., Wagner B. 2004. The diatom flora and limnology of lakes in the Amery Oasis, East Antarctica. Polar Biology. 27: 513-531.

Fermani P., Mataloni G., Van de Vijver B. 2007. Soil microalgal communities on an antarctic active volcano (Deception Island, South Shetlands). Polar Biology. 30: 1381-1393.

Flower R.J. 2005. A taxonomic and ecological study of diatoms from freshwater habitats in the Falklands Islands, South Atlantic. Diatom Research. 20 (1): 23-96.

Flower R.J., Jones V.J., Round F.E. 1996. The distribution and classification of the problematic *Fragilaria* (*virescens* v.) *exigua* Grun./ *Fragilaria exiguiformis* (Grun.) Lange-Bertalot: a new species or a new genus? Diatom Research. 11 (1): 41-57.

Foged N. 1974. Freshwater diatoms in Iceland. Bibliotheca Phycologica. 15: 1-118 + 36 plates.

Gibson J.A.E., Roberts D., Van de Vijver B. 2006. Salinity control of the distribution of diatoms in lakes of the Bunger Hills, East Antarctica. Polar Biology. 29: 694-704.

Hawes I., Brazier P. 1991. Freshwater stream ecosystems of James Ross Island, Antarctica. Antarctic Science. 3 (3): 265-271.

Heywood R.B., Dartnall H.J.G., Priddle J. 1979. The freshwater lakes of Signy Island, South Orknei Islands, Antarctica: data sheets. British Antarctic Survey Data, n° 3, 44 pp.

Heywood R.B., Dartnell H.J.G., Priddle J. 1980. Characteristics and classification of the lakes of Signy island, South Orkney Islands. Freshwater Biology, 10, 47-59.

Hobbs G.J. 1968. The geology of the South Shetland Islands. IV. The Geology of Livingston Island. British Antarctic Survey Reports. N° 47: 1-34.

Hodgson D.A., Convey P. 2005. A 7000-year Record of Oribatid Mite Communities on a Maritime-Antarctic Island: Responses to Climate Change. Arctic, Antarctic, and Alpine Research. 37 (2): 239-245.

Hustedt F.R. 1930. Die Süsswasser-flora Mitteleuropas (herausgegeben von A. Pascher). Heft 10: Bacillariophyta (Diatomea) 2^{e} Auflage, Gustav Fischer, Jena. 466 pp.

Hustedt F.R. 1942. Aërophile Diatomeen in der nordwestdeutschen Flora. Berichte der Deutsche Botanische Gesellschaft. 60: 55-73.

Jones V., Juggins S. 1995. The construction of a diatom-based chlorophyll a transfer function and its application at three lakes on Signy Island (maritime Antarctic) subject to differing degrees of nutrient enrichment. Freshwater biology. 34: 433-445.

Jones P. D., Limbert D. W. S. 1989. Antarctic surface temperature and pressure data. ORNL/CDIAC-27, NDP-032. Oak Ridge National Laboratory, Oak Ridge, Tennessee.

Jones V., Juggins S., Ellis-Evans J.C. 1993. The relationship between water chemistry and surface sediment diatom assemblages in maritime Antarctic lakes. Antarctic Science. 5 (4): 339-348.

Kellogg D.E., Stuiver M., Kellogg T.B., Denton G.H.D. 1980. Non-marine diatoms from Late Wisconsin perched deltas in Taylor Valley, Antarctica. Palaeogeography, Palaeoclimatology, Palaeoecology. 30: 157-189.

Kellogg T.B., Kellogg D.E. 2002. Non-marine and littoral diatoms from Antarctic and sub-Antarctic locations. Distribution and updated taxonomy. Diatom Monographs. 1: 1-795.

Kelly M.G., Bennion H., Cox E.J., Goldsmith B., Jamieson J., Juggins S., Mann D.G., Telford R.J. (2005). Common freshwater diatoms of Britain and Ireland: an interactive key. Environment Agency, Bristol. (http://craticula.ncl.ac.uk/EADiatomKey.html).

Kociolek J.P., Jones V.J. 1995. *Gomphonema signyensis* sp. nov., a freshwater diatom from maritime Antarctica. Diatom Research. 10 (2): 269-276.

Ko-Bayashi T. 1965. Variations on some pennate diatoms from Antarctica (Part 2): XII. Variations of Navicula muticopsis Van Heurck. Japanese Antarctic Research Expedition 1956-1962, Scientific Reports Series E. 24: 1-28 (31 plates).

Kopalova K., Elster J., Nebalová L., Van de Vijver B. In press. Three new terrestrial diatom species from seepage areas on James Ross Island (Antarctic Peninsula region). Diatom Research.

Krammer K. 1992. *Pinnularia*, eine Monographie der europäischen Taxa. Bibliotheca Diatomologica, Band 26, J. Cramer, Berlin, Stuttgart. 353 pp.

Krammer K. 2000. The genus *Pinnularia*. Diatoms of Europe. 1: 1-703.

Krammer K., Lange-Bertalot H. 1986. Süsswasserflora von Mitteleuropa, Band 2: Bacillarophyceae, Teil 1: Naviculaceae. Gustav Fischer Verlag, Stuttgart, New York, 876 pp.

Krammer K., Lange-Bertalot H. 1988. Süsswasserflora von Mitteleuropa, Band 2: Bacillarophyceae, Teil 2: Bacillariaceae, Epithemiaceae, Surirellaceae. Gustav Fischer Verlag, Stuttgart, New York, 596 pp.

Krammer K., Lange-Bertalot H. 1991a. Süsswasserflora von Mitteleuropa, Band 2: Bacillarophyceae, Teil 3: Centrales, Fragilariaceae, Eunotiaceae. Gustav Fischer Verlag, Stuttgart, New York, 576 pp.

Krammer K., Lange-Bertalot H. 1991b. Süsswasserflora von Mitteleuropa, Band 2: Bacillarophyceae, Teil 4: Achnanthaceae. Gustav Fischer Verlag, Stuttgart, New York, 437 pp.

Krasske K. 1939. Zür Kieselalgenfloras Südchiles. Archiv fur Hydrobiologie. 35: 349-468.

Lange-Bertalot H. 2001. Diatoms of Europe Vol. 2 *Navicula* sensu stricto 10 genera separated from *Navicula* sensu lato, *Frustulia*. ARG Gartner Verlag KG, Ruggell. 526 pp.

Lange-Bertalot H. 1993. 85 neue taxa. Bibliotheca Diatomologica. 27 (vol. 2/1-4): 1-454.

Lange-Bertalot H. 1996. Annotated diatom micrographs. Iconographia Diatomologica Vol. 4. O. Koeltz scientific books, 288 pp.

Lange-Bertalot H., Krammer K. 1989. *Achnanhtes* eine Monographie der Gattung. Bibliotheca Diatomologica, 18, J. Cramer, Stuttgart, 393 pp.

Lange-Bertalot H., Genkal S.I. 1999. Diatoms from Siberia I. Iconographia Diatomologica, 6, 1-292, Koeltz Scientific Books, Königstein.

Lange-Bertalot H., Metzeltin D. 1996. Indicators of oligotrophy – 800 taxa representative of three ecologically distinct lake types. In: Lange-Bertalot (Ed.), Iconographia Diatomologica, Vol. 2. Königstein: Koeltz Scientific Books, 390 pp.

Lange-Bertalot H., Külbs K., Lauser T., Nörpel-Schlemm M., Willmann M. 1996. Dokumentation und Revision der von Georg Krasske beschriebenen Diatomeen-Taxa Iconographia Diatomologica. 3: 1-358.

Lange-Bertalot H., Moser G. 1994. *Brachysira*, Monographie der Gattung Bibliotheca Diatomologica. 29: 1-212.

Le Cohu R. 1999. Review of the principal species of Fragilariales (Bacillariophyta) in the Kerguelen Islands. Canadian Journal of Botany. 77: 821-834.

Le Cohu R., Maillard R. 1986. Diatomées d'eau douce des îles Kerguelen (à l'exclusion des Monoraphidées). Annales de Limnologie 22 (2) : 99-118.

Le Cohu R., Van de Vijver B. 2002. Le genre *Diadesmis* (Bacillariophyta) dans les archipels de Crozet et de Kerguelen avec la description de cinq espèces nouvelles. Annales de Limnologie. 38 (2): 119-132.

Mann D. 1999. The species concept in diatoms. Phycologia. 38: 437-495.

Moser G., Lange-Bertalot H., Metzeltin D. 1998. Insel der Endemiten. Geobotanisches Phänomen Neukaledonien. Bibliotheca Diatomologica. 38: 1-464.

Oppenheim D.R., Greenwood R. 1990. Epiphytic diatoms in two freshwater maritime Antarctic lakes. Freshwater Biology. 24: 303-314.

Oppenheim D.R. 1994. Taxonomic studies of *Achnanthes* (Bacillariophyta) in freshwater maritime antarctic lakes. Canadian Journal of Botany. 72: 1735-1748.

Patrick R., Reimer C.W. 1966. The diatoms of the United States, exclusive of Alaska and Hawaii. Volume 1. Academy of Natural Sciences of Philadelphia, Philadelphia: 688 pp.

Paull T.M., Hamilton P.B., Gajewski K., LeBlanc M. 2008. Numerical analysis of small Arctic diatoms (Bacillariophyceae) representing the Staurosira and Staurosirella species complexes. Phycologia. 47: 213-224.

Reichardt E. 1999. Zur Revision der Gattung *Gomphonema*. Die Arten um *G. affine*/*insigne*, *G. angustatum/micropus*, *G. acuminatum* sowie gomphonemoide Diatomeen aus dem Oberoligozän in Böhmen. In: Lange-Bertalot H. (Ed.): Iconographia Diatomologica. Annotated Diatom Micrographs, Vol. 8. A. R. G. Gantner Verlag Kommanditgesellschaft, FL Rugell: 203 pp.

Renberg I. 1990. A procedure for preparing large sets of diatom slides from sediment cores. Journal of Paleolimnology. 4: 87-90.

Riaux-Gobin C., Compère P. 2004. Two marine cocconeid diatoms from Kerguelen's Land (Austral Ocean, Indian Sector): *Cavinula kerguelensis* nom. nov. and *Cocconeiopsis wrightii*. Diatom Research. 19: 59-69.

Roberts D., McMinn A. 1999. Diatoms from the saline lakes of the Vestfold Hills, Antarctica. Bibliotheca Diatomologica. 44: 1-83. J. Cramer, Berlin, Stuttgart.

Round F.E., Bukhtiyarova L. 1996. Four new genera based on Achnanthes (Achnanthidium) together with a re-definition of Achnanthidium. Diatom Research. 11 (2): 345-361.

Round F.E., Crawford R.M., Mann D.G. 1990. The diatoms: Biology and Morphology of the genera. Cambridge University Press, 747pp.

Rumrich U., Lange-Bertalot H., Rumrich M. 2000. Diatomeen der Anden, Von Venezuela bis Patagonien/Feureland, und zwei weitere Beiträge.

Sabbe K., Verleyen E., Hodgson D.A., Vanhoutte K., Vyverman W. 2003. Benthic diatom flora of freshwater and saline lakes in the Larsemann Hills and Rauer Islands, East Antarctica. Antarctic Science. 15 (2): 227-248.

Schmidt R., Mäusbacher R., Müller J. 1990. Holocene diatom flora and stratigraphy from sediment cores of two Antarctic lakes. Journal of Paleolimnology. 3: 55-74.

Simonsen R. 1987. Atlas and Catalogue of the Diatom Types of Friedrich Hustedt. J. Cramer, Berlin, Stuttgart, 3 volumes, 525 pp, 395 pp, 772 pp.

Smith R.I.L. 1972. Vegetation of the South Orkney Islands with particular reference to Signy Island. Scientific Report of the British Antarctic Survey. 68: 1-124.

Smol J.P., Stoermer E.F. In press. The diatoms: applications for the environmental and earth sciences. 2nd Edition. Cambridge University press, Cambridge.

Spaulding S.A., Stoermer E.F. 1997. Taxonomy and distribution of the genus *Muelleria* Frenguelli. Diatom Research. 12 (1): 95-115.

Spaulding S.A., Esposito R., Lubinski D., Horn S., Cox M., McKnight D., Alger A., Hall B., Mayernick M., Whittaker T., Yang C. 2008. Antarctic Freshwater Diatoms web site, McMurdo Dry Valleys LTER, visited 12 Nov 2008 at http://huey.colorado.edu/diatoms/.

Spaulding S., Kociolek J.P., Wong D. 1999. A taxonomic and systematic revision of the genus *Muelleria* (Bacillariophyta). Phycologia. 38 (4): 314-341.

Spaulding S.A., Van de Vijver B., Hodgson D.A., McKnight D.M., Verleyen E., Stanish, L. In press. Diatoms as indicators of environmental change in Antarctic and subantarctic freshwaters. In: Smol J.P., Stoermer E.F. (Eds.). In press. The diatoms: applications for the environmental and earth sciences. 2nd Edition. Cambridge University Press, Cambridge.

Stoermer E.F., Kreis R.G., Andresen N.A. 1999. Checklist of diatoms from the Laurentian Great Lakes, II, Journal of Great Lakes Research. 25 (3): 515-566.

Sugden D.E. 1982. Arctic and Antarctic: a modern geographical synthesis. Oxford: Basil Blackwell. 472 pp.

Temniskova-Topalova D., Chipev N., Manoilova K. 1996. Preliminary report on diatoms from the Livingston Island, South Shetland Islands, Antarctic. - Bulg. Antarc. Res., Life Sciences. 1: 31-61.

Van de Vijver B., Beyens L. 1997. The epiphytic diatom flora of mosses from Stromness Bay area, South Georgia. Polar Biology. 17: 492-501.

Van de Vijver B., Beyens L. 1997. Freshwater diatoms from some islands in the maritime Antarctic region. Antarctic Science. 9 (4): 418-425.

Van de Vijver B., Frenot Y., Beyens L. 2002. Freshwater diatoms from Ile de la Possession (Crozet Archipelago, Subantarctica). Bibliotheca Diatomologica. 46: 1-412.

Van de Vijver B., Beyens L., Lange-Bertalot H. 2004a. The genus *Stauroneis* in the Arctic and (Sub-) Antarctic regions. Bibliotheca Diatomologica. 51. J. Cramer, Berlin, Stuttgart, 317 pp.

Van de Vijver B., Beyens L., Vincke S., Gremmen N.J.M. 2004b. Moss-inhabiting diatom communities from Heard Island, sub-Antarctica. Polar Biology. 27: 532-543.

Van de Vijver B., Gremmen N.J.M., Beyens L. 2005. The genus *Stauroneis* (Bacillariophyceae) in the Antarctic region. Journal of Biogeography. 32: 1791-1798.

Van de Vijver B., Van Dam H., Beyens L. 2006. *Luticola higleri* sp. nov., a new diatom species from King George Island (South Shetland Islands, Antarctica). Nova Hedwigia. 82 (1-2): 69-79.

Van de Vijver B., Gremmen N., Smith V. 2008a. Diatom communities from the sub-Antarctic Prince Edward Islands: diversity and distribution patterns. Polar Biology. 31: 795-808.

Van de Vijver B., Kelly M., Blanco S., Jarlman A., Ector L. 2008b. The unmasking of a sub-Antarctic endemic: *Psammothidium abundans* (Manguin) Bukhtiyarova et Round in European rivers. Diatom Research. 23 (1): 233-242.

Van de Vijver B., Mataloni G. 2008. New and interesting species in the genus Luticola D.G. Mann (Bacillariophyta) from Deception Island (South Shetland Islands). Phycologia. 47 (5): 451-467.

Van de Vijver B., Agius J.T., Gibson J.A.E., Quesada A. in press. An unusual spine-bearing *Pinnularia* species from the Antarctic Livingston Island (South Shetland Islands). Diatom Research.

Van Heurck H. 1909. Diatomées. In: Résultats du Voyage du S.Y. Belgica en 1897-1898-1899. Rapports Scientifiques. Botanique. Imprimerie J.-E. Buschmann, Antwerpen. Botanique. 6: 1-129.

Verleyen E., Hodgson D.A., Vyverman W., Roberts D., McMinn A., Vanhoutte K., Sabbe K. 2003. Modelling diatom responses to climate induced fluctuations in the moisture balance in continental Antarctic lakes. Journal of Paleolimnology. 30: 195-215.

Wasell A., Håkansson H. 1992. Diatom stratigraphy in a lake on Horseshoe Island, Antarctica: a marine-brackish-fresh water transition with comments on the systematics and ecology of the most common diatoms. Diatom research, 7 (1): 157-194.

West W., West G.S. 1911. Freshwater algae. British Antarctic Expedition (1907-1909). Science Report, Biology. 1 (7): 263-298.

Witkowski A., Lange-Bertalot H., Metzeltin D. 2000. Diatom flora of marine coasts I. Iconographia Diatomologica. 7: 1-925.

Chapter 5:

Five new non-marine diatom taxa from islands in the Atlantic sector of the Southern Ocean

Bart Van de Vijver, Mieke Sterken, Wim Vyverman, Gabriela Mataloni, Linda Nedbalova, Katerina Kopalova, Elie Verleyen & Koen Sabbe

Abstract

A survey of the non-marine diatoms from several islands in the Atlantic sector of the Southern Ocean (a.o. South Shetlands, South Georgia, James Ross Island) resulted in the description of five species new to science: *Chamaepinnularia gerlachei* Van de Vijver & Sterken sp. nov., *Craticula antarctica* Van de Vijver & Sabbe sp. nov., *Craticula subpampeana* Van de Vijver & Sterken sp. nov., *Diadesmis australis* Van de Vijver & Sabbe sp. nov. and *Navicula australoshetlandica*. Van de Vijver sp. nov. The morphology of each species is described on the basis of light and electron microscopy, and they are compared to similar species, especially with those present in the Subantarctic and Antarctic Region. Preliminary observations on the ecology and biogeography of each species are provided.

This chapter is a manuscript in preparation

Contribution of the author: diatom size measurements and identification in the LSB dataset (see Chapter 4), revision/writing parts of the manuscript..

5.1. Introduction

During the last century, taxonomic and floristic studies of freshwater and terrestrial environments in the Subantarctic and Antarctic revealed the presence of diverse diatom communities, often comprising a large number of new taxa which to date have only been reported from the Antarctic (e.g. Kellogg et al., 1980, Spaulding et al., 1999, West & West 1911). Other taxa, which have been commonly reported from the Antarctic for decades, appeared to have been consistently wrongly identified as a result of force-fitting to species described in European and North-American floras [see Sabbe et al. (2003) for a detailed discussion of this issue]. Indeed, recent taxonomic revisions have shown that many of these constitute species in their own right, which has resulted in a spate of descriptions of new taxa (a.o. Schmidt et al., 1990; Kociolek & Jones 1995; Spaulding et al., 1999; Van de Vijver & Mataloni 2008 and references therein). These revisions also resulted in a more complete understanding of the geographical distributions of Antarctic non-marine diatoms and diatom biogeography in general, suggesting that at least some diatoms do possess more restricted geographic ranges (Van de Vijver et al., 2005, Vyverman et al., 2007). The present paper adds to the increasing body of evidence supporting widespread endemism in the non-marine diatom floras of the Antarctic region through the description of five new taxa belonging to four different genera.

5.2. Material and Methods

Sediment and moss samples were collected from various terrestrial and freshwater habitats in the following islands in the Atlantic sector of the Southern Ocean: South Shetland Islands (King George Island, Livingston Island, Deception Island), South Georgia, James Ross Island, Signy Island and Beak Island.

Diatom samples were prepared following the method of Van der Werff (1955). Small parts of the samples were cleaned by adding 37 % H_2O_2 and heating to 80°C for about 1 hour whereafter the reaction was completed by addition of $KMnO_4$. Following digestion and centrifugation (3 times 10 minutes at 3500 rpm), the material was diluted with distilled water to avoid excessive concentrations of diatom valves that may hinder reliable observations. Samples from Beak Island were processed according to methods described in Chapters 6 and 7; most of the samples from Livingston & Signy Island were prepared according to Jones et al. (1993) and Jones & Juggins (1995). Cleaned diatom valves were mounted in Naphrax®. Samples and slides are stored at the National Botanic

Garden of Belgium (BR), Department of Bryophytes and Thallophytes, the Research Group of Protistology and Aquatic Ecology of Ghent University, and the Geography Department of University College London. Light microscope (LM) observations were conducted using an Olympus BX51 microscope equipped with Differential Interference Contrast (Nomarski) optics or an Olympus CX 41 microscope at a magnification of 10x100x (Sterken et al., in prep. a). For scanning electron microscopy (SEM), part of the suspension was filtered through polycarbonate membrane filters with a pore diameter of 3 µm, pieces of which were fixed on aluminium stubs after air-drying. The stubs were sputter-coated with 50 nm of Au and studied in a JEOL-5800LV at 20 kV. Terminology of valve morphology is based on Barber & Haworth (1981) and Round et al. (1990).

5.3. Observations

Chamaepinnularia gerlachei Van de Vijver & Sterken sp. nov. (Figs. 1-18)

DIAGNOSIS: Valvae lineares marginibus parallellibus apicibusque rotundatis non-protractis. Longitudo 12-30 µm, latitudo 3.3-4.9 µm. Area axialis moderate lata, dilatans graduatim in aream centralem. Area centralis rhombica-lanceolata, formans fasciam potius latam. Raphe recta, filiformis teminationibus distalis rectis, leviter expansis fissurisque terminalibus unilateraliter uncinatis. Striae transapicales parallelae ad leviter radiatas prope aream centralem, 15-20 in 10 µm, interruptae ad marginem valvae linea hyalina. Striae continuantes circa polos.

HOLOTYPUS: BR-XXX (National Botanic Garden, Meise, Belgium)
ISOTYPI : PLP-XXX (UA, University of Antwerp, Belgium), BRM-ZUHXXX (Hustedt Collection, Bremerhaven, Germany)
TYPE LOCALITY: James Ross Island, Muddy Lake Sample JRI2008-18 (Coll. L. Nedbalová, 01/02/2008)
ETYMOLOGY: This species is dedicated to Adrien de Gerlache (1866-1934), the commander of the first Belgian expedition to the Antarctic, and the first ever to spend winter there, after their ship called “Belgica” was trapped in the ice of the Bellingshausen Sea in 1899.

MORPHOLOGY: Frustules rectangular in girdle view (Fig. 16). Valves linear with more or less parallel margins and broadly rounded apices, 12-30 µm long, 3.3-4.9 µm wide (n =

41). Axial area lanceolate widening to a rectangular central area which forms a rather broad fascia. Raphe straight, filiform with straight, weakly expanded central endings and terminal fissures hooked in the same direction. Striae parallel to weakly radiate near the central area, 15-20 in 10 µm, sometimes interrupted near the valve margin by a small hyaline line (Figs. 1, 4-5), which runs from the central area and terminates somewhat before the apices (Fig. 17). Internally, this line is visible as a rib-like structure inside the alveoli (Fig. 18). The striae consist of alveoli which are externally covered by hymenate occlusions (Fig. 17). Short striae continue around the valve apices. Terminal fissures bent to the same side, continuing onto the mantle (Fig. 17). Central endings expanded, drop-like. Internally, central nodule present (Fig. 18).

DISTRIBUTION: Northeast Antarctic Peninsula (James Ross Island, Beak Island), South Shetland Islands (Deception Island, Livingston Island), South Orkney Islands (Signy Island), South Georgia. This species has to date not been observed in localities in the southern Indian Ocean (Van de Vijver B, unpubl. obs.)

ECOLOGY: The type population of *Chamaepinnularia gerlachei* was found in a dried soil sample from Muddy Lake on James Ross Island (pH 6.85, conductivity about 600 µS/cm). The lake has a moderately high degree of sulphate (152.4 µg/l) and a moderate to very low amount of phosphate (46.5 µg/l) and nitrogen (0.00 µg/l). The associated diatom flora is dominated by *Nitzschia* cf. *pusilla* Grunow with *Achnanthes taylorensis* Kellogg et al., *Navicula cincta* (Ehrenberg) Ralfs and *Luticola* cf. *cohnii* (Hilse) Mann as subdominant species. On Deception Island, the species was mostly found near Turbio Lake, accompanied by *Chamaepinnularia krookiiformis* (Krammer) Lange-Bertalot & Krammer, *Stauroneis latistauros* Van de Vijver & Lange-Bertalot, *Psammothidium metakryophilum* (Lange-Bertalot & Schmidt) Sabbe and *Planothidium lanceolatum* s.l. (Brébisson) Lange-Bertalot.

C. gerlachei was identified as *Pinnularia* sp. *1*, in Jones & Juggins (1995), where its chlorophyll *a* optimum was estimated at c. 0.80 µg/l. The species was also found in fossil diatom assemblages from lake sediment cores retrieved from two isolation lakes on Beak Island (Chapters 6 and 7), where its increased abundance near the marine-freshwater transitions and the marine sections of these cores suggest a preference for brackish to saline waters.

***Craticula antarctica* Van de Vijver & Sabbe sp. nov**. (Figs 49-66)

DIAGNOSIS: Valvae lancolatae ad ellipticas-lanceolatas marginibus claro convexis apicibus capitatis. Longitudo 23.5-36 µm, latitudo (6.2-)6.5-8.0 µm. Area axialis angusta, linearis. Area centralis parva, elliptica ad ovalem. Raphe filiformis, recta terminationibus centralis distantibus. Striae transapicales rectae radiataeque in medio parte valvae, convergentae fortiter arcuatae ad etiam geniculatas prope apices, 17-20 in 10 µm. Areolae non visibiles in microscopico photonico.

HOLOTYPE: BR-XXX (National Botanic Garden, Meise, Belgium)
ISOTYPE: PLP- XXX (UA, University of Antwerp, Belgium), BRM-XXX (Hustedt Collection, Bremerhaven, Germany)
TYPE LOCALITY: James Ross Island, Nadeje Lake Sample JRI2008-25 (Coll. L. Nedbalová, 13/02/2008)

MORPHOLOGY: Valves elliptical to lanceolate-elliptical with rostrate to capitate apices, 31-36 µm long, 6.5-8.0 µm wide (n=14, type population). Axial area narrowly linear. Central area indistinct, narrowly elliptical. Raphe filiform with straight, simple, rather distant central endings. Central raphe endings simple, straight to very weakly bent, terminal fissures hooked in the same direction (Figs 59-62, 64). Terminal raphe endings straight, ending in a slightly swollen hyaline area (Fig. 63). Striae straight to radiate in the centre, becoming convergent to arcuate-geniculate towards the apices, 17-20 in 10 µm (n=23). Areolae indistinct in LM, roundish (Fig. 64) to apically elongate (Fig. 62) in SEM. Near the apices, areolae rather irregularly organized (Fig. 61). Internally, the striae are separated by thickened virgae (Figs. 60, 63-64), but less so near the centre; they appear to be occluded by vela (Fig. 64). A small proportion of the population consisted of valves that were entirely coated with silica (Figs 58, 65-66).

CONFIRMED DISTRIBUTION: Northeast Antarctic Peninsula (James Ross Island, Beak Island), Antarctic Continent (Bunger Hills, Larsemann Hills, Rauer Islands, Skarvsness ice-free area, Vestfold Hills, Kazumi Iwa, see Ko-bayashi 1965, as *C. molesta*, Roberts & McMinn 1999, as *C. molesta*, Sabbe et al., 2003, as *C.* cf. *molesta*, Gibson et al., 2006, as *Craticula* sp. a, Ohtsuka et al., 2006, as *Craticula* sp.). In Crozet and Signy Island the closely similar *C. submolesta* (Van de Vijver et al., 2002) is present.

ECOLOGY: The type population of *Craticula antarctica* was observed in alkaline Nadeje Lake on James Ross Island in a sediment sample taken at a depth of 6 m (pH 8.38, conductivity 710 µS/cm). Phosphate level is moderate (61 µg/l), sulphate (8.4 µg/l) and nitrogen (0.01 µg/l) are low. The accompanying diatom flora consists of *Nitzschia inconspicua* Grunow, *N. perminuta* (Grunow) Peragallo and *Planothidium* cf. *haynaldii*. On Beak Island this species was exclusively found in fossil assemblages from a sediment core retrieved in an isolation basin (Beak-1), where it only occurred in sediment samples that correspond with, or immediately postdate the timing of isolation of the lake basin from the sea (i.e. between c. 6930-6580 cal. yr. BP or 76-71 cm depth; Chapter 7).

***Craticula subpampeana* Van de Vijver & Sterken sp. nov**. (Figs 43-48, 67-70)

DIAGNOSIS: Valvae lanceolatae apicibus acute rotundatis, non protractis. Longitudo 80-110 µm, latitudo 15.0-20.5 µm. Area axialis linearis, angusta. Area centralis semper distincte dilatata. Raphe filiformis terminationibus distantibus uncinatis. Striae transapicales, 13-17 in 10 µm, ad nodulem centralem versus distantiores positae. Areolae 25-28 in 10 µm.

HOLOTYPE: BR-XXX (National Botanic Garden, Meise, Belgium)
ISOTYPE: PLP- XXX (UA, University of Antwerp, Belgium), BRM-XXX (Hustedt Collection, Bremerhaven, Germany)
TYPE LOCALITY: James Ross Island, Monolith Lake, Sample JRI2008-11 (Coll. L. Nedbalová, 01/02/2008)

MORPHOLOGY: Valves lanceolate with acutely rounded, non-protracted ends. 80-110 µm long, 15.0-20.5 µm wide (n=13). Axial area narrowly linear, central area slighty wider, elliptic-lanceolate. Raphe filiform, slightly wider near the apices. Central raphe endings rather distant, expanded, hooked in the same direction (Figs. 48, 67). Internally, they are indistinct, slightly deflected (Fig. 69). Terminal fissures hooked in the same direction, to the opposite side as the central raphe endings (Figs. 43-47, 68). Internally, the distal raphe endings terminate in a small helictoglossa (Fig. 70). Striae 13-17 in 10 µm, distinctly lineolate (25-28 areolae in 10 µm), slightly more distantly spaced and radiate in the centre of the valve, becoming more or less parallel throughout the rest of the valve to slightly convergent near the apices. Externally, the areolae are apically elongate connected by slight, longitudinal grooves in the centre and separated by thick

longitudinal ribs towards the apices (Figs 67-68). Internally, the areolae are covered by vela and appear more roundish (Fig. 69). Heribaudii stage not observed.

CONFIRMED DISTRIBUTION: South Shetland Islands (South Georgia, Livingston Island), South Orkney Islands (Signy Island), Northeast Antarctic Peninsula (James Ross Island, Beak Island). It is possible that some of the records of *C. cuspidata* in Kellogg & Kellogg (2002) refer to *C. subpampeana*; these should be verified. *Craticula subpampeana* was identified as *Navicula cuspidata* (Kützing) Kützing in Håkansson & Jones (1994).

ECOLOGY: The type population was epilithic in Monolith Lake on James Ross Island, a large lake with circumneutral pH, low conductivity (120 µS/cm) and low values of phosphate (9.7 µg/l), nitrogen (0.00 µg/l) and sulphate (14.8 µg/l). The diatom flora in this lake was dominated by *Achnanthidium* cf. *exiguum* (Grunow) Czarnecki, *Nitzschia perminuta*, *Navicula libonensis* Schoeman, *Diadesmis australis* Van de Vijver & Sabbe and *Fragilaria capucina* s.l. Desmazières. In Signy, Livingston and Beak Islands (Chapter 6), it was also only found in lakes with relatively low conductivities (86-172 µS/cm).

***Diadesmis australis* Van de Vijver & Sabbe sp. nov**. (Figs 19-29)

DIAGNOSIS: Valvae lineares parte centrale claro inflata apicibusque lato rotundatis vel interdum leviter inflatis. Longitudo 6-19 µm, latitudo 2.0-5.0 µm. Area axialis moderate lata, area centralis rotunda. Raphe filiformis, recta terminationibus centralis potius distantibus. Striae transapicales distinguibiles in microscopico photonico, 32-36 in 10 µm, parallellae ad leviter radiatas.

HOLOTYPE: BR-XXX (National Botanic Garden, Meise, Belgium)
ISOTYPE: PLP- XXX (UA, University of Antwerp, Belgium), BRM-XXX (Hustedt Collection, Bremerhaven, Germany)
TYPE LOCALITY: James Ross Island, Monolith Lake Sample JRI2008-10 (Coll. L. Nedbalová, 01/02/2008)

MORPHOLOGY: Valves linear but distinctly inflated in the centre, with broadly rounded, sometimes slightly swollen apices, 6-19 µm long, 2.0-5.0 µm wide (n=40). Axial area moderately broad, widening towards a rounded central area. Raphe straight, filiform, with

central endings rather distant. In SEM (Fig. 29), external central and terminal raphe endings simple, straight, flanked by two small elongate depressions. Striae usually distinct in LM, especially in the centre of the valve, 32-36 in 10 µm. They are parallel to slightly radiate, curve around the centre and extend beyond the terminal raphe fissures. On the valve face, the striae consist of a single, slightly transapically elongate areola. Striae bordering the central area slightly shorter than those bordering the axial area. Towards the poles, striae tend to diverge near the terminal raphe endings. A single row of areolae, continuous around the apices, is present on the mantle. Spines absent.

CONFIRMED DISTRIBUTION: Northeast Antarctic Peninsula (James Ross Island, Beak Island), South Shetland Islands (King George Island, Livingston Island) and South Orkney Islands [Signy Island (Jones & Juggins 1995, as *Navicula perpusilla*)], Antarctic Continent [Bunger Hills (Gibson et al., 2006 as *Diadesmis* sp. a, Larsemann Hills & Rauer Islands (Sabbe et al., 2003 as *D.* cf. *perpusilla*)]. Due to confusion with *D. perpusilla*, the species is probably more widespread than indicated here. However, it was hitherto never observed on the sub-Antarctic Islands of the southern Indian Ocean (Van de Vijver B., unpubl. obs.).

ECOLOGY: The type population of this species was found in the epipelon of Monolith Lake (James Ross Island, see. *Craticula subpampeana).* Jones & Juggins (1995) modelled a low chlorophyll-a optimum for this species (i.e. 0.80 µg/l). In a combined surface dataset from Livingston, Signy and Beak Island, the species typically occurred in lakes with low nutrient concentrations, but occurred in high abundances in the shallow lakes from Beak Island (Beak-3, Beak-2 and Beak-5; see Chapter 6).

Navicula australoshetlandica **Van de Vijver sp. nov. (**Figs. 30-42)

DIAGNOSIS: Valvae angustae, lineares-lanceolatae apicibus cuneatim rotundatis, non-protractis. Longitudo 13-22.5 µm, latitudo 3.9-5.0 µm. Area axialis angusta. Area centralis symmetrica, dilatata transversaliter, marginata 2-3 striis curtis. Raphe filiformis terminationibus centralis poris expansis. Striae transapicales claro radiatae leviterque curvatae prope aream centralem, rectae parallellaeque ad etiam convergentes ad polos, 12-15 in 10 µm. Lineolae leviter distinguibiles in microscopico photonico, ca. 35 in 10 µm.

HOLOTYPE: BR-XXX (National Botanic Garden, Meise, Belgium)
ISOTYPE: PLP- XXX (UA, University of Antwerp, Belgium), BRM-XXX (Hustedt Collection, Bremerhaven, Germany)
TYPE LOCALITY: King George Island, South Shetland Islands, Sample W625, Bellingshausen, (coll. L. Beyens, 19/01/1998)

MORPHOLOGY: Valves narrow, linear-lanceolate to lanceolate with cuneate apices, 13-22.5 µm long, 3.9-5.0 µm wide (n=53). Axial area narrow. Central area rectangular, bordered by 2-3 shortened striae. Raphe filiform with straight, expanded, rather distant central endings. Terminal fissures hooked in the same direction. Striae radiate and slightly curved near the centre, to convergent near the apices, 12-15 in 10 µm. Areolae indistinct in LM, ca. 35 in 10 µm.

CONFIRMED DISTRIBUTION: Northeastern Antarctic Peninsula (Beak Island), South Shetland Islands (King George Island, Livingston Island), South Georgia. This taxon was recognized as *Navicula* sp. 1 (ZZZ952) as well as 'ZZZ959' in samples from Livingston Island (Jones et al., 1993).

ECOLOGY: The type population of *Navicula australoshetlandica* was found near the Bellingshausen Station on King George Island (South Shetland Islands). The species was present in a small, shallow, mud pool surrounded by mosses (pH 8.8, conductivity 250 µS/cm). The associated diatom community was composed of *Nitzschia homburgiensis*, *N. perminuta*, *N. debilis* Arnott, various *Luticola* taxa (e.g. *L. higleri* Van de Vijver, Van Dam & Beyens, *Amphora* cf. *veneta* and various *Pinnularia* taxa (e.g. *P.* cf. *microstauron*). In Jones et al. (1993), *Navicula australoshetlandica* was identified as *Navicula* species 1 (code ZZZ952), and was found in a few low-elevation coastal lakes Livingston Island. On Beak-Island, this species was only found in fossil diatom assemblages in a sediment core retrieved from a shallow coastal lake (Beak-3; Sterken et al., unpubl. data).

5.4. Discussion

Chamaepinnularia gerlachei presents all features to justify its position within the genus *Chamaepinnularia*, such as small size and the interruption of the striae near the valve face/mantle junction. *C. gerlachei* can be separated from other *Chamaepinnularia* species by its quite distinct fascia. *C. gandrupii* (Petersen) Lange-Bertalot & Krammer shows a similar linear valve outline but has undulating margins and lacks the typical fascia. In *C. krasskei* Lange-Bertalot, some specimens have a very small fascia but the striae are never interrupted near the valve face/mantle junction, as is the case in *C. gerlachei*. *C. krookiiformis* (Krammer) Lange-Bertalot & Krammer has typical capitate valve apices and convex margins. *C. amphiborealis* Lange-Bertalot & Werum has a large central area that is however always bordered by shortened striae. The striation pattern is also different with clearly radiate striae near the central area and convergent striae near the apices. The Antarctic *C. australomediocris* (Lange-Bertalot & Schmidt) Van de Vijver is shorter (valve length 8-15 µm versus 12-30 µm in *C. gerlachei*) with a more lanceolate outline (compared to the linear outline in *C. gerlachei*) and a narrower axial area.

Craticula antarctica has incorrectly been reported from the Antarctic as *Craticula* (*Navicula*) *molesta* (Krasske) Lange-Bertalot & Willmann, an Arctic species (e.g. Kobayashi (1965); see Sabbe et al. (2003) and Gibson et al. (2006) for a detailed discussion). *C. antarctica* closely resembles *C. buderi* (Hustedt) Lange-Bertalot *sensu* Lange-Bertalot (2001), which according to Lange-Bertalot (2001) is conspecific with *C. pseudohalophila* Cholnoky (cf. also Schoeman & Archibald 1977), both taxa occupying opposite ends of the size spectrum. *N. pseudohalophila* can be separated from *C. antarctica* on the basis of valve outline (less capitate and more rostrate in the former) and striation pattern (*C. pseudohalophila* has several shortened striae near the central area and lacks the typical geniculate striae near the apices). Other small *Craticula* species such as *C. accomoda* (Hustedt) Mann, *C. molestiformis* (Hustedt) Lange-Bertalot and *C. submolesta* (Hustedt) Lange-Bertalot differ sufficiently with respect to valve dimensions and valve outline to avoid confusion with *C. antarctica*. *C. riparia* var. *mollenhaueri* Lange-Bertalot has a different valve outline with more protracted apices and a higher stria density (21-23 vs. 17-20 in *C. antarctica*).

There are slight but potentially significant differences in width (6.5-8.0 vs. 4.9-6.2 µm respectively) and stria density (17-20 vs. 22 striae in 10 µm respectively) between the James Ross Island type population and populations from the Bunger Hills (unpubl. data), Rauer Islands and the Larsemann Hills (Sabbe et al., 2003), which need to be further

investigated. Solid valves were observed in material from James Ross Island and Beak Island (Fig. 58). While larger *Craticula* species such as *C. cuspidata* have typical Héribaud structures (series of parallel transverse bars attached to the internal sternum), smaller species tend to irregularly deposit silica on the valve interior, resulting in a continuous siliceous covering of the valve (Kusber & Cocquyt, 2007).

Craticula subpampeana can easily be distinguished from several other larger *Craticula* species such as *C. pampeana* (Frenguelli) Lange-Bertalot or *C. acidoclinata* Lange-Bertalot & Metzeltin but bears nevertheless some similarities such as the typically hooked central raphe endings. *C. pampeana* is much larger with a valve width exceeding 30-35 µm (versus 15-20.5 in *C. subpampeana*) and a lower number of striae in 10 µm (10 vs. 13-17 in *C. subpampeana*). *C. pampeana* was described from a fossil deposit in Argentina (Frenguelli, 1926). *C. acidoclinata* has a more elliptical-lanceolate valve outline and undulating raphe branches. In addition, this species is mainly found in oligotrophic to dystrophic environments. Carlson (1913) described *Navicula megacuspidata* from South Georgia, a species that without doubt should be transferred to *Craticula*. This species is much larger than *C. subpampeana* (180-245 µm long vs. 80-110 in the latter). Cosmopolitan species such as *C. ambigua* (Ehrenberg) Mann and *C. cuspidata* (Kützing) Mann differ in valve outline, raphe structure and valve dimensions (Lange-Bertalot 2001).

Many (if not all) reports of *Diadesmis* (cf.) *perpusilla* (Grunow) Mann or *Diademis* (*Navicula*) *gallica* var. *perpusilla* (Grunow) Lange-Bertalot from the Antarctic (see Kellogg & Kellogg 2002) most probably concern *Diadesmis australis*. As the type material of *Navicula perpusilla* Grunow can not be traced, we have based our comparison with *D. australis* on *D. perpusilla sensu* Werum & Lange-Bertalot (2004). *D. perpusilla* has a more lanceolate to lanceolate-elliptical valve outline usually lacking the inflated central part and striae which converge (Round et al., 1990: p.530 fig.d) around the terminal raphe endings, and not diverge like in Fig. 29 and Sabbe et al. (2003, Fig. 80). In addition, in *D. perpusilla* the depressions flanking the central raphe endings sometimes connect forming a spathulate groove (Werum & Lange-Bertalot 2004, p.325 Fig. 2), and *D. perpusilla* sometimes possesses spines. *D. gallica* is a chain-forming species bearing linking spines. Specimens present in these chains have a tendency to loose their raphe system, a feature never observed in *D. australis*. *D. laevissima* has a lanceolate to elliptical-lanceolate valve outline with short striae composed of very small, rounded areolae, contrary to *D. australis* which always has a tumescent central part and

transapically elongated areolae. *D. ingeae* Van de Vijver, *D. ingeaeformis* Hamilton & Antoniades, *D. arcuata* (Heiden) Lange-Bertalot, *D. arcuatoides* Lange-Bertalot and *D. tabellariaeformis* (Krasske) Lange-Bertalot & Wojtal all have an inflated central part but apart from *D. ingeaeformis*, they all lack the depressions flanking the raphe endings. *D. ingeaeformis* has inflated apices which are usually larger than the inflated central part. *D. tabellariaeformis* has an extremely large central part, resembling (hence the name) members of the genus *Tabellaria*.

Navicula australoshetlandica shows some similarities to other *Navicula* species such as *N. lauca* Rumrich & Lange-Bertalot, *N. doehleri* Lange-Bertalot, *N. veneta* Kützing, *N. wiesneri* Lange-Bertalot and *N. vekhovii* Lange-Bertalot & Genkal. Apart from *N. veneta*, none of these species has been recorded from the Antarctic Region to date. *N. lauca*, described from the Altiplano in Chile (Rumrich et al., 2000), is similar in outline but has slightly produced valve apices and a lower stria density (10-12 vs. 12-14 in *N. australoshetlandica*). *N. doehleri*, only found in Svalbard (Lange-Bertalot, 2001) has a lower striadensity (8-9 vs. 12-14 in 10 µm in *N. australoshetlandica*). *N. veneta* can be easily separated based on its valve outline, which is more elliptic-lanceolate with clearly convex margins and wedge-shaped, protracted ends, and width (5-6 µm vs. 3.9-5.0 µm in *N. australoshetlandica*). *N. wiesneri* has a coarser striation pattern, more convex margins and a rather irregularly shaped central area. Finally, *N. vekhovii* has a lanceolate valve outline with acutely rounded apices and a clearly wedge-shaped central area. The smaller *Navicula* taxa from the complex around *N. tenelloides* Hustedt such as *N. arctotenelloides* Lange-Bertalot & Metzeltin all have a typically lanceolate valve outline with more convex margins and protracted valve apices.

Acknowledgments

The authors wish to thank Prof. Dr. Louis Beyens (University of Antwerp) who collected the sample from King George Island in 1998 and Dr. Viv Jones who collected the Signy and Livingston Island materials. Mrs. Myriam de Haan is acknowledged for technical assistance using the Scanning Electron Microscope.

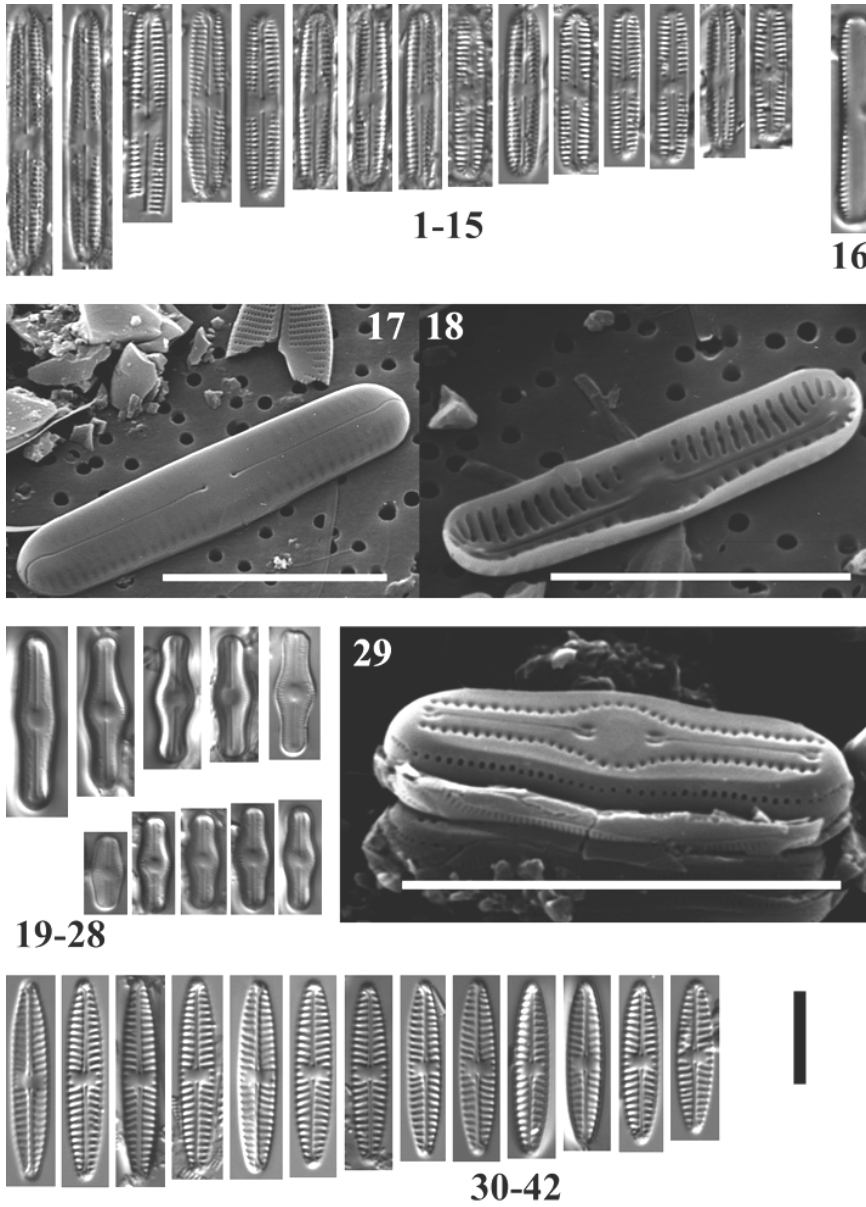

Plate 1: Figs 1-18. *Chamaepinnularia gerlachei* sp.nov. Figs 1-15 LM valve views of the type population. Fig. 16. LM girdle view. Fig. 17. SEM external view of an entire valve showing the raphe structure and the hyaline line interrupting the striae. Fig. 18. SEM internal view of an entire valve showing the typical *Chamaepinnularia* features. Figs. 19-29 *Diadesmis australis* sp.nov. Figs. 19-28 LM views of the type population. Fig. 29. SEM external view of an entire valve. Figs. 30-42. *Navicula australoshetlandica* sp.nov. LM type population. Scale bars represent 10 µm.

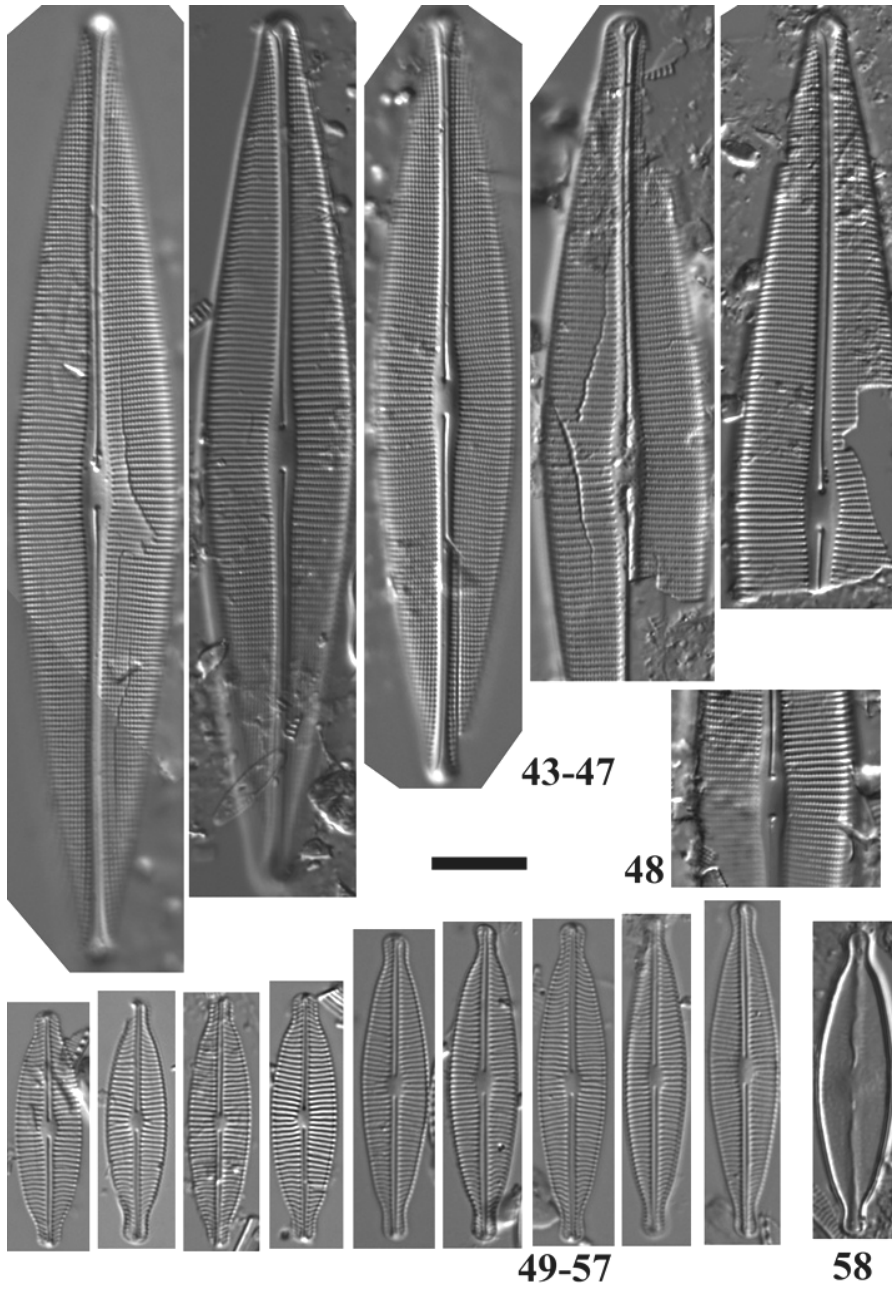

Plate 2: Figs 43-48. *Craticula subpampeana* sp.nov. Figs 43-47 LM views of the type population. Fig. 48. LM detail view of the hooked central raphe endings. Figs. 49-58. *Craticula antarctica* sp.nov. Figs. 49-57 LM views of the type population. Fig. 58. LM view of a valve with excessive silica coverings. Scale bars represent 10 µm.

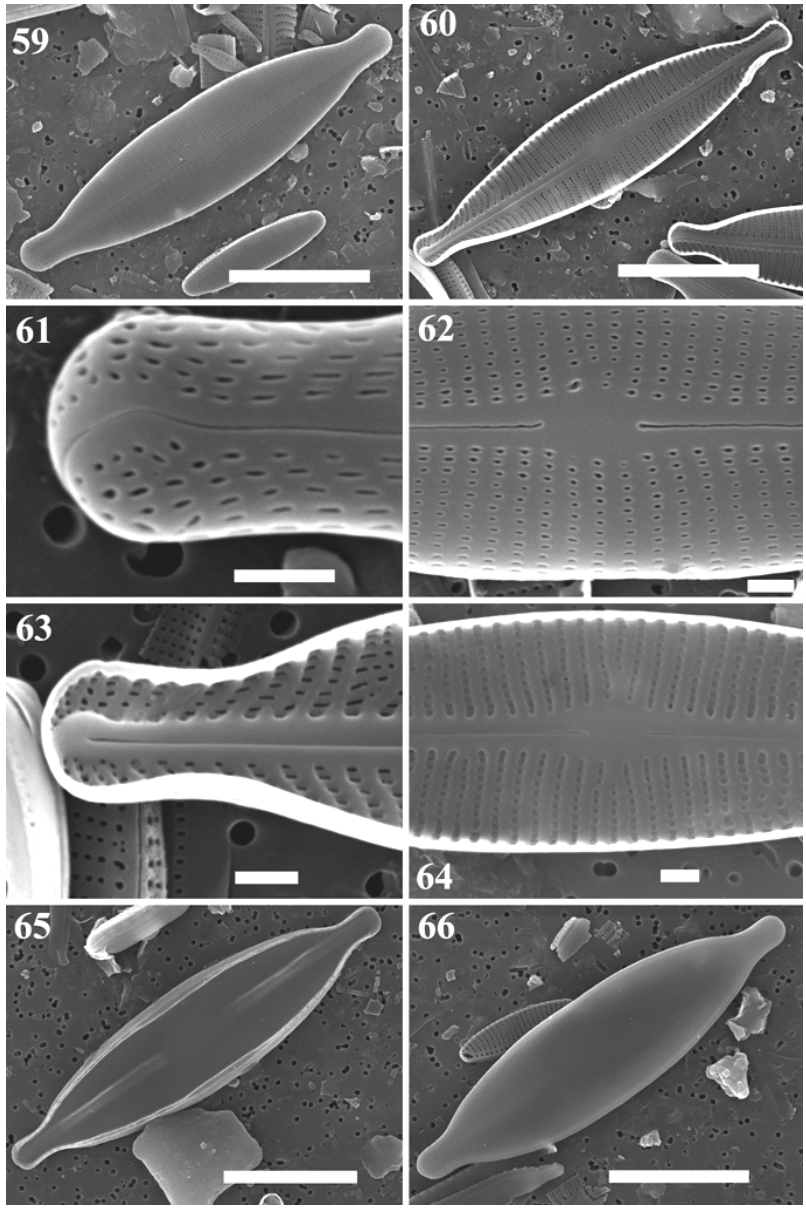

Plate 3: Figs 59-66. *Craticula antarctica* sp. nov. Fig. 59. SEM external view of an entire valve. Fig. 60. SEM internal view of an entire valve. Fig. 61. SEM external detail of a valve apex with the irregularly organized areolae. Fig. 62. SEM external detail of the central area with the central raphe endings. Fig. 63. SEM internal detail of a valve apex with the irregularly organized areolae. Fig. 64. SEM internal detail of the central area with the central raphe endings. Note the vela covering the areolae. Figs 65-66. SEM external view of two valves with excessive silica coverings. Scale bare represents 10 µm except for figs 61-64 where scale bar = 1 µm.

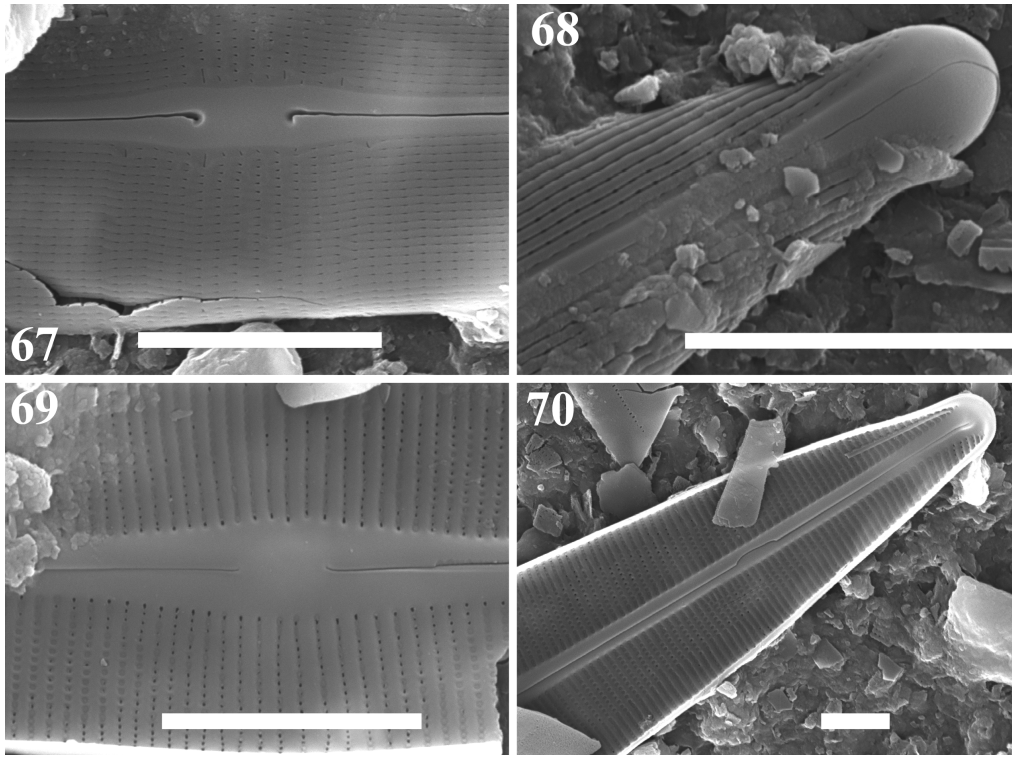

Plate 4: Figs 67-70. *Craticula subpampeana* sp.nov. SEM, external (Figs 67-68) and internal (Figs 69-70) views.

References

Barber H.G., Haworth E.Y. 1981. A guide to the morphology of the diatom frustule. The Freshwater Biological Association, Scientific Publication, 44, 111p.

Carlson G.W.F. 1913. Süsswasseralgae aus der Antarktis, Südgeorgien und den Falkland Inseln. Wissenschaftliche Ergebnisse der Schwedischen Südpolar-Expedition 1901-1903, unter leitung von dr. Otto Nordenskjøld. 4 (Botanique): 1-94 + 3 plates.

Frenguelli J. 1926. Diatomeas fósiles del Prebelgranense de Miramar (Contr. IV) Bolletim del Academia nacional de Ciencias de Cordoba. 29: 5-108.

Gibson J.A.E., Roberts D., Van de Vijver B. (2006) Salinity control of the distribution of diatoms in lakes of the Bunger Hills, East Antarctica. Polar Biology. 29: 694-704.

Håkansson H., Jones V.J. 1994. The compiled freshwater diatom taxa list for the maritime region of the South Shetland and South Orkney Islands. In: Hamilton P.B. 1994. Proceedings of the fourth Arctic-Antarctic diatom symposium.

Jones V., Juggins S., Ellis-Evans J.C. 1993. The relationship between water chemistry and surface sediment diatom assemblages in maritime Antarctic lakes. Antarctic Science. 5 (4): 339-348.

Jones V., Juggins S. 1995. The construction of a diatom-based chlorophyll a transfer function and its application at three lakes on Signy Island (maritime Antarctic) subject to differing degrees of nutrient enrichment. Freshwater biology. 34: 433-445.

Kellogg T.B., Kellogg D.E. 2002. Non-marine and littoral diatoms from Antarctic and subantarctic regions. Distribution and updated taxonomy. Diatom monographs. 1: 1-795.

Kellogg D.E., Stuiver M., Kellogg T.B., Denton G.H.D. 1980. Non-marine diatoms from Late Wisconsin perched deltas in Taylor Valley, Antarctica. Palaeogeography, Palaeoclimatology, Palaeoecology. 30: 157–189.

Ko-Bayashi T. 1965. Variations on some pinnate diatoms from Antarctica. 2. JARE Science Report (Biology). 24: 1-28.

Kociolek J., Jones V.J. 1995. *Gomphonema signyensis* sp. nov., a freshwater diatom from Maritime Antarctica. Diatom Research. 10: 269-276.

Krasske G. 1938. Beiträge zur Kenntnis der Diatomeen-Vegetation von Island un Spitsbergen. Archiv für Hydrobiologie. 33: 503-533.

Kusber W-H., Cocquyt C. 2007. *Craticula elkab* (O.) Müller Lange-Bertalot, Kusber & Cocquyt comb. Nov. – typification and observations based on African sediment core material. Diatom Research. 22: 117-126.

Lange-Bertalot H. 2001. *Navicula* sensu stricto, 10 genera separated from *Navicula* sensu lato, *Frustulia*. Diatoms of Europe. 2: 1-526.

Ohtsuka T., Kudoh S., Imura S., Ohtani S. 2006. Diatoms composing benthic microbial mats in freshwater lakes of Skarvness ice-free area, East-Antarctica. Polar Bioscience. 20: 113-131.

Roberts D., McMinn A. 1999. Diatoms of the saline lakes of the Vestfold Hills, Antarctica. Bibliotheca Diatomologica. 44: 1-83.

Round F.E., Crawford R.M., Mann D.G. 1990. The diatoms. Biology & Morphology of the genera. Cambridge University Press, Cambridge, 747pp.

Rumrich U., Lange-Bertalot H., Rumrich M. 2000. Diatomeen der Anden. Iconographia diatomologica. 9: 1-649.

Sabbe K., Verleyen E., Hodgson D.A., Vanhoutte K., Vyverman W. 2003. Benthic diatom flora of freshwater and saline lakes in the Larsemann Hills and Rauer Islands, East-Antarctica. Antarctic Science. 15(2): 227-248.

Schmidt R., Mäusbacher R., Müller J. 1990. Holocene diatom flora and stratigraphy from sediment cores of two Antarctic lakes. Journal of Paleolimnology. 3: 55-74.

Schoemann F.R., Archibald R.E.M. 1977. The diatom flora of Southern Africa. CSIR special report WAT 50, Pretoria.

Spaulding S.A., Kociolek J.P., Wong D. 1999. A taxonomic and systematic revision of the genus *Muelleria* (Bacillariophyta). Phycologia. 38: 314-341.

Tyler P.A. 1996. Endemism in freshwater algae, with special reference to the Australian region. In: Biogeography of freshwater algae (Ed. by J. Kristiansen). Hydrobiologia. 336: 127-135.

Van de Vijver B., Frenot Y., Beyens L. 2002. Freshwater diatoms from Ile de la Possession (Crozet Archipelago, Subantarctica). Bibliotheca Diatomologica. 46: 412pp.

Van de Vijver B., Beyens L., Lange-Bertalot H. 2004. The genus *Stauroneis* in Arctic and Antarctic locations. Bibliotheca Diatomologica. 51: 1-311.

Van de Vijver B., Gremmen N.J.M., Beyens L. 2005. The genus *Stauroneis* (Bacillariophyceae) in the Antarctic region. Journal of Biogeography. 32: 1791-1798.

Van de Vijver B., Van Dam H., Beyens L. 2006. *Luticola higleri sp. nov.*, a new diatom species from King George Island (South Shetland Islands), Antarctica. Nova Hedwigia. 82(1-2): 69-79.

Van de Vijver B. 2008. *Pinnularia obaesa* sp. nov. and *P. australorabenhorstii* sp. nov., two new large *Pinnularia* (sect. *Distantes*) from the Antarctic King George Island (South Shetland Islands). Diatom Research. 23: 221-232.

Van de Vijver B., Mataloni G. 2008. New and interesting species in the genus *Luticola* D.G. Mann (Bacillariophyta) from Deception Island (South Shetland Islands). Phycologia. 47: 451-467.

Van der Werff A. 1955. A new method for cleaning and concentrating diatoms and other organisms. Verhandlungen der Internationalen Vereinigung für theoretische und angewandte Limnologie. 12: 276-277.

Vyverman W., Verleyen E., Sabbe K., Vanhoutte K., Sterken M., Hodgson D.A., Mann D.G., Juggins S., Van de Vijver B., Jones V., Flower R., Roberts D., Chepurnov V.A., Kilroy C., Vanormelingen P., de Wever A. 2007. Historical processes constrain patterns in global diatom diversity. Ecology. 88: 1924-1931.

Werum M., Lange-Bertalot H. 2004. Diatoms in springs. Iconographia Diatomologica. 13: 1-417.

West W., West G.S. 1911. Freshwater algae. In: Murray J. (Ed.) Biology. vol. 1. Reports on the Scientific Investigations, British Antarctic expedition 1907–09. London: Heinemann: 263–298.

Chapter 6

A diatom and pigment-based reconstruction of Holocene climate change on Beak Island, the Antarctic Peninsula

Mieke Sterken, Elie Verleyen, Koen Sabbe, Dominic A. Hodgson, Stephen J. Roberts, Vivienne J. Jones, Andrea Balbo, S. Moreton, Wim Vyverman

Abstract

The recent global climate change is most pronounced in the Antarctic Peninsula and Maritime Antarctica, where a dramatic regional warming has affected glacier and sea ice dynamics, as well as many ecosystems. Lakes in Maritime Antarctica have proven to be early warning systems for temperature variability, through changes in their water temperature, ice cover and nutrient concentrations. Diatoms and other algae quickly respond to such changes, and are therefore traditionally used as indicators to reconstruct climate-related limnological changes. In order to assess the relationship between diatom species and their environment, diatom calibration datasets are developed. Here, we examined an existing diatom calibration dataset from Livingston Island (South Shetlands) and Signy Island (South Orkney Islands), and extended it with six new sites from Beak Island (northeast Antarctic Peninsula). For this, a revised taxonomy and more up-to-date statistical techniques were used, which resulted in a new model to reconstruct changes in nutrient concentrations (NH_4^+) of lakes in the region. We further applied this model to fossil diatom assemblages in a lake sediment core from a shallow isolation basin on Beak Island. The core dated back to c. 5700 cal. yr. BP, and the basin only became isolated from the sea at c. 3000-2700 cal. yr. BP. On the basis of diatom indicator taxa and fossil pigment compositions, we inferred cold coastal marine conditions for the period between 5700 and 3000 cal. yr. BP. Short-term oscillations in diatom species composition presumably reflecteded glacial oscillations on nearby land masses. After the isolation of the basin, low NH_4^+ concentrations were reconstructed for the lake between 2700 and 1600 cal. yr. BP, despite the observed high diatom, total pigment and UV-screening pigment concentrations, which suggested a warmer climate. An abrupt change was observed in all proxies at c. 1600 cal. yr. BP (91 cm depth), where a short-term oscillation in magnetic susceptibility and organic matter content suggested locally increased allochtonous sedimentation. Due to uncertainties in the age depth model, it was difficult to assess when the following period of low pigment and diatom concentrations exactly ended, but an increase in pigment concentrations occurred at c. 40 cm depth, coinciding with a moderate increase in total diatom and organic matter concentrations.

This chapter is a manuscript in preparation

Contribution of the author: diatom microscopy, statistical analyses, partly constructing age-depth model, data interpretation, writing largest part of the paper.

6.1. Introduction

Assessments of Antarctic temperature change have shown that recent global warming is most pronounced in the Antarctic Peninsula region, with mean temperature increases being six times the global mean of 0.6 ± 0.2°C during the 20th century (Vaughan et al., 2003; Houghton et al., 2001). This warming has resulted in the collapse of ice shelves and the enhanced recession of glaciers (Cook et al., 2005; Scambos et al., 2003, 2004; De Angelis & Skvarca, 2003), and has affected many ecosystems (Walther et al., 2002; Lewis, 1994). Lakes, in particular, have been shown to respond very quickly to this warming. Because summer temperatures in the Antarctic Peninsula (AP) are close to freezing, and because of the small size of lakes in the AP, any minor degree of warming may significantly alter the physical and chemical properties of these lakes (Vaughan, 2006; Quayle et al., 2002). The variations in snow and ice-cover on the lakes, and the deglaciation of their catchments markedly affect their water temperatures, albedo, light availability, nutrient concentrations and the length of the growing season (Lyons et al., 2006; Quayle et al., 2002). Due to the simple structure of their ecosystems, polar lake biota quickly respond to these changes (Pearce, 2005; Butler 1999; Quayle et al., 2002), and their remains, preserved in the sediments of the lakes, may serve as good paleo-ecological indicators for reconstructing past environmental changes.

Diatoms and fossil pigments from coastal Antarctic and maritime Antarctic lakes have, in this respect, been successfully used in order to reconstruct past climatic and environmental changes (e.g. Jones et al., 2000; Hodgson et al., 2005). Diatoms generally preserve well, and the specific ornamentation of their silica-rich cell walls allows them to be determined up to species level. Since many lacustrine diatom species occupy distinct ecological niches, they have been used successfully to build inference models (i.e. transfer functions) that enable the quantitative reconstruction of changes in nutrient concentrations (e.g. Canada: Lim et al., 2007, 2008; Macquarie Island: Saunders et al., 2008), salinity (East-Antarctica: Roberts et al., 2004; Verleyen et al., 2003), pH (Svalbard: Jones & Birks, 2004; Macquarie Island: Saunders et al., 2008), temperature/altitude (Siberia: Kumke et al., 2004; Kerguelen: Gremmen et al., 2007; Macquarie Island: Saunders et al., 2008), soil moisture content (Van de Vijver et al., 2002). In the Antarctic Peninsula region, a transfer function for chlorophyll *a* has been successfully constructed (Jones & Juggins, 1995), on the basis of a diatom dataset from Livingstone and Signy Islands (Jones et al., 1993). Apart from diatoms, fossil pigments are also useful in paleoecological and paleoclimatic studies, as they have recently been shown to be valuable indicators of past algal and bacterial populations in high-latitude

lakes and coastal ecosystems (e.g. Verleyen et al., 2004a,b; Hodgson et al., 2005; Leavitt & Hodgson, 2001).

In addition to reconstructing changes in freshwater environments, diatoms can well be used to reconstruct past oceanic conditions and sea-ice extent, derived from marine sediment records (e.g. Crosta et al., 2005; Armand et al., 2005; Cremer et al., 2003). Fossil pigments and marine diatom indicator taxa have proven to be good proxies for reconstructing shallow coastal environmental conditions, as was observed in marine sections of sediment cores retrieved from isolation basins (e.g. Verleyen et al., 2004a,b). These lakes provide excellent opportunities to retrieve relatively undisturbed coastal marine sediment records, as they are formed after isolation from the sea caused by isostatic recovery of the land (Verleyen et al., 2004a,b).

The aims of this paper are twofold. First we extend an existing diatom calibration dataset from Livingston Island (South Shetlands) and Signy Island (South Orkneys) with additional samples from Beak Island (Trinity Peninsula), to develop diatom-based inference models. A particular focus is the development of a transfer function to reconstruct nutrient levels and trophic status, which is believed to be related with climate in maritime Antarctic lakes (Quayle et al., 2002).

Second, we reconstruct past lake trophic status and climate change on Beak Island, by applying the transfer function to the lacustrine diatom record of a sediment core from an isolation lake (Beak-2) on Beak Island, and by interpreting these data together with the the fossil pigment record from the core. In the marine section of this core, we use indicator diatom taxa and fossil pigment compositions to reconstruct changes in the marine environment.

6.2. Material and Methods

6.2.1. Site description

Beak Island (63°36'S, 57°20'S) is situated in Prince Gustav Channel, between Vega Island and the Tabarin Peninsula, at the northeastern tip of the Antarctic Peninsula (Fig.1). The island is assumed to have the same continental climate as James Ross Island (50 km to the southwest), which is typified by negative mean monthly temperatures (Björck et al., 1996). The regional climate is influenced by (1) the Westerly storm tracks bringing humid, warm air from northwest, or (2) the cold barrier winds bringing arid air-masses from south and southwest (i.e. the Weddell Sea) (Björck et al., 1996). The region is influenced by the rain shadow effect of the Antarctic Peninsula mountains (Sugden,

1982), and is characterized by yearly maximum precipitation values of 100-200 mm yr^{-1} (Sugden, 1982) or 0.31 m yr^{-1} in the NE-Antarctic Peninsula (Peel, 1992). Snowfall periodically occurs during summer, followed by rapid melting and long dry periods. Beak Island is currently free of permanent snow fields, ice caps or glaciers.
The geology of Beak Island, which is formed by the partially emerged periphery of an inactive volcanic caldera (Fig. 2), is composed of Miocene rocks belonging to the James Ross Volcanic Island group (Bibby, 1966). A few lakes and ponds occur on the island (see 6.3.1. in this Chapter).

Livingston Island (62°40'S, 61°00'W; South Shetland Islands) is located at about 160 km NW from the northernmost tip of the Antarctic Peninsula. It falls within the Maritime Antarctic climate zone, which implies high precipitation rates (1000-1500 mm yr^{-1}; Robin & Adie, 1964) and mean monthly air temperatures raise above 0°C at least one month a year (Björck et al., 1996). The climate on the western side of the AP (including Livingston Island) is generally warmer and wetter than on the eastern side (Beak and James Ross Island). As a result, the Equilibrium Line Altitude (ELA) often lies at or less than 100 m above present sea level instead of 400 m at James Ross Island. This is because the South Shetlands climate is subject to the effects of comparatively warm, saturated air masses approaching from the west, while the eastern side of the AP is influenced by the rain shadow effect of the AP mountains and cold dry air masses coming from the Weddell Sea Region.

The geology of the island consists of Jurassic-Cretaceous shales and sandstones, and Upper-Jurassic-Cretaceous volcanic rocks (Hobbs, 1968). The snow-free ground is usually barren and rocky with a sparse vegetation mainly comprising lichens and mosses (in inland sites), with a more extensive vegetation cover of lichens, mosses and two flowering plants (*Deschampsia antarctica* Desvaux and *Colobanthus quitensis* (Kunth) Bartl.) in coastal sites. Large bird colonies (mainly penguins) dominate the shoreline (Jones et al., 1993).

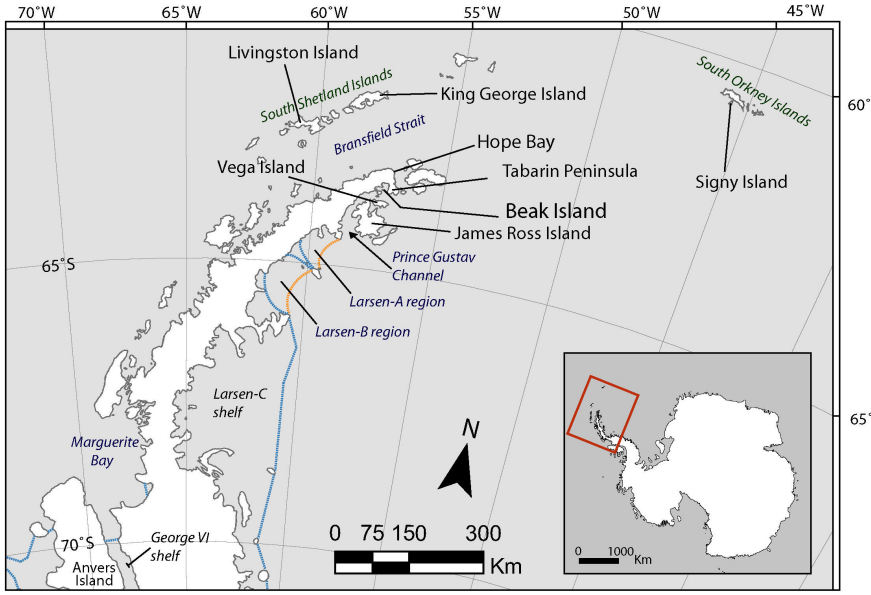

Figure 1: Map of the northern tip of the Antarctic Peninsula, showing Beak Island north of James Ross Island, Livingston Island (South Shetland Islands) and Signy Island (South Orkney Islands), as well as some locations mentioned in the text.

Signy Island (60°43'S, 45°38'W; South Orkney Islands) is a small (20 km^2) island located to the northeast of the Antarctic Peninsula, between the Weddell Sea and South Georgia. The South Orkney Islands have the same Maritime Antarctic climate as the South Shetlands. Signy Island is currently 32 % covered by permanent snow and ice, and the geology consists of folded metamorphic rocks (mainly quartz-mica-schists, with some amphibolites and marbles) (Matthews & Malling, 1967).

The ice-free areas are well vegetated with patches of moss and lichens, and the same flowering plants *(D. antarctica* and *C. quitensis*) as in Livingston Island occur on Signy Island (Smith, 1972). Lakes on Signy Island have generally more densely vegetated catchments, with more stable and acid soils. Most of the lakes are of glacial origin, and are deeper than 10 m. The biology of several Signy Island lakes has been studied extensively (Hawes, 1985; Ellis-Evans, 1981; 1984; 1985; 1991; Ellis-Evans & Wynn-Williams, 1985). Recent rapid warming has also been observed on the island, and has proven to severely impact the lake physical, chemical and biological parameters (Quayle et al., 2002). An increase in surface air temperature of 1°C during the past 40 years resulted in a four fold increase in lake primary productivity in 15 years.

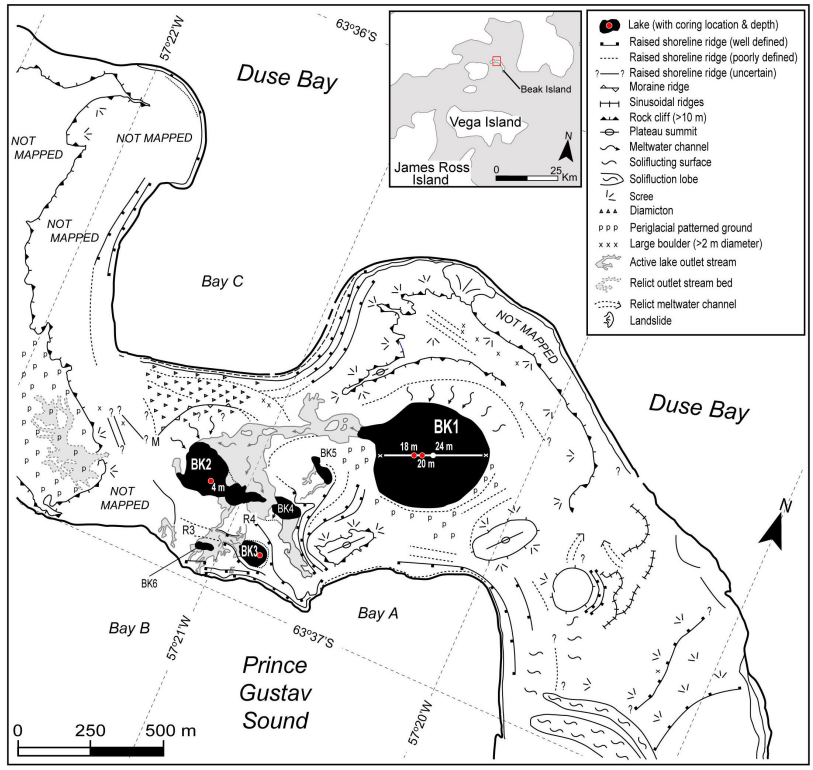

Figure 2a: Map of the geomorphology of the central part of Beak Island, where the lakes Beak 1-6 are situated (S. Roberts).

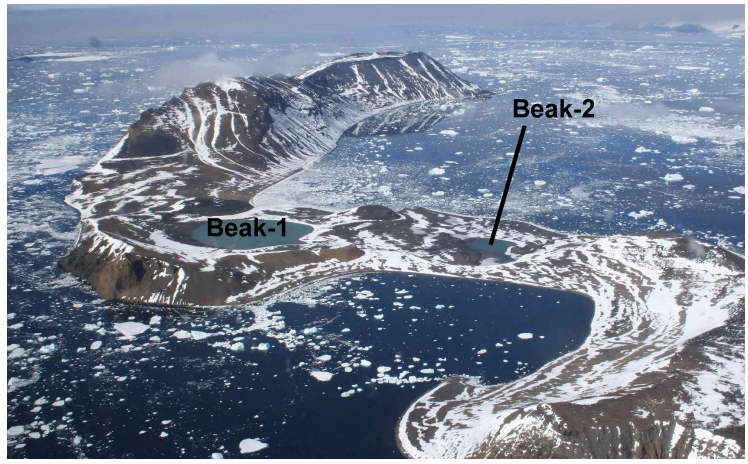

Figure 2b: Picture of Beak Island, seen from Duse Bay, looking towards the south. Lakes Beak-1 and Beak-2 are indicated (picture: D. Hodgson).

6.2.2. Lake surveying and sampling

Sill heights of three lakes/ponds (Beak 1-3) on Beak Island were measured using a Trimble GPS system. Water depths were measured in these lakes/ponds using a hand-held echo sounder, deployed at fixed positions along a static line, in order to identify the deepest point in each lake (Hodgson et al., 2005a). Surface water conductivity, temperature and oxygen saturation were measured in six lakes (Beak 1-6) using a YSI MDS 600 water quality meter, and vertical profiles of these variables were measured in the deepest lake (Beak-1, 24 m deep). Water samples from all lakes were collected in acid-washed Nalgene bottles. 125 ml was collected for ion chemistry, and 125 ml was filtered for nutrient analysis.

Sampling procedures of the Livingston and Signy Island lakes are described in Jones et al. (1993) and Jones & Juggins (1995).

6.2.3. Coring

Sediment cores were retrieved from the deepest parts of lakes Beak-1, -2 and -3 (Fig. 2a; see Chapter 7 for Beak-1). A composite sediment core was recovered from the deepest part of Lake Beak-2 using a UWITEC gravity corer for surface sediments and a 1 m Livingstone corer for deeper sediments (Wright 1967), with overlaps of c. 20 cm between core drives for intermediate to basal sediments. Three cores, BK2A-C with a total sediment depth of 244 cm were extracted and sliced at 1 cm intervals in the field. A duplicate surface core was retained intact. Core samples were sealed in sterile Whirlpack bags and stored at –20°C for transport to the British Antarctic Survey (Cambridge).

6.2.4. Geochronology

A chronology was established by accelerated mass spectrometry (AMS) radiocarbon (AMS ^{14}C) dating of macrofossil remains (moss strands, leaves and organic cyanobacterial mat fragments) and bulk sediments. Dates are reported as conventional radiocarbon years BP (^{14}C BP), and as calibrated years BP (cal BP relative to AD 1950) using the Intcal 04.14C dataset (Reimer et al., 2004) for freshwater samples, the Marine calibration curve (Hughen et al., 2004) for marine samples, and a mixed marine-Intcal 04 curve (50 % marine) for samples at the marine-lacustrine transition. For the marine curve a ΔR was set at 900 years, which corresponds to a reservoir effect of 1300 years (Berkman et al., 1998). All dates were calibrated in the Calib 5.0.1 program (Stuiver & Reimer 1993).

6.2.5. Stratigraphy (Lithology, Magnetic susceptibility (MS), LOI950, LOI550, wet density)

The Beak-2 core was photographed, macroscopically described, and analysed for wet density, dry weight, % weight loss on ignition (LOI_{550}, after combustion at 550°C for two hours) and % carbonate composition (LOI_{950}; % weight loss after combustion at 950°C for two hours) (Dean, 1974). Wet density (g cm^{-3}) and magnetic susceptibility (g^{-1} cm^3) were measured at 1 cm resolution in the upper 20 cm, and at 2 cm resolution in the rest of the core. Wet mass, volume specific magnetic susceptibility was measured using a Bartington 1 ml MS2G sensor.

6.2.6. Fossil pigment analyses

Fossil pigments were extracted from bulk sediments following standard protocols (Leavitt and Hodgson, 2001; Squier et al., 2002). All samples were freeze dried immediately prior to extraction. Pigments were extracted from freeze-dried sediments by sonication (30 seconds at 40 W) in 2-5 ml high-performance liquid chromatography (HPLC)-grade acetone (90 %), and filtered through a nylon filter (mesh size 0.20 um).

All compounds were isolated and quantified using an Agilent technologies 1100 series HPLC system equipped with an autosampler at -10°C, a diode array spectrophotometer (400-700 nm), an absorbance detector and a fluorescence detector. A reversed phase Spherisorb ODS2 column was used (internal diameter: 4.6 mm, particle size of 5 pm). Three solvents were used (Wright et al., 1991): A (80:20 methanol:0.5 M ammonium acetate (aq.; pH 7.2 v/v)), B (90:10 acetonitrile (210 nm UV cut-off grade) : water (v/v)) and C (ethyl acetate; HPLC grade).

The HPLC system was calibrated by use of authentic pigment standards from the U.S. Environmental Protection Agency, and compounds isolated from reference cultures following Scientific Committee on Oceanic Research (SCOR) protocols (Jeffrey et al., 1997). The taxonomic affinities of the pigments were derived from Jeffrey et al., (1997) and Leavitt and Hodgson (2001). Pigments with unknown affinity were labeled as derivatives of the pigment with which it showed the closest match based on the retention time and the absorption spectrum.

6.2.7. Siliceous Microfossils

Surface sediment and core samples from Beak Island were prepared using H_2O_2, according to a slightly modified procedure following Renberg (1990) (see Chapter 7). In order to calculate absolute diatom abundances, the samples were spiked with polystyrene

microspheres (concentration: 6.81 x 10^6 l^{-1}) (Battarbee and Kneen 1982). The material was mounted in Naphrax medium (refractive index 1.710). Random fields were scanned at a magnification of 10x100x with an Olympus CX 41 microscope, and LM pictures were taken with an Olympus DP50 camera (see Chapter 4). At least 450 valves were counted in the samples from Beak-2.

For the identification of all freshwater taxa we refer to Chapters 4 and 5. Marine diatoms were identified according to Cremer et al. (2003) and Roberts & McMinn (1999).

The diatom data from the Beak Island sediment cores and six surface samples were intercalibrated with previously existing diatom datasets from Livingston and Signy Island (Jones & Juggins, 1995; Jones et al., 1993). Refer to these papers for details on the methods of sample preparation. For intercalibrating the datasets, the original slides of Jones et al. (1993) and Jones & Juggins (1995) were screened, all taxa were photographed and measured, and were compared with the original counting results of these studies. In case of doubt about the delineation of certain taxa (e.g. due to new taxonomic descriptions and reviews of species complexes since the ´90s), species or taxa were merged into a species group or complex (Table 5). These 'recombined' taxonomic groups were applied in the analyses of this chapter, and may similary also contain multiple taxa from Chapter 4. All taxa (including those from Chapter 4) are listed in Table 5. Marine species were not included in Chapter 4, but some were identified by Jones et al. (1993) and Jones & Juggins (1995) and were intercalibrated as such. Taxa occurring exclusively in the marine parts of the Beak Island cores are listed in Table 5 as well, and were photographed (unpubl. data) but not described.

Apart from diatoms, siliceous fossils like chrysophyte cysts and scales/plates of testate amoebae were also observed and enumerated in the Beak-2 sediment samples. In temperate areas, chrysophytes mainly occur in low-productivity lakes with low nutrient concentrations (Zeeb & Smol, 2001). In high arctic ponds, their cysts have been found in highest percentages in semi-aquatic mosses (as compared to epilithic habitats) (Douglas & Smol, 1995). The ratio cysts to diatoms has also been proposed as an estimate of lake ice cover in high polar regions (Smol, 1983; 1988).

Testate amoebae are a group of free-living, heterotrophic protists, that are particularly abundant in acid peats and mosses (Smith, 1992), but can also occur in desert soils or streams and lakes (Tolonen 1985). They have been widely recorded in Antarctic and sub-Antarctic regions (Smith, 1992; Vincke et al., 2006 and references therein),

where they are frequently observed in mosses (Vincke et al., 2006). Climate seems to have a significant impact on the distribution of testate amoebae, as a decrease in species diversity and population size is observed from the sub-Antarctic islands towards the Pole (Schmidt, 1992). The plates found in our sediment samples were identified according to Douglas & Smol (2001), and most of them probably belong to the genus *Euglypha*. It is possible that a few (less than 10 %) belong to the genus *Assulina* (hence the name '*Euglypha* type plates'; Fig. 3) and it could be that other small *Assulina* plates were not recognised/enumerated in the samples (see Douglas & Smol, 2001 for a review).

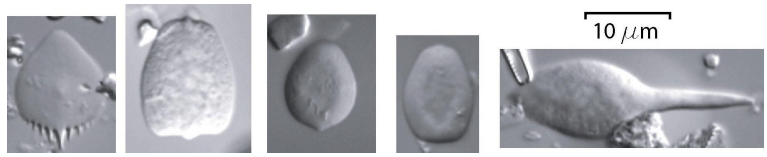

Figure 3: Light micrographs of *Euglypha* type siliceous plates found in the Beak-2 sediment core.

6.2.8. Statistical analyses

Indirect ordinations were performed in order to explore the limnological characteristics of the surface datasets from Livingston, Signy and Beak Island, whereas direct ordinations were used to investigate the relationship between the measured environmental variables and the diatom taxa from these datasets. For these analyses, species data were log (x+1) transformed to reduce the influence of dominant taxa and all environmental variables (except pH) were log (x+1) transformed to reduce or remove skewness. All ordinations were performed using CANOCO 4.5 for Windows (ter Braak and Smilauer, 2002).

Diatom-based transfer functions were developed in C2 version 1.5.1 (Juggins, 2003) using simple weighted averaging (WA) and weighted averaging partial least squares (WA-PLS) algorithms (Birks, 1998). The same program was used for determining WA-based species optima for all reconstructed variables. Outlier samples were detected according to Jones & Juggins (1995). The optimal number of components in the WA-PLS model was determined following the criteria in Eggermont et al. (2006) and Verleyen et al. (2003).

Diatom and fossil pigment compositions in the Beak-2 sediment core were analyzed and plotted using Tilia 2.0.b.4 (Grimm 1991-1993) and TGView version 2.0.2. (Grimm, 2004). The cores were divided into stratigraphical zones using stratigraphically constrained cluster analysis of the diatom data (CONISS; Grimm, 1987).

6.3. Results

6.3.1. Lake surveying and sampling on Beak Island

A summary of lake characteristics (temperature, conductivity, salinity, oxygen content, pH, altitude (i.e. sill height), maximum depth, nutrient and ionic concentrations, and total (TOC) and dissolved (DOC) organic carbon) in the six lakes from Beak Island is given in Table 1 (Hodgson et al., 2005a). For Beak-1 (the largest (diameter c. 400 m) and deepest (24 m) lake) the temperature, conductivity, oxygen content and pH are given for both the water surface and the bottom of the lake. Beak-1 is most likely formed by a depression created by a secondary eruption vent (Chapter 7; Hodgson et al., 2005a). Lake Beak-2 is an irregularly shaped lake/pond (surface area: c. 200 x 300 m) with a maximum depth of four meters, and a rapidly shelving lake-bed being mostly shallower than two meters. Beak 3-6 are ponds which occupy small depressions in the landscape or have formed in dammed outflow channels. Thick orange and green cyanobacterial mats had developed in the shallow littoral of Beak 2-6. The outflow of Beak-1 is linked to Beak-2 and Beak-3 (Fig. 2a,b) forming an inter-connected lacustrine system between 11 and 1 meter a.s.l. The outflow is vegetated by thick orange and green microbial mats, but was nearly inactive at the time of sampling (January 2006). At high water levels Beak-2 and Beak-4 may form a single water body (Fig. 2a).

***Table 1**:* Summary of environmental variables measurements for lakes Beak 1 to 6.

Sample	Temp (^{0}C)	Sp.Cond. (uS/cm^2)	Cond. (uS/cm)	Salinity (‰)	DOX (%)	DOX (mg/l)	PH	Altitude (m)	Max Dept (m)
Beak 1 surface	4.82	280	172	0.13	107.3	13.75	7.37	10.955	24
Beak 1 bottom (24 m)	4.29	293	177	0.14	80.3	10.38	6.87		
Beak 2	12.2	250	188	0.12	112.5	12.05	8.61	2.365	4
Beak 3	14.29	311	247	0.15	111.3	11.46	8.95	0.515	1
Beak 4	12.85	612	470	0.3	114.1	12.03	9.77	-	0.5
Beak 5	12.82	312	239	0.15	115.3	12.2	9.12	-	0.5
Beak 6	13.32	272	212	0.13	110.2	11.57	9.16	-	0.5

Table 1 *(continued)*

Sample	NO_3 (µg/l)	NH_4 (µg/l)	PO_4-P (µg/l)	Si (µg/l)	Cl^- (mg/l)	TDN (µg/l)	Na (mg/l)	K (mg/l)	Mg (mg/l)	Ca (mg/l)	TOC (mg/l)	DOC (mg/l)	SO_4-S (mg/l)	Al (mg/l)	Fe (mg/l)
Beak 1	<100	<10	17	1220	68.8	140	37.7	2.03	6.57	5.05	0.75	0.99	32.7	0.126	0.109
Beak 2	<100	25	6	349	59.6	490	34.2	2.49	5.97	3.7	2.4	2.67	33.2	0.009	0.018
Beak 3	<100	21	<5	887	73.6	580	40.9	3.12	8.67	5.24	3.1	3.86	46.6	0.011	0.045
Beak 4	<100	<10	<5	2970	144	1700	108	6.52	8.55	3.72	7.7	11	10	0.079	0.063
Beak 5	<100	45	41	704	68.7	570	39.4	3.44	10	4.87	2.9	3.25	60.1	0.035	0.084
Beak 6	<100	<10	<5	1070	62.5	660	31.1	4.08	8.96	4.86	4.3	4.62	35.1	<0.002	0.093

6.3.2. Extension of the diatom-based calibration dataset and development of inference models to reconstruct changes in variables related to lake primary productivity

The original 133 taxa from the Livingston and Signy Islands database (hereafter called LS-dataset; Jones et al., 1993; Jones & Juggins, 1995) were examined and recombined into 113 entities (Table 5), of which the taxonomic boundaries of 84 taxa/complexes were traced back and illustrated (taxa indicated in bold in Table 5, and illustrated in Chapter 4). The addition of the Beak surface samples to the LS-dataset yielded five additional taxa in the newly compiled dataset (Beak-Livingston-Signy or BLS-dataset). These taxa were *Achnanthes* cf. *muelleri*, *Chamaepinnularia cymatopleura*, *Hantzschia* spp. (containing *Hantzschia* sp. 1 and *Hantzschia* sp. 2), *Navicula cincta* and Species 12 (Table 5).

Compared with the LS-dataset, maximum depth was added as a new environmental variable, and the range of some variables (pH, silica, altitude, chloride) was extended (Table 2). The variables chlorophyll *a* (Chl*a*) and phaeopigment concentration were not measured for the Beak samples, and were thus not included in the BLS-dataset (Beak-Livingston-Signy) as we prefer to directly measure fossil Chl*a* concentrations in the core samples using HPLC rather than indirectly reconstructing the past Chl*a* levels by use of a diatom-based transfer function. In some samples from Beak Island, the concentrations of NO_3, NH_4, PO_4-P and TP were below the detection limits of the instrument (indicated with '<' in Table 1), and were set by default at half the given detection limit (i.e. at 50 µg/ l for NO_3, 5 µg/l for NH_4 and 2.5 µg/l for O-P).

***Table 2*:** Summary of environmental variables in the dataset (LS) of Jones et al. (1993) and the combined Beak-Livingston-Signy (BLS) dataset. Values in bold indicate where the addition of the Beak samples extend the environmental range.

Variable	LS		BLS	
	min	max	min	max
Chlorophyll *a* (µg/l)	0.04	13.5	0.04	13.5
Phaeopigments (µg/l)	0.21	11.5	0.21	11.5
NO_3^- (µg/l)	0.5	737	0.5	737
NH_4^+ (µg/l)	0.5	288	0.5	288
O-P (SRP) (µg/l)	0.29	405	0.29	405
pH	6.61	8.89	6.61	**9.77**
Conductivity (µS/cm)	40	2960	40	2960
Altitude (m)	4	150	**0.52**	150
Silica (µg/l)	56.2	1980	56.2	**2970**
Chloride (mg/l)	9.5	644	**1.78**	644
Max. Depth (m)	0.1	15	0.1	**24**
TDN (µg/l)	31	3311	31	3311
TP (mg/l)	0.5	314	0.5	314
Na (mg/l)	1.5	188	1.5	188
K (mg/l)	0.05	9.5	0.05	9.5
Mg (mg/l)	0.48	34	0.48	34
Ca (mg/l)	0.48	33.6	0.48	33.6

A PCA ordination analysis on the standardised measured environmental variables in the BLS-dataset shows the position of the Beak samples/lakes in relation to the Livingston and Signy samples/lakes, in terms of their physical and chemical properties (Fig. 4). The eigenvalue of the first PCA axis was 0.453, and that of the second axis 0.212. Based on the conclusions from Jones & Juggins (1995) and on the PCA diagram (Fig. 4) the environmental variables can be grouped into three types (with the exception of the newly included variable 'maximum depth'), each of which representing:

(1) trophic status and/or productivity (NO_3^-, NH_4^+, O-P, TDN),

(2) conductivity/hardness (pH, conductivity, Cl^-, Na^+, Mg^{2+}, Ca^{2+}) and

(3) location: geological/chemical differences between islands (Silicate, K^+).

The lakes from Livingston, Signy and Beak Islands are clearly separated on the PCA diagram (Fig. 4), with Signy Island lakes being generally deeper (situated at the negative side of the second ordination axis), and less conductive than those from Livingston Island and Beak Island. Additionally, the samples from Livingston Island can be divided in two groups, of which the 'Livingston inland sites' generally contain less nutrients and salts than the lower

elevation coastal sites (see Fig. 4; and Jones et al., 1993). To illustrate this, all lakes situated at less than 300 m from the coast are indicated with filled symbols in Fig. 4. The water chemistry and physical properties of the (shallow) lakes from Beak Island is at the high conductivity- and nutrient-range in Fig. 4. Only Beak-1 (a 24 m deep lake) shows greater similarites to the Signy Island lakes than to the Livingston coastal sites (Fig. 4).

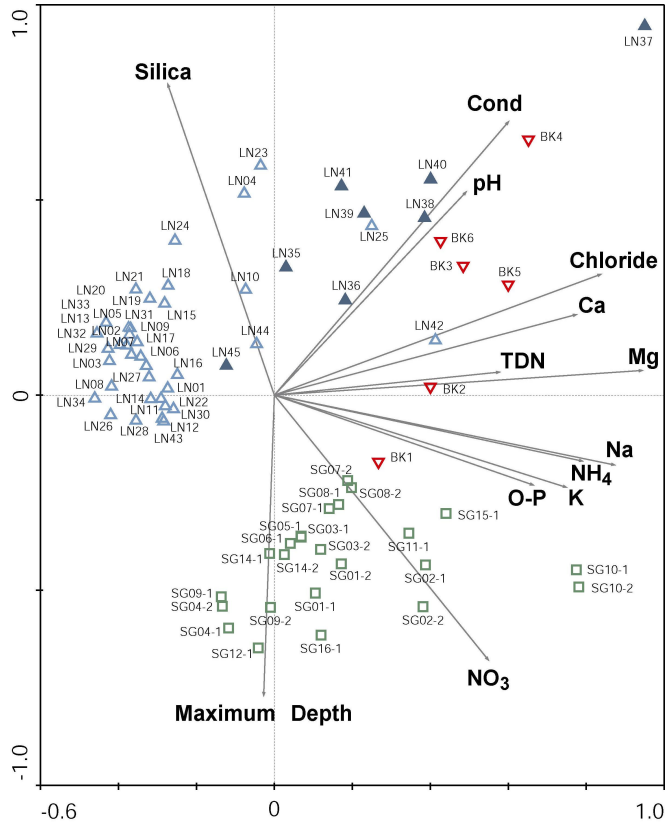

Figure 4: PCA biplot on the environmental variables of the BLS-dataset. Red downside triangles represent Beak samples; filled blue triangles: Livingston coastal (< 300 m from the coastline) samples; empty blue triangles: Livingston non-coastal samples; green squares: Signy Island samples.

The diatom communities from Beak Island tend to be slightly more similar to those from Livingston than those from Signy Island (Figs. 5, 6). Four taxa (*Nitzschia paleacea*, *Planothidium haynaldii*, *Luticola higleri* and *Achnanthidium* cf. *exiguum*) were present (though in low abundances) in both Beak and Livingston Islands, while absent in Signy Island (Fig. 5).

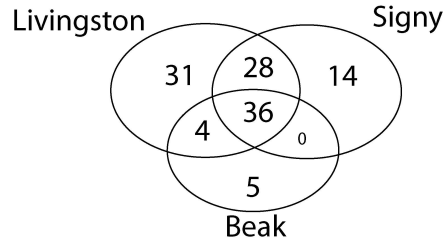

Figure 5: diagram showing the number of taxa or species complexes in the BLS-dataset.

In order to explore the diatom species communities from Livingston, Beak and Signy Islands, a Detrended Correspondence Analysis (DCA) was employed on the BLS-dataset, [using the detrending by segments option and no downweighting of rare species, and with species data log(x+1) transformed], revealing a Total Inertia of 2.542. The gradient lengths of the first and second ordination axes were 2.581 and 2.188 standard deviation (SD) units respectively. For representation purposes the same analysis was done on the complete dataset but omitting all species that have a maximum relative abundance of 0.4 % and occurring in less than two samples (Total inertia: 2.343; gradient lengths: 2.624 and 2.096 for the first and second axes) (Fig. 6).

The lakes from Beak Island are mainly dominated by *Nitzschia frustulum/inconspicua*, except for Lake Beak-1, which has high abundances of *Brachysira minor*, *Planothidium* cf. *lanceolatum*, *P. renei* and *P. delicatulum*. The diatom communities of the Signy Island lakes are mainly characterized by *Stauroforma inermis, Planothidium renei, Mayamaea atomus* and by the virtual absence of *Planothidium* cf. *lanceolatum* (Fig. 6). The Livingston inland (high elevation) lakes are characterized by the Antarctic endemic *Brachysira minor* (a species typically associated with mosses; Van de Vijver & Beyens, 1997), by the epilithic *Eolimna minima*, *Planothidium* cf. *lanceolatum*, *Psammothidium abundans* (although this species is also present in lakes from Signy Island), and *Staurosirella pinnata* (Fig. 6). Most of these taxa are typical of low-nutrient, high light-availability conditions. The Livingston coastal lakes are characterized by *Staurosira alpestris, Nitzschia frustulum, and Planothidium delicatulum* (Fig. 6), which are all typical of high-nutrient, high-productivity lakes.

The maximum amount of variation in the species data was determined by DCA ordination (as described in the previous paragraph). Because the gradient length of the first DCA axis was between 2 and 3 (i.e. 2.581 SD units), both linear or unimodal ordinations could be used to further infer the relationships between the diatom assemblages and the measured environmental variables (ter Braak & Prentice, 1988; Jongman et al., 1995).

Canonical correspondence analysis (CCA) with forward selection and Monte Carlo permutation tests (999 permutations), were subsequently applied on the BLS-dataset. Species data were log(x+1) transformed and rare species were downweighted. The results of the CCA are summarized in Table 3, and showed that all measured variables explained a significant portion of the total variance in species data (being 1.728). All variables together explained 0.633 (i.e. 36.6 % of the total variance). The variables explaining the largest portions of all variance were related to location (L) and conductivity/hardness (C-h). However, both of these have a strong spatial component, the first one caused by the geology of the islands, and the second one being partly related to the distance from the coast (see 6.4.: discussion). Therefore, we sought the best nutrient/trophy-related variable, since these variables are largely climate-dependent in Maritime Antarctica (e.g. Quayle et al., 2002; see 6.4.: discussion).

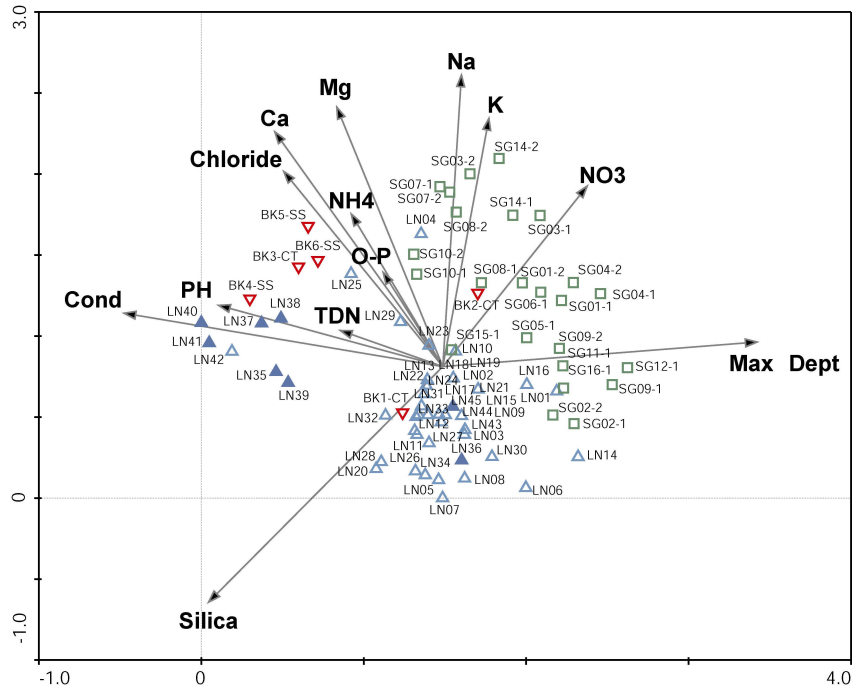

Figure 6a: Sample plot of a DCA analysis on the total diatom database from Livingston, Signy (Jones et al., 1993) and Beak Island (i.e. BLS dataset). Environmental variables are plotted passively on the sample plot. Species with a relative abundance lower than 0.5 % and in less than 2 samples in the surface dataset or in the cores are not included in the DCA analysis. Detrending was by segments, rare species were not downweighted. Red downside triangles represent Beak samples; filled blue triangles: Livingston coastal (< 300 m from the coastline) samples; empty blue triangles: Livingston non-coastal samples; green squares: Signy Island samples. For the samples from Beak-1, -2 and -3, the code CT stands for core-top sample, and SS for (littoral) surface sediment sample.

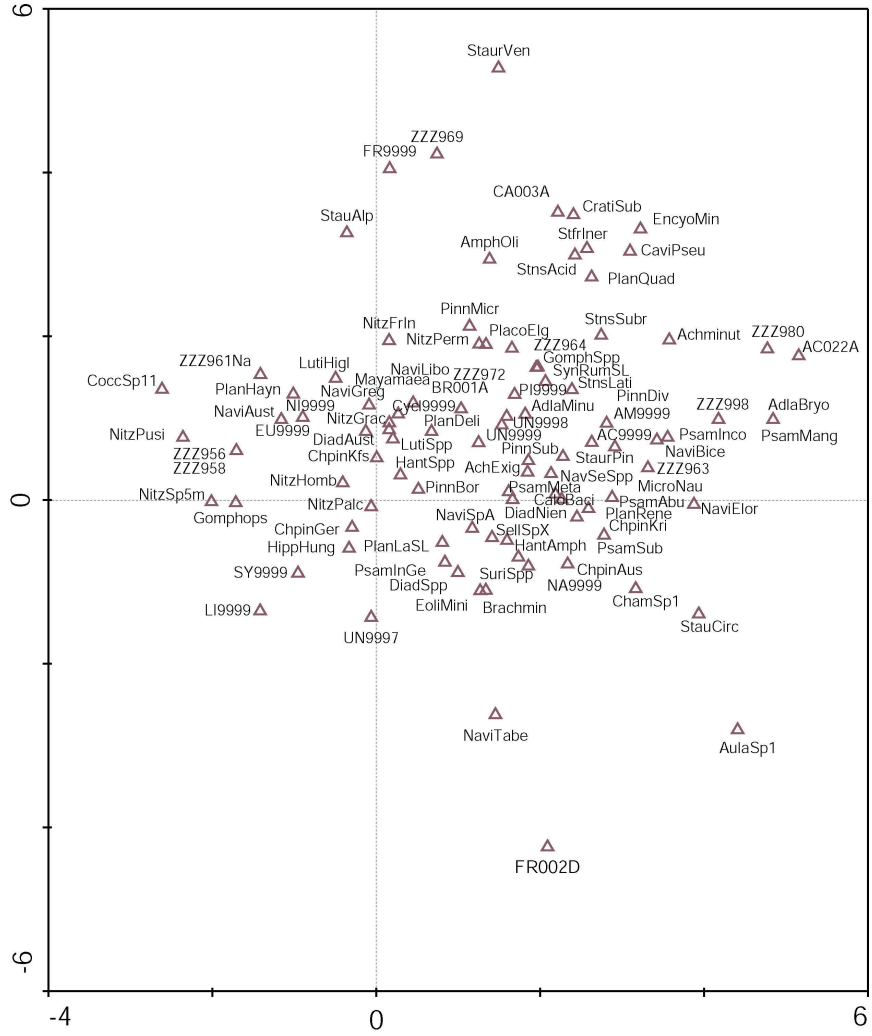

Figure 6b: Species plot of a DCA analysis on the total diatom database from Livingston, Signy (Jones et al., 1993) and Beak Island (i.e. BLS dataset). Species with a relative abundance lower than 0.5 % and in less than 2 samples in the surface dataset or in the cores are not included in the DCA analysis. Detrending was by segments, rare species were not downweighted. The full names of the diatom taxa and their codes are listed in Table 5.

CCA-tests of each of the nutrient-related variables showed that they all significantly explained a portion of the diatom distribution in the dataset. NH_4^+, however, explained the largest part (6.3 % of the total variation), and was the only nutrient-related variable that still significantly explained part of the variation in diatom data after partialling out all the better

explaining (thus forward selected) variables (see Table 3). Moreover, the ratio of the eigenvalue for the first CCA axis, with NH_4^+ as the sole predictive variable, to the eigenvalue for the second (unconstrained) CCA axis, was highest for NH_4^+ (i.e. 0.48, while it was 0.45, 0.34 and 0.23 for NO_3, O-P and TDN respectively).

Table 3: Summary of the CCA analysis on the BLS-dataset for all measured variables. 'Group' refers location (L), conductivity/hardness (C-h), maximum depth (MD) or trophic state/nutrients (Troph). Expl. var. is the total variance explained by the respective variable, and it is given as a percentage of the variance explained by all significant variables together, and as a percentage of the total variance in diatom data. Significance levels are indicated (p value).

Group	variable	expl. var.	% of explained variance	% of total variance	p value
L	Silica	0,158	25,0	9,1	0.001
C-h	Na^+	0,135	21,3	7,8	0.001
C-h	Mg	0,131	20,7	7,6	0.001
C-h	Cond	0,125	19,7	7,2	0.001
C-h	Ca	0,125	19,7	7,2	0.001
MD	Max Depth	0,123	19,4	7,1	0.001
L	K	0,118	18,6	6,8	0.001
Troph	NO_3^-	0,109	17,2	6,3	0.001
Troph	**NH_4^+**	**0,108**	**17,1**	**6,3**	0.001
C-h	Cl^-	0,103	16,3	6,0	0.001
C-h	pH	0,088	13,9	5,1	0.001
Troph	O-P	0,079	12,5	4,6	0.001
Troph	TDN	0,049	7,7	2,8	0.003

Initial WA and WA-PLS regression and calibrations for NH_4^+ showed the best results (RMSEP= 0.323 log(x+1) units, and jackknifed R^2 = 0.607) for the WA-PLS-2 analysis. This analysis produced 7 outliers (samples LN-09, LN-14, LN-23, LN-38, LN-42, SG-01 and SG-12) with an absolute residual greater than the standard deviation of the observed values. Deletion of these samples from the model did not cause any important shift in species scores, as observed when plotting WA-PLS coefficients of all species before vs. after deleting the outliers. The new model had a jackknifed R^2 of 0.724 and an RMSEP of 0.267 log(x+1) units. WAPLS-2 was preferred above WAPLS-1 since the addition of one component improved the model by 13.4 %.

6.3.3. Geochronology

The age-depth model of Beak-2 is based on eight ^{14}C dates (Table 4; Fig. 7). The top sediments of this core were 339 ± 35 ^{14}C years old. These were dated on the living microbial mat at the bottom of the lake, in contrast to the samples at 50.5, 70.5 and 72.5 cm, which were dated on macroremains of mosses. It remains unclear whether this age resulted from dating or coring problems, or from sediment disturbance due to the relatively shallow (4 meter) depth of the lake. It is, however, unlikely that the topmost sediments are contaminated with old carbon from the catchment area, since the island was not glaciated nor covered by a permanent ice field, and its geology mainly consists of volcanic rocks. Moreover, the sediment core-top sample from nearby Lake Beak-1 (see Chapter 7) was of modern age, and no inconsistencies were found in the age-depth curve of the freshwater section of that core (Chapter 7).

An age inversion was observed in the core at 72.5 cm depth. We assigned an intermediate age of 1285 cal. yr. BP between 70.5 and 72.5 cm depth, presuming that this inversion is a possible dating artefact caused by the lack of sufficient material to apply an independent $\delta^{13}C$ analysis on the 72.5 cm date (which was hence corrected using an estimated $\delta^{13}C$ correction factor). Moreover, the stratigraphic zonations in sedimentological, geochemical and biological proxies in the core (Figs. 7, 8, 9) may point to only minor disturbances in this upper section of the core, although we admit that the record would benefit from additional datings and perhaps grain size analyses in order to confirm or reject this argument. Therefore, we adopted a provisionary age-depth model (Fig. 7), remaining careful in interpreting the upper meter of the core.

6.3.4. Sediment stratigraphy

The bottom part of the Beak-2 sediment core (245-198 cm) is composed of silt and fine sandy organic mud with clasts, and is interrupted by an interval with coarser sand (with clasts) between 214 and 208 cm. Between 198 and 173 cm sediments become much finer (i.e. clay/silt in a black organic mud matrix), and are overlain by dark fine organic muds between 170 and 166 cm, and between 162 and 144 cm.

The main lithological shift in the core occurs at 144 cm depth, where diffuse decomposed mats appear (144-5 cm), overlain by a living orange microbial mat at the top of the core (5-0 cm) (Fig. 7). Laminations/bands are visible between c. 84 and 132 cm depth.

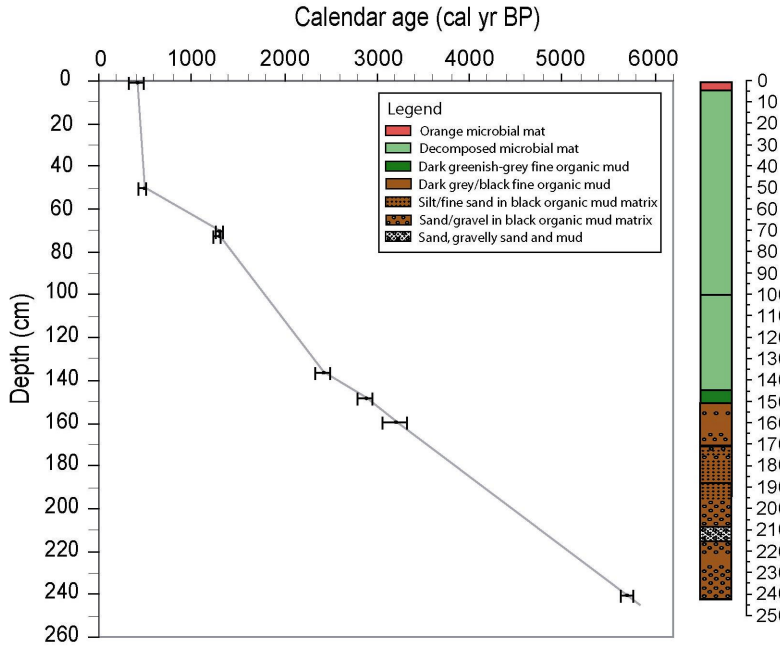

Figure 7: Age-depth model and lithological description of the Beak-2 core.

Table 4: ^{14}C dates of sediment core Beak-2

AMS Lab number	14-C date	14-C error	Type of material	Depth in core	Min. cal. age	Max. cal. age	Median cal. age	Pprobability of 2 Sigma interval	Date used in model	Curve used
SUERC-12568	339	35	Bulk/ macro	0.5	309	483	396	1.000	396	Intcal 04.14C
SUERC-12387	400	35	Macro	50.5	426	515	470.5	0.744	470.5	Intcal 04.14C
SUERC-12388	1377	35	Macro	70.5	1260	1351	1305.5	0.987	1284.	Intcal 04.14C
SUERC-12391	1329	35	Macro	72.5	1224	1303	1263.5	0.775	1284.5	Intcal 04.14C
SUERC-12569	2374	35	Bulk	136.5	2337	2490	2413.5	0.952	2413.5	Intcal 04.14C
SUERC-12946	2780	35	Bulk	148.5	2787	2957	2872	1.000	2872	Intcal 04.14C
SUERC-12570	3632	35	Bulk	159.5	3055	3321	3188	0.999	3188	50 % mixed
SUERC-12947	4990	36	Bulk	240.5	5641	5761	5701	0.777	5701	Marine dR 900

Wet density values generally slightly decrease from the bottom to the top of the core, with a local minimum at 209 cm where the coarser material is observed, and local maxima occur at c. 180-177 cm and 44 cm. A sharp peak is observed at 111 cm depth (Fig. 8). Magnetic susceptibility (MS) is high (c. 14-20 g^{-1} cm^3) at the bottom of the core (239-227 cm depth). Low values persist between c. 227-193 cm and roughly delimits the zone of coarser sediments, and a second maximum is found between 189-184 cm. Lower values are measured between 155 and 119 cm depth. In the upper part of the core, two local maxima are found at 98, 44 and 3 cm depth. LOI_{925} is generally higher in the bottom half of the core, where it is highest between 171 and 145 cm, and between c. 215-195 cm depth. In the upper 145 cm of the core, LOI_{925} remains relatively stable, with the exception of a rise between c. 11 cm towards the core top, and a local peak at 28 cm depth.

LOI_{550} is minimal (3.2 % on average) between the bottom of the core and 155 cm, after which it rises to 25.6 % at 137 cm depth. A subsequent increase towards c. 29-30 % is observed at 82-76 cm, followed by a decrease towards c. 19.8 % at 38 cm depth. A peak of 38.1 % is observed at 32 cm, and values remain high towards the top of the core, with the exception of a minor decline between 30 and 24 cm depth (ca. 29-27 %).

6.3.5. Fossil diatom assemblages

A stratigraphically constrained cluster analysis on all fossil diatom compositions divides the Beak-2 sediment core in two marine sections between 237-153 cm and four freshwater zones between 153 cm and the top of the core (Fig. 9).

* *Marine zones*

In general, the marine sections (Zones Beak 2m-1 and 2m-2) are dominated by the sea-ice related diatom *Navicula glaciei*, and by *Craspedostauros* sp., *N. criophila*, *N. phyllepta*, and an increasing abundance of *N. cryptotenella* towards the top (153 cm; Fig. 9). Species richness is higher than in the freshwater part of Beak-2, and the turnover rates and number of broken valves are high (Fig. 9).

The bottom zone 2m-1 (237-223 cm) starts with high abundances of *Nanofrustulum shiloi*, *Navicula glaciei*, *Achnanthes* cf. *brevipes* and *Craspedostauros* sp. at 237 cm depth. Peaks in diatom species turnover rate at 220 and 195 cm depth mark the boundaries of zone 2m-2 (223-188 cm) where also a small increase in diatom total abundances, centered around 203 cm, occurs. Between 220 and 208 cm depth, minor

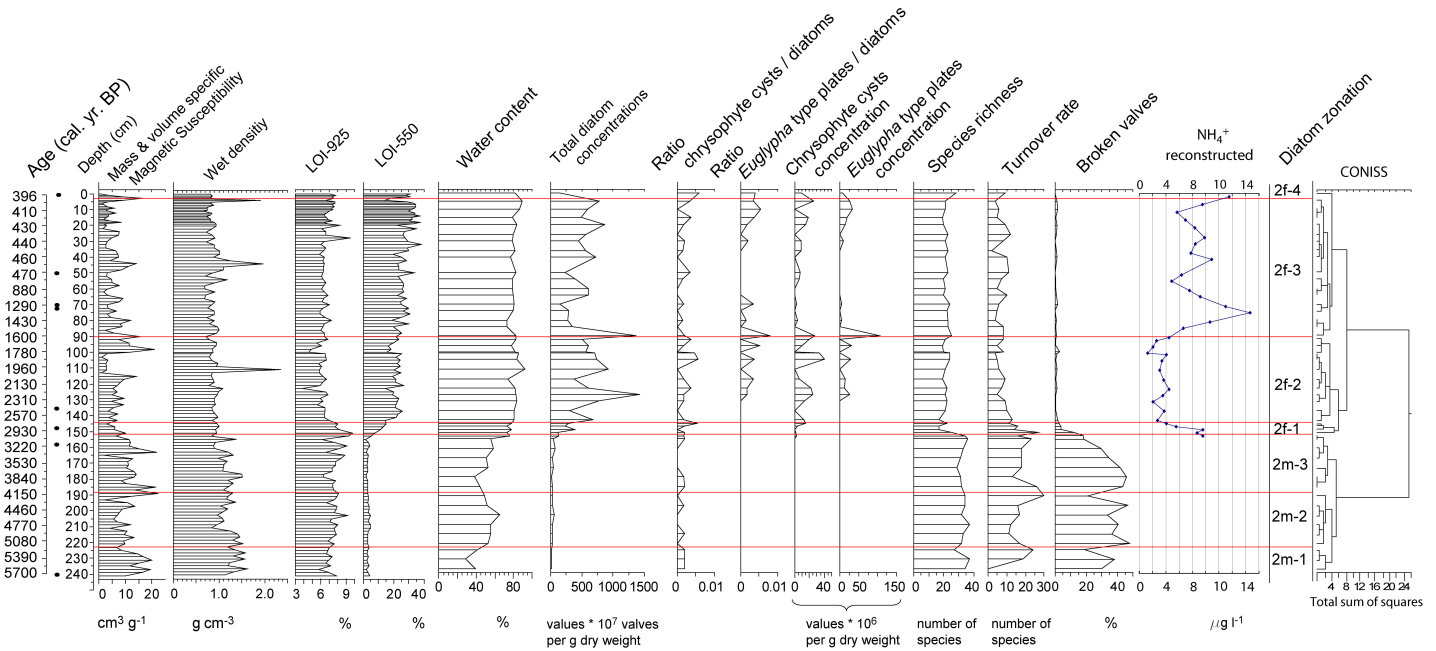

***Figure 8*:** Sedimentological, geochemical and microfossil-related stratigraphies of the Beak-2 core, plotted against depth (cm). Corresponding interpolated calibrated ages are given, and depths of ^{14}C dates (Table 4 and Fig. 7) are indicated by black dots.
LOI stands for loss-on-ignition. Diatom species turnover rates are the total number of species lost and gained from one sample to the next (above). The percentage of broken species is calculated with Chaetoceros RS excluded. WA-PLS-2 reconstructed NH_4^+ concentrations are shown for the freshwater zone of the core (in µg/l). Zonation of the cores is based on a CONISS cluster analysis on the diatom species data (Fig. 9).

increases are observed in *Achnanthes* cf. *brevipes*, *Amphora* spp., *Chaetoceros* resting spores, *Synedra kerguelensis*, *Fragilariopsis* spp., *Berkeleya* sp. and *Synedropsis* spp., the latter three being related to (sea) ice or ice-melting (Smith et al., 2007; Buffen et al., 2007; Gersonde & Zielinski, 2000; Crosta et al., 2008). A short-term disappearance of *Chamaepinnularia* spp. and suppression of *Navicula directa* is observed between 220-190 cm. Similar species compositions are observed at 173-166 cm depth (c. 3620-3010 cal. yr. BP) in zone 2m-3.

Zone 2m-3 (188-152 cm) is dominated by *Navicula glaciei*, *Craspedostauros* and *Navicula cryptotenella*, the latter steadily increasing towards 152 cm depth. *Navicula perminuta* becomes less abundant towards the top of this section, except for a small peak at 173 cm, which coincides with a peak in *Berkeleya* sp. and *Synedra kerguelensis*.

* *Transition zone*

Zone 2f-1 (152-144 cm): The main transition to freshwater conditions occur between 153 and 144 cm depth (zone 2f-1), and starts with high relative abundances in *Nitzschia perminuta*, *N. gracilis* and *Navicula gregaria*, followed by peaks in *Nitzschia frustulum/inconspicua*, *Stauroforma inermis*, *Navicula* cf. *libonensis* and *Gomphonema* spp., which are all high conductivity or eutrophic indicator taxa (Björck et al., 1996; Van de Vijver et al., 2008; and as observed in our surface dataset (Fig. 6) and in Jones & Juggins (1995).

* *Freshwater zones*

Zone 2f-2 (144-91 cm) is dominated by *Nitzschia frustulum/inconspicua*, *N. perminuta*, *Naviculadicta seminulum*, *Gomphonema* spp. and *Stauroforma inermis* (Fig. 9). *Naviculadicta seminulum* starts with a high peak between 131-127 cm, but rapidly decreases between 125-100 cm depth. A similar, but less pronounced trend is found in *Achnanthidium* cf. *exiguum* and *Navicula* cf. *libonensis* and *Psammothidium abundans*. Diatom total abundances are high between 144 and 91 cm depth, coinciding with the first appearance of the testacean *Euglypha* type plates, and a slight increase in Chrysophycean cyst concentrations (Fig. 9). Sharp peaks in diatom total abundances occur at 127 and 90 cm, both depths associated with high *Naviculadicta seminulum* abundances.

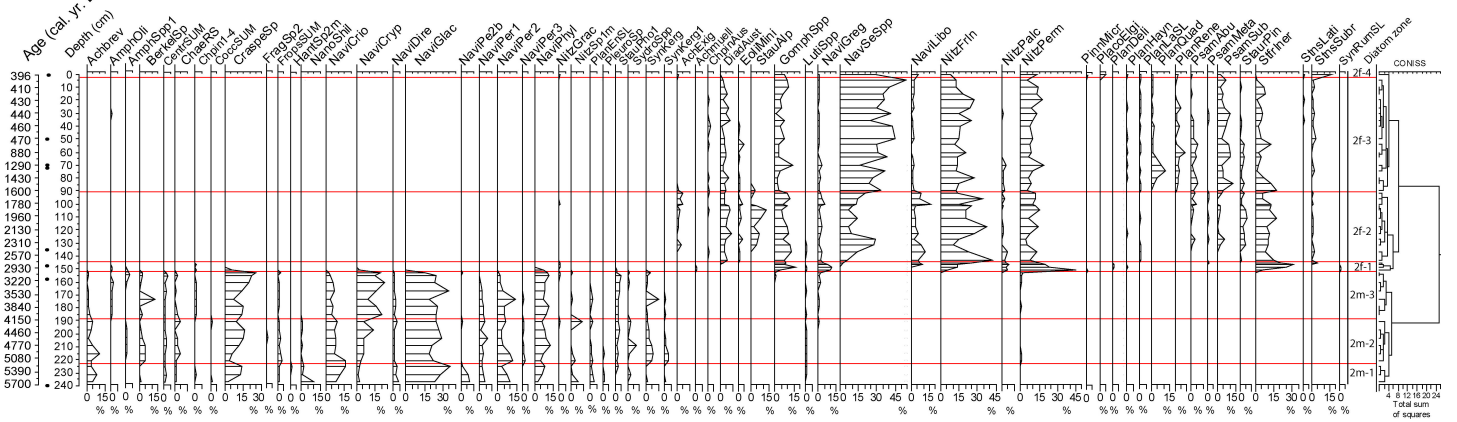

***Figure 9*:** Diatom stratigraphy of the BK2 core, plotted against depth (cm). Corresponding interpolated calibrated ages are given, and depths of ^{14}C dates (Table 4 and Fig. 7) are indicated by black dots. Only species with a relative abundance exceeding 2 % or occurring in five or more samples are shown, Chpin1-4 is an assemblage of *C. gerlachei*, C. sp. 2, *C.* sp. 3 and *C. cymatopleura*. Centric species are summed (CentrSUM), as well as all species of the genera *Cocconeis* (CoccSUM) and *Fragilariopsis* (FropsSUM). Abbreviations of the species and their corresponding full names are listed in Table 5. Zonation of the cores is based on a CONISS cluster analysis on the diatom data.

Zone 2f-3 (91-3 cm) starts with the disappearance of *Staurosira alpestris* and *Achnanthidium* cf. *exiguum.* Diatom species compositions in this zone are dominated by *Naviculadicta seminulum* s.l., which increases towards the top of the core. This zone is further characterized by suppressed abundances of *Navicula* cf. *libonensis*, the appearance of *Planothidium renei* and a maximum in *Planothidium quadripunctatum* between 80 and 64 cm depth. Although *Planothidium haynaldii* and *Chamaepinnularia australomediocris* appear in very low abundances, they are present in more samples from zone 2f-3 than in the previous zone. Between 84 and 70 cm depth, total diatom abundances are low, and between 60 and 40 cm, *Euglypha* type plates temporally disappear. Chrysophycean cyst concentrations remain present in the samples, though in suppressed concentrations between 91 and 50 cm.

Zone 2f-3 shows a change at 50 cm, whereafter *Eolimna minima* disappears, *Staurosirella pinnata* and *Psammothidium abundans* decrease, *P. metakryophilum* reappears and *Stauroneis latistauros* appears (though in very low abundances). This upper part of zone 2f-3 is also characterized by increasing total diatom abundances and the reappearance of *Euglypha* type plates after 40 cm.

In the core top sample (zone 2f-4; 3-0 cm), *Stauroneis* cf. *subgracilior* and *Placoneis elginensis* become abundant, while *Naviculadicta seminulum* dramatically decreases in relative abundance. Diatom species richness is high in this core-top sample, while absolute diatom abundances, *Euglypha* type plates and chrysophyte cyst concentrations decrease, although the ratio cysts/diatoms is high in this sample (Fig. 9).

WA-PLS-2 reconstructed values for NH_4^+ concentrations (µg/l) are shown in Fig. 8. NH_4^+ starts high (9.6 µg/l) in zone 2f-1 immediately after isolation of the lake, and drops quickly to minimal values in zone 2f-2, especially at the beginning and the end of the zone (Fig. 8). Values are generally higher in zone 2f-3, with a major peak at 74 cm (c. 1320 cal. yr. BP). Values remain higher in zone 2f-3 than in 2f-2, and increase again towards the top of the core. Still, these reconstructed values remain, with their maximum at 16.7 µg/l lower than the actual measured value of 24 µg/l. The high peak at 74-70 cm depth is probably caused by increases in *Planothidium renei*, *Nitzschia perminuta* and *Gomphonema* spp. at these depths. Indeed, these species are known to thrive in more productive or eutrophied systems.

6.3.6. Fossil pigment compositions

The fossil pigment stratigraphy of core Beak-2 broadly follows the diatom stratigraphy (Fig. 10), revealing changes in total abundances and compositions at the same depths as those in the diatom stratigraphy.

* *Marine zones*

Zone 2m-1 (237-223 cm) contains almost no pigments. The carotenoids that do occur in this zone are mainly composed of diatoxanthin and a lutein derivative, a chlorophyll/carotenoid mixture is observed as well, and phaeophytin *a* is the most important chlorophyll derivative found in this zone.

Changes in pigment composition at c. 220 and 190 cm depth corroborate the delineation of diatom zone 2m-2 (223-188 cm), which is characterized by the absence of *ß*-carotene, an increase in lutein/zeaxanthin and a complementary decrease in diatoxanthin, with respectively a local maximum (respectively minimum) centered at 203 cm depth. In the chlorophyll-group phaeophytin *a* remains high in this zone, as well as two co-eluting pigments identified as a chlorophyll-carotenoid mixture (Fig. 10). A small increase in total pigment concentrations is observed in this zone 2m-2. A modest peak in concentrations is observed at 203 cm, and coincides with a minor peak in diatom absolute abundances at the same depth.

Zone 2m-3 (188-152 cm) is marked by the abrupt (re-)appearance of *ß*-carotene at 188 cm, the apperance of small concentrations of scytonemin, and the disappearance of an *a*-carotene like pigment. A decrease (increase) in diatoxanthin (lutein/zeaxanthin) is observed towards 153 cm depth, and a slightly lower percentage of lutein-derived pigment 1 is observed. Total carotenoid concentrations show a (small) increase/peak at 173 cm, and corresponds with a very short lived change in pigment composition (e.g. disappearance of scytonmin and an unknown carotenoid, appearance of chlorophyll *c2*) and diatom compositions (cfr. short-lived *Berkeleya* sp. and *Synedra* peak at 173 cm).

The chlorophyll pigments are dominated by pyrophaeophytin *a* like pigments instead of the earlier dominant chlorophyll-carotenoid mixture (Fig. 10). Towards the top of this section (152 cm), chlorophyll *a* concentrations reach their maximum (Fig. 10).

* *Transition zone*

Zone 1f-1 (152-144 cm) contains high peaks of total carotenoid and chlorophyll concentrations. Carotenoids shift from being dominated by lutein/zeaxanthin at 152 cm towards scytonemin at 144 cm, where total carotenoid concentrations have declined.

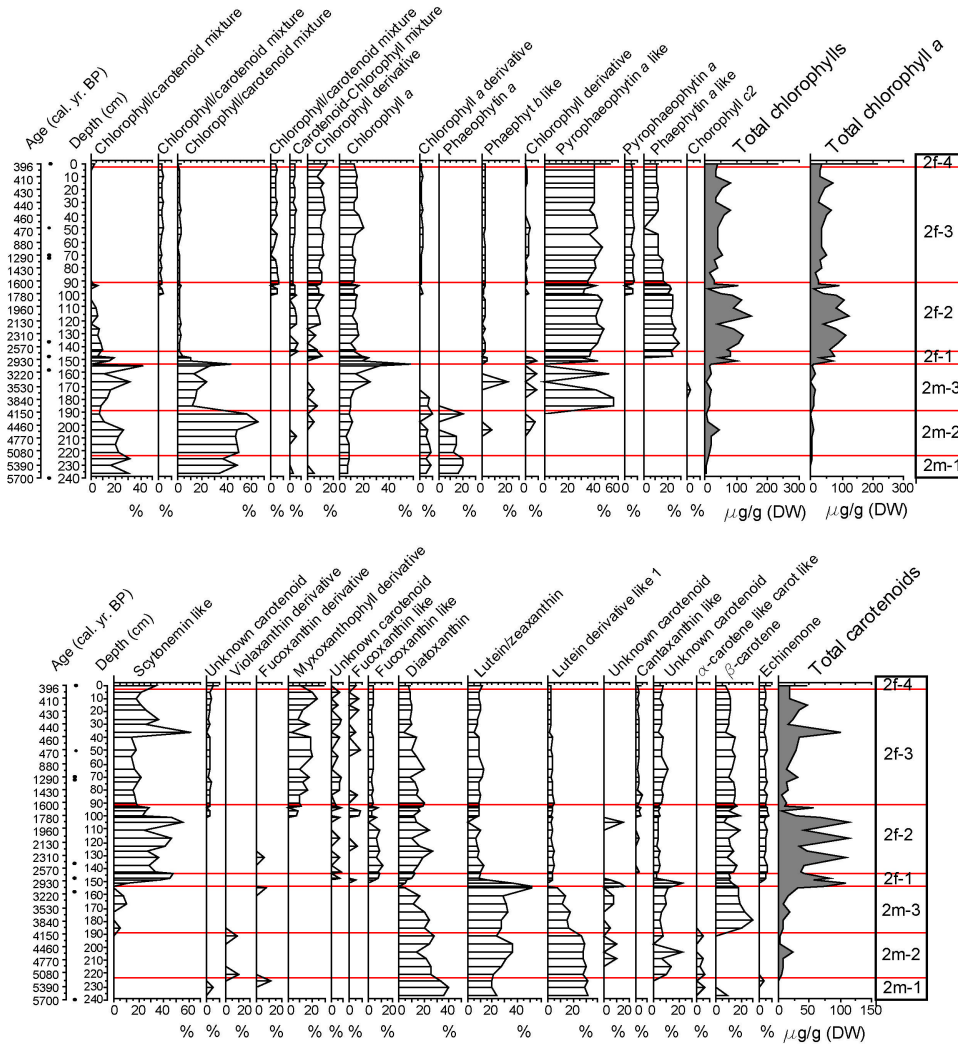

Figure 10: Fossil pigment stratigraphy of the Lake Beak-2 sediment core, plotted against depth (cm). Corresponding interpolated calibrated ages are given, and depths of ^{14}C dates (Table 4 and Fig. 7) are indicated by black dots. Only pigments constituting more than 2 % of the total carotenoids or total chlorophylls are shown. Total pigment concentrations (grey shaded graphs) are expressed in µg/g dry weight (DW). Zonation of the core is based on a CONISS cluster analysis performed on the diatom data (Fig. 9).

* *Freshwater zones*

Freshwater zone 1f-2 (144-91 cm) contains maximal concentrations of both total carotenoids and chlorophylls (Fig. 10), although the total carotenoid concentrations show a large variability in this zone.

The carotenoids are highly dominated by scytonemin in this zone, together with modest (c. 15-35 %) fractions of diatoxanthin, lutein/zeaxanthin and ß-carotene. The lutein derivative that was found in high percentages in the marine sections of the core is lower in the freshwater zones, as well as some unknown carotenoids that were detected. Echinenone, fucoxanthin and canthaxanthin like pigments, as well as some unknown carotenoids appear in this zone for the first time, and remain present throughout the whole freshwater core section (Fig. 10). The chlorophyll group is dominated by Pyrophaeophytin *a* like pigments, which had appeared already in the marine section of the core at 188 cm depth. Further, phaeophitin-a like pigments appear, and are particularly high in zone 1f-2, and slightly decreasing in the next zone (1f-3). Chlorophyll *a* and some chlorophyll derivatives are present in lower proportions in this zone.

Zone 1f-3 (91-3 cm) is characterized by a decrease in total pigment (especially carotenoids) concentrations between 91 and c. 40 cm depth. An increase was observed again between c. 40 and 15 cm. In the carotenoid group, scytonemin percentages followed the same trend, i.e. low values between 91 and 40 cm, and high values between 40 and 15 cm. Some canthaxanthin like, and an unknown carotenoid that were recognized in zone 1f-2 slightly increased in percentage in this zone, and one of the fucoxanthin-like pigments slightly decreased. Myxoxanthophyll and an unknown carotenoid appeared for the first time, and remained stable throughout this zone (Fig. 10). In the chlorophyll group, pyrophaeophytin *a*, a chlorophyll *a* derivative and some chlorophyll/carotenoid mixtures appeared for the first time in this zone, and remained stable to the top of the core. No large changes in chlorophyll compositions were observed throughout this zone.

Zone 1f-4 (3-0 cm) contains a surface sample with very high pigment concentrations (mainly chlorophylls). In the carotenoid group a high peak in a myxoxantophyll derivative is responsible for this increase, together with a modest increase in scytonemin pigments. In the chlorophyll group a peak in pyrophaeophytin is observed, but other pigment percentages remain more or less stable (Fig. 10).

6.4. Discussion

In this paper, we constructed a diatom-based transfer function for reconstructing NH_4^+ levels in maritime Antarctic lakes, and applied it to fossil diatom assemblages from a shallow (4 m) lake sediment core from Beak Island (NE Antarctic Peninsula). Of all environmental variables measured, many explained a larger proportion of the diatom variance in the dataset than NH_4^+ (see Table 3). However, these variables were either (a) related to the geology of the respective islands (hence location of the lakes) or (b) related to salinity/conductivity in the lakes, which we believe is not a direct function of the water balance of the lakes (many of which are not closed basins), like it is the case in drier climatic regions (e.g. in East-Antarctica; Roberts et al., 2004; Verleyen et al., 2003). Instead, changes in conductivity are mainly influenced by the distance to the coast, and hence again by location. Indeed, when applying a CCA on a subset of our dataset, containing only lakes at more than 300 meter away from any coast, conductivity was left not to explain an additional significant portion of the variance in diatom compositions after partialling out the more significant variables (Silicate). Similarly, the variable "maximum depth", which was newly added to our dataset in comparison with the dataset of Jones et al. (1993), proved to be strongly dependent of the respective island the lakes are on, as Signy Island mainly contained deeper basins, whereas lakes on Livingston Island ranged from shallow at the coast to deeper at inland sites (Fig. 4).

The selection of a single variable that is clearly linked with climate seems rather difficult in maritime Antarctic lakes. Trophic status related variables like nutrient concentrations and lake primary productivity, seem to be the most promising variables for reconstructing cilimate in Maritime Antarctica. Indeed, lake primary productivity and nutrient concentrations have been shown recently to significantly increase in response to climate warming on Signy Island (Quayle et al., 2002). An increase in lake primary productivity in these lakes is related to an increase in the growing season and higher water temperatures. Increased nutrient concentrations are likely related to the melting of glaciers and snowbanks and the subsequent development of vegetation in the catchment area.

6.4.1. Paleoclimate changes in Beak Island

6.4.1.1. Cold marine conditions between c. 5860-3015 cal. yr. BP

Between c. 5860 and 3015-2720 cal. yr. BP the core sediments from Beak-2 contained coarse the basin of Beak-2 was below sea level. Diatom assemblages were dominated by fast/shore ice related species (*Navicula glaciei;* Whitehead & McMinn, 1997), ice edge (*Navicula criophila*; Kang & Fryxell, 1993) and sub-ice (*Berkeleya* and *Synedropsis* sp.;

Riaux-Gobin & Poulin, 2004) related species, together with benthic/tychoplanktonic marine and brackish water diatoms like *Navicula phyllepta* and *N. perminuta* (Zacher et al., 2007; Underwood & Povot, 2000).

This high amount of ice-related species, and the relatively low diatom total abundances may reflect a period with extensive sea-ice cover and cold climatic conditions. However, the poor preservation of the diatoms and the presence of coarse material at several depths in the marine organic mud matrix of Beak-2 may as well point to the presence of decaying icebergs stranded in or near the shallow marine basin at that time, thus indicating episodic melting.

A gradual decrease in *Achnanthes* cf. *brevipes*, and increase in *Craspedostauros* sp. and *Navicula cryptotenella* towards 3015-2720 cal. yr. BP probably reflects the shallowing of the basin through isostatic recovery. This evolution is also reflected in the pigment data, which show very low total concentrations at the bottom of the core, increasing from c. 5080 cal. yr. BP (220 cm) onwards, and gradually shifting from high diatoxanthin towards higher lutein/zeaxanthin pigments. This is indicative of an increasing importance of non-diatom algal blooms, which typically become more dominant in meltwater related stratified marine environments. Moreover, the appearance of the UV-screening scytonemin like pigments and *b*-carotene at c. 4150 cal. yr. BP (190 cm) may point to the presence of cyanobacteria (Squier et al., 2004), and may thus, together with the increased non-diatom algal abundances, be explained by (1) the shallowing environment and/or (2) increasingly warming temperatures.

Our interpretation of cold conditions between 5860 and 3015 cal. yr. BP are roughly in accordance with a low productivity period between c. 6000 and 3500 cal. yr. BP deduced from fossil diatom and pigment data in the freshwater core section from Lake Beak-1 (Chapter 7). This would corroborate the inference of cold conditions starting at c. 4700 ^{14}C BP (c. 5360 cal. yr. BP) in Hope Bay, as inferred from the low productivity in Lake Boeckella during that time (Gibson & Zale, 2006). These cold conditions are also said to explain the occurrence of glacier advances after 5360 cal. yr. BP in Hope Bay (Zale, 1994). However, in James Ross Island, cold and arid conditions were inferred for the 5000-4200 ^{14}C BP period (c. 5700-4700 cal. yr. BP), causing glaciers to retreat due to snow starvation. However, a milder climate with higher precipitation was said to explain glacier re-advances on the island at c. 4700 cal. yr. BP (Björck et al., 1996).

6.4.1.2. Isolation of Beak-2 and high productivity between c. 3015-2720 cal. yr. BP.

The isolation of Beak-2 occurred between c. 3015 and 2720 cal. yr. BP, and the associated species succession was similar to that observed in another isolation lake sediment core from Beak Island (Beak-1; Chapter 7), with high peaks of *Nitzschia perminuta* followed by *N. frustulum/inconspicua* and *Naviculadicta seminulum*. This succession is most likely a response to the change from marine to brackish and finally freshwater conditions, and therefore prevents us from reconstructing climate conditions for this period in our core. The rapid decrease in inferred NH_4^+ concentrations is related to the high peak of *Naviculadicta seminulum* after 2720 cal. yr. BP and which may have taken over from *Nitzschia* spp. due to a continuing decrease in lakewater salinity and nutrient depletion resulting from a combination of high productivity and decreasing nutrient supplies from the marine environment as the lake became isolated.

After the isolation phase of the basin, generally low nutrient concentrations and productivity were reconstructed for the lake between c. 3015 and 1600 cal. yr. BP. This seems to contradict the markedly higher total diatom abundances and very high pigment concentrations in this zone, as well as the appearance of *Euglypha* type plates and very high relative abundances of UV-screening pigments (scytonemin) in this zone, which all may point to a warmer climate (Leavitt & Hodgson, 2001).

A change towards low pigment and diatom concentrations co-occurred with a decrease of *Euglypha* type plates, scytonemin-like pigments and the appearance of a myxoxanthophyll- and a chlorophyll-derivative at c. 1600 cal. yr. BP (91 cm depth). This change occurred rather abruptly, and coincided with a short term oscillation in magnetic susceptibility and a local minimum in organic matter (Loss on Ignition; LOI_{550}), pointing to a sudden increase in clastic input. The timing of this shift at 1600 cal. yr. BP corresponds with a moment of large changes in the upstream Lake Beak-1 (Chapter 7), which shifted towards a less productive stage with more acid-associated diatom species. It is possible that such an ecological change in Beak-1 severely affected the ecology of Lake Beak-2, which is situated immediately downstream Beak-1 (Fig. 2a). The more acid nature of the Beak-1 lakewater would corroborate the presence of *Euglypha* type plates in this section of the Beak-2 core, since protozoan plates are especially common in cores associated with bogs, or may be indicative for the growth of mosses in the catchment of a lake (Douglas & Smol, 2001; and references therein). Although the ratio of chrysophyte cysts to diatom valves does not show large variations through the lacustrine section of

core Beak-2, the presence of these cysts may as well point to the existence of aquatic mosses in the lake (Douglas & Smol, 1995).

This moment of abrupt change corresponds with the start of a 'neoglacial cooling' in many sites in the Antarctic Peninsula region, with the reformation of ice shelves [e.g. Larsen-A (Fig. 1): Brachfeld et al. (2003); Prince Gustav Channel (Fig. 1): Pudsey & Evans (2001)], and a deteriorating climate in the South Shetlands and South Orkneys (Björck et al., 1991; Liu et al., 2006), although in the South Orkneys the Mid-Holocene hypsithermal ended slightly later than 1600 cal. yr. BP (Jones et al., 2000; Hodgson & Convey, 2005). A remarkable high peak in reconstructed NH_4^+ values was observed at c. 1320 cal. Yr. BP (74 cm), and was caused by an increased abundance of *Nitzschia frustulum* and *N. perminuta*, *Gomphonema* spp. and *Planothidium quadripunctatum*. This event was marked by low diatom total abundances, and only a minor increase in total chlorophylls and total carotenoids (Fig. 10). A minor increase in scytonemin percentages was also observed.

Due to uncertainties in the age depth model, it was difficult to assess when this period exactly ended, but a clear change back to high concentrations of total carotenoids and diatoms occurred at c. 40 cm depth. This coincided with an increase in total diatom concentrations, a shift towards higher LOI_{550} and the reappearance of *Euglypha* type plates.

6.5. Conclusions

In this Chapter, we intercalibrated an existing diatom reference dataset from Livingston and Signy Islands with diatoms from lake sediment cores and surface sediments from Beak Island (NE Antarctic Peninsula). Diatom species distributions in the dataset were mainly explained by silicate and conductivity, both being variables with a high spatial component that could not clearly be linked with climate. Trophic or productivity indicator variables, such as pigment or nutrient concentrations, do show a firm response to climate change however, and of these, NH_4^+ explained the largest portion of variance in the diatom data. We constructed a WA-PLS-2 based transfer function for NH_4^+ and applied it to the lacustrine fossil diatom record of Lake Beak-2 (Beak Island).

The environmental history of Beak-2 was reconstructed on the basis of fossil diatom and pigment concentrations. The lake is an isolation basin, and marine sediments at the bottom of the core suggest the presence of many decaying icebergs and probably also cold climate conditions at the site between c. 5860 and 3015 cal. yr. BP. After isolation of

the basin, a high productivity (as seen in the diatom and pigment concentrations) was maintained until c. 1600 cal. yr. BP. Reconstructed NH_4^+ values were, however, low during this period. After 1600 cal. yr. BP, dating of the sediments becomes uncertain, and prohibits us to draw firm conclusions about the timing of climate shifts.

***Table 5*:** List of taxa identified in the BLS-surface dataset and Beak sediment cores. In case of doubt about the delineation of certain taxa (e.g. due to new taxonomic descriptions and reviews of species complexes since the ´90s), species or taxa were merged into a species group or complex. Taxa indicated in bold are photographed and described in Chapter 4. For each (recombined) taxon the respective species codes used in Jones et al. (1993) and Jones & Juggins (1995) are given. Columns A, B and C represent the presence/absence of each taxon in the surface dataset (A), the freshwater parts of the Beak sediment cores (B) and both (C). Column A is divided into LN (Livingston Island), SG (Signy Island) and BK (Beak Island), and in column C '1' refers to the presence of a taxon in A or B, and '2' refers to the presence in both A and B. Species marked with zero in column C represent taxa that were identified (either in the surface dataset or the cores), but were not positively identified with one of the taxa listed in Jones et al. (1993) and Jones & Juggins (1995). The asterisk (*) marks species that are newly described in Chapter 5, and 'm' indicates that the respective taxon occurred exclusively in the marine parts of the cores.

New code (this paper)	**A** LN	SG	BK	**B**	**C**	**New name of taxon or species complex**		**Old code (Jones et al., 1993; Jones & Juggins, 1995)**
AC014C	1	0	0	0	1	*Achnanthes austriaca* var. *helvetica*		AC014C
AC022A	0	1	0	0	1	*Achnanthes* cf. *marginulata*		AC022A
AC9968	1	0	0	0	1	*Achnanthes [marginulata]* major Uaine		AC9968
AC9999	1	1	0	0	1	*Achnanthes* sp.		AC9999
Achbrev	0	0	0	1	1	*Achnanthes* cf. *brevipes*		-
AchExig	1	0	1	1	2	***Achnanthidium* cf. *exiguum***		AC008A
Achminut	1	1	0	0	1	***Achnanthidium minutissimum* s.l.**		AC013A
Achmuell	0	0	1	1	2	***Achnanthes* cf. *muelleri***		-
AchSp1						*Achnanthes* sp. 1	m	-
AdlaBryo	0	1	0	0	1	***Adlafia bryophila***		NA045A
AdlaMinu	1	1	0	1	2	***Adlafia* cf. *minuscula***		ZZZ978
AM9999	1	1	0	0	1	*Amphora* sp.		AM9999
AmphiSpp	1				0	***Amphipleura* sp.**		-
AmphOli	1	1	1	1	2	***Amphora* cf. *oligotraphenta***		AM004A + ZZZ975
AmphSpp1	0	0	0	1	1	*Amphora* spp. 1		-
AulaSp1	1	0	0	0	1	***Aulacoseira* sp. 1**		ZZZ950
BerkelSp	0	0	0	1	1	*Berkeleya* sp.		-
BR001A	1	0	0	0	1	*Brachysira* cf. *vitrea*		BR001A
Brachmin	1	1	1	1	2	***Brachysira minor***		BR008A
CA003A	1	1	0	0	1	*Caloneis ventricosa*		CA003A

Table 5 (continued)

New code (this paper)	A LN	A SG	A BK	B	C	New name of taxon or species complex		Old code (Jones et al., 1993; Jones & Juggins, 1995)
CaloBaci	1	1	1	1	2	***Caloneis* cf. *bacillum***		CA002A
CaviPseu	0	1	0	0	1	***Cavinula pseudoscutiformis***		NA013A
Centr_1						Centric sp. 1	m	-
Centr_11						Centric sp. 11	m	-
Centr_12						Centric sp. 12	m	-
Centr_13						Centric sp. 13	m	-
Centr_14						Centric sp. 14	m	-
Centr_15						Centric sp. 15	m	-
Centr_16						Centric sp. 16	m	-
Centr_17						Centric sp. 17	m	-
Centr_18						Centric sp. 18	m	-
Centr_19	0	0	0	1	1	Centric sp. 19		-
Centr_2	0	0	0	1	1	Centric sp. 2		-
Centr_21						Centric sp. 21	m	-
Centr_22						Centric sp. 22	m	-
Centr_3						Centric sp. 3	m	-
Centr_4						Centric sp. 4	m	-
Centr_5						Centric sp. 5	m	-
Centr_6	0	0	0	1	1	Centric sp. 6		-
Centr_7						Centric sp. 7	m	-
Centr_8						Centric sp. 8	m	-
Centr_9						Centric sp. 9	m	-
ChaeRS	0	0	0	1	1	*Chaetoceros* resting spore		-
Chaetoc						*Chaetoceros* valve	m	-
ChamAl		1			0	***Chamaepinnularia aliena***		-
ChamSp1	1	1	0	0	1	***Chamaepinnularia* sp. 1**		ZZZ988
ChpinAus	1	1	1	1	2	***Chamaepinnularia australomediocris***		NA734A
ChpinCym	0	0	1	1	2	***Chamaepinnularia cymatopleura***		-
ChpinGer	1	1	1	1	2	***Chamaepinnularia gerlachei***	*	ZZZ946
ChpinKfs	1	1	1	1	2	***Chamaepinnularia krookiformis***		ZZZ944 + ZZZ947
ChpinKri	1	1	0	1	2	***Chamaepinnularia krookii***		PI169A
ChpinSp2						*Chamaepinnularia* sp. 2	m	-
ChpinSp3	0	0	0	1	1	*Chamaepinnularia* sp. 3		-
CM9999	0	1	0	0	1	*Cymbella* sp.		CM9999
CoccSp1						*Cocconeis* sp. 1 (cf. *pinnata*)	m	-
CoccSp11	1	0	0	0	1	*Cocconeis* sp. 11		ZZZ960
CoccSp3						*Cocconeis* sp. 3	m	-

Table 5 (continued)

New code (this paper)	A LN	A SG	A BK	B	C	New name of taxon or species complex		Old code (Jones et al., 1993; Jones & Juggins, 1995)
CoccSp5						*Cocconeis* sp. 5	m	-
CoccSp6						*Cocconeis* sp. 6	m	-
CoccSp7						*Cocconeis* sp. 7	m	-
CoccSp9a						*Cocconeis* sp. 9a	m	-
CoccSp9b						*Cocconeis* sp. 9b	m	-
CoccSpp	0	1	0	0	1	*Cocconeis* spp. (containing: **Cocconeis placentula var. euglypta**)		CO9999
CraspeSp	0	0	0	1	1	*Craspedostauros* sp.		-
CratiAnt	0	0	0	1	1	***Craticula antarctica***	*	-
CratiSub	1	1	0	1	2	***Craticula subpampeana***	*	NA056A
Cycl9999	1	1	0	0	1	*Cyclotella* spp.		CY9999
DiadAust	1	1	1	1	2	***Diadesmis australis***	*	NA036A
DiadNien	1	1	0	0	1	***Diadesmis* cf. *langebertalotii***		ZZZ948
DiadSp13	0	0	0	1	1	*Spec. 13*		-
DiadSpp	1	1	1	1	2	*Diadesmis* spp. (containing: ***Diadesmis* sp. 1** + ***Diadesmis* sp. 2**)		NA046A
DiplSpp	1	0	0	1	2	*Diploneis* spp.		DP9999
EncyoMin	1	1	0	0	1	***Encyonema minutum***		CM031A
EoliMini	1	1	1	1	2	***Eolimna minima***		NA086A
EU9999	1	1	0	0	1	***Eunotia* spp.**		EU9999
FR002A	0	1	0	0	1	*Fragilaria construens* var. *construens*		FR002A
FR002D	1	0	0	0	1	*Fragilaria construens* var. *exigua*		FR002D
FR9999	1	1	0	0	1	*Fragilaria* sp.		FR9999
FragSp2	0	0	0	1	1	*Fragilaria* sp. 2		-
FragSp2b						*Fragilaria* sp. 2b	m	-
FragSp2c						*Fragilaria* sp. 2c	m	-
FropsCfr						*Fragilariopsis cylindroformis*	m	-
FropsCur	0	0	0	1	1	*Fragilariopsis curta*		-
FropsCyl	0	0	0	1	1	*Fragilariopsis cylindrus*		-
FropsOb2						*Fragilariopsis* cf. *obliquecostata* f. 2	m	-
FropsObl						*Fragilariopsis* cf. *obliquecostata*	m	-
FropsSp1						*Fragilariopsis* sp. 1	m	-
FropsVhi						*Fragilariopsis vanheurckii*	m	-
Gomphops	1	0	0	0	1	***Gomphonemopsis* sp.**		ZZZ959
GomphSpp	1	1	1	1	2	***Gomphonema* spp.**		GO003A + GO003B + GO004A + GO013A + ZZZ992 + ZZZ962 + GO9999

Table 5 (continued)

New code (this paper)	A LN	A SG	A BK	B	C	New name of taxon or species complex		Old code (Jones et al., 1993; Jones & Juggins, 1995)
HantAmph	1	0	0	1	2	***Hantzschia* cf. *amphioxys***		HA001A
HantSp1m						*Hantzschia* sp. 1 marine	m	-
HantSp2m						*Hantzschia* sp. 2 marine	m	-
HantSpp	0	0	1	1	2	*Hantzschia* spp. (containing: ***Hantzschia* sp. 1** and ***Hantzschia* sp. 2**)		-
HantSppm						*Hantzschia* spp. marine	m	-
HippHung	1	0	0	0	1	***Hippodonta hungarica***		NA066B
LI9999	1	0	0	0	1	*Licmophora* sp.		LI9999
LutiCohn	0	0	0	0	1	***Luticola* cf. *cohnii***		-
LutiHigl	1	0	1	1	2	***Luticola higleri***		ZZZ954
LutiSpp	1	1	1	1	2	*Luticola* spp. (containing: ***Luticola* cf. *australomutica***, ***L.* cf. *muticopsis* s.s.**, ***L. muticopsis* f. *reducta/evoluta***)		NA555A + NA025A + ZZZ986
Mayamaea	1	1	1	1	2	***Mayamaea* cf. *atomus* var. *permitis***		NA084A
ME019A	1	0	0	0	1	*Melosira arentii*		ME019A
MicroNau	1	1	1	1	2	***Microcostatus* cf. *naumanni***		NA150A
MuellAeq	1				0	***Muelleria aequistriata***		-
MuellAus	1	0	0	0	1	***Muelleria australoshetlandica***		NA397A
NA099A	1	0	0	0	1	*Navicula* cf. *bremensis*		NA099A
NA9999	1	1	0	0	1	*Navicula* sp.		NA9999
NanoShil						*Fragilaria construens* var. *venter* (f.1 + f.2)	m	-
NaviAust	1	0	0	1	2	***Navicula austroshetlandica***	*	ZZZ952
NaviBice	1	1	0	0	1	***Navicula bicephala***		NA740A
NaviCinc	0	0	1	1	2	***Navicula cincta***		-
NaviCrio	0	0	0	1	1	*Navicula criophila*		-
NaviCryp	0	0	0	1	1	*Navicula cryptotenella*		-
NaviDire	0	0	0	1	1	*Navicula directa*		-
NaviElor	1	1	0	1	2	***Naviculadicta' elorantana***		NA005C
NaviGlac	0	0	0	1	1	*Navicula glaciei*		-
NaviGreg	1	1	1	1	2	***Navicula gregaria***		NA023A
NaviJoub	0	0	0	1	1	*Navicula joubaudii*		-
NaviLibo	1	1	1	1	2	***Navicula* cf. *libonensis***		NA007B
NaviPe2b	0	0	0	1	1	*Navicula perminuta* var. 2b		-
NaviPer1	0	0	0	1	1	*Navicula perminuta* var. 1		-
NaviPer2	0	0	0	1	1	*Navicula perminuta* var. 2		-
NaviPer3						*Navicula perminuta* var. 3	m	-
NaviPhyl	0	0	0	1	1	*Navicula phyllepta*		-
NaviSp1m						*Navicula* sp. 1 marine	m	-

Table 5 (continued)

New code (this paper)	A LN	A SG	A BK	B	C	New name of taxon or species complex		Old code (Jones et al., 1993; Jones & Juggins, 1995)
NaviSp2m						*Navicula* sp. 2 marine	m	-
NaviSp3m	0	0	0	1	1	*Navicula* sp. 3 marine		-
NaviSp4m						*Navicula* sp. 4 marine	m	-
NaviSpA	1	0	0	0	1	*Navicula* sp. a		ZZZ949
NaviTabe	1	0	0	0	1	***Diadesmis tabellariaeformis***		NA735A
NavSeSpp	1	1	1	1	2	*Naviculadicta seminulum* s.l. (containing: ***Navicula* cf. *obsoleta***, ***N.* cf. *seminulum***)		NA005A + ZZZ977 + ZZZ976 + ZZZ940
NE003A	1	0	0	0	1	*Neidium affine* var. *affine*		NE003A
NE9999	1	0	0	0	1	*Neidium* sp.		NE9999
NI9999	1	1	0	0	1	*Nitzschia* sp.		NI9999
NitzAngu						*Fragilaria* sp. 1	m	-
NitzFrIn	1	1	1	1	2	*Nitzschia frustulum/inconspicua* complex (***N. inconspicua*** + ***N. frustulum***)		NI008A
NitzGrac	1	1	1	1	2	***Nitzschia gracilis***		NI017A + NI009A
NitzHomb	1	1	1	1	2	***Nitzschia homburgiensis***		NI197A
NitzPalc	1	0	1	1	2	***Nitzschia paleacea***		NI033A
NitzPerm	1	1	1	1	2	***Nitzschia perminuta***		NI005A
NitzPusi	1	0	0	0	1	***Nitzschia* cf. *pusilla***		ZZZ955
NitzSp1l	0	0	0	1	1	*Nitzschia* sp. 1 lacustrine		-
NitzSp1m	0	0	0	1	1	*Nitzschia* sp. 1 marine		-
NitzSp4m	0	0	0	1	1	*Nitzschia* sp. 4 marine		-
NitzSp5m	1	0	0	0	1	*Nitzschia* sp. 5 marine		ZZZ957
NitzSp6m	0	0	0	1	1	*Nitzschia* sp. 6 marine		-
NitzSp7m						*Nitzschia* sp. 7 marine	m	-
NitzSppM	0	0	0	1	1	*Nitzschia* spp. marine		-
Obj3						Object 3	m	-
Obj4						Object 4	m	-
Obj6						Object 6	m	-
OrthRhoe	0	0	0	1	2	***Orthoseira roeseana***		-
PI014A	1	0	0	0	1	*Pinnularia* cf. *appendiculata*		PI014A
PI9999	1	1	0	0	1	*Pinnularia* spp. (containing: ***P. obscura, P. splendida, P. spp., P. gemella***)		PI9999
PinnBor	1	1	0	1	2	***Pinnularia borealis***		PI012A
PinnDiv	1	1	0	0	1	***Pinnularia* cf. *divergens* var. *linearis***		PI008A
PinnKolb	1				0	***Pinnularia* cf. *kolbei***		-
PinnMicr	1	1	1	1	2	*Pinnularia microstauron* s.l. (= ***P. microstauron* + *P. microstauron* var. *nonfasciata***)		PI011A + PI011G
PinnSp2						*Pinnularia* sp. 2	m	-

Table 5 (continued)

New code (this paper)	A			B	C	New name of taxon or species complex		Old code (Jones et al., 1993; Jones & Juggins, 1995)
	LN	SG	BK					
PinnSpp2	0	0	0	1	1	*Pinnularia* spp. 2		-
PinnSub	1	1	0	0	1	***Pinnularia subantarctica* var. *elongata***		PI022A
PlacoElgi	1	1	1	1	2	***Placoneis* cf. *elginensis***		NA057A
PlanDeli	1	1	1	1	2	***Planothidium delicatulum***		AC016A
PlanEnSL						*Planothidium* cf. *engelbrechtii* s.l.	m	-
PlanHayn	1	0	1	1	2	***Planothidium* sp. 1**		AC001A
PlanLaSL	1	1	1	1	2	*Planothidium* cf. *lanceolatum* s.l. (= ***P. lanceolatum s.l. + P. frequentissimum***)		AC031A
PlanoSp2						*Planothidium* sp. 2	m	-
PlanoSpp						*Planothidium* spp.	m	-
PlanQuad	1	1	1	1	2	***Planothidium quadripunctatum***		AC040A
PlanRene	1	1	1	1	2	***Planothidium renei***		AC144A
PleuroSp	0	0	0	1	1	*Pleurosigma* sp.		-
PsamAbu	1	1	1	1	2	***Psammothidium abundans***		AC135A
PsamInco	1	1	0	1	2	***Psammothidium incognitum***		AC137A
PsamInGe	1	1	0	1	2	*Psammothidium* cf. *investians/germainii* complex (= ***P.* cf. investians** + **P. germainii (f. 1 + f. 2)**)		AC083A + AC138A + (0)
PsamMang	1	1	0	0	1	***Psammothidium manguinii***		AC139A
PsamMeta	1	1	1	1	2	***Psammothidium metakryophilum***		AC145A
PsamSub	1	1	1	1	2	***Psammothidium subatomoides***		AC136A
SA9999	1	0	0	0	1	*Stauroneis* sp.		SA9999
SellSpX	1	0	0	0	1	***Sellaphora* sp. 1**		SA004A + ZZZ953 + ZZZ941
Spec					0	Spec.		-
Spec10m						Spec. 10 marine	m	-
Spec12m	0	0	1	1	2	*Species* 12		-
Spec13m						*Caloneis* sp. 1	m	-
Spec1m						Spec. 1 marine	m	-
Spec2	0	0	0	1	1	Spec. 2		-
Spec2m						Spec. 2 marine	m	-
Spec3m						Spec. 3 marine	m	-
Spec5m						Spec. 5 marine	m	-
Spec6m						Spec. 6 marine	m	-
Spec7m						Spec. 7 marine	m	-
Spec8m						Spec. 8 marine	m	-
SpecX					0	Spec. X		-
StauAlp	1	1	1	1	2	***Staurosira alpestris***		FR002B

Table 5 (continued)

New code (this paper)	A LN	A SG	A BK	B	C	New name of taxon or species complex		Old code (Jones et al., 1993; Jones & Juggins, 1995)
StauCirc	0	1	0	0	1	***Staurosira* cf. *circula***		FR018A
StauPho1	0	0	0	1	1	*Staurophora* sp. 1		-
StaurPin	1	1	1	1	2	***Staurosirella pinnata***		FR001A
StaurVen	0	1	0	0	1	***Staurosira* cf. *venter***		FR002C
StfrIner	1	1	1	1	2	***Stauroforma inermis***		FR005D
StnsAcid	1	1	1	1	2	***Stauroneis* aff. *acidoclinata***		SA006A
StnsHusv	1				0	***Stauroneis husvikensis***		-
StnsLati	1	1	1	1	2	***Stauroneis latistauros***		ZZZ996
StnsSubr	1	1	1	1	2	***Stauroneis* cf. *subgracilior* species complex (including 4 forms)**		SA001A + AC032A
SuriSpp	1	1	0	0	1	***Surirella* sp. 1**		SU9999
SY9999	1	0	0	0	1	*Synedra* sp.		SY9999
SydroSpp	0	0	0	1	1	*Synedropsis* spp.		-
SydroSpp						*Synedropsis* spp. (*S.* cf. *fragilis* + *S.* sp. 2, 3, 5)	m	-
SynKerg	0	0	0	1	1	*Synedra* cf. *kerguelensis*		-
SynKerg1	0	0	0	1	1	*Synedra* cf. *kerguelensis* var. 1		-
SynRumSL	1	1	1	1	2	*Synedra rumpens* s.l. (containing: ***Fragilaria capucina* var. *capucina* s.l.**)		SY002A + FR9986
UN9997	1	0	0	0	1	plankton		UN9997
UN9998	1	1	0	0	1	unknown *naviculaceae*		UN9998
UN9999	1	1	0	0	1	unknown		UN9999
ZZZ951	1	0	0	0	1	*Navicula* cf. *vertebrae* 1		ZZZ951
ZZZ956	1	0	0	0	1	*Navicula* spp. 1 GP		ZZZ956
ZZZ958	1	0	0	0	1	*Fragilariopsis* sp.		ZZZ958
ZZZ961Na	1	0	0	0	1	*Navicula* spp. 1 Devil's		ZZZ961
ZZZ963	0	1	0	0	1	*Navicula* sp.1 krob		ZZZ963
ZZZ964	1	1	0	0	1	*Nitzschia frustulum/perminuta* or *Navicula* sp. 1 Tran		ZZZ964
ZZZ965	0	1	0	0	1	*Amphora* spp. 2		ZZZ965
ZZZ969	0	1	0	0	1	*Achnanthes* spp. 1 or *Gomph* spp. 2		ZZZ969
ZZZ972	1	0	0	0	1	*Achnanthes* cf. *abundans*		ZZZ972
ZZZ980	0	1	0	0	1	*Navicula* cf. *dificilima*		ZZZ980
ZZZ990	0	1	0	0	1	*Navicula* sp. 1 Pumphouse		ZZZ990
ZZZ998	0	1	0	0	1	Spp.		ZZZ998

References

Armand L., Crosta X., Romero O., Pichon J.J. 2005. The biogeography of major diatom taxa in Southern Ocean sediments. 1. Sea ice related species. Palaeogeography, Palaeoclimatology, Palaeoecology. 223: 93-126.

Battarbee R.W., Kneen M. 1982. The use of electronically counted microspheres in absolute diatom analysis. Limnology and Oceanography. 27: 184-188.

Berkman P.A., Andrews J.T., Björck S., Colhoun E.A., Emslie S.D., Goodwin I.D., Hall B.L., Hart C.P., Hirakawa K., Igarashi A., Ingólfsson O., López-Martínez J., Lyons W.B., Mabin M.C.G., Quilty P.G., Taviani M., Yoshida Y. 1998. Circum-Antarctic coastal environmental shifts during the Late Quaternary reflected by emerged marine deposits. Antarctic Science. 10 (3): 345-362.

Birks H.J.B. 1998. Numerical tools in palaeolimnology – progress, potentialities, and problems. Journal of Paleolimnology. 20: 307-332.

Buffen A., Leventer A., Rubin A., Hutchins T. 2007. Diatom assemblages in surface sediments of the northwestern Weddell Sea, Antarctic Peninsula. Marine Micropaleontology. 62: 7-30.

Butler H.G. 1999. Seasonal dynamics of the planktonic microbial community in a maritime Antarctic lake undergoing eutrophication. Journal of plankton research. 21: 2393-2419.

Bibby J.S. 1966. The stratigraphy of part of north-east Graham Land and the James Ross Island Group. British Antarctic Survey, Scientific Reports. 53: 1-37.

Björck S., Håkansson H., Zale R., Karlen W., Jönsson BL. 1991. A late Holocene lake sediment sequence from Livingston Island, South Shetland Islands, with palaeoclimatic implications. Antarctic Science. 3 (1): 61-72.

Björck S., Olsson S., Ellis-Evans C., Håkansson H., Humlum O., de Lirio J.M. 1996. Late Holocene palaeoclimatic records from lake sediments on James Ross Island, Antarctica. Palaeogeography, Palaeoclimatology, Palaeoecology. 121: 195-220.

Brachfeld S.A., Domack E.W., Kissel C., Laj C., Leventer A., Ishman S.E., Gilbert R., Camerlenghi A., Eglinton L.B. 2003. Holocene History of the Larsen-A Ice Shelf Constrained by Geomagnetic Paleointensity Dating. Geology. 31: 749-752.

Cook A.J., Fox A.J., Vaughan D.G., Ferrigno J.G. 2005. Retreating glacier fronts on the Antarctic Peninsula over the past half-century. Science. 308: 541-544.

Cremer H., Roberts D., McMinn A., Gore D., Melles M. 2003. The Holocene diatom flora of marine bays in the Windmill Islands, East Antarctica. Botanica Marina. 43: 82-106.

Cremer H., Gore D., Hultzsch N., Melles M., Wagner B. 2004. The Diatom Flora and Limnology of Lakes in the Amery Oasis, East Antarctica. Polar Biology. 27: 513-531.

Crosta X., Romero O., Armand L., Pichon J.J. 2005. The biogeography of major diatom taxa in Southern Ocean sediments. 2. Open Ocean related species. Palaeogeography, Palaeoclimatology, Palaeoecology. 223: 66-92.

Crosta X., Denis D., Ther O. 2008. Sea ice seasonality during the Holocene, Adélie Land, East Antarctica. Marine Micropaleontology. 66: 222-232.

De Angelis H., Skvarca P. 2003. Glacier Surge After Ice Shelf Collapse. Science. 299: 1560-1562.

Dean W.E. 1974. Determination of Carbonate and Organic-Matter in Calcareous Sediments and Sedimentary-Rocks by Loss on Ignition - Comparison With Other Methods. Journal of Sedimentary Petrology. 44: 242-248.

Douglas M.S.V., Smol J.P. 1995. Paleolimnological significance of observed distribution patterns of chrysophyte cysts in Arctic pond environments. Journal of Paleolimnology. 13: 1-5.

Douglas M.S.V., Smol J.P. 2001. Siliceous protozoan plates and scales. Chapter 13. In: Smol J.P., Birks H.J.B., Last W.M. (Eds.). Tracking Environmental Change Using Lake Sediments. Vol. 3: Terrestrial, Algal, and Siliceous Indicators. Kluwer Academic Publishers, Dordrecht, The Netherlands: 265-279.

Eggermont H., Heiri O., Verschuren D. 2006. Subfossil Chironomidae (Insecta: Diptera) as quantitative indicators for past salinity variation in African lakes. Quaternary Science Reviews. 25: 1966-1994.

Ellis-Evans J.C. 1981. Freshwater microbiology in the Antarctic: II. Microbial numbers and activity in nutrient-enriched Heywood Lake, Signy Island. British Antarctic Survey Bulletin. 54: 105-121.

Ellis-Evans J.C. 1984. Methane in Maritime Antarctic freshwater lakes. Polar Biology. 3: 63-71.

Ellis-Evans J.C. 1985. Decomposition processes in Maritime Antarctic Lakes. . In: Siegfried W.R., Condy P.R., Laws R.M., Antarctic nutrient cycles and food webs. Springer-Verlag Berlin, Heidelberg.

Ellis-Evans J.C. 1991. Numbers and activity of bacterio- and phytoplankton in contrasting maritime Antarctic lakes. Verhandlungen des Internationalen Verein Limnologie. 24: 1149-1154.

Ellis-Evans J.C., Wynn-Williams D.D. 1985. The interaction of soil and lake microflora at Signy Island. In: Siegfried W.R., Condy P.R., Laws R.M., Antarctic nutrient cycles and food webs. Springer-Verlag Berlin, Heidelberg.

Gersonde R., Zielinski U. 2000. The reconstruction of late Quaternary Antarctic sea-ice distribution – The use of diatoms as a proxy for sea-ice. Palaeogeography, Palaeoclimatology, Palaeoecology. 162: 263-286.

Gibson J.A.E., Zale R. 2006. Holocene Development of the Fauna of Lake Boeckella, Northern Antarctic Peninsula. Holocene. 16: 625-634.

Gremmen N.J.M., Van de Vijver B., Frenot Y., Lebouvier M. 2007. Distribution of moss-inhabiting diatoms along the altitudinal gradient at sub-Antarctic Iles Kerguelen. Antarctic Science. 19: 17-24.

Grimm E.C. 1987. Coniss - a Fortran-77 Program for Stratigraphically Constrained Cluster-Analysis by the Method of Incremental Sum of Squares. Computers & Geosciences. 13: 13-35.

Grimm E.C. 1991-1993. Tilia 2.0 Version b.4 and TiliaGraph, Ilinois State Museum, Springfield, Ilinois.

Grimm E.C. 2004. TGView Version 2.0.2., Illinois State Museum, Springfield, Ilinois.

Hawes I. 1985. Factors controlling phytoplankton populations in Maritime Antarctic lakes. In: Siegfried W.R., Condy P.R., Laws R.M. Antarctic nutrient cycles and food webs. Springer-Verlag Berlin, Heidelberg.

Hobbs G.J. 1968. The geology of the South Shetland Islands. IV. The Geology of Livingston Island. British Antarctic Survey Scientific Reports. 47: 34 pp.

Hodgson D.A., Convey P. 2005. A 7000-year Record of Oribatid Mite Communities on a Maritime-Antarctic Island: Responses to Climate Change. Arctic, Antarctic, and Alpine Research. 37 (2): 239-245.

Hodgson D.A., Roberts S.J., Verleyen E., Vyverman W., Lole A. 2005a. Field report – Sledge Uniform 2005-2006. Project: Natural climate variability – extending the Americas palaeoclimate transect through the Antarctic Peninsula to the pole (CACHE-PEP). Ref n°: R/2005/NT3.

Hodgson D.A., Verleyen E., Sabbe K., Squier A.H., Keely B.J., Leng M.J., Saunders K.M., Vyverman W. 2005b. Late Quaternary climate-driven environmental change in the Larsemann Hills, East Antarctica, multi-proxy evidence from a lake sediment core. Quaternary Research. 64: 83-99.

Hodgson D.A., Roberts D., McMinn A., Verleyen E., Terry B., Corbett C., Vyverman W. 2006. Recent rapid salinity rise in three East Antarctic lakes. Journal of Paleolimnology. 18: 385-406.

Houghton J.T., Ding Y., Griggs D.J., Noguer M., van der Linden P.J., Dai X., Maskell K., Johnson C.A., Eds. 2001. Climate Change 2001: The Scientific Basis. Contribution of Working Group I to the Third Assessment Re;ort of the Intergovernmental Panel on Climate Change. New York, Cambridge University Press.

Hughen K.A., Baillie M.G.L., Bard E., Beck J.W., Bertrand C.J.H., Blackwell P.G., Buck C.E., Burr G.S., Cutler K.B., Damon P.E., Edwards R.L., Fairbanks R.G., Friedrich M., Guilderson T.P., Kromer B., McCormac G., Manning S., Ramsey C.B., Reimer P.J., Reimer R.W., Remmele S., Southon J.R., Stuiver M., Talamo S., Taylor F.W., Van Der Plicht, J., Weyhenmeyer C.E. 2004. Marine04 Marine Radiocarbon Age Calibration, 0-26 cal. kyr BP. Radiocarbon. 46: 1059-1086.

Jeffrey S.W., Mantoura R.F.C., Bjornland T. 1997. Data for the identification of 47 key phytoplankton pigments. In: Jeffrey SW, Mantoura RFC, Wright SW (Eds.): Phytoplankton pigments in oceanography, guidelines to modern methods. Monographs on oceanographic methodology (SCOR), 10, UNESCO Publishing: 447-554.

Jones V., Juggins S, Ellis-Evans JC. 1993. The relationship between water chemistry and surface sediment diatom assemblages in maritime Antarctic lakes. Antarctic Science. 5 (4): 339-348.

Jones V., Juggins S. 1995. The construction of a diatom-based chlorophyll *a* transfer function and its application at three lakes on Signy Island (maritime Antarctic) subject to differing degrees of nutrient enrichment. Freshwater biology. 34: 433-445.

Jones V.J., Hodgson D.A., Chepstow-Lusty A. 2000. Palaeolimnological evidence for marked Holocene environmental changes on Signy Island, Antarctica. The Holocene. 10 (1): 43-60.

Jones V.J., Birks H.J.B. 2004. Lake-sediment records of recent environmental change on Svalbard: results of diatom analysis. Journal of Paleolimnology. 31: 445-466.

Jongman R.H.G., ter Braak C.J.F., van Tongeren O.F.R. 1995. Data analysis in community and landscape ecology. Cambridge University Press, Cambridge. 299 pp.

Juggins S. 2003-2007 C2 data analysis Version 1.5.1, University of Newcastle.

Kang S.H., Fryxell G.A. 1993. Phytoplankton in the Weddell Sea, Antarctica – composition, abundance and distribution in water-column assemblages of the marginal ice-edge zone during austral autumn. Marine Biology. 116 (2): 335-348.

Kumke T., Kienel U., Weckstrom J., Korhola A., Hubberten H.W. 2004. Inferred Holocene paleotemperatures from diatoms at Lake Lama, Central Siberia. Arctic Antarctic and Alpine Research. 36: 624-634.

Leavitt P.R., Hodgson D.A. 2001. Sedimentary pigments. In Smol JP & Last WS (Eds): Developments in palaeoenvironmental research, v. 3: Tracking environmental changes using lake sediments, biological techniques and indicators. Kluwer: 295-325.

Lewis S.R. 1994. Vascular plants as bioindicators of regional warming in Antarctica. Oecologia. 99: 322-328.

Lim D.S.S., Smol J.P., Douglas M.S.V. 2007. Diatom assemblages and their relationships to lakewater nitrogen levels and other limnological variables from 36 lakes and ponds on Banks Island, N.W.T., Canadian Arctic. Hydrobiologia. 586: 191-211.

Lim D.S.S., Smol J.P., Douglas M.S.V. 2008. Recent environmental changes on Banks Island (N.W.T., Canadian Arctic) quantified using fossil diatom assemblages. Journal of Paleolimnology. 40: 385-398.

Liu X.D., Li H.C., Sun L.G., Yin X.B., Zhao S.P., Wang Y.H. 2006. d13C and d15N in the ornithogenic sediments from the Antarctic maritime as palaeoecological proxies during the past 2000 yr. Earth and Planetary Science Letters. 243: 424-438.

Lyons W.B., Laybourn-Parry J., Welch K.A., Priscu J.C. 2006. Antarctic lake systems and climate change. Chapter 13. In: Bergstrom D.M., Convey P., Huiskes H.L. (Eds.). Trends in Antarctic terrestrial and limnetic ecosystems. Springer, Dordrecht, The Netherlands: 273-295.

Matthews D.H., Malling D.H. 1967. The geology of the South Orkney Islands. I. Signy Island. Scientific Report Falkland Islands Dependencies Survey. 25: 32 pp.

Pearce D.A., van der Gast C.J., Woodward K., Newsham K.K. 2005. Significant changes in the bacterioplankton community structure of a maritime Antarctic freshwater lake following nutrient enrichment. Microbiology. 151. 3237-3248.

Peel D.A. 1992. Spatial temperature and accumulation rate variations in the Antarctic Peninsula. In: Morris EM (Ed.), The contribution of Antarctic Peninsula ice to sea level rise. British Antarctic Survey Ice & Climate Special Report 1: 11-15.

Pudsey C.J., Evans J. 2001. First survey of Antarctic sub-ice shelf sediments reveals mid-Holocene ice shelf retreat. Geology. 29 (9): 787-790.

Quayle W.C., Peck L.S., Peat H., Ellis-Evans J.C., Harrigan P.R. 2002. Extreme responses to climate change in Antarctic lakes. Science. 295: 645-645.

Reimer P.J., Baillie M.G.L., Bard E., Bayliss A., Beck J.W., Bertrand C., Blackwell P.G., Buck C.E., Burr G., Cutler K.B., Damon P.E., Edwards R.L., Fairbanks R.G., Friedrich M., Guilderson T.P., Hughen K.A., Kromer B., McCormac F.G., Manning S., Bronk Ramsey C., Reimer R.W., Remmele S., Southon J.R., Stuiver M., Talamo S., Taylor F.W., van der Plicht J., Weyhenmeyer C.E. 2004. Radiocarbon. 46: 1029-1058.

Renberg I. 1990. A procedure for preparing large sets of diatom slides from sediment cores. Journal of Paleolimnology. 4: 87-90.

Riaux-Gobin C., Poulin M. 2004. Possible symbiosis of *Berkeleya adeliensis* Medlin, *Synedropsis fragilis* (Manguin) Hasle et al. and *Nitzschia lecointei* Van Heurck (Bacillariophyta) associated with land-fast ice in Adelie Land, Antarctica. Diatom Research. 19: 265-274.

Roberts D., McMinn A. 1999. Diatoms of the saline lakes of the Vestfold Hills, Antarctica. Bibliotheca Diatomologica. Band 44: 82 pp.

Roberts D., McMinn A., Cremer H., Gore D.B., Melles M. 2004. The Holocene evolution oand palaeosalinity history of Beall Lake, Windmill Islands (East Antarctica) using an expanded diatom-based weighted averaging model. Palaeogeography, Palaeoclimatology, Palaeoecology. 208: 121-140.

Roberts S.J., Hodgson D.A., Bentley M.J., Smith J.A., Millar I.L., Olive V., Sugden D.E. 2008. The Holocene history of George VI Ice Shelf, Antarctic Peninsula from clast-provenance analysis of epishelf lake sediments. Palaeogeography, Palaeoclimatology, Palaeoecology. 259: 258-283.

Robin G. de Q., Adie R.J. 1964. The ice cover. Chapter 8. In: Priestley R., Adie R.J., Robin G. de Q. (Eds.). Antarctic Research. London, Butterworths: 100-117.

Saunders K.M., Hodgson D.A., McMinn, A. 2008. Quantitative relationships between benthic diatom assemblages and water chemistry in Macquarie Island lakes and their potential for reconstructing past environmental changes. Antarctic Science. doi: 10.1017/S0954102008001442.

Sabbe K., Hodgson D.A., Verleyen E., Taton A., Wilmotte A., Vanhoutte K., Vyverman W.G. 2004. Salinity, depth and the structure and composition of microbial mats in continental Antarctic lakes. Freshwater Biology. 49: 296-319.

Scambos T., Hulbe C., Fahnestock M. 2003. Climate-Induced Ice Shelf Disintegration in the Antarctic Peninsula. Antarctic Peninsula Climate Variability: Historical and Paleoenvironmental Perspectives, 79, 79-92. International Workshop on Antarctic Peninsula Climate Variability, Date: APR, 2002 Hamilton Coll Clinton NY.

Scambos T.A., Bohlander J.A., Shuman C.A., Skvarca P. 2004. Glacier acceleration and thinning after ice shelf collapse in the Larsen B embayment, Antarctica. Geophysical research letters. 31 (18): Article number L18402.

Smith J.A., Bentley M.J., Hodgson D.A., Roberts S.J., Leng M.J., Lloyd J.M., Barrett M.S., Bryant C., Sugden D.E. 2007. Oceanic and Atmospheric Forcing of Early Holocene Ice Shelf Retreat, George Vi Ice Shelf, Antarctica Peninsula. Quaternary Science Reviews. 26: 500-516.

Smith H.G. 1992. Distribution and ecology of the testate rhizopod fauna of the continental Antarctic zone. Polar Biology. 12: 629-634.

Smith R.I.L. 1972. Vegetation of the South Orkney Islands with particular reference to Signy Island. Scientific Report of the British Antarctic Survey. 68: 1-124.

Smol J.P. 1983. Paleophycology of a high arctic lake near Cape Herschel, Ellesmere Island. Canadian Journal of Botany. 61: 2195-2204.

Smol J.P. 1988. Chrysophycean microfossils in paleolimnological studies. Palaeogeography, Palaeoclimatology, Palaeoecology. 62: 287-297.

Squier A.H., Hodgson D.A., Keely B.J. 2002. Sedimentary Pigments as Markers for Environmental Change in an Antarctic Lake. Organic Geochemistry. 33: 1655-1665.

Squier A.H., Hodgson D.A., Keely B.J. 2004. A Critical Assessment of the Analysis and Distributions of Scytonemin and Related Uv Screening Pigments in Sediments. Organic Geochemistry. 35: 1221-1228.

Stuiver M., Reimer P.J. 1993. Extended C-14 Data-Base and Revised Calib 3.0 C-14 Age Calibration Program. Radiocarbon. 35: 215-230.

Sugden D.E. 1982. Arctic and Antarctic: a modern geographical synthesis. Oxford: Basil Blackwell. 472 pp.

ter Braak C.J.F., Prentice I.C. 1988. A theory of gradient analysis. Advances in Ecological Research. 18: 271-317.

ter Braak C.J.F., Smilauer P. 2002. CANOCO for Windows 4.5., Biometris – Plant Research International, Wageningen, The Netherlands.

Tolonen K. 1985. Rhizopod analysis. In: Berglund B.E. (Ed.). Handbook of Holocene Palaeoecology and Palaeohydrology. J. Wiley & Sons, New York: 645-666.

Underwood G.J.C., Povot L. 2000. Determining the environmental preferences of four estuarine epipelic diatom taxa: growth across a range of salinity, nitrate and ammonium conditions. European Journal of Phycology. 35: 173-182.

Van de Vijver B., Beyens L. 1997. The epiphytic diatom flora of mosses from Stromness Bay area, South Georgia. Polar Biology. 17: 492-501.

Van de Vijver B., Ledeganck P., Beyens L. 2002. Soil diatom communities from Ile de la Possession (Crozet, sub-Antarctica). Polar Biology. 25: 721-729.

Van de Vijver B., Gremmen N., Smith V. 2008. Diatom communities from the sub-Antarctic Prince Edward Islands: diversity and distribution patterns. Polar Biology. 31 (7): 795-808.

Vaughan D.G., Marshall G.J., Connolley W.M., Parkinson C., Mulvaney R., Hodgson D.A., King J.C., Pudsey C.J., Turner J. 2003. Recent Rapid Regional Climate Warming on the Antarctic Peninsula. Climatic Change. 60: 243-274.

Vaughan D.G. 2006. Recent trends in melting conditions on the Antarctic Peninsula and their implications for ice-sheet mass balance and sea level. Arctic, Antarctic and Alpine Research. 38 (1). 147-152.

Verleyen E., Hodgson D.A., Vyverman W.G., Roberts D., McMinn A., Vanhoutte K., Sabbe K. 2003. Modelling diatom responses to climate induced fluctuations in the moisture balance in continental Antarctic lakes. Journal of Paleolimnology. 30: 195-215.

Verleyen E., Hodgson D.A., Leavitt P.R., Sabbe K., Vyverman W. 2004a. Quantifying habitat-specific diatom production: a critical assessment using morphological and biogeochemical markers in Antarctic marine and lake sediments. Limnology & Oceanography. 49 (5): 1528-1539.

Verleyen E., Hodgson D.A., Sabbe K., Vanhoutte K., Vyverman W. 2004b. Coastal oceanographic conditions in the Prydz Bay region (East Antarctica) during the Holocene recorded in an isolation basin. The Holocene. 14 (2): 246-257.

Verleyen E., Hodgson D.A., Sabbe K., Vyverman W. 2004c. Late Quaternary deglaciation and climate history of the Larsemann Hills (East Antarctica). Journal of Quaternary Science. 19(4): 361-375.

Vincke S., Van de Vijver B., Gremmen N., Beyens L. 2006. The moss dwelling testacean fauna of the Stromness Bay (South Georgia). Acta Protozoologica. 45: 65-75.

Walther G.-R., Post E., Convey P., Menzel A., Parmesan C., Beebee T.J.C., Fromentin J.-M., Hoegh-Guldberg O., Barlein, F. 2002. Ecological responses to recent climate change. Nature. 416: 389-395.

Whitehead J.M., McMinn A. 1997. Paleodepth determination from Antarctic benthic diatom assemblages. Marine Micropaleontology. 29 (3-4): 301-318.

Wright H.E. 1967. A square-rod piston sampler for lake sediments. Journal of Sedimentary Petrology. 37: 976.

Wright S., Jeffrey S., Mantoura R., Llewellyn C., Bjornland T., Repeta D., Welschmeyer N. 1991. Improved HPLC method for the analysis of chlorophylls and carotenoids from marine phytoplankton. Marine Ecology Progress Series. 77: 183-196.

Zacher K., Hanelt D., Wiencke C., Wulff A. 2007. Grazing and UV radiation effects on an Antarctic intertidal microalgal assemblage: a long-term field study. Polar Biology. 30: 1203-1212.

Zeeb B.A., Smol J.P. 2001. Chrysophyte scales and cysts. (Chapter 9) In: Smol J.P., Birks H.J.B., Last W.M. (Eds.). 2001. Tracking Environmental Change Using Lake Sediments. Vol. 3: Terrestrial, Algal and Siliceous Indicators. Kluwer Academic Publishers, Dordrecht, The Netherlands: 203-223.

Zale R. 1994. Changes in Size of the Hope Bay Adelie Penguin Rookery as Inferred From Lake Boeckella Sediment. Ecography. 17: 297-304.

Chapter 7

Deglaciation history and Holocene climate dynamics to the North of Prince Gustav Channel, northeastern Antarctic Peninsula

Mieke Sterken, Stephen J. Roberts, Dominic A. Hodgson, Wim Vyverman, Andrea Balbo, Koen Sabbe, S. Moreton, Elie Verleyen

Abstract

The Antarctic Peninsula is one of the most rapidly warming regions on Earth, as evidenced by a recession of sea-ice, snowfields and glaciers and by the retreat and collapse of ice shelves. Despite this, only a limited number of well-dated shallow marine and lake sediment based climate records exist from the region. Here we reconstruct the deglaciation history and changes in sea-ice and climate using sedimentological proxies, diatoms and fossil pigments in a sediment core collected from an isolation basin on Beak Island (Prince Gustav Channel, NE Antarctic Peninsula). The onset of marine sedimentation at c. 10.6 cal. ka BP provides a minimum age for deglaciation. Conditions remained cold and perennial sea-ice persisted in this part of Prince Gustav Channel until c. 9.2 cal. ka BP when a transition took place from near perennial sea-ice cover and high iceberg concentrations, to a seasonally open marine environment until at least 6.6 cal. ka BP. The isolation of the lake prevents paleoclimate reconstructions to be made for the period between c. 6.6 and 6 ka BP. Between c. 6 and 3.5 ka BP relatively cold climate conditions on land prevail as reflected in low primary productivity levels. Between c. 3.5 and 1.7 cal. ka BP, a wetter and milder climate likely resulted in higher organic sedimentation rates and a well-developed planktonic community, which we link to the Mid-Holocene Hypsithermal (MHH) previously recorded elsewhere in the north and northeastern Antarctic Peninsula. This warm period occurs slightly later than a warm period near the western margin of the Antarctic Peninsula, which might point to different forcing and/or mechanisms being present in the different regions. Neoglacial cooling is evident from c. 1.7 cal. ka BP onwards, which is interrupted by an increase in primary productivity and a shift in diatom diversity and species composition in the uppermost core sections, likely related to the recent temperature rise recorded in several regions of the Antarctic Peninsula.

This chapter is a manuscript in preparation

Contribution of the author: d*iatom microscopy, partly constructing age-depth model, interpretation, statistical analyses, writing largest part of the paper.*

7.1. Introduction

The Antarctic Peninsula (AP) is particularly sensitive to climate change. Currently it is one of the most rapidly warming regions on Earth, with temperatures rising at six times the global mean (0.6±0.2°C) during the 20th century (Vaughan et al., 2003; Houghton et al., 2001). This warming has resulted in the recent recession of snowfields and glaciers (Cook et al., 2005), a reduction in the duration of sea-ice cover (Parkinson, 2002) and the retreat and collapse of ice shelves (e.g. Vaughan & Doake, 1996; Rott et al., 1998; Scambos et al., 2003); the latter causing increased flow velocities of feeder glaciers upstream of the ice shelves (De Angelis and Skvarca, 2003; Scambos et al., 2004).

In order to better understand the longer-term context of these anomalies, ice, marine and, lake sediment cores together with geomorphological evidence are being used to reconstruct changes in ice and climate throughout the Holocene. To date, most ice cores from the AP region have spanned only a few thousand years, although new records extracted from the Detroit Plateau and James Ross Island will cover the full Holocene (e.g. Simoes et al., 2008). Investigations of the deglaciation of the Antarctic Peninsula Ice Sheet (APIS) from its Last Glacial Maximum (LGM) limits and Holocene climate evolution have largely concentrated on marine sediment cores, for example in Marguerite Bay (Ó Cofaigh et al., 2005), Lallemand Fjord (Taylor et al., 2001), Bismark Strait (Domack et al., 2001; Shevenell et al., 1996; Brachfeld et al., 2002; Leventer et al., 2002) and Bransfield Strait (e.g. Banfield & Anderson, 1995; Barcena et al., 1998). On land, records have been derived from lake sediment records, for example from Alexander Island (Bentley et al., 2005; Smith et al., 2007; Roberts et al., 2008; subm.; Hjort et al., 2001), Horseshoe Island (Wasell & Håkanson, 1992), the western and northern islands of the Antarctic Peninsula (e.g. the South Shetland Islands (Björck et al., 1991; 1993; 1996), James Ross Island (e.g. Björck et al., 1996), and the South Orkney Islands (Jones et al., 2000; Hodgson and Convey, 2005). Well dated terrestrial and shallow marine records spanning the entire Holocene are however still rare. This is particularly the case for the northeastern margin of the AP, the Weddell Sea region, and the eastern margin of the AP south of the South Shetland Islands (Bentley et al., 2009; Hodgson et al., in press).

Although the pattern of deglaciation of the APIS since the LGM, and Holocene environmental and climate changes are poorly constrained, some recent attempts have been made to formulate a 'regional consensus' (e.g. Hjort et al., 2003; Hodgson et al., in press; Bentley et al., 2009). The retreat of the APIS (~18,000 cal. yr. BP) from the shelf

occurred progressively from the outer to the inner continental shelf regions, and from north to south (Heroy & Anderson, 2005; Heroy et al., 2007). By ~10,000 cal. yr. BP the APIS grounding line reached the inner shelf, but the retreat was diachronous and not well spatially constrained (Hodgson et al., in press). Ice core records from the central plateau (Masson-Delmotte et al., 2006) record an Early Holocene warm optimum (between 11 and 9.5 ka BP), which coincided with this continued deglaciation. Interestingly, at the same time relatively cold conditions are recorded in Palmer Deep (Western AP) (e.g. Sjunneskog & Taylor, 2002; Domack, 2002). The period following the Early Holocene optimum shows complex patterns, with differences in timing and duration of warm periods and events (including ice shelf collapse) between different regions (Bentley et al., 2009). This period of contrasting climate patterns is followed by the Mid-Holocene Hypsithermal (MHH), which is observed in ice cores and marine and lake sediment records and can be roughly placed somewhere in the period between 4.8 ka BP and 1.5 ka BP although dating problems prevent detailed comparison of records from different regions. Following the MHH a 'neoglacial' cooling is observed in several records, coincident with the reformation of ice shelves near the eastern margin of the AP (e.g. Pudsey et al., 2006; Brachfeld et al., 2003) and a temperature related decline in lacustrine primary productivity North of the AP (e.g. Hodgson & Convey, 2005). To date, the number of records from the AP is clearly too scarce to make good comparisons of Holocene climate between both margins of the AP and between other regions in the high latitudes of the Southern Hemisphere.

In this paper, we analyse the record of paleoenvironmental change from shallow marine and lake sediments deposited in a lake basin on Beak Island, northern Prince Gustav Channel (Figs. 1, 2). We integrate sedimentological, fossil diatom and pigment analyses to reconstruct changes in marine and freshwater environments, and as such to identify the glaciological and paleoclimate events occurring there during the Holocene.

7.2. Site description

Beak Island (63°36'S, 57°20'S) is a partially emerged periphery of an inactive volcanic caldera situated in Prince Gustav Channel between Vega Island and the Tabarin Peninsula (Figs. 1, 2a). The island is composed of Miocene volcanic rocks, mainly porphyritic basalt, hyaloclastites and pillow lavas, belonging to the James Ross Volcanic Island group (Bibby, 1966). Beak Island is currently free of permanent snow fields, ice

caps or glaciers, and is assumed to have the same continental climate regime as James Ross Island (50 km to the southwest), typified by negative mean monthly temperatures (Björck et al., 1996). The regional climate is influenced by (1) the Westerly storm tracks bringing humid, warm air from northwest, or (2) the cold barrier winds bringing arid air-masses from south and southwest (i.e. the Weddell Sea) (Björck et al., 1996). The region is influenced by the rain shadow effect of the Antarctic Peninsula mountains (Sugden, 1982). Snowfall periodically occurs during summer, followed by rapid melting and long dry periods.

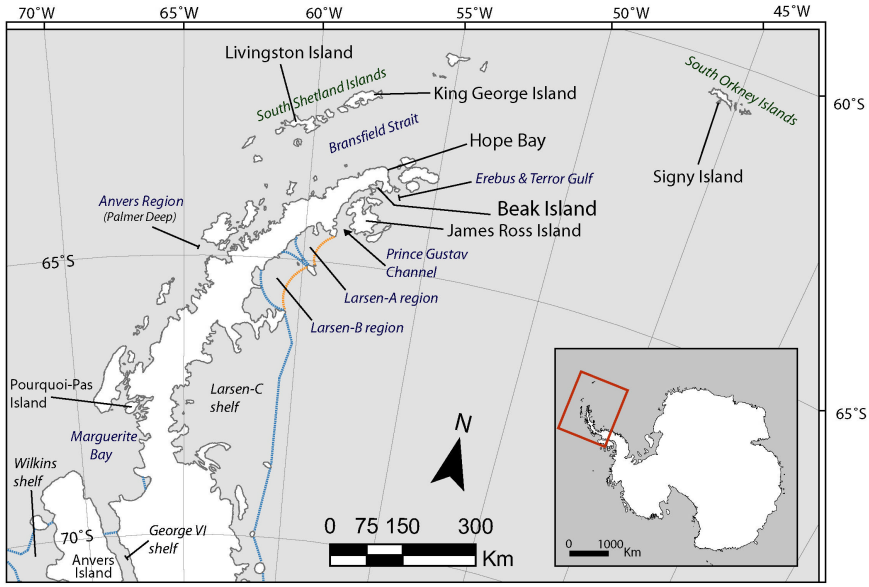

Figure 1: Map of the northern tip of the Antarctic Peninsula, showing Beak Island north of James Ross Island, and some locations mentioned in the text.

Several lakes and pools occur on the island (Fig. 2a,b). Beak-1, the largest and deepest lake with a diameter of c. 400 m is most likely a depression created by a secondary eruption vent. It is flanked by a rock cliff (higher than 10 m) at 200 m to the west, and is bordered by periglacially patterned ground to the north and east. Moss banks occur on the (north)western shores of the lake, and are dissected by a series of small, braided meltwater streams emanating from a snowbank on the adjacent slope. It has one outflow to the southwest. The outlet, which is vegetated by thick orange and green microbial mats, was nearly inactive at the time of sampling (January 2006). The lake remains ice covered for 8-9 months per year.

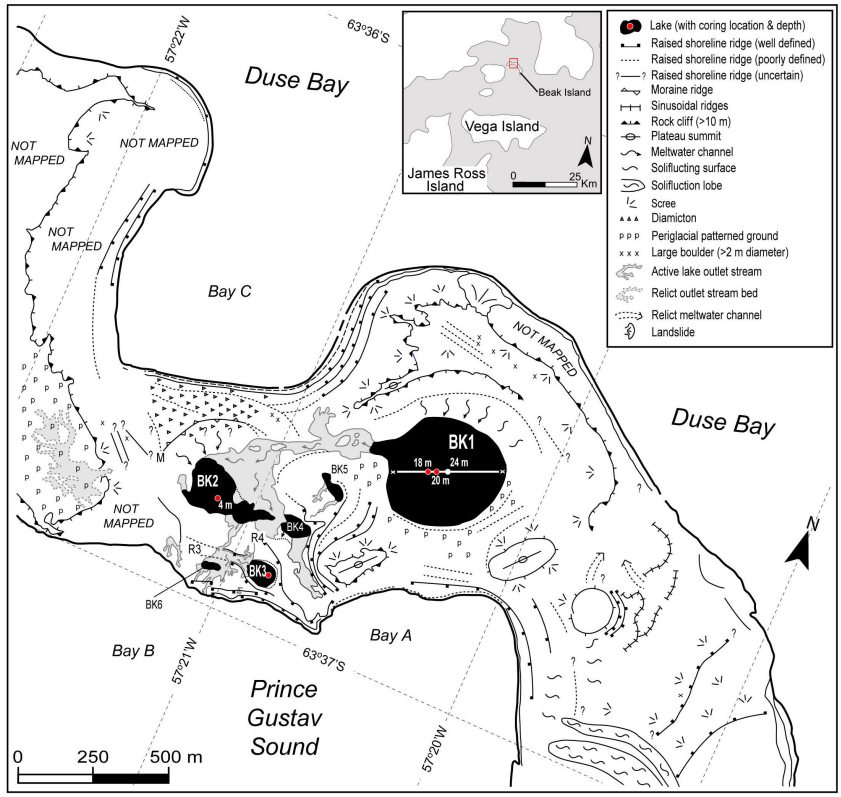

Figure 2a: Map of Beak Island showing the study site and the position of the lake sediment core.

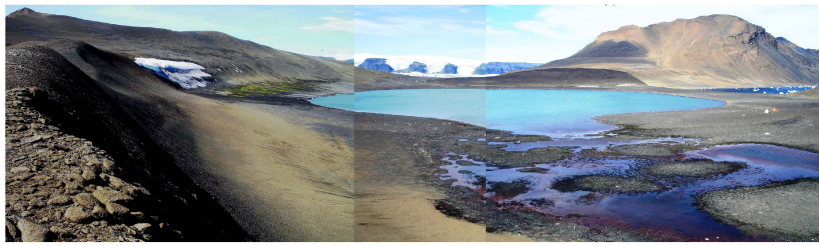

Figure 2b: View on Lake Beak-1 from the west, looking towards the northeast (Picture: W. Vyverman).

7.3. Methods

7.3.1. Lake surveying, limnology and coring

The sill height of the lake was measured using a Trimble GPS system. Water depth and bathymetric cross sections were measured using a hand-held echo sounder deployed at fixed positions along a static line. Surface and vertical profiles of lake water conductivity, temperature and oxygen saturation were measured using a YSI MDS 600 water quality meter. Water samples were collected in acid-washed Nalgene bottles. 125 ml was collected for ion chemistry and 125 ml was filtered for nutrient analysis.

Cores were taken at 20 m depth rather than the deepest point of the lake at 25 m because the maximum length of the coring rods was 22 m. A Livingstone corer (Wright, 1967) was used to retrieve both surface and deeper sediments, as a 5 cm thick layer of moss prevented the UWITEC gravity corer penetrating the surface sediments. The principal cores from the lake (BK 1E and BK 1D) were sectioned at 0.5 cm resolution in the field. The samples were sealed in sterile Whirlpack bags and stored at –20°C for transport to the UK. A duplicate 100 cm long core (BK1G) was extracted from 20 m depth and two shorter cores were extracted from 18 m depth and retained intact for high resolution, non-destructive measurements.

7.3.2. Stratigraphy and sedimentary properties

The cores were photographed, macroscopically described, and analysed for wet density, dry weight, % weight loss on ignition (LOI_{550}, after combustion at 550°C for two hours) and % carbonate composition (LOI_{950}; % weight loss after combustion at 950°C for two hours) (Dean, 1974). LOI_{550} will serve as a proxy for primary productivity, given the assumption of nearly constant sedimentation rates, which has recently been shown to vary in response to climate warming in Maritime Antarctic lakes (Quayle et al., 2002). Wet density (g cm^{-3}) and magnetic susceptibility (g^{-1} cm^3) were measured at 1 cm resolution. Wet mass, volume specific magnetic susceptibility was measured using a Bartington 1 ml MS2G sensor.

7.3.3. Geochronology

A chronology was established by accelerated mass spectrometry radiocarbon (AMS ^{14}C) dating of macrofossil remains (moss strands, leaves and organic cyanobacterial mat fragments) and bulk sediments. Dates are reported as conventional radiocarbon years BP (^{14}C BP), and as calibrated years BP (cal. BP relative to AD 1950) using the Intcal

04.14C dataset (Reimer et al., 2004) for freshwater samples, the marine calibration curve (Hughen et al., 2004) for marine samples, and a mixed marine-Intcal 04 curve (50 % marine) for samples at the marine-lacustrine transition (Table 2). For the marine curve a dR was set at 900 years, which corresponds to a reservoir effect of 1300 years (Berkman et al., 1998). All dates were calibrated in the Calib 5.0.1 program (Stuiver & Reimer, 1993).

7.3.4. Siliceous Microfossils

Subsamples of 0.07-0.21 g wet sediment were taken throughout the cores. The samples were weighed, then dried at 60°C for 24 hours, and reweighed to calculate the water content. Samples were oxidized using hydrogen peroxide (see Renberg, 1990). In order to calculate absolute diatom abundances, the samples were spiked with polystyrene microspheres with a known concentration of 6.81×10^6 l^{-1} (Battarbee and Kneen, 1982). The material was mounted in Naphrax® medium (refractive index 1.710). Random fields were scanned at a magnification of 10x100x with an Olympus CX 41 microscope. Species area curves (by noting down the number of species and valves counted after each random view field) were used to evaluate the minimum number of valves to be counted, which was more than 400 valves per sample. Marine diatoms were mainly identified according to Cremer et al., (2003) and Roberts & McMinn (1999). Freshwater diatoms were mainly identified using Sabbe et al. (2003); Cremer et al. (2004); Van de Vijver & Beyens (1997); Patrick & Reimer (1966); Round et al. (1990), Van de Vijver et al. (2002) and Chapters 4 and 5.

The diatom sequence was divided to zones using stratigraphically constrained cluster analysis (CONISS; Grimm, 1987) and plotted using Tilia 2.0.b.4 (Grimm, 1991-1993) and Tilia Graph View version 2.0.2. (Grimm, 2004). Changes in the marine diatom communities were interpreted based on indicator taxa. For example, *Chaetoceros* resting spores are indicative for near ice, meltwater-related, high productive open water conditions, whereas *Fragilariopsis curta*, *F. cylindrus* and *Navicula glaciei* are typical (spring) sea-ice organisms (Armand et al., 2005; Crosta et al., 2008; Whitaker & Richardson, 1980). Changes in the lacustrine diatom communities were interpreted using an existing diatom datasets from Livingston Island (45 lakes, South Shetland Islands; 62°40'S, 61°00'W) and Signy Island (24 lakes, South Orkney Islands; 60°43'S, 45°38'W; Jones et al., 1993), which was extended with six lakes from Beak Island (Chapter 6). A transfer function based on this combined dataset was constructed for the NH_4^+ level, in order to reconstruct changes in nutrient levels, because (1) this variable has

been shown to significantly explain the variation in diatom community structure in Maritime Antarctic lakes, and (2) its concentration is directly related to temperature changes through soil development in the catchment area of the lakes (Quayle et al., 2002; Chapter 6). The diatom-based transfer-function has a jack-knifed R^2 of 0.742 and a root mean square error of prediction (RMSEP) of 0.267 log(x+1) units (Chapter 6).

Apart from diatoms, we also enumerated siliceous cysts of chrysophytes and scales/plates of testate amoebae in core Beak-1. Chrysophyte cysts can be an indicator of low productivity in temperate lakes, but have been correlated with the presence of mosses and/or with lake ice cover in high latitude lakes (Zeeb & Smol, 2001; Douglas & Smol, 1995; Smol, 1983, 1988). Testate amoebae are particularly abundant in moss habitats in sub-Antarctica (Vincke et al., 2006), and are most abundant in acid peats and bogs (Smith, 1992). The scales in our samples were identified according to Douglas & Smol (2001), and most of them probably belong to the genus *Euglypha*. It is possible that a few (less than 10 %) belong to the genus *Assulina* (hence the name '*Euglypha* type plates') and it could be that other small *Assulina* plates were not recognised/enumerated in the samples (see Douglas & Smol, 2001 for a review).

7.3.5. Fossil pigments

Fossil pigments were extracted from bulk sediments following standard protocols (Leavitt & Hodgson, 2001; Squier et al., 2002). All samples were freeze dried immediately prior to extraction. Pigments were extracted from freeze-dried sediments by sonication (30 seconds at 40 W) in 2-5 ml high-performance liquid chromatography (HPLC)-grade acetone (90 %), and filtered through a nylon filter (mesh size 0.20 um).

All compounds were isolated and quantified using an Agilent technologies 1100 series HPLC system equipped with an autosampler at -10°C, a diode array spectrophotometer (400-700 nm), an absorbance detector and a fluorescence detector. A reversed phase Spherisorb ODS2 column was used (internal diameter: 4.6 mm, particle size of 5 pm). Three solvents were used (Wright et al., 1991): A (80:20 methanol:0.5 M ammonium acetate (aq.; pH 7.2 v/v)), B (90:10 acetonitril (210 nm UV cut-off grade): water (v/v)) and C (ethyl acetate; HPLC grade).

The HPLC system was calibrated by use of authentic pigment standards from the U.S. Environmental Protection Agency, and compounds isolated from reference cultures following Scientific Committee on Oceanic Research (SCOR) protocols (Jeffrey et al., 1997). The taxonomic affinities of the pigments were derived from Jeffrey et al. (1997) and Leavitt and Hodgson (2001). Pigments with unknown affinity were labeled as

derivatives of the pigment with which it showed the closest match based on the retention time and the absorption spectrum.

7.4. Results

7.4.1. Lake survey and limnology

The Beak-1 basin is near circular (Fig. 2b), and has a simple concentric bathymetric profile, with a maximum depth of 24 m. The current retaining sill height of 10.95 above the present high tidewater mark is lower than a likely Holocene marine limit, mapped in the catchment at 14.91 m a.s.l. (Fig. 2a; Hodgson et al., 2005). The lake is circumneutral (pH ranging from 7.37 at the surface to 6.92 at the bottom; Table 1), and has a summer water temperature between 4.82°C (surface) and 4.26°C (bottom). Salinity is 0.13-0.14, and conductivity and specific conductivity range between 172-177 µS/cm and 280-293 µS/cm respectively. Nutrient levels and ion compositions are relatively low and below detection limit for ammonium and nitrite, which is similar to other lakes in the region (Table 1).

Table 1: Summary of limnological measurements in Lake Beak 1.

Sample	Temp (^{0}C)	Sp.Cond. (µS/cm^2)	Cond. (µS/cm)	Salinity	DOX (%)	DOX (mg/l)	pH	Altitude	Maxi. Dept
Beak 1 surface	4.82	280	172	0.13	107.3	13.75	7.37	10.955	24
Beak 1 bottom (24 m)	4.29	293	177	0.14	80.3	10.38	6.87		
Beak 2	12.2	250	188	0.12	112.5	12.05	8.61	2.365	4
Beak 3	14.29	311	247	0.15	111.3	11.46	8.95	0.515	1
Beak 4	12.85	612	470	0.3	114.1	12.03	9.77	-	0.5
Beak 5	12.82	312	239	0.15	115.3	12.2	9.12	-	0.5
Beak 6	13.32	272	212	0.13	110.2	11.57	9.16		0.5

Table 1 *(continued)*

Sample	NO_3 (µg/l)	NH_4 (µg/l)	PO_4-P (µg/l)	Si (µg/l)	Cl (mg/l)	TDN (µg/l)	Na (mg/l)	K (mg/l)	Mg (mg/l)	Ca (mg/l)
BK_1	<100	<10	17	1220	68.8	140	37.7	2.03	6.57	5.05
BK_2	<100	25	6	349	59.6	490	34.2	2.49	5.97	3.7
BK_3	<100	21	<5	887	73.6	580	40.9	3.12	8.67	5.24
BK_4	<100	<10	<5	2970	144	1700	108	6.52	8.55	3.72
BK_5	<100	45	41	704	68.7	570	39.4	3.44	10	4.87
BK_6	<100	<10	<5	1070	62.5	660	31.1	4.08	8.96	4.86

Table 1 *(continued)*

Sample	TOC (mg/l)	DOC (mg/l)	SO_4-S (mg/l)	Al (mg/l)	Fe (mg/l)
BK_1	0.75	0.99	32.7	0.126	0.109
BK_2	2.4	2.67	33.2	0.009	0.018
BK_3	3.1	3.86	46.6	0.011	0.045
BK_4	7.7	11	10	0.079	0.063
BK_5	2.9	3.25	60.1	0.035	0.084
BK_6	4.3	4.62	35.1	<0.002	0.093

7.4.2. Geochronology

The principal cores from 20 m depth consisted of two drives (BK-1E and BK-1D) with a total of 1.66 m of sediment recovered. Eighteen samples were ^{14}C dated (Table 2). Most dates were chronologically consistent. Exceptions occurred at 32.5 cm, where the dated moss-stem was probably translocated downward during the coring process, and at 103.5 and 129.5 cm depth, where ages of 10,901 ± 53 and 10,752 ± 62 ^{14}C BP were older than the basal sediment age of 10,625 ± 54 ^{14}C BP (166-167 cm depth; Fig. 3). These last two age inversions likely reflect a very rapid deposition of sediments between 167 and 100 cm depth. The presence of rough zonations in lithofacies (Fig. 3), diatom and pigment compositions (Figs. 4, 5) between 167-100 cm suggest, at worst, only minor disturbance in the marine environment. Moreover, with a sill height at c. 7-8 m below sea level at the time of deposition (Hodgson et al., unpubl. data), it is likely that the deepest parts of the basin became a sediment trap, protected from large disturbance by marine currents or large icebergs.

7.4.3. Sedimentological properties

Seven distinct lithological units were observed, all well defined by sharp transitional contacts (Fig.3). The basal unit, which is composed of coarse gravel that prevented deeper penetration, is overlain by a unit of gravelly sand, gravel, sand and mud (166-147 cm). From 147-102 cm, lenses of gravel, sand, fine sand and silt are embedded in a black organic mud matrix, and overlain by a unit of dark grey/black fine organic mud (102-75 cm). The main lithological change in the core occurs at c. 75 cm, where greenish-grey fine organic muds are overlain by a unit of light greenish grey to olive green clay rich laminated muds (74-45 cm) and a unit of olive green, fine organic mud (45-30 cm). A unit of olive green laminated fine organic mud between c. 28-5 cm, is capped by matted

Table 2: ^{14}C dates of the sediment core from Maritime Antarctica. A mixed curve was used for the calibration of the samples at 78.5 and 79.5 cm depth, (Intcal 04.14C and Marine Curve, 50 %; Reimer et al., 2004; Hughen et al., 2004). Samples from depths greater than 80 cm were calibrated with the Marine Curve (ΔR=900 years) (Hughen et al., 2004).

AMS Lab number	14-C date	14-C error	Type of material	depth in core	minimum calibrated	maximum calibrated	median cal. age	probability of 2 Sigma interval	date used in model	curve used
SUERC-12385	modern		Macro	0.5	modern	modern	modern	-	0	Intcal 04.14C
SUERC-1239	1563	35	Bulk/ macro	15.5	1379	1532	1455.5	1.000	1456	Intcal 04.14C
SUERC-1239	2305	35	Bulk	31.5	2300	2360	2330	0.743	2330	Intcal 04.14C
SUERC-1238	1101	35	Macro	32.5	932	1069	1000.5	1.000	-	Intcal 04.14C
SUERC-1239	2345	35	Bulk	34.5	2311	2473	2392	0.991	2392	Intcal 04.14C
SUERC-1239	2940	35	Bulk	43.5	2973	3214	3093.5	1.000	3094	Intcal 04.14C
SUERC-1239	3280	35	Bulk	46.5	3440	3587	3513.5	0.958	3514	Intcal 04.14C
SUERC-1240	4048	35	Bulk	55.5	4422	4621	4521.5	0.944	4522	Intcal 04.14C
SUERC-1240	4346	35	Bulk	59.5	4844	4976	4910	0.956	4910	Intcal 04.14C
SUERC-1240	6010	36	Bulk	73.5	6774	6945	6859.5	0.962	6860	Intcal 04.14C
SUERC-1240	6735	35	Bulk	78.5	6864	7089	6976.5	0.953	6977	50 % mixed
SUERC-1256	6098	35	Bulk	73.5	6881	7031	6956	0.818	-	Intcal 04.14C
SUERC-1256	7393	36	Bulk	79.5	7557	7677	7617	1.000	7617	50 % mixed
SUERC-1294	10901	53	Bulk	103.5	10756	11140	10948	1.000	-	Marine dR 900
SUERC-1256	9626	48	Bulk	108.5	9282	9496	9389	1.000	9389	Marine dR 900
SUERC-1294	10752	62	Bulk	129.5	10575	11022	10798.5	1.000	-	Marine dR 900
SUERC-1294	10147	46	Bulk	140.5	9910	10190	10050	1.000	10050	Marine dR 900
SUERC-1256	10625	54	Bulk	166.5	10480	10723	10601.5	1.000	10602	Marine dR 900

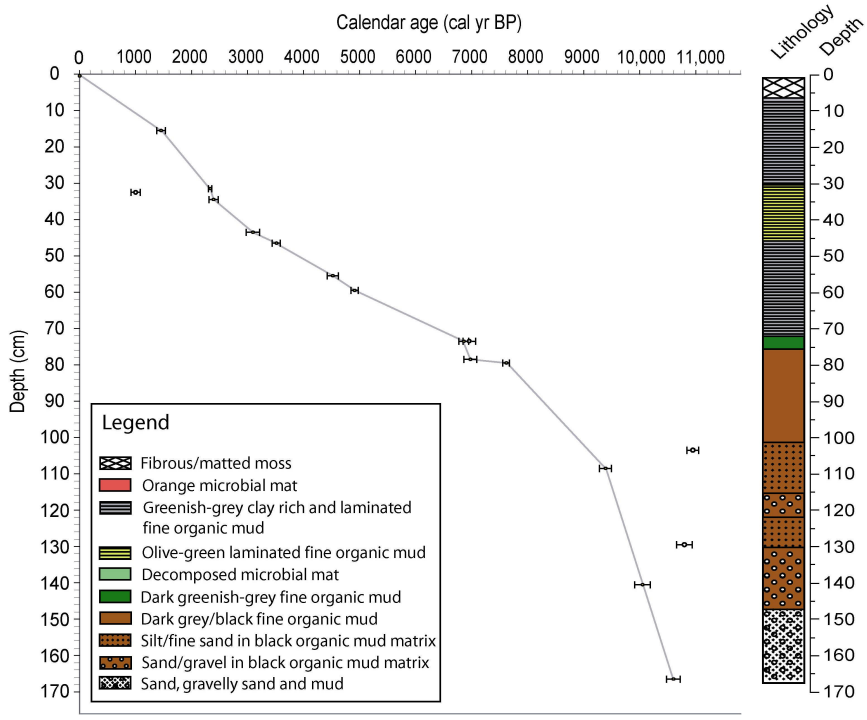

Figure 3: Age-depth model and lithology of the Beak-1 core.

moss in the uppermost 5 cm of the core. Mosses were also visually present during subsampling at 15-17.5 cm and 32-33 cm and in small quantities throughout 20-9 cm. There is no evidence of slumps or other discontinuities in the cores and the upper c. 70 cm is finely laminated.

Four tephra layers were visually identified, namely at c. 138-134, 59, 44 and 34-33 cm depth. These layers correspond with peaks in magnetic susceptibility (MS) and distinct local minima in LOI_{550} (Fig. 4). The MS is generally highest between 160 and 150 cm depth, and minimal between 90 and 85 cm, after which it gradually rises between 55 and 35 cm, followed by a decrease towards the top of the core (Fig. 4). Wet density is relatively high and variable between 166 and 80 cm depth, where it sharply declines until 76 cm (Fig. 4). Between 76 and the top of the core the wet density increases again, but remains lower than the bottom sediments. LOI_{925} a proxy for carbonate content, is fairly constant throughout the core, with the exception of minima near the tephra layers and a sharp drop at 20 cm depth (Fig. 4). LOI_{550} remains lower than 3.5 % between 166 and 104 cm, and only

rises above 5 % at 96 cm depth. A peak in LOI_{550} occurs at the main transition to fine organic-rich mud (75cm). A second peak occurs between 45 and 25 cm, culminating at 30 cm briefly interrupted by the tephra layer at 33 cm. LOI_{550} increases for a third time from 10 cm upwards and subsequently declines again at 2 cm towards the top of the core, where the wet density is lowest.

7.4.4. Siliceous microfossils and the diatom based reconstruction of NH_4^+ concentration

The diatom stratigraphy of the Lake Beak-1 is divided into 8 zones, based on the CONISS cluster analysis (Fig.4&5), namely two marine zones (m-1 and m-2), one transition zone (1t-1) and five freshwater zones (1f-1 to -5).

Marine zones

Zone 1m-1 (166-105 cm): this zone is characterized by a low species diversity and total diatom abundances, and a relatively high percentage of broken valves (Fig.5). The diatom communities are composed of a mixture of marine and sea-ice related taxa, such as *Navicula glaciei* and *Navicula perminuta* (Fig. 5), and open water taxa (*Chaetoceros* resting spores). Sparse freshwater diatoms are also found at some depths (e.g. *Planothidium renei, Staurosirella pinnata, Brachysira minor* at 166 cm). The bottom of this zone contains a slightly higher percentage of centric diatom species, *Cocconeis* spp. and some terrestrial/freshwater species (*Brachysira minor*, *Staurosirella pinnata*; Fig. 5).

Zone 1m-2 (105-76 cm): in this zone, total diatom abundances and diversity increase, and the fraction of broken valves decreases. *Chaetoceros* RS, which are mainly found in open ocean assemblages, increase up to 76.7 % at 96 cm depth. *Chaetoceros* RS reach two minima at 94 and 88 cm depth, where total diatom abundances are low, and a sudden peak in centric species (94 cm) and *Craspedostauros* and *Berkeleya* species (88 cm) occurs (Fig. 5). Other sea-ice zone related species (e.g. *Fragilariopsis* spp.), and brackish-water diatoms (e.g. *Craspedostauros laevissimus*) become increasingly abundant in this zone, which precedes the transition to lacustrine conditions. A decline in *Achnanthes* cf. *brevipes* occurs at 100 cm (Fig. 5).

Transition zone

Zone 1t-1 (76-70 cm): the main transition from marine to freshwater diatom communities coincides with the marked transition in lithology at 76 cm depth and extremely low reconstructed NH_4^+ concentrations (Fig.4). Diatom species richness, turnover rate, and

percentage of broken valves, is at a maximum between 76 and 74 cm depth, and at a minimum between 73-71 cm. Diatoms are dominated by taxa characteristic for relatively high productive water (e.g. *Nitzschia perminuta*, and *N. frustulum)*, *Gomphonema spp.*, and taxa known to have a broad salinity tolerance (e.g. *Craticula antarctica)* between 76 and 74 cm, and by *Naviculadicta seminulum* and *Brachysira minor* between 73 and 70 cm depth (Fig. 5).

Freshwater zones

Zone 1f-1 (70-44 cm): in this zone the number of *Euglypha* type plates is low to nearly zero. After 67 cm depth, *Achnanthidium* cf. *exiguum, Chamaepinnularia australomediocris* and *Planothidium renei* appear and the reconstructed NH_4^+ concentration increases. *A.* cf. *exiguum* sharply declines at 49 cm and *Chamaepinnularia australomediocris* gradually declines towards the top of the core, but the abundance of *Planothidium renei* varies widely (Fig. 5).

Zone 1f-2 (44-20 cm): in this zone the concentration of stomatocysts and *Euglypha* type plates is relatively high. The reconstructed NH_4^+ concentration is highly variable and similar to the previous zone. The diatoms in this zone are dominated by *Planothidium renei*, and are characterized by a minor increase in *P. delicatulum*, by the appearance of the tychoplanktonic diatom *Staurosirella pinnata* (with a maximum abundance at 27 cm depth), and the presence of aerophilic taxa such as *Stauroneis* cf. *subgracilior, Caloneis bacillum*, *Mayamaea atomus* var. *permitis*, *Stauroneis cf. subgracilior* and *Diadesmis spp*. (Fig. 5).

Zone 1f-3 (20-14 cm): at 20 cm the concentration of the moss-associated *Brachysira minor* starts to rise towards a high peak at 15 cm depth, causing diatom total abundances to peak, and inferred $NH4^+$ concentration to be low (Fig. 5). The number of plates and stomatocysts is similarly low. The start of this rise in *Brachysira* coincides with the appearance of *Psammothidium abundans*, a diatom common in deep freshwater (> 5 m) lakes in the Larsemann Hills (Verleyen et al., 2003), and indicative for low phosphorous concentrations and high light intensities. The appearance of this species also coincides with the sudden decline of LOI_{950} at 20 cm depth.

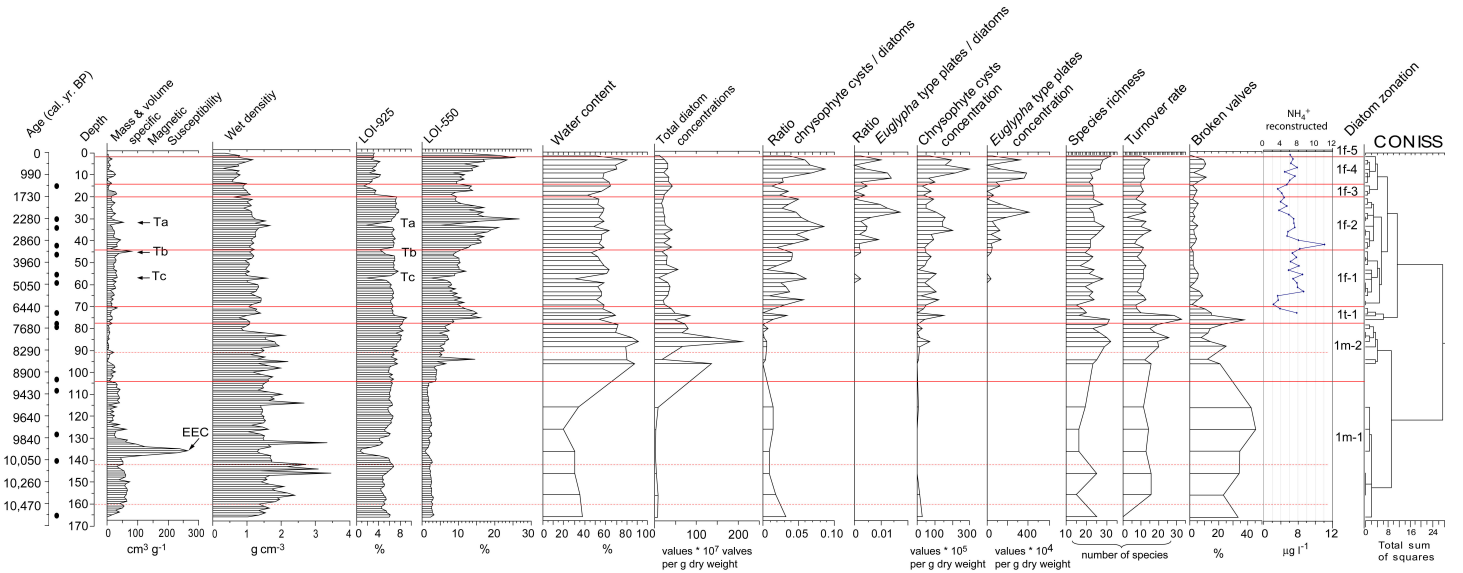

Figure 4: Sedimentological, geochemical and microfossil-based proxies in the Beak-1 sediment core, plotted against depth (cm). Corresponding interpolated calibrated ages are given, and depths of ^{14}C dates (Table 2 and Fig. 3) are indicated by black dots.
LOI stands for Loss on Ignition. The stomatocysts versus diatoms and the total abundance of cysts are an approximation for the amount of planktonic chrysophytes. Diatom species richness is the number of taxa in each sediment sample. The diatom turnover rate is calculated as the sum of the number of taxa gained and the number of taxa lost when moving from one sample to the next (above). The amount of broken valves is calculated as a percentage of the total number of diatoms counted, with the exclusion of *Chaetoceros* RS. Reconstructed NH_4^+ concentrations (µg/l) are calculated using a diatom based transfer function (Chapter 6). The zonation of the core is based on the CONISS analysis of the diatom species compositions (Fig. 5). Ta, Tb and Tc represent tephra layers in the core, EEC stands for a core extrusion extention between 138 and 134 cm depth.

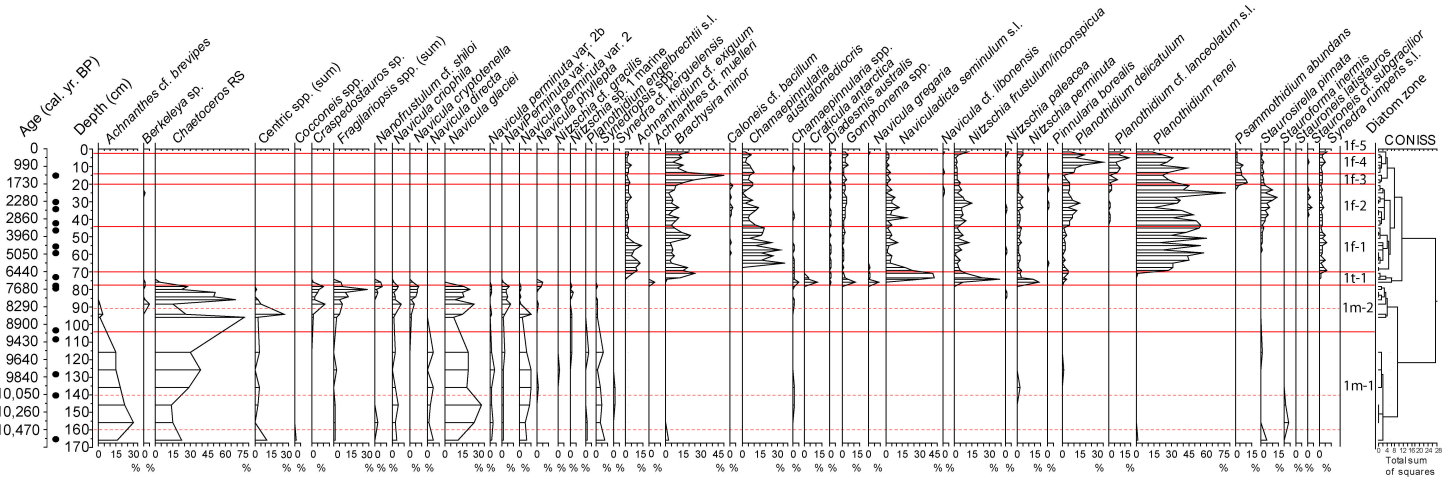

Figure 5:
Diatom stratigraphy of the BK1 core, plotted against depth (cm). Corresponding interpolated calibrated ages are given, and depths of ^{14}C dates (Table 2 and Fig. 3) are indicated by black dots. Only species with a relative abundance exceeding 5 % or occurring in five or more samples are shown, as well as species with a specific (ecologically meaningful) distribution in the core. *Chamaepinnularia* spp. is an assemblage of *C. gerlachei*, C. sp. 2, *C.* sp. 3 and *C. cymatopleura*. Centric species are summed, as well as all species (see Table 5 in Chapter 6) of the genera *Cocconeis* and *Fragilariopsis*. The zonation of the core is based on the CONISS analysis of the diatom species compositions.

Zone 1f-4 (14-2 cm): total diatom abundances, as well as *Euglypha* type plate and chrysophyte concentrations are again high between 10 and 5 cm (Fig. 4), and decline towards the top of the core. At 7 cm, a maximum in inferred NH_4^+ concentration and *Planothidium delicatulum* occurs, a species currently occurring in low-elevation lakes in Signy and Livingston islands. It is an epilithic species, found at sea spray associated sites and/or in meltwater streams (Jones et al., 1993; Jones & Juggins 1995; Chapters 4 and 6). *P. lanceolatum* increases towards a maximum at the top of the core. This species is currently found in high-elevation, low productivity lakes with low nutrient concentrations (Jones et al., 1993; Jones & Juggins 1995; Sterken et al., in prep.).

Zone 1f-5 (1 cm): this zone is composed of the core-top and differs from the previous zone by its high diatom richness and the higher abundances in *Nitzschia frustulum* which was also abundant in zone 1f-2 and immediately after lake isolation.

7.4.5 Fossil pigments

Changes in pigment concentrations and relative abundances in the core are broadly consistent with the zones based on diatom species compositions and the sedimentological characteristics. Changes in pigment stratigraphy are therefore discussed following the diatom zonation. Total carotenoid and chlorophyll concentrations are highly correlated, both in the marine and freshwater sections of the core (Fig. 6).

* *Marine zones*

Zone 1m-1 (166-105 cm): the total pigment concentrations were moderately low throughout this zone and the carotenoid concentration is composed of pigments produced in diatoms, dinophytes and chrysophytes (diatoxanthine), and chlorophytes (lutein). The basal core levels of this zone (165-145 cm depth) contain high amounts of ***b***-carotene and chlorophyll derivatives, including (pyro)phaeophitin ***a***. In addition, some very short-term peaks in terrestrial/lacustrine cyanobacteria specific pigments (myxoxanthophyl, canthaxanthin) are present in the bottom sediments, suggesting that this part of zone 1m-1 is of marine and terrestrial origin. The upper parts (145-105 cm) are similarly dominated by a pigment which is likely a derivative of ***b***-carotene, and chlorophyll derivatives. A (pyro)phaeophitin ***a*** like derivative is virtually absent.

Zone 1m-2 (105-76 cm): the carotenoid and chlorophyll composition is largely similar to that observed in the bottom parts of zone 1m-1, but the total pigment

concentration is generally higher, pointing to more productive conditions. Phaeohytin *b* becomes subdominant. In the bottom sediments of the zone (105-85 cm), a pigment present in diatoms and chrysophytes (fucoxanthin) becomes more important. Phaeophorbide becomes more abundant in the upper parts of the zone together with de chlorophyll derivative that dominated the bottom parts of zone 1m-1.

* *Transition zone*

Zone 1t-1 (76-70 cm): At the marine-lacustrine transition in core Beak-1 (76 cm depth), the diversity in pigment composition and the total concentration were high. Zeaxanthin appeared for the first time between 80 and 70 cm depth, lutein (indicative for chlorophytes and bryophytes; Leavitt and Findlay 1994) showed a maximum between 74 and 70 cm depth (~ diatom zone 1f-1), and at 74 cm depth, small peaks of rare pigments with characteristics similar to those of hexanoyloxi-fucoxanthin, canthaxanthin and vaucheriaxanthin occur. At 75 cm, a short lived peak of an unknown pigment is found. Percentages of phaeophytin *b* (an indicator of the presence of chlorophytes and mosses; Leavitt and Findlay 1994) were maximal at the marine-freshwater transition depths.

* *Freshwater zones*

Zone 1f-1 (70-44 cm): this zone is characterised by very low total pigment concentrations. In some samples carotenoids were even below detection limits. Pyrophaeophytin *a* dominates the chlorophylls and phaeophytin *b* is subdominant.

Zone 1f-2 (44-20 cm): increased pigment concentrations in this zone coincide with a diverse pigment composition, comparable with the samples at the marine-freshwater transition. Carotenoids are again present in relatively high amounts and dominated by pigments produced in diatoms, cryptofytes and cyanobacteria and green algae/mosses, such as fucoxanthin and fucoxanthin derivatives, diadinoxanthin, a high peak of alloxanthin-like pigments (almost 100 % at 21 cm depth), diatoxanthin, lutein, vaucheriaxanthin like pigments and *b*-carotene. Non-degraded chlorophyll *a* re-appears in this zone in low abundances and phaeophorbide *a*, a pigment produced under grazing conditions, reappears in similar percentages as it was between 85 and 75 cm depth.

Zone 1f-3 (20-14 cm): between 20 and 15 cm depth, the samples are devoid of carotenoids, and contain only small concentrations of chlorophyll-derived pigments, which is coincident with the sudden shifts in diatom communities (Fig. 5).

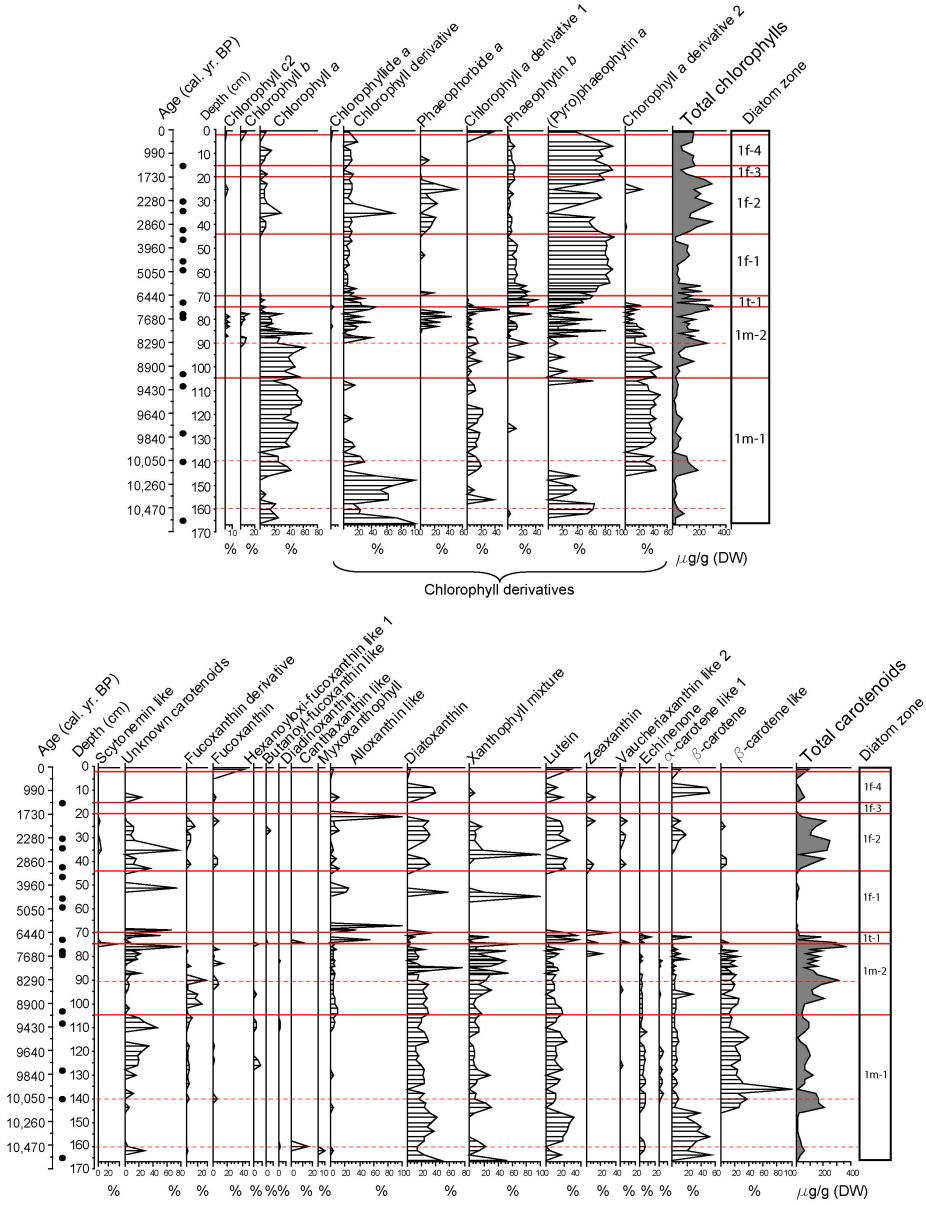

Figure 6: Fossil pigment stratigraphy of the Beak-1 sediment core, plotted against depth (cm). Corresponding interpolated calibrated ages are given, and depths of ^{14}C dates (Table 2 and Fig. 3) are indicated by black dots. Only pigments constituting more than 2 % of the total carotenoids or total chlorophylls are shown. Total pigment concentrations (grey shaded graphs) are expressed in µg/g dry weight (DW). The zonation of the core is based on the CONISS analysis of the diatom species compositions (Fig. 5).

Zone 1f-4 (14-2 cm): this zone shows slightly higher total pigment concentrations, and compositions that are similar, but less pronounced, to those of zone 1f-3 (70-40 cm). The carotenoids present are produced by diatoms, cryptofytes and cyanobacteria and green algae/mosses.

Zone 1f-5 (1 cm): the core-top sample differs from other samples, by its high peak in fucoxanthin (a pigment produced by chrysophytes and diatoms), lutein (chlorophytes and bryophytes), *b*-carotene (chlorophytes and cyanobacteria), chlorophyll *b* (likely related to mosses) and a chlorophyll *a* derivative.

7.5. Discussion

7.5.1. c. 10,600 cal. yr. BP – 9200 cal. yr. BP: deglaciation and the onset of marine sedimentation

The zone corresponding to c. 10,600 - 9200 cal. yr. BP shows many characteristics of glaciomarine sediments derived from the decaying Antarctic Peninsula Ice Sheet (APIS) and transported to the site by ice bergs (e.g. Pushkar et al., 1999; Brachfeld et al., 2003; Domack et al., 2005). This can be concluded from several lines of evidence, namely from the minimal diatom total abundances, the high amount of broken valves, the presence of a some terrestrial diatoms and pigments derived from terrestrial cyanobacteria, the low organic carbon values (LOI_{550}), the low water content, the high magnetic susceptibility, the high sedimentation rates, a lithology composed of coarse material of varied size and the ^{14}C dates being out of stratigraphic order. Although the diatoms are likely to be a mixture of autochtonous growing and allochtonous derived specimens, the communities in this zone are mainly composed of sea-ice indicator taxa (*Navicula glaciei*) and thus likely reflect the presence of a nearly permanent ice cover over the coring site (e.g. Burckle & Cirilli, 1987). This interpretation does not rule out the presence of a large amount of decaying icebergs at the site, since icebergs can penetrate through pack-ice (Reece, 1950; Pudsey & Evans, 2001).

Although the glaciomarine sediments might potentially be contaminated with old carbon, the ^{14}C dates set a minimum age for deglaciation of the area around Beak Island, and extend the terrestrial based estimates by several thousand years (Hjort et al., 1992; 1997). These dates also slightly predate the minimum age of deglaciation of some islands

to the north of the AP around 9500 ^{14}C BP (Jones et al., 2000), and previous estimates based on glacial stratigraphy and morphology in Vega Island (Zale & Karlén, 1989) at about 10,000 yr. BP. Interestingly, the deglaciation is as early as that inferred for Erebus and Terror Gulf to the SE of Beak and Eagle Islands, the Greenpeace Trough and the Larsen-A and -B ice shelves (Fig. 1; Brachfeld et al., 2003; Domack et al., 2005), and implies a rapid disintegration of the north eastern part of the APIS on the inner shelf. This melting is largely coincident with the melting of other parts of the APIS (Heroy & Anderson, 2007) in phase with the Early Holocene warm period detected in ice cores from the central plateau (Masson-Delmotte et al., 2006). It is however unlikely that changing climate conditions alone led to the destabilisation of the APIS. Together with internal dynamics, the rising sea level at the start of the Holocene is also expected to have affected the marine based APIS, as melting of parts of the ice sheet were in phase with the collapse of the ice sheets in the Northern Hemisphere and coincided with melting water pulse (MWP) 1b, a period of rapid global sea level rise (Hodgson et al., in press). The inferred presence of long sea ice cover during this period could corroborate the inference of a 'climatic reversal' between c. 11,000 and 9000 BP in Palmer Deep on the northwestern side of the Antarctic Peninsula, although our record does not extend further than 10,600 cal. yr. BP, and interestingly this reversal was still characterized by seasonally open water at the Palmer Deep site (Taylor & Sjunneskog, 2002).

7.5.2. c. 9200-6930 cal. BP: Seasonally open water marine environment

Between 9200 and 6930 cal. yr. BP (105-76 cm) relatively high productive, open water conditions influenced by seasonal meltwater were likely present. This is reflected in the higher LOI_{550} values and the diatom and pigment data. Diatom species richness and absolute abundances, mainly driven by *Chaetoceros* resting spores (CRS), were maximal. CRS are often found in near-ice open water assemblages, where surface waters are strongly stratified due to the melting of ice (Karl 1991; Crosta et al., 2008; Buffen et al., 2007). They typically occur in high productivity zones, especially where non-diatomaceous plankton blooms occur (Leventer et al., 1992; Comiso et al., 1990; Smith and Nelson, 1990). Highly productive open water conditions are furthermore evidenced by the peaks in total pigment concentrations at 98 and 90 cm depth, and the appearance of alloxanthin-like pigments at 108 cm depth. Alloxanthin is indicative of the presence of cryptophytes (Buchaca & Catalan 2007; Jeffrey et al., 1997), which have recently been associated with environments under increased meltwater runoff and reduced surface water salinities caused by regional warming along the Western AP margin (Moline et al., 2004). The disappearance of coarse-grained debris and the slower sedimentation rate

were probably caused by the continued retreat of glaciers and ice shelves in the area, leaving a lower amount of icebergs or only debris-poor icebergs at distal sites.

Between c. 8290 and 6930 cal. yr. BP (90-76 cm), a mixture of species with very different ecological optima is present. The assemblages are composed of nearshore marine and brackish water taxa (e.g. *Craspedostauros* sp., *Navicula cryptotenella* and different *Nitzschia* species), sea-ice and ice-melt related species (e.g. *Navicula glaciei)* and several ice-edge species (e.g. *Fragilariopsis cylindrus*). The rapid shifts in diatom assemblages and pigment stratigraphies is difficult to interpret and could be related to (1) climate change, (2) an effect of the isostatic uplift and the related availability of ecological niches, or (3) a combination of both.

The period between 9200 and c. 6930 cal. yr. BP is not well documented in the paleoclimate records in the AP. The records that do exist show contrasting patterns in the timing and duration of events (Bentley et al., 2009). Along the southwestern margin of the AP, there is evidence for glacier thinning and ice margin retreat until at least 7–8 cal. ka BP (Bentley et al., 2006), and the collapse of the King George VI Ice Shelf (Alexander Island) between c. 9.6 and 7.9 cal. ka BP (Bentley et al., 2005). This coincides with the first part of a prolonged climate optimum in the Palmer Deep record between c. 9 and 3.7 cal. ka BP (Domack et al., 2001). Interestingly, the ice shelves on the eastern margin of the AP remained intact (Domack et al., 2005), while our record is also in favor for warmer conditions. This is in agreement with a recent study by Hey et al. (pers. comm.) on marine fossil diatoms from the southern Prince Gustav Channel, which suggests a change in diatom compositions towards seasonally open water conditions at the ice shelf edge around 8.7-7.4 cal. ka BP and with some early studies of Quaternary glacial stratigraphy and morphology in northern James Ross Island. The latter studies suggested a glacial readvance between 7300 and 6700 ^{14}C BP (resp. c. 8100 and 7550 cal. yr. BP), which was partly ascribed to a Holocene warming (Ingólfsson et al., 1998). The reason why ice shelves in this part of the Antarctic remained intact while the King George VI Ice Shelf collapsed is still unclear and needs further investigation (Hodgson et al., in press).

7.5.3. c. 6600 - 6400/6000 cal. yr. BP: lake isolation

The period between 6600 and 6400-6000 cal. yr. BP (76-70 cm) coincides with the isolation of the lake, which prevents the use of this part of the core for the reconstruction of past climate changes as also seen in other isolation basins around Antarctica (e.g. Wasell & Håkansson, 1992; Verleyen et al., 2004a,b). This isolation event dominates all

analysed proxies. The diatom turnover and diversity is highest at the start of this zone after which they rapidly decline. The zone is dominated by diatoms, which are generally found today in coastal lakes that are influenced by sea birds and mammals (e.g. the *Nitzschia frustulum*/*inconspicua* complex, *N. perminuta* and *Naviculadicta seminulum*; Björck et al., 1996; Van de Vijver et al., 2008; Chapter 6). Together with the relatively high organic carbon content (LOI_{550}) and total diatom and pigment concentrations, the presence of these diatoms point to highly productivity conditions due to marine derived nutrients.

Although this period of increased primary productivity is likely related to the isolation event, it coincides with relatively warm conditions elsewhere in Antarctica, such as in the Bransfield Basin between 6.8-5.9 cal. ka BP (Heroy et al., 2007), near the inner Larsen-A region at c. 6300 ± 500 yr. BP with ice shelf margin and open water conditions present across the inner-middle shelf (Evans et al., 2005) and in Hope Bay, where the earliest penguin colonies were dated at c. 5500 ^{14}C BP (~ c. 6300 cal. yr. BP), shortly after deglaciation (Zale, 1994a,b; Gibson & Zale, 2006)

7.5.4. c. 6000 and 3500 cal. yr. BP: decreased primary productivity

The period between c. 6000 and 3500 cal. yr. BP is characterized by relatively low primary productivity, likely the result of cold climate conditions that are reflected in all the proxies studied. The total organic carbon (LOI_{550}) and chlorophyll content are relatively low; fossil carotenoid concentrations were even below detection limits in some core levels. The diatom assemblages were characterized by relatively high abundances of *Achnanthidium* cf. *exiguum* and *Brachysira minor*, two species typical of high-altitude, nutrient-poor lakes on Livingston Island with low Chlorophyll *a* concentrations (Jones & Juggins, 1995).

The paleoclimate records from the AP spanning this period are difficult to interpret due to problems with ^{14}C dating and the lack of well dated records (Bentley et al., 2009). Cool conditions, with extensive sea-ice cover as evidenced by the diatom communities were also found in Lake Beak-2 on Beak Island between 6600 and 3500 cal. yr. BP (Chapter 6). Low nutrients and productivity was inferred from an extensive growth of aquatic mosses in Lake Boeckella (Hope Bay) after 4700 ^{14}C BP (Gibson & Zale, 2006), which broadly corresponds with the start of and the low productivity conditions in the core. In addition, Mid-Holocene glacier oscillations/advances were inferred for the region of Hope Bay after 4700 ^{14}C BP (Zale, 1994a), and on James Ross Island after 4600 ^{14}C

BP, which was linked to increased precipitation (Hjort et al., 1997). In contrast, cold and arid climatic conditions between c. 5.0 and 4.2 ^{14}C kyr BP (c. 5.7-4.7 cal. ka BP) were reconstructed from lake sediment cores on James Ross Island (Björck et al., 1996), which followed rapid glacier retreat just before 5.0 ^{14}C kyr BP. No such cold climate conditions were reported from marine sediment records in the NW-Weddell Sea region during this period (Pudsey & Evans, 2001). In contrast to cold an arid conditions, a Holocene climate optimum occurred near the western margin of the AP which lasted until 3.7 cal. ka BP (Domack et al., 2001).

7.5.5. c. 3500 and 1730 cal. yr. BP: Mid-Holocene Hypsithermal

Sedimentological and biological proxies clearly point to the prevalence of a period of higher primary productivity between 3500 and 1730 cal. yr. BP, which may indicate a warmer climate. The relatively high organic carbon content coincides with a high diatom species diversity, the presence of non-diatom indicator carotenoids (e.g. lutein, zeaxanthin, vaucheriaxanthin-like; Fig. 6), representing a diverse community of possibly planktonic algae, high pigment concentrations and the reappearance of phaeophorbide-a, which is likely related to increased grazing activity by zooplankton and the development of a planktonic community. The presence of a well developed planktonic community is also supported by the sub-dominance of the tychoplanktonic species *Staurosirella pinnata*. The reconstructed NH_4^+ concentration remains however relatively constant, implying that the observed increase in primary productivity is likely related to changes in the duration of ice cover (and the length of the growing season) rather than to changes in nutrient levels in the catchment area. This is not unexpected as the catchment area of the lake was likely devoid of glaciers during the past 6000 years, implying that increased nutrient concentrations following deglaciation and soil development are expected to exert only a small influence on the lake's metabolism in contrast to the lakes in more glaciated areas (e.g. Quayle et al., 2002). However, the presence (although in small numbers) of some typical aerophilic diatoms could indicate an increased input from algae which were able to colonize damp littoral areas in the catchment area as a result of warmer and moister summer conditions. The presence of *Euglypha* type plates in this zone could corroborate this interpretation, pointing to moss growth in the catchment or littoral area of the lake (Vincke et al., 2006; Douglas & Smol, 2001).

The period of increased primary productivity between 3500 and 1730 cal. yr. BP coincides with the Mid-Holocene Hypsithermal (MHH), a warm period found in several parts of the AP (Hodgson et al., 2004). The exact timing of this event is however still a

matter of debate (Hodgson et al., in press.). The best dated records are situated north of Beak Island in the South Orkney Islands and west in the South Sheltland Islands and put the MHH respectively between 3300 to 1200 ^{14}C yr. BP (Jones et al., 2000; Hodgson & Convey, 2005) and 3250 to 1850 ^{14}C yr. BP (Björck et al., 1991). Less well dated evidence for a warm period along the eastern margin of the AP ending at c. 1900 ^{14}C BP also exists further South in Prince Gustav Channel, when the ice shelf reformed (Pudsey & Evans 2001; Hey et al., pers. comm.), as well as in the Larsen-A region, where fluctuations in ice-shelf stability/extent were recorded until c. 1400 ^{14}C BP (Brachfeld et al., 2003). Interestingly, some marine records from the western part of the AP south of the South Shetland Islands place the MHH earlier. A Holocene climate optimum starts at c. 9 ka and ends at c. 3.2 ka in Palmer Deep (Domack et al., 2001) which clearly precedes the MHH in terrestrial records from the eastern part of the AP (this study), the South Shetland Islands (Hodgson & Convey, 2005) and the South Orkney Islands (Jones et al., 2000). One of the explanations for this apparent difference between marine records from the west and terrestrial records from other areas in the AP is that the proxies in these environments are responding to environmental conditions expressed at different times of the year (Bentley et al., 2009). In other words, marine cores are reflecting springtime phytoplankton blooms whereas the terrestrial records respond to forcing mechanisms present during summer blooms, when the lake ice is absent and lacustrine productivity is highest (Bentley et al., 2009). Other explanations might include the influence of circumpolar deep water, which is more important on the western margin (Bentley et al., 2009). It is evident that more terrestrial records and particularly from the western part of the AP are highly needed to test this hypothesis.

7.5.6. c. 1730 cal. yr. BP – 1370 (20-14 cm): low productivity

The period between c. 1730 and 1370 cal. yr. BP is characterized by a relatively low primary productivity, which is likely dominated by benthic communities composed of diatoms and mosses. This is consistent with the disappearance of phaeophorbide, a pigment pointing to a high grazing activity. The abrupt changes in the diatom species compositions are related to the rise of *Brachysira minor* and *Psammothidium abundans*, which indicate low nutrient and, together with the low carbonate content (LOI_{950}), more acidic conditions. This is probably caused by the establishment of a benthic moss vegetation in the lake which survived at low-light conditions. Mosses often have an acidifying influence on their direct environment (Wetzel, 2001) and were shown to be indicators for low productivity and low nutrient conditions in similar lakes in the AP (Gibson & Zale, 2006).

This period of rapid environmental changes in Lake Beak corresponds to the reformation of ice shelves in the Prince Gustav Channel (1900 ^{14}C BP; Pudsey & Evans, 2001) and Larsen-A regions (1400 ^{14}C BP, dating uncertain; Brachfeld et al., 2003), as well as neoglacial cooling in other parts of the AP (e.g. the S-Shetland Islands: Björck et al., 1991, 1993; Bransfield Strait: Fabrés et al., 2000).

7.5.7. c. 1460 – present: climate deterioration and the recent temperature rise

From c. 1460 cal. yr. BP onwards the organic carbon content gradually increases towards the top of the core, which can be consistent with relatively cold conditions being interrupted by the recent temperature rise, at least, if considering possible changes in the sedimentation rate or (de)compaction of the sediments at the top of the core, as evidenced by the low wet density between 15 and 0 cm depth (Fig. 4). The core top is furthermore characterized by a relatively high diatom diversity and the rise of species favoring moderately high nutrient concentrations (e.g. *Nitzschia frustulum/inconspicua*). Inferred nutrient concentrations remain low however. This could be possibly related to the fact that, in combination with the large depth of Lake Beak-1, diatoms are less sensitive to changes in lakewater nutrient concentrations in Antarctica as they are largely restricted to the benthos (e.g. Bonilla et al., 2005).

The period of low lake productivity starting c. 1730 cal. yr. BP is consistent with Björck et al. (1996), who inferred a mild, humid but still colder than the Mid-Holocene climate for the period between 3000 ^{14}C BP and recent times in Hope Bay. In other regions of the AP, a neoglacial cooling is inferred for the past 1500 years (Bentley et al., 2009). A positive shift in primary productivity and the siliceous microfossils and pigments in our record is likely related to the recent temperature rise recorded elsewhere in the AP. This temperature increase already affected the physical and chemical environment of ecosystems in the AP and likely caused the recent recession of snowfields and glaciers (Cook et al., 2005), a reduction in the duration of sea-ice cover (Parkinson, 2002) and the disintegration of ice shelves (e.g. Vaughan and Doake, 1996; Rott et al., 1998; Scambos et al., 2003). The sediment core from Beak Island is thus amongst the first long term records showing a response of lacustrine ecosystems to recent global change, similar to Arctic water bodies, where the temperature rise since the industrial revolution resulted in significant shifts in lakes (e.g. Smol et al., 2005; Smol & Douglas, 2007).

7.6. Conclusions

Here we present one of the first continuous, well-dated reconstructions of Holocene climate and environmental change in the inner shelf regions north of James Ross Island, derived from lithological, diatom and fossil pigment analyses of sediment cores from an isolation basin in Beak Island.

1) Our results showed marine deposits in the basin, extending the minimum age for deglaciation of the surrounding area north of James Ross to as early as 10,600 cal. yr. BP.

2) A transition of a nearly permanent sea-ice cover and high iceberg concentrations to a seasonally open marine environment occurred around 9200 cal. yr. BP, which broadly corresponds with the early retreat/disintegration of the ice shelf in the southern Prince Gustav Channel.

3) Between c. 6 and 3.5 cal. ka BP colder climate conditions prevailed, followed by a Mid-Holocene climate optimum between c. 3500 and 1730 cal. yr. BP. This Mid-Holocene Hypsithermal is similarly found in other records from the eastern and northern part of the AP, yet it occurs earlier in the western part of the AP, south of the South Shetland Islands.

4) Lake productivity decreased from c. 1730 cal. yr. BP onwards, and corresponds with a reconstructed neoglacial cooling elsewhere in Antarctica. This period was interrupted by a strong increase in the lake's primary production and a shift in the diatom communities, probably related with the recent regional warming trend. The core is thus amongst the first long term records to show evidence of ecosystem changes as a result of the recent warming in the AP.

5) More well-dated past climate change records are needed to test the apparent phase difference in the dating of Holocene warm periods between the eastern en western margin of the AP and to provide a long term context for the recent temperature anomaly and its effect on polar ecosystems in other areas of the AP.

Acknowledgements

This study was funded by the British Antarctic Survey CACHE-PEP core program (led by Dominic Hodgson) and the Belgian Science Policy Office project HOLANT (led by Wim Vyverman). Elie Verleyen is a postdoctoral research fellow of the Fund for Scientific Research Flanders, Belgium. Andy Lole is thanked for his assistance in the field and the captain and crew of the HMS Endurance for the logistic support.

References

Armand L., Crosta X., Romero O., Pichon J.J. 2005. The biogeography of major diatom taxa in Southern Ocean sediments. 1. Sea ice related species. Palaeogeography, Palaeoclimatology, Palaeoecology. 223: 93-126.

Banfield L.A. & Anderson J.B. 1995. Seismic facies investigation of the late Quaternary glacial history of Bransfield Basin, Antarctica. Antarctic Research Series. 68: 123-140.

Barcena M.A., Fabrés J., Isla E., Flores J.A., Sierro F.J., Canals M., Palanques A. 1998. Holocene neoglacial events in the Bransfield Strait (Antarctica). Palaeocenographic and palaeoclimatic significance. Scientia Marina. 70: 607-619.

Battarbee R.W., Kneen M. 1982. The use of electronically counted microspheres in absolute diatom analysis. Limnology and Oceanography. 27: 184-188.

Bentley M.J., Hodgson D.A., Sugden D.E., Roberts S.J., Smith J.A., Leng M.J., Bryant C. 2005. Early Holocene Retreat of the George VI Ice Shelf, Antarctic Peninsula. Geology. 33: 173-176.

Bentley M.J., Hodgson D.A., Smith J.A., Ó Cofaigh C., Domack E.W., Larter R.D., Roberts S.J., Brachfeld S., Leventer A., Hjort C., Hillenbrand C-D., Evans J. 2009. Mechanisms of Holocene palaeoenvironmental change in the Antarctic Peninsula region. The Holocene. 19: 51-69.

Berkman P.A., Andrews J.T., Björck S., Colhoun E.A., Emslie S.D., Goodwin I.D., Hall B.L., Hart C.P., Hirakawa K., Igarashi A., Ingólfsson O., López-Martínez J., Lyons W.B., Mabin M.C.G., Quilty P.G., Taviani M., Yoshida Y. 1998. Circum-Antarctic coastal environmental shifts during the Late Quaternary reflected by emerged marine deposits. Antarctic Science. 10 (3): 345-362.

Bibby J.S. 1966. The stratigraphy of part of north-east Graham Land and the James Ross Island Group. British Antarctic Survey, Scientific Reports. 53: 1-37.

Björck S., Håkansson H., Zale R., Karlén W., Jönssen B.L. 1991. A Late Holocene lake sediment sequence from Livingston Island, South Shetland Islands, with palaeoclimatic implications. Antarctic Science. 3 (1): 61-72.

Björck S., Håkansson H., Olssen S., Banekow L., Janssens J. 1993. Palaeoclimatic studies in South Shetland Islands, Antarctica, base don numerous stratigraphic variables in lake sediments. Journal of Paleolimnology. 8: 233-272.

Björck S., Olsson S., Ellis-Evans C., Håkansson H., Humlum O., de Lirio J.M. 1996. Palaeogeography, Palaeoclimatology, Palaeoecology. 121: 195-220.

Bonilla S., Villeneuve V., Vincent W.F. 2005. Benthic and planktonic algal communities in a high Arctic lake : pigment structure and contrasting responses to nutrient enrichment. Journal of Phycology. 41: 1120-1130.

Brachfeld S.A., Banerjee S.K., Guyodo Y., Acton G.D. 2002. A 13 200 Year History of Century to Millennial-Scale Paleoenvironmental Change Magnetically Recorded in the Palmer Deep, Western Antarctic Peninsula. Earth and Planetary Science Letters. 194: 311-326.

Brachfeld S., Domack E., Kissel C., Laj C., Leventer A., Ishman S., Gilbert R., Camerlenghi A., Eglinton L.B. 2003. Holocene History of the Larsen-A Ice Shelf Constrained by Geomagnetic Paleointensity Dating. Geology. 31: 749-752.

Buchaca, T. & Catalan, J. 2007. Factors Influencing the Variability of Pigments in the Surface Sediments of Mountain Lakes. Freshwater Biology. 52: 1365-1379.

Buffen A., Leventer A., Rubin A., Hutchins T. 2007. Diatom Assemblages in Surface Sediments of the

Northwestern Weddell Sea, Antarctic Peninsula. Marine Micropaleontology. 62: 7-30.

Burckle L.H. & Cirilli J. 1987. Origin of Diatom Ooze Belt in the Southern-Ocean - Implications for Late Quaternary Paleoceanography. Micropaleontology. 33: 82-86.

Comiso J.C., Maynard N.G., Smith W.O., Sullivan C.W. 1990. Satellite Ocean Color Studies of Antarctic Ice Edges in Summer and Autumn. Journal of Geophysical Research-Oceans. 95: 9481-9496.

Cook A.J., Fox A.J., Vaughan D.G., Ferrigno J.G. 2005. Retreating glacier fronts on the Antarctic Peninsula over the past half-century. Science. 308: 541-544.

Cremer H., Gore D., Hultzsch N., Melles M., Wagner B. 2004. The Diatom Flora and Limnology of Lakes in the Amery Oasis, East Antarctica. Polar Biology. 27: 513-531.

Cremer H., Roberts D., McMinn A., Gore D., Melles M. 2003. The Holocene diatom flora of marine bays in the Windmill Islands, East Antarctica. Botanica Marina. 43: 82-106.

Crosta X., Denis D., Ther O. 2008. Sea Ice Seasonality During the Holocene, Adelie Land, East Antarctica. Marine Micropaleontology. 66: 222-232.

De Angelis, H. & Skvarca, P. 2003. Glacier Surge After Ice Shelf Collapse. Science. 299: 1560-1562.

Dean W.E. 1974. Determination of Carbonate and Organic-Matter in Calcareous Sediments and Sedimentary-Rocks by Loss on Ignition - Comparison With Other Methods. Journal of Sedimentary Petrology. 44: 242-248.

Domack E.W. 2002. A synthesis for Site 1098: Palmer Deep. In: Barker P.F., Camerlenghi A., Acton G.D., Ramsay A.T.S. (Eds.): Proceedings of ODP Scientific Results, 178, 1-14. (available online http://www-odp.tamu.edu/publications/178_SR/VOLUME/CHAPTERS/SR178_34.pdf [2008-10-03].

Domack E., Leventer A., Dunbar R., Taylor F., Brachfeld S., Sjunneskog C., ODP Leg 178 Scientific Party. 2001. Chronology of the Palmer Deep Site, Antarctic Peninsula: a Holocene Palaeoenvironmental Reference for the Circum-Antarctic. Holocene. 11: 1-9.

Domack E., Duran D., Leventer A., Ishman S., Doane S., Mccallum S., Amblas D., Ring J., Gilbert R., Prentice M. 2005. Stability of the Larsen B Ice Shelf on the Antarctic Peninsula During the Holocene Epoch. Nature. 436: 681-685.

Douglas M.S.V., Smol J.P. 1995. Paleolimnological significance of observed distribution patterns of chrysophyte cysts in Arctic pond environments. Journal of Paleolimnology. 13: 1-5.

Douglas M.S.V., Smol J.P. 2001. Siliceous protozoan plates and scales. Chapter 13. In: Smol J.P., Birks H.J.B., Last W.M. (Eds.). Tracking Environmental Change Using Lake Sediments. Vol. 3: Terrestrial, Algal, and Siliceous Indicators. Kluwer Academic Publishers, Dordrecht, The Netherlands: 265-279.

Evans J., Pudsey C.J., Ó Cofaigh C., Morris P., Domack E. 2005. Late Quaternary Glacial History, Flow Dynamics and Sedimentation Along the Eastern Margin of the Antarctic Peninsula Ice Sheet. Quaternary Science Reviews. 24: 741-774.

Fabrés J., Calafat A.M., Canals M., Bárcena M.A., Flores J.A. 2000. Bransfield Basin fine grained sediments: Late Holocene sedimentary processes and oceanographic and climatic conditions. Holocene. 10 (9): 703-718.

Gibson J.A.E. & Zale R. 2006. Holocene Development of the Fauna of Lake Boeckella, Northern Antarctic Peninsula. Holocene. 16: 625-634.

Grimm E.C. 1987. Coniss - a Fortran-77 Program for Stratigraphically Constrained Cluster-Analysis by the Method of Incremental Sum of Squares. Computers & Geosciences. 13: 13-35.

Grimm E.C. 1991-1993. Tilia 2.0 Version b.4 and TiliaGraph, Ilinois State Museum, Springfield, Ilinois.

Grimm E.C. 2004. TGView Version 2.0.2., Illinois State Museum, Springfield, Ilinois.

Heroy D.C. & Anderson J.B. 2005. Ice-sheet extent of the Antarctic Peninsula region during the Last Glacial Maximum (LGM) – Insights from glacial geomorphology. Geological Society of America Bulletin. 117: 1497-1512.

Heroy D.C., Sjunneskog C., Anderson J.B. 2007. Holocene climate change in the Bransfield Basin, Antarctic Peninsula: evidence from sediment and diatom analysis. Antarctic Science. DOI: 10.1017/S0954102007000788.

Hjort C., Ingólfsson Ó., Björck S. 1992. The last major deglaciation in the Antarctic Peninsula region. A review of recent Swedish Quaternary research. In: Yoshida Y., Kaminuma K., Shiraishi K. (Eds.). Recent Progress in Antarctic Earth Science, 741-743. Terra Scientific Publishing Company, Tokyo.

Hjort C., Ingólfsson Ó., Möller P., Lirio J.M. 1997. Holocene glacial history and sea-level changes on James Ross Island, Antarctic Peninsula. Journal of Quaternary Science. 12 (4): 259-273.

Hjort C., Bentley M.J., Ingólfsson Ó. 2001. Holocene and pre-Holocene temporary disappearance of the George VI Ice Shelf, Antarctic Peninsula. Antarctic Science. 13: 296-301.

Hodgson D.A. & Convey P. 2005. A 7000-Year Record of Oribatid Mite Communities on a Maritime-Antarctic Island: Responses to Climate Change. Arctic Antarctic and Alpine Research. 37: 239-245.

Hodgson D.A., Vyverman W., Sabbe K. 2001. Limnology and Biology of Saline Lakes in the Rauer Islands, Eastern Antarctica. Antarctic Science. 13: 255-270.

Hodgson D.A., Doran P., Roberts D., McMinn A. 2004. Paleolimnological studies from the Antarctic and subantarctic islands. In: Pienitz R., Douglas S.V., Smol J.P. Long-term Environmental Change in Arctic and Antarctic Lakes: 419-474. Springer, Dordrecht.

Hodgson D.A., Roberts S.J., Verleyen E., Vyverman W., Lole A. 2005. Field report – Sledge Uniform 2005-2006. Project: Natural climate variability – extending the Americas palaeoclimate transect through the Antarctic Peninsula to the pole (CACHE-PEP). Ref n°: R/2005/NT3.

Hodgson D.A., Abram N., Anderson J., Bargelloni L., Barrett P., Bentley M.J., Bertler N.A.N., Chown S., Clarke A., Convey P., Crame A., Crosta X., Curran M., di Prisco G., Francis J.E., Goodwin I., Gutt J., Massé G., Masson-Delmotte V., Mayewski P.A., Mulvaney R., Peck L., Pörtner H-O., Röthlisberger R., Stevens M.I., Summerhayes C.P., van Ommen T., Verde C., Verleyen E., Vyverman W., Wiencke C., Zane L. In Press. Antarctic climate and environment history in the pre-instrumental period. In: Turner J., Convey P., di Prisco G., Mayewski P.A., Hodgson D.A., Fahrbach E., Bindschadler R., Gutt J. (Eds.). Antarctic Climate Change and the Environment. Scientific Committee for Antarctic Research, Cambridge.

Houghton J.T., Ding Y., Griggs D.J., Noguer M., van der Linden P.J., Dai X., Maskell K., Johnson C.A. (Eds.). 2001. Climate Change 2001: The Scientific Basis. Contribution of Working Group I to the Third Assessment Report of the Intergovernmental Panel on Climate Change. New York, Cambridge University Press.

Hughen K.A., Baillie M.G.L., Bard E., Beck J.W., Bertrand C.J.H., Blackwell P.G., Buck C.E., Burr G.S., Cutler K.B., Damon P.E., Edwards R.L., Fairbanks R.G., Friedrich M., Guilderson T.P., Kromer B., McCormac G., Manning S., Ramsey C.B., Reimer P.J., Reimer R.W., Remmele S., Southon J.R., Stuiver M., Talamo S., Taylor F.W., Van Der Plicht J., Weyhenmeyer C.E. 2004 Marine04 Marine Radiocarbon Age Calibration, 0-26 cal. Kyr Bp. Radiocarbon. 46: 1059-1086.

Ingólfsson O., Hjort C., Björck S., Smith R.I.L. 1992. Late Pleistocene and Holocene Glacial History of James-Ross-Island, Antarctic Peninsula. Boreas. 21: 209-222.

Ingólfsson O., Hjort C., Berkman P., Björck S., Colhoun E., Goodwin I.D., Hall B., Hirakawa K., Melles M., Möller P., Prentice M. 1998. Antarctic glacial history since the Last Glacial Maximum: an overview of the record on land. Antarctic Science. 10: 326-344.

Ingólfsson O., Hjort C., Humlum O. 2003. Glacial and Climate History of the Antarctic Peninsula Since the Last Glacial Maximum. Arctic Antarctic and Alpine Research. 35: 175-186.

Jeffrey S.W., Mantoura R.F.C., Bjornland T. 1997. Data for the identification of 47 key phytoplankton pigments. In: Jeffrey SW, Mantoura RFC, Wright SW (Eds.): Phytoplankton pigments in oceanography, guidelines to modern methods. Monographs on oceanographic methodology (SCOR), 10, UNESCO Publishing, 447-554.

Jones V.J. & Juggins S. 1995. The Construction of a Diatom-Based Chlorophyll a Transfer Function and Its Application at Three Lakes on Signy Island (Maritime Antarctic) Subject to Differing Degrees of Nutrient Enrichment. Freshwater Biology. 34: 433-445.

Jones V.J., Juggins S., Ellis-Evans J.C. 1993. The Relationship Between Water Chemistry and Surface Sediment Diatom Assemblages in Maritime Antarctic Lakes. Antarctic Science. 5: 339-348.

Jones V.J., Hodgson D.A., Chepstow-Lusty A. 2000. Palaeolimnological evidence for marked Holocene environmental changes on Signy Island, Antarctica. The Holocene. 10 (1): 43-60.

Jones, P. D. & Limbert, D.W.S. 1989. Antarctic surface temperature and pressure data. In Bowden, T.A. (Ed.) Carbon dioxide information analysis centre. Tennessee: Oak Ridge National Laboratory, 52 pp.

Karl D.M., Tilbrook B.D., Tien G. 1991. Seasonal coupling of organic matter production and particle flux in the Antarctic Peninsula region. Deep-Sea Research. 38: 1097–1126.

Leavitt P.R. & Findlay D.L. 1994. Comparison of Fossil Pigments With 20 Years of Phytoplankton Data From Eutrophic Lake-227, Experimental Lakes Area, Ontario. Canadian Journal of Fisheries and Aquatic Sciences. 51: 2286-2299.

Leavitt P.R. & Hodgson D.A. 2001. Sedimentary pigments. In Smol JP & Last WS (Eds): Developments in palaeoenvironmental research, v. 3: Tracking environmental changes using lake sediments, biological techniques and indicators. Kluwer: 295-325.

Leventer A. 1992. Modern Distribution of Diatoms in Sediments From the George-V-Coast, Antarctica. Marine Micropaleontology. 19: 315-332.

Leventer A., Domack E., Barkoukis A., McAndrews B., Murray J. 2002. Laminations From the Palmer Deep: a Diatom-Based Interpretation. Paleoceanography. 17: art. n° 1027.

Liu X.D., Li H.C., Sun L.G., Yin X.B., Zhao S.P., Wang Y.H. 2006. Delta C-13 and Delta N-15 in the Ornithogenic Sediments From the Antarctic Maritime as Palaeoecological Proxies During the Past 2000 Yr. Earth and Planetary Science Letters. 243: 424-438.

Masson-Delmotte V., Kageyama M., Braconnot P., Charbit S., Krinner G., Ritz C., Guilyardi E., Jouzel J., Abe-Ouchi A., Crucifix M., Gladstone R.M., Hewitt C.D., Kitoh A., Le Grande A., Marti O., Merkel U., Motoi T., Ohgaito R., Otto-Bliesner B., Peltier W.R., Ross I., Valdes P.J., Vettoretti G., Weber S.L., Wolk F., Yu Y. 2006. Past and future polar amplification of climate change: climate model intercomparisons and ice-core constraints. Climate Dynamics. 26 (5): 513-529.

McMinn A. 1996. Preliminary Investigation of the Contribution of Fast-Ice Algae to the Spring Phytoplankton Bloom in Ellis Fjord, Eastern Antarctica. Polar Biology. 16 (4): 301-307.

McMinn A. 1998. Species succession in fast ice algal communities; a response to UV-B radiation? Korean Journal of Polar Research. 8: 47-52.

Moline M.A., Claustre H., Frazer T.K., Schofield O., Vernet M. 2004. Alteration of the Food Web Along the Antarctic Peninsula in Response to a Regional Warming Trend. Global Change Biology. 10: 1973-1980.

Ó Cofaigh C., Dowdeswell J.A., Allen C.S., Hiemstra J.F., Pudsey C.J., Evans J., Evans D.J.A. 2005. Flow dynamics and till genesis associated with a marine-based Antarctic palaeo-ice stream. Quaternary Science Reviews. 24: 709-740.

Parkinson C.L. 2002. Trends in the length of the Southern Ocean sea-ice season, 1979-99. In: Winther J.G., Solberg R. (Eds.). Annals of Glaciology. 34: 435-440. 4th International Symposium on Remote Sensing in Glaciology, Date: June 03-08, 2001, Univ. Maryland College pk Maryland.

Patrick R. & Reimer C.W. 1966. The diatoms of the United States, exclusive of Alaska and Hawaii, Volume 1-Fragilariaceae, Eunotiaceae, Achnanthaceae, Naviculaceae. Academy of Natural Sciences of Philadelphia Monograph No. 13, 688 pp.

Peel D.A. 1992. Spatial temperature and accumulation rate variations in the Antarctic Peninsula. In: Morris EM (Ed.), The contribution of Antarctic Peninsula ice to sea level rise. British Antarctic Survey Ice & Climate Special Report 1: 11-15.

Pudsey C.J. & Evans, J. 2001. First Survey of Antarctic Sub-Ice Shelf Sediments Reveals Mid-Holocene Ice Shelf Retreat. Geology. 29: 787-790.

Pudsey C.J., Murray J.W., Appleby P., Evans J. 2006. Lee Shelf History From Petrographic and Foraminiferal Evidence, Northeast Antarctic Peninsula. Quaternary Science Reviews. 25: 2357-2379.

Pushkar V.S., Roof S.R., Cherepanova M.V., Hopkins D.M., Brigham-Grette J. 1999. Paleogeographic and Paleoclimatic Significance of Diatoms From Middle Pleistocene Marine and Glaciomarine Deposits on Baldwin Peninsula, Northwestern Alaska. Palaeogeography, Palaeoclimatology, Palaeoecology. 152: 67-85.

Quayle W.C., Peck L.S., Peat H., Ellis-Evans J.C., Harrigan P.R. 2002. Extreme responses to climate change in Antarctic lakes. Science. 295: 645-645.

Quesada A., Fernández-Valiente E., Hawes I., Howard-Willems I. 2008. Benthic primary production in polar lakes and rivers. Chapter 10 In: Polar Books Collection:Polar Lakes and Rivers: Limnology of Arctic and Antarctic Aquatic Ecosystems. Oxford University Press, 320 pp.

Rabassa J. 1983. Stratigraphy of the glacigenic deposits in northern James Ross Island, Antarctic Peninsula. In Tills and related deposits, Ed. E. Evenson, C. Schlüchter and J. Rabassa, Rotterdam, A.A. Bakema Publishers, 329-340.

Rabassa J. 1987. Drumlins and drumlinoid forms in northern James Ross Island, Antarctic Peninsula. In Drumlin Symposium, Ed. Menzies J., Rose J., Rotterdam, A.A. Balkema Publishers: 267-288.

Reece A. 1950. The ice of Crown Prince Gustav Channel, Graham Land, Antarctica. Journal of Glaciology. 1: 404-409.

Reimer P.J., Baillie M.G.L., Bard E., Bayliss A., Beck J.W., Bertrand C., Blackwell P.G., Buck C.E., Burr G., Cutler K.B., Damon P.E., Edwards R.L., Fairbanks R.G., Friedrich M., Guilderson T.P., Hughen K.A., Kromer B., McCormac F.G., Manning S., Bronk Ramsey C., Reimer R.W., Remmele S., Southon J.R., Stuiver M., Talamo S., Taylor F.W., van der Plicht J., Weyhenmeyer C.E. 2004. Radiocarbon. 46: 1029-1058.

Renberg I. 1990. A procedure for preparing large sets of diatom slides from sediment cores. Journal of Paleolimnology. 4: 87-90.

Riaux-Gobin C. & Poulin M. 2004. Possible symbiosis of *Berkeleya adeliensis* Medlin, Synedropsis fragilis (Manguin) Hasle et al. and Nitzschia lecointei Van Heurck (Bacillariophyta) associated with land-fast ice in Adelie Land, Antarctica. Diatom Research. 19: 265-274.

Roberts D. & McMinn A. 1999. Diatoms of the saline lakes of the Vestfold Hills, Antarctica. Bibliotheca Diatomologica. 44: 83 pp.

Roberts S.J., Hodgson D.A., Bentley M.J., Smith J.A., Millar I.L., Olive V., Sugden D.E. 2008. The Holocene History of George Vi Ice Shelf, Antarctic Peninsula From Clast-Provenance Analysis of Epishelf Lake Sediments. Palaeogeography Palaeoclimatology Palaeoecology. 259: 258-283.

Round F.E., Crawford R.M., Mann D.G. 1990. The Diatoms: Biology and Morphology of the Genera. Cambridge University Press. Cambridge. 747 pp.

Rott H., Rack W., Nagler T., Skvarca P. 1998. Climatically Induced Retreat and Collapse of Northern Larsen Ice Shelf, Antarctic Peninsula. Annals of Glaciology. 27: 86-92.

Sabbe K., Verleyen E., Hodgson D.A., Vanhoutte K., Vyverman W. 2003. Benthic Diatom Flora of Freshwater and Saline Lakes in the Larsemann Hills and Rauer Islands, East Antarctica. Antarctic Science. 15: 227-248.

Scambos T., Hulbe C., Fahnestock M. 2003. Climate-Induced Ice Shelf Disintegration in the Antarctic Peninsula. Antarctic Peninsula Climate Variability: Historical and Paleoenvironmental Perspectives. 79: 79-92. International Workshop on Antarctic Peninsula Climate Variability, Date: April, 2002. Hamilton College Clinton, NY.

Scambos T.A., Bohlander J.A., Shuman C.A., Skvarca P. 2004. Glacier acceleration and thinning after ice shelf collapse in the Larsen B embayment, Antarctica. Geophysical research letters. 31 (18): Art. n° L18402.

Shevenell A., Domack E.W., Kernan G.M. 1996. Record of Holocene paleoclimate change along the Antarctic Peninsula: evidence from glacial marine sediments, Lallemand Fjord. Pap. Proceedings of the Royal Society of Tasmania. 130: 55-64.

Simoes J.C., Alencar A.S., Aquino F.E., Arevalo M., Handley M.J., Introne D., Jana R., Kurbatov A.V., Mayewski P.A., Travassos J.M., Passos H.R., Reis L.F.M. 2008. Detroit Plateau: a new ice core site in the Antarctic Peninsula. SCAR/IASC/IPY Open Science Conference: Polar Research, Arctic & Antarctic Perspectives in the International Polar Year. St-Petersburg, Russia, July, 8-11th, 2008.

Skvarca P., Rack W., Rott H., Donangelo T.I.Y. 1999. Climatic Trend and the Retreat and Disintegration of Ice Shelves on the Antarctic Peninsula: an Overview. Polar Research. 18: 151-157.

Smith H.G. 1992. Distribution and ecology of the testate rhizopod fauna of the continental Antarctic zone. Polar Biology. 12: 629-634.

Smith J.A., Bentley M.J., Hodgson D.A., Roberts S.J., Leng M.J., Lloyd J.M., Barrett M.S., Bryant C., Sugden D.E. 2007. Oceanic and Atmospheric Forcing of Early Holocene Ice Shelf Retreat, George Vi Ice Shelf, Antarctica Peninsula. Quaternary Science Reviews. 26: 500-516.

Smith W.O. & Nelson D.M. 1990. Phytoplankton growth and new production in the Weddell Sea marginal ice zone during austral spring and autumn. Limnology & Oceanography. 35: 809-821.

Smol J.P. 1983. Paleophycology of a high arctic lake near Cape Herschel, Ellesmere Island. Canadian Journal of Botany. 61: 2195-2204.

Smol J.P. 1988. Chrysophycean microfossils in paleolimnological studies. Palaeogeography, Palaeoclimatology, Palaeoecology. 62: 287-297.

Smol J.P., Douglas M.S.V. 2007. Crossing the final ecological threshold in high Arctic ponds. Proceedings of the National Academy of Sciences. 104 (30): 12395-12397.

Smol J.P., Wolfe A.P., Birks H.J.B., Douglas M.S.V., Jones V.J., Korhola A., Pienitz R., Rühland K., Sorvari S., Antoniades D., Brooks S.J., Fallu M.-A., Hughes M., Keatley E., Laing T.E., Michelutti N., Nazarova L., Nyman M., Paterson A.M., Perren B., Quinlan R., Rautio M., Saulnier-Talbot E., Siitonen S., Solovieva N., Weckström J. 2005. Climate-driven regime shifts in the biological communities of arctic lakes. Proceedings of the National Academy of Sciences. 102 (12): 4397-4402.

Squier A.H., Hodgson, D.A., Keely, B.J. 2002. Sedimentary Pigments as Markers for Environmental Change in an Antarctic Lake. Organic Geochemistry. 33: 1655-1665.

Squier A.H., Hodgson D.A., Keely B.J. 2004. A Critical Assessment of the Analysis and Distributions of Scytonemin and Related Uv Screening Pigments in Sediments. Organic Geochemistry. 35: 1221-1228.

Stuiver M. & Reimer P.J. 1993. Extended C-14 Data-Base and Revised Calib 3.0 C-14 Age Calibration Program. Radiocarbon. 35: 215-230.

Sugden D.E. 1982. Arctic and Antarctic: a modern geographical synthesis. Oxford: Basil Blackwell. 472 pp.

Taylor F., Whitehead J., Domack E. 2001. Holocene paleoclimate change in the Antarctic Peninsula: evidence from the diatom, sedimentary and geochemical record. Marine Micropaleontology. 41 (1-2): 25-43.

Taylor F., Sjunneskog C. 2002. Postglacial marine diatom record of the Palmer Deep, Antarctic Peninsula (ODP Leg 178, Site 1098) 2. Diatom assemblages. Paleoceanography. 17 (3): Art. N°8001.

Sjunneskog C., Taylor F. 2002. Postglacial marine diatom record of the Palmer Deep, Antarctic Peninsula (ODP Leg 178, Site 1098) 1. Total diatom abundance. Paleoceanography. 17 (3): Art. n° 8003.

Van de Vijver B. & Beyens L. 1997. Freshwater Diatoms From Some Islands in the Maritime Antarctic Region. Antarctic Science. 9: 418-425.

Van de Vijver B., Frenot Y., Beyens L. 2002. Freshwater diatoms from Ile de la Possession (Crozet Archipelago, Subantarctica), Bibliotheca Diatomologica. 46: 412 pp.

Van de Vijver B., Gremmen N., Smith V. 2008. Diatom communities from the sub-Antarctic Prince Edward Islands: diversity and distribution patterns. Polar Biology. 31 (7): 795-808.

Vaughan D.G. & Doake C.S.M. 1996. Recent Atmospheric Warming and Retreat of Ice Shelves on the Antarctic Peninsula. Nature. 379: 328-331.

Vaughan D.G., Marshall G.J., Connolley W.M., Parkinson C., Mulvaney R., Hodgson D.A., King J.C., Pudsey C.J., Turner J. 2003. Recent Rapid Regional Climate Warming on the Antarctic Peninsula. Climatic Change. 60: 243-274.

Verleyen E., Hodgson D.A., Vyverman W., Roberts D., McMinn A., Vanhoutte K., Sabbe K. 2003. Modelling diatom responses to climate induced fluctuations in the moisture balance in continental Antarctic lakes. Journal of Paleolimnology. 30(2): 195-215.

Verleyen E., Hodgson D.A., Sabbe K., Vanhoutte K., Vyverman W. 2004a. Coastal oceanographic conditions in the Prydz Bay region (East Antarctica) during the Holocene recorded in an isolation basin. The Holocene. 14(2): 246-257.

Verleyen E., Hodgson D.A., Sabbe K., Vyverman W. 2004b. Late Quaternary deglaciation and climate history of the Larsemann Hills (East Antarctica). Journal of Quaternary Science. 19(4): 361-375.

Vincke S., Van de Vijver B., Gremmen N., Beyens L. 2006. The moss dwelling testacean fauna of the Stromness Bay (South Georgia). Acta Protozoologica. 45: 65-75.

Wasell A., Håkansson H. 1992. Diatom stratigraphy in a lake on Horseshoe Island, Antarctica: a marine-brackish-fresh water transition with comments on the systematics and ecology of the most common diatoms. Diatom research, 7 (1): 157-194.

Wetzel R.G. 2001. Limnology: Lake and River Ecosystems. Academic Press, 1006 p.

Whitaker T.M. & Richardson M.G. 1980. Morphology and Chemical-Composition of a Natural-Population of an Ice-Associated Antarctic Diatom Navicula-Glaciei. Journal of Phycology. 16: 250-257.

Wright H.E. 1967. A square-rod piston sampler for lake sediments. Journal of Sedimentary Petrology. 37: 976.

Wright S.W., Jeffrey S.W., Mantoura R.F.C., Llewellyn C.A., Bjornland T., Repeta D., Welschmeyer N. 1991. Improved Hplc Method for the Analysis of Chlorophylls and Carotenoids From Marine-Phytoplankton. Marine Ecology-Progress Series. 77: 183-196.

Zacher K., Hanelt D., Wiencke C., Wulff A. 2007. Grazing and Uv Radiation Effects on an Antarctic Intertidal Microalgal Assemblage: a Long-Term Field Study. Polar Biology. 30: 1203-1212.

Zale R. 1994a. Changes in Size of the Hope Bay Adelie Penguin Rookery as Inferred From Lake Boeckella Sediment. Ecography. 17: 297-304.

Zale R. 1994b. C-14 Age Corrections in Antarctic Lake-Sediments Inferred From Geochemistry. Radiocarbon. 36: 173-185.

Zale R. & Karlen W. 1989. Lake Sediment Cores From the Antarctic Peninsula and Surrounding Islands. Geografiska Annaler Series A - Physical Geography. 71: 211-220.

Zeeb B.A., Smol J.P. 2001. Chrysophyte scales and cysts. (Chapter 9) In: Smol J.P., Birks H.J.B., Last W.M. (Eds.). 2001. Tracking Environmental Change Using Lake Sediments. Vol. 3: Terrestrial, Algal and Siliceous Indicators. Kluwer Academic Publishers, Dordrecht, The Netherlands: 203-223.

Chapter 8

Discussion

8.1. Introduction

Global research efforts on postglacial millennial-scale climatic changes originally focused on the North-Atlantic region, because of its important role in the modulation of the thermohaline circulation (THC), and hence in the redistribution of heat across the world. Recently, scientific attention has shifted to the Southern Hemisphere, where especially the Southern Ocean and Antarctica appeared to be important players in the regulation of global climate variations (e.g. Knorr & Lohmann, 2003; Anderson et al., 2009).

An increasing number of studies also point towards tropical regions as one of the missing pieces in our understanding of Pleistocene glacial-interglacial climate variability (Pena & Cacho, 2009). More particularly, long-term changes in frequency and amplitude of interannual/decadal modes, like El Niño Southern Oscillation (ENSO), may have played a substantial role in global climate modulation (Lamy et al., 2004; Shulmeister et al., 2006; Moreno, 2004), and at present are significantly correlated with extratropical climate modes and anomalies (e.g. Trenberth & Caron, 2000; Yuan & Martinson, 2000; Yuan 2004). The tropospheric and oceanic physical links between these (Pacific) tropical and Antarctic climate anomalies are the Southern Westerly Wind belt (SWW) and the associated Antarctic Circumpolar Current (ACC). More knowledge however is needed about past changes in the position and strength of these Westerlies, and about their link with both tropical and Antarctic climate variations, against a background of changing climate-forcing mechanisms through time. Regional climates in western South America and the Antarctic Peninsula are under direct influence of the Southern Westerlies, and therefore provide opportunities to better understand past global climate changes, through local/regional palaeoclimatic reconstructions in these areas.

In this thesis, lake sediments were analyzed for biological, sedimentological and geochemical proxies, in order to infer past climatic changes at two key sites along a latitudinal transect from southern South America (40°S) to the Antarctic Peninsula (63°S).

8.2. South America

8.2.1. Lago Puyehue: research approach

The first two chapters of this thesis deal with a reconstruction of the late Quaternary environmental history of Lago Puyehue (northern Patagonia, 40°40'S, 72°28'W). The lake is selected because of its position at the eastern side of the Andes and at the northern boundary of the Southern Westerlies, and is under direct seasonal influence of these Westerly Winds. During winter, the Westerlies cause high amounts of precipitation and a deep mixing of the lake, during summer the Westerly Wind belt shifts southward, and causes a drier climate and a stratification of the water column. Latitudinal shifts in the mean position of the Westerlies would thus most probably have resulted in, at least, changes in the seasonality of precipitation, and could be recorded in the sediments of Lago Puyehue. With its surface area of 165.4 km^2 and maximum depth of 123 m (Campos et al., 1989), this lake is one of the first large lakes that has been cored in southern South America, together with the Argentinian lakes Cardiel (48°55'S; surface area 370 km^2; maximum depth: 76 m; Gilli et al., 2005) and Mascardi (41°10'S; surface area 38 km^2; maximum depth: 200 m; Hajdas et al., 2003). The size of the lake permitted a well-considered coring site selection based on a detailed seismic survey (Charlet et al., 2008; Figure 2 in Chapter 2).

The sediment core (PU-II) is dated with 10 bulk AMS ^{14}C dates, of which one (near the base of the core) was omitted from the age-depth model. The chronology of the upper 20 cm is supported by ^{210}Pb and ^{137}Cs dating (Arnaud et al., 2006) and by varve counting (Boës and Fagel, 2008). In general, the chronostratigraphical resolution of our record is comparable to that of other studies in the region (Table 1), and shows no major inconsistencies. We consider the risk of having a problematic reservoir effect as minimal, because of (a) the volcanic nature of the catchment, (b) the water mixing to the bottom of the lake during winter, and (c) the (primarily) aquatic origin of the organic matter (see 8.2.2., and Chapter 3). Moreover, a downcore varve-chronology, anchored at 767 cm (c. 10.9 cal. ka BP) showed a basal date of c. 17.2 cal. ka BP for core PU-II (Boës and Fagel, 2008). Although the age-depth model of our core is well underpinned, the chronology may still benefit from additional radiocarbon dates from the period just before the high variability in atmospheric ^{14}C concentrations (i.e. before 12.9-11.1 cal. ka BP; Hughen et al., 2000), in order to better constrain the age uncertainties of the point where the varve sequence is anchored to the radiocarbon chronology. This would permit us to make detailed comparisons with the records of e.g. Hajdas et al. (2003), where 20 radiocarbon dates were used in a time frame of c. 5000 years (i.e. between 9695 ± 90 and

14,450 ± 110 ^{14}C BP). Additionally, some more dates downcore from 767 cm, and a detailed microscopical re-examination of the varves in different sections of the core may further confirm (or reject) the inferred yearly nature of the varves between 767 and 1122 cm depth.

Environmental reconstruction in the L. Puyehue record was primarily based on fossil diatoms (Chapter 2) and on organic matter content and composition (Chapter 3). In the large Patagonian lakes at 40°S, diatoms mainly occur during the winter mixing period, with the tychoplanktonic genus *Aulacoseira* dominating over more oligotrophic species like *Cyclotella* cf. *stelligera*. During summer, mainly chlorophytes and cyanobacteria prevail (Campos 1989). We link high diatom biovolumes (mainly driven by the productivity of *Aulacoseira* spp.) to high nutrient availability and/or well-mixed water columns. Changes in the relative abundance of *Aulacoseira* and *Cyclotella* are then interpreted as changes in nutrient availability caused by (a) altered mixing regimes and (b) changing precipitation patterns, which in turn are both influenced by temperature and wind stress.

Carbon and nitrogen content of the sedimentary organic matter was used to partition total organic carbon (TOC) into an aquatic and a terrestrial component (Chapter 3). The rationale behind this approach was to be able to trace changes in both catchment development and in total phytoplankton productivity. In order to calculate these organic aquatic and terrestrial fractions in the core, we measured the N/C values of different aquatic and terrestrial sources and specifically selected some of these "end-members" to serve as aquatic (i.e. lake particulate organic matter) and terrestrial (i.e. Holocene paleosols) parameters in a mixing equation. In addition, a "biogenic silica index", based on the ratio between the biogenic silica (Bertrand et al., 2008) versus aquatic organic carbon concentrations, was developed to evaluate the relative importance of the diatoms in the whole aquatic community.

8.2.2. Paleoclimatic interpretations

8.2.2.1. Paleoclimate studies in Patagonia

Since the start of the ENSO-Chile project (see 1.2. in this thesis) and since the publication of Sterken et al. (2008; see Chapter 1) the number of palaeoclimatic reconstructions in southern South America has increased considerably. An overview of paleo-environmental studies from the region between 33°S and 55°S is given in Fig. 1, and includes an update on the recent literature. While early research in this region was

mainly based on combined geomorphology and geochronology (e.g. Bentley, 1997; Denton et al., 1999), most of the recent studies are based on pollen and charcoal records from peat bogs, mires and - to a lesser extent - lakes (e.g. Hajdas et al., 2003; Fig. 1). Recently, lacustrine chironomid records (Massaferro et al., 2009) and marine sediment cores (e.g. Lamy et al., 2004; 2007; Mohtadi et al., 2008; Boyd et al., 2008) have been added to these studies. The studies in Chapters 2 and 3 of this thesis are unique in being part of a multiproxy approach that not only combines sedimentological and pollen proxies, but also varve-, geochemical- and diatom-based reconstructions. In fact, the results from Chapter 2 are one of the first diatom-based climate reconstructions in southern South America, apart from the large (Argentinian) lakes Mascardi and Cardiel (Markgraf et al., 2003; Wille et al., 2007), and a few diatom-based limnological reconstructions covering the last century (Urrutia et al., 2000; Cruces et al., 2001).

From the overview in Fig. 1, some general trends can be observed. Many records show a first deglaciation or warming step at c. 18.2-17.6 cal. ka BP. This is observed at nearly all latitudes, but was centered around 17.2 cal. ka BP in southern Patagonia (Sugden et al., 2005; McCulloch & Davies, 2001), and at 17.8 cal. ka BP in northern Patagonian terrestrial records (e.g. Moreno & Léon, 2003). Interestingly, the marine records of Lamy et al. (1999) and Lamy et al. (2004, 2007) show an earlier start (18.2 and 18.8 ka BP respectively) of drier conditions and SST increase than most terrestrial based records (Fig. 1).

The climate studies between 33 and 36°S all agree in showing a progressively decreasing trend of Westerly Wind influences towards 10 cal. ka BP. However, at 40-41°S there is some degree of controversy about the possible influence of a cold reversal coinciding with the Antarctic Cold Reversal (14.0-12.5 ka BP; Jouzel et al., 2001), the northern hemispheric Younger Dryas (12.89-11.65 ka BP; Stuiver et al., 1995) or during the so-called Huelmo-Mascardi cold reversal (HMCR; 11.4-10.2 ^{14}C ka BP or c. 13.5-11.5 cal. ka BP; Hajdas et al., 2003). This HMCR is usually interpreted as a cool and dry period, mainly deduced from pollen and chironomids in lake sediments from 41°S in southern South America (Fig. 1; Moreno & Léon, 2003; Massaferro et al., 2009). Similarly, although less well constrained, glacier advances or stabilisations were observed between c. 15.0 and 12.8 cal. ka BP in the region between 46 and 51°S (Turner et al., 2005b; Moreno et al., 2009; Sugden et al., 2005). However, such a temperature stagnation or reversal has not been observed in records from 44°S (Haberle & Bennett, 2004; Bennett et al. 2000), and has provoked considerable scientific debate.

During the Early Holocene, a warm and dry climate was observed in nearly all sites between 33 and 55°S, although there are many discrepancies in the exact timing of this

period (Fig. 1). Also, this generalization does not apply for all sites, as it would be an oversimplification of records where winter precipitation increased and summers became drier during the Early Holocene (e.g. Markgraf et al., 2007).

In a similar way, the Late-Holocene could be summarized as a period of enhanced climate variability in the entire Patagonian region (Fig. 1), with increasingly wetter conditions in most of the sites. In North-Patagonia (especially between 33 and 38°S, where seasonal precipitation is currently strongly linked with El Niño; Montecinos & Aceituno, 2003), this was attributed to an increased seasonal influence of the Westerlies. At higher resolution, however, the millennial- to centennial scale climate variations were more difficult to compare between sites, partly due to dating constraints and the lack of high resolution records.

8.2.2.2. Lago Puyehue: deglaciation of the lake, and catchment development

The presence of high diatom abundances starting at the base of the core (1,122 cm; 17.9 cal. ka BP) and the absence of coarse glacial debris at any depth in the core led us to conclude that the lake was deglaciated before 17.9 cal. ka BP. This timing narrows down previous age ranges of the lake's deglaciation, which was broadly placed between c. 23.2 and 14.1 cal. ka BP (19,500-12,230 ^{14}C yr. BP; Bentley, 1997; see Fig. 5 in Chapter 2). This retreat roughly corroborates the widely accepted dating of the Patagonian Ice Sheet LGM stage between 25,000 and 23,000 BP, with a third less extensive maximum centered at 17,500 BP (Sugden et al., 2005).

The N/C analyses (Chapter 3) generally revealed that the organic carbon in the lower part of the core (between 17.9 and 12.8 cal. ka BP) was almost entirely of aquatic origin. This indicates that (1) dating in this part of the core was not influenced by old catchment-derived carbon, and thus did probably not suffer from a carbon reservoir effect, and (2) that the catchment vegetation (at least to the east of the lake) only started to develop after 12.8 cal. ka BP, suggesting the presence of a glacier in the catchment area between 17,900 and 12.8 cal. ka BP. The influence of a glacier from the lake watershed was mentioned in Chapter 2 as a possible explanation for the low diatom concentrations, the low LOI_{550} values and the presence of a smectite type of clay (Bertrand et al., 2006) between c. 17.9 and 12.8 cal. ka BP. The additional analyses in Chapter 3 increased the plausibility of this interpretation.

8.2.2.3.: Deglacial warming step in Lago Puyehue

At c. 17.3 cal. ka BP, a sudden increase in diatom productivity was observed, with an increase in terrestrial organic carbon at c. 16.0 cal. ka BP. These changes coincide with a

warming/deglaciation step found in many terrestrial records of Patagonian Ice Sheet deglaciation (McCulloch et al. 2000; Fig. 1). However, this event lags behind the start of a 5°C rise in SST off the Chilean coast at 41°S, which occurred between 18.8-16.7 ka BP (Lamy et al., 2007) or 2-3°C between 19.2-17.4 ka BP (Lamy et al., 2004).

If dating is correct in both cores, and if the warming inferred from the Puyehue record was not preceded by a warming before 17.9 cal. ka BP (i.e. the bottom age of our core), then this lag could be explained by feedback mechanisms caused by the presence of a glacier in the catchment of the lake. The initial increase in SST may, for example, have caused an increased moisture advection to the North-Patagonian Ice Sheet (NPIS), causing a stagnation in the mass balance of the associated glaciers. A similar mechanism is assumed to have caused a delayed decrease in Fe-concentrations and salinity at the oceanic ODP-1233 site reflecting melting of the Ice Sheet and glaciers between 17.8 and 15.8 cal. ka BP (41°S; Lamy et al., 2004).

8.2.2.4. Lago-Puyehue: late-glacial cooling or reversal

The Lago Puyehue diatom record (Chapter 2) shows no clear evidence for a rapid and short-lived late-glacial cooling event at the time of the Antarctic Cold Reversal, the Huelmo-Mascardi event, or the northern hemispheric Younger Dryas cold episode. However, there are indications that some climate instability may have occurred between 13.4 and 11.7 cal. ka BP during/after a relatively long period (between 16.9 and 12.8 cal. ka BP) of low absolute diatom abundances and biovolumes.

A major increase in diatom abundances and biovolumes was observed between 12.8-11.8 cal. ka BP, but could originally be explained by different mechanisms (Chapter 2). Diatom biovolumes in the core are strongly driven by the genus *Aulacoseira*, which thrives well in comparably nutrient rich, well-mixed waters (see Chapter 2). Depending on whether (a) nutrients and light, or (b) temperature were the most limiting factors for the growth of *Aulacoseira*, both a warming or cooling climate could explain the increase in diatom biovolumes. Despite this uncertainty, we interpreted the diatom biovolume increase as mainly reflecting a wetter/windier, and perhaps also warmer period (Chapter 2). In Chapter 3, the observed increase in diatom biovolumes and silica content coincided with a major increase in amount of terrestrial organic matter. This was interpreted in terms of enhanced catchment development and the final retreat of any glacier remnants in the Puyehue catchment area, caused by a major warming pulse.

The timing of this warming coincides with an important rise in SST observed between 12.7 and 12.1 cal. ka BP at the marine ODP-1233 site (41°S; Lamy et al., 2004,

2007), and with the retreat of glaciers at 46-48° and 51°S (Fig. 1; Turner et al., 2005b; Moreno et al., 2009). Such an increase in SST off the Chilean coast could well explain the high diatom biovolumes, because (under assumption of unchanged wind speeds) a rise in SST would cause an increased atmospheric advection of warmth and moisture to the Chilean coast. Still, we cannot explain the apparent discrepancies with the pollen record of Lago Puyehue which points to warm and dry conditions (Vargas-Ramirez et al., 2008), and with the Huelmo-Mascardi (cold, dry) event observed at 41°S (c. 13.5-11.5 cal. ka BP; Hajdas et al., 2003). We can, however, conclude, that a climate cooling similar to (and coinciding with) the Northern Hemisphere Younger Dryas chronozone [12.89-11.65 cal. ka BP; Stuiver et al. (1995)] was not evident in our record. This corroborates the arguments that the Younger Dryas was not expressed as a Southern Hemispheric or global cooling, but that any Patagonian glacier advances may have been more related to changes in the Southern Hemispheric Westerly circulation (e.g. Ackert et al., 2008).

8.2.2.5. Lago-Puyehue: The Holocene

The Holocene epoch was characterized by an abundant vegetation cover probably linked to high temperatures, and by several centennial-scale changes in lake plankton and terrestrial vegetation. The N/C ratios revealed that during the Holocene, changes in TOC (and thus in LOI_{550} as was measured in Chapter 1) were mainly driven by changes in input of terrestrial organic matter. After 9.6 cal. yr. BP, stronger and more persistent summer stratification may have been the result of higher temperatures associated with an Early Holocene thermal optimum.

Towards the Mid-Holocene lower precipitation values, culminating at 5.0 cal. ka BP, were tentatively inferred from the lower total diatom abundances and a temporary disappearance of epiphytic taxa in the core. The mid- and late-Holocene were characterized by high centennial to millennial variability in both total diatom abundances and sedimentological proxies (Chapters 2, 3 and Bertrand et al., 2008). This probably reflects enhanced climate variability, as was also observed in records elsewhere in South America. Still, an observed increase in volcanic activity between c. 6.9-3.3 cal. ka BP (Bertrand et al., in press) may also have influenced the total diatom and organic matter concentrations in the core (see Chapter 3). An increase in both *Cyclotella* and *Aulacoseira* during the last 3000 years was tentatively interpreted in terms of changing precipitation seasonality, possibly linked with an increased frequency of El Niño occurrences. This is supported by modern-day measurements which show that El Niño currently leads to drier summers and slightly moister winters in the Puyehue area.

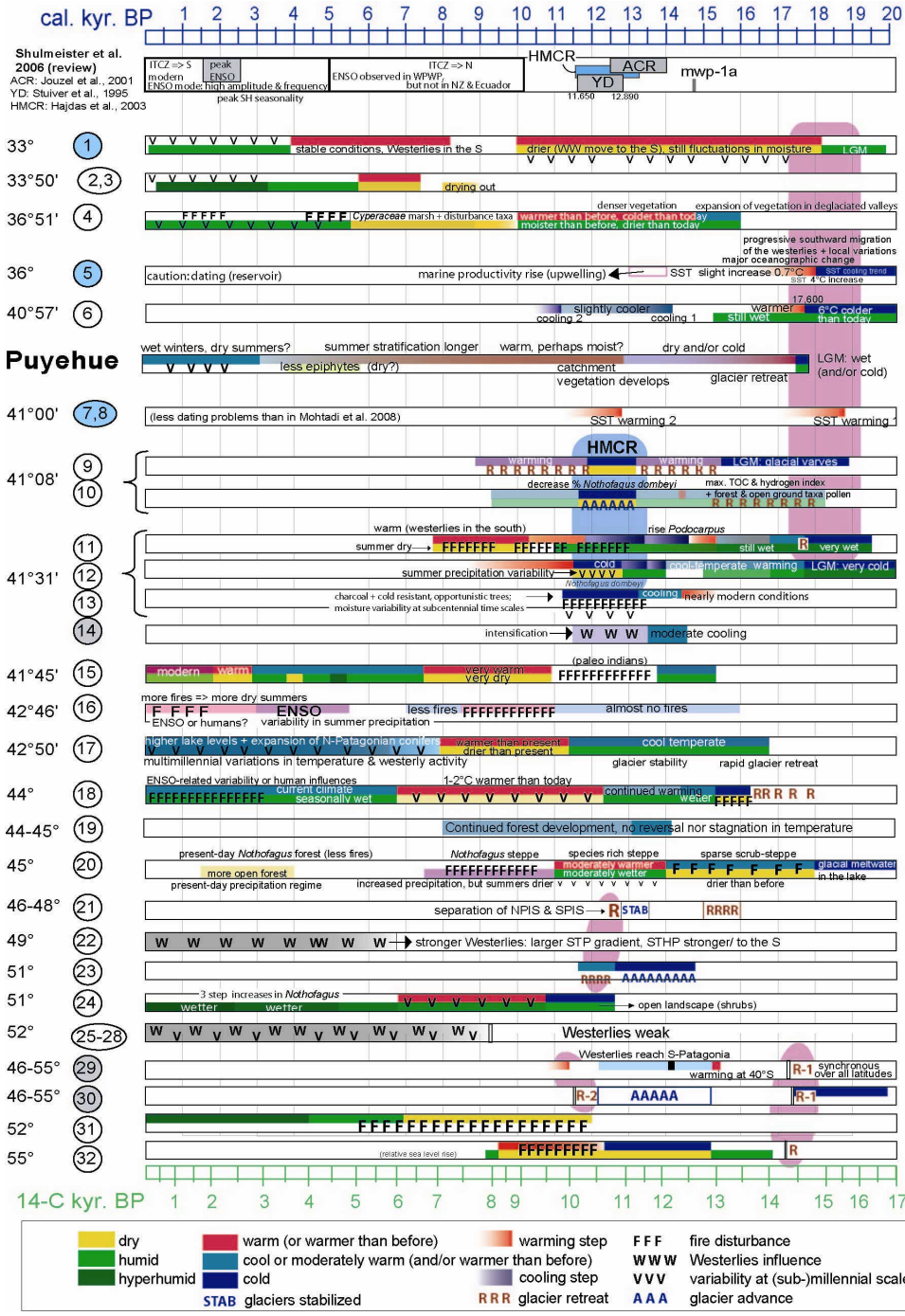
cal. kyr. BP
1 2 3 4 5 6 7 8 9 10 11 12 13 14 15 16 17 18 19 20
Shulmeister et al. 2006 (review)
ACR: Jouzel et al., 2001
YD: Stuiver et al., 1995
HMCR: Hajdas et al., 2003
ITCZ => S
peak ENSO
modern ENSO mode: high amplitude & frequency
peak SH seasonality
ITCZ => N
ENSO observed in WPWP, but not in NZ & Ecuador
HMCR
ACR
YD
11.650
12.890
mwp-1a
33°
1
stable conditions, Westerlies in the S
drier (WW move to the S), still fluctuations in moisture
LGM
33°50'
2,3
drying out
36°51'
4
Cyperaceae marsh + disturbance taxa
denser vegetation
expansion of vegetation in deglaciated valleys
warmer than before, colder than today
moister than before, drier than today
36°
5
progressive southward migration of the westerlies + local variations
major oceanographic change
caution: dating (reservoir)
marine productivity rise (upwelling)
SST slight increase 0.7°C
SST cooling trend
SST 4°C increase
40°57'
6
17.600
slightly cooler
cooling 2
cooling 1
warmer
still wet
6°C colder than today
Puyehue
wet winters, dry summers?
summer stratification longer
warm, perhaps moist?
dry and/or cold
less epiphytes (dry?)
catchment vegetation develops
glacier retreat
LGM: wet (and/or cold)
41°00'
7,8
(less dating problems than in Mohtadi et al. 2008)
SST warming 2
SST warming 1
41°08'
9
10
HMCR
Warming
Warming
LGM: glacial varves
decrease % Nothofagus dombeyi
max. TOC & hydrogen index
+ forest & open ground taxa pollen
41°31'
11
12
13
14
warm (westerlies in the south)
rise Podocarpus
summer dry
still wet
very wet
summer precipitation variability
cold
cool temperate
warming
LGM: very cold
Nothofagus dombeyi
charcoal + cold resistant, opportunistic trees; moisture variability at subcentennial time scales
cooling
nearly modern conditions
intensification
moderate cooling
41°45'
15
modern
warm
very warm
very dry
(paleo indians)
42°46'
16
more fires => more dry summers
ENSO or humans?
ENSO
variability in summer precipitation
less fires
almost no fires
42°50'
17
higher lake levels + expansion of N-Patagonian conifers
warmer than present
drier than present
cool temperate
multimillennial variations in temperature & westerly activity
glacier stability
rapid glacier retreat
44°
18
ENSO-related variability or human influences
current climate
seasonally wet
1-2°C warmer than today
continued warming
wetter
44-45°
19
Continued forest development, no reversal nor stagnation in temperature
45°
20
present-day Nothofagus forest (less fires)
more open forest
present-day precipitation regime
Nothofagus steppe
increased precipitation, but summers drier
species rich steppe
moderately warmer
moderately wetter
sparse scrub-steppe
drier than before
glacial meltwater in the lake
46-48°
21
separation of NPIS & SPIS
STAB
49°
22
stronger Westerlies: larger STP gradient, STHP stronger/ to the S
51°
23
51°
24
3 step increases in Nothofagus
wetter
wetter
open landscape (shrubs)
52°
25-28
Westerlies weak
46-55°
29
Westerlies reach S-Patagonia
warming at 40°S
R-1
synchronous over all latitudes
46-55°
30
R-2
R-1
52°
31
55°
32
(relative sea level rise)
14-C kyr. BP
1 2 3 4 5 6 7 8 9 10 11 12 13 14 15 16 17
dry
humid
hyperhumid
warm (or warmer than before)
cool or moderately warm (and/or warmer than before)
cold
STAB glaciers stabilized
warming step
cooling step
RRR glacier retreat
FFF fire disturbance
WWW Westerlies influence
VVV variability at (sub-)millennial scale
AAA glacier advance

Figure 1 *(opposite page):* Overview of recent literature on the deglacial and Holocene climate variability recorded in southern South America. The locations of the sites are shown in Fig. 3, the corresponding publications and authors are listed in Table 1. Blue encircled numbers represent marine cores, grey circles represent summaries, reviews or references to other literature sources.

Table 1: List of references shown in Figs. 1 and 3, and their corresponding study area or site names.

1	Lamy et al., 1999	GeoB 3302, GIK 17748-2
2	Jenny et al., 2003	Laguna Aculeo
3	Villa-Martinez et al., 2004	Laguna Aculeo
4	Markgraf et al., 2009	Neuquen, Argentina
5	Mohtadi et al., 2008	GeoB 7165-1
6	Moreno et al., 1999	Canal de la Puntilla
7	Lamy et al., 2004	ODP 1233
8	Lamy et al., 2007	ODP 1233
9	Ariztegui et al., 1997	Laguna Mascardi
10	Hajdas et al. 2003	Laguna Mascardi
11	Moreno & Léon, 2003	Huelmo site
12	Massaferro et al. 2009	Huelmo site
13	Hajdas et al. 2003	Huelmo site
14	Moreno et al., 2009	Torres del Paine (4 mires)
15	Moreno, 2004	Lago Condorito
16	Abarzua & Moreno, 2008	Isla Grande de Chiloé
17	Abarzua et al., 2004	Isla Grande de Chiloé
18	Haberle & Bennett, 2004	Chonos Archipelago
19	Bennett et al., 2000	Chonos Archipelago
20	Markgraf et al., 2007	Mallin Pollux, Coyhaique
21	Turner et al., 2005b	N-Patagonian Ice Sheet, E-Andes
22	Gilli et al., 2005	Lago Cardiel
23	Moreno et al., 2009	Torres del Paine (4 mires)
24	Villa-Martinez & Moreno, 2007	Torres del Paine (Vega Nandu)
25	Mayr et al., 2007	Laguna Potrok Aike
26	Haberzettl et al., 2005	Laguna Potrok Aike
27	Haberzettl et al., 2007	Laguna Potrok Aike
28	Haberzettl et al., 2008	Laguna Potrok Aike
29	McCulloch et al., 2000	Patagonia (review)
30	Sugden et al., 2005	Strait of Magellan region
31	Huber et al., 2004	S-Patagonia
32	McCulloch & Davies, 2001	Strait of Magellan

8.2.2.6. Lago-Puyehue: summary

In conclusion, the Puyehue record exhibits two major changes, which, at sub-orbital time scales broadly coincided with two major climate changes recorded in most sites from southern South America (Fig. 1). Although the deglaciation of the lake and its catchment had started before 17.9 cal. ka BP, an abrupt change was observed at c. 17.3 cal. ka BP in the Puyehue record, marked by very high diatom biovolumes, immediately followed by a minor increase in terrestrial vegetation. This was tentatively interpreted as a warming, and broadly coincided with a warming or deglaciation step recorded in other terrestrial records in Patagonia, but lagging behind the start of an SST increase off the Chilean coast at 41°S by c. 1000 years (Lamy et al., 2004). This lag could be explained by feedback mechanisms caused by the presence of a glacier in the catchment of the lake at that time.

The second major change in the record, occurring between c. 12.8 and 11.8 cal. ka BP, was marked by a steep increase in diatom productivity and by the expansion of vegetation in the Puyehue catchment area (Chapters 2 and 3). This increase, tentatively interpreted as a rise in temperature and precipitation, coincides with an important warming in SST observed between 12.7 and 12.1 cal. ka BP at the marine ODP-1233 site (41°S), and with the retreat of glaciers at 46-48° and 51°S (Fig. 1). Although discrepancies still exist both in the timing of events and the interpretation of proxies (e.g. diatoms vs. pollen), we can still conclude that a climate cooling similar to and coinciding with the Northern Hemisphere Younger Dryas period (12.89-11.65 cal. yr. BP) was not evident in our record.

The diatom compositions in the upper part of the core were tentatively interpreted in terms of a changing precipitation seasonality, which could be linked with increased El Niño occurrences (Montecinos & Aceituno, 2003). An increased centennial- to millennial variability was observed, as has been observed in most of the Patagonian paleoclimate studies (Fig. 1). However, at present, detailed interpretations about these short-term climate changes are not possible because higher resolution analyses are still lacking.

8.3. The Antarctic Peninsula

The second site studied in this thesis was Beak Island (63°S), located at the southern end of the Patagonian-Antarctic paleoclimate transect. Beak Island is situated at the (north)eastern side of the Antarctic Peninsula, an area which - in contrast to the northwestern side - is virtually unexplored in terms of terrestrial climate records. Studies in this region however are important in order to further extend our understanding of the climate evolution east of the Peninsula. Indeed, today's climate differs significantly between the Weddell Sea area and the western side of the Antarctic Peninsula.

8.3.1. Beak Island: research approach

In Antarctica, coastal lakes are very interesting for reconstructing climate, because they quickly respond to changes in climate, due to their size and relatively simple ecosystem structure (see Chapter 6). Isolation lakes, which have emerged from the sea after isostatic recovery of the land, are particularly interesting because they contain marine as well as freshwater sediment layers that can inform us about former coastal oceanographic conditions and relative sea level changes (e.g. Bentley et al., 2005b). Moreover, they have the advantage of being less hampered by problematic dating than many deep-sea marine cores, since reservoir problems can be partly controlled of, by radiocarbon dating of the freshwater part of the cores.

The lakes cored on Beak Island are basins that were isolated from the sea during the Holocene. The sediment core from the deepest lake (Beak-1; 24 m deep) is chosen as a starting point for paleoclimatic reconstructions on Beak Island, because the depth of the lake makes it less prone to drying out at any time during the past, and because its high position above sea level resulted in a longer paleoclimatic record. Apart from this core, an additional record from the shallow Lake Beak-2 was investigated. Although this lake is only 4 m deep and dating is less certain than in Beak-1 (see Chapter 6), past oceanic and limnological inferences made for Beak-2 corroborate some of the paleoclimatic signals interpreted from Beak-1 (see 8.3.2.).

Because pollen and many faunal proxies are not present in Antarctic lake sediments, algal/cyanobacterial pigments and diatoms are one of the primary biological proxies for reconstructing paleo-environments in Antarctic terrestrial areas. In order to maximize the use of diatoms as paleo-environmental indicators, reference datasets are used to constrain their current ecological preferences by examining their distributions in a set of contemporary lakes covering a wide range of values for several environmental variables

of interest. The value and applicability of these reference datasets critically depends upon consistent species delineations. To date, only a few diatom reference datasets exist for (sub-) Antarctica, and many of the earlier diatom studies used northern hemispheric diatom flora to identify the diatoms. This has often resulted in a 'force-fitting' of unique Antarctic diatom species to existing taxa (cf. Sabbe et al., 2003, for a detailed discussion of this problem).

Recent taxonomic and systematic studies in (sub-) Antarctica have revealed the presence of many new Antarctic endemic species, many of which had previously been misidentified as existing northern hemispheric species. These recent insights are changing our views on the biogeography of certain groups of micro-organisms (e.g. Vyverman et al., 2007; Verleyen et al., in press). For these reasons, we first re-investigated and extended an existing diatom calibration database (Jones et al., 1993; Jones & Juggins, 1995) from Maritime Antarctica, providing a systematic update and description of the diatom communities in this dataset (Chapter 4). We described five new species (Chapter 5), belonging to the genera *Chamaepinnularia*, *Craticula*, *Diadesmis* and *Navicula*. Some of these were previously reported under other names (or in other studies from the Antarctic region (e.g. Sabbe et al., 2003; Jones et al., 1993; Jones & Juggins, 1995). These new species add further evidence for significant endemism among Antarctic diatoms (Sabbe et al., 2003; Vyverman et al., 2007).

In Chapter 6, we reanalysed this intercalibrated and expanded dataset, in order to link diatoms species distributions to ecological gradients. Diatom species composition in the six Beak Island samples was intermediate between that of the Livingston and Signy Islands, with the shallowest lakes (Beak 3-6) being more similar to the Livingston coastal lakes (i.e. 'group 3' in Jones et al., 1993), and the deeper lakes (Beak-2; depth: 4 m, and Beak-1: depth 24 m) being more similar to the Signy and Livingston inland sites respectively (see Chapter 6). We subsequently used the dataset to construct quantitative inference models (transfer functions) for reconstructing NH_4^+ concentrations in both lakes Beak-1 and Beak-2. This, together with measured fossil pigment compositions allowed us to infer past changes in the lakes environment (see 8.3.2.). Lake Beak-1 is an outlier in terms of depth in the calibration dataset. This has consequences for the application of a depth transfer function on the fossil diatom record from this lake, and may also result in different responses of the benthic diatom communities to nutrient enrichment in the lake (e.g. Bonilla et al., 2005).

In Chapters 6 and 7, we investigated assemblages of siliceous microfossils and fossil pigments in sediment cores from Lakes Beak-1 and Beak-2, in order to reconstruct past changes in oceanic and climate conditions during the entire Holocene. We applied the NH_4^+ transfer function on the freshwater sections of both cores, as a proxy for past nutrient levels in the lakes.

8.3.2. Paleoclimatic interpretations

8.3.2.1. Paleoclimate studies in the Antarctic Peninsula

An overview of paleoclimatic studies from the Antarctic Peninsula (AP) is given in Fig. 2. As for the South American records, some general climate trends could be distilled from the climate studies in and around the AP, although many inconsistencies or shifts in the timing of warm and cold events do exist [see also Bentley et al. (2009); Hodgson et al. (in press) and Ingólfsson (2004) for reviews].

Although there is a deficiency of radiocarbon dates constraining the deglaciation from the Antarctic Peninsula shelf area, some trends could be observed. In general, the initial retreat of the grounded ice from outer shelf zones occurred around 18.5 cal. ka BP, and deglaciation of the outer and middle shelf was still ongoing in many sites by 13.0 cal. ka BP. Early deglaciation of inner shelf areas occurred by 11.0 cal. ka BP, but most other inner shelf sites only deglaciated by 8.0-6.0 cal. ka BP (Fig. 2; Ingólfsson et al., 2004; Heroy & Anderson, 2005). Deglaciation seems to have started earlier in the northern and western parts of the AP (e.g. Palmer Deep: 13.3-11.0 cal. ka BP vs. the Larsen region: 10.7-10.5 cal. ka BP; Fig. 2). Because many marine sites, and almost all terrestrial sites, were glaciated or strongly influenced by glacial deposits, climate and environmental conditions at the start of the Holocene are not well known in the AP.

A composite of isotopic temperature proxies in Antarctic ice cores revealed an Antarctic-wide Early Holocene climate optimum (c. 11.5-9.2 cal. ka BP; Masson et al., 2000). However, one of the rare Early-Holocene environmental reconstructions that exist for the AP region reported a rapid deglaciation (11.0-10.0 cal. ka BP) followed by cold proxy results between 10.0 and 8.0 cal. ka BP, which would conflict with such an Early Holocene optimum (see Figs. 2 and 3; Palmer Deep marine site; Sjunneskog & Taylor, 2002; Domack, 2002).

Shortly after the Early Holocene warm period, some ice shelves from the western side of the AP experienced an early collapse. The George VI shelf (Bentley et al. 2005b; Smith et al., 2007; Roberts et al., 2005) was absent between c. 9.60 and 7.73 cal. ka BP,

while at Palmer Deep (NW-AP) advection of warm water was inferred (Fig. 2). In contrast, ice shelves to the east of the peninsula did not disappear during the Early Holocene (Domack et al., 2005).

In the presently ice-free terrestrial regions, deglaciation began as early as 9.5 cal. ka BP, as observed from early lake sedimentation records (Hodgson et al., in press). There is, however, large variability in the timing of ice margin retreat, as some areas were only ice-free by 5.0-3.0 cal. ka BP (Björck et al., 1991; 1996).

This patchiness in terrestrial deglaciation timing is superadded by records of Mid-Holocene glacier advances, that could be explained[3] by both increased precipitation through advection of warm, humid air from cyclonic Westerly storm tracks), or by increased influence of the anticyclonic cold barrier winds that bring cold, arid air masses from the south(east) (Hjort et al., 1997). Some freshwater and marine based studies indicate colder temperatures for this period between c. 5.3 and 3.0 cal. ka BP, but the evidence is sparse and dating is often poor (see Fig. 2), and in Palmer Deep no Mid-Holocene glacial event was detected (Domack et al., 2001). More well-dated high-resolution paleoclimate reconstructions for this period in the northeastern margin of the Antarctic Peninsula are needed to resolve this issue.

The Mid-Holocene is generally marked by significant warming in many Antarctic Peninsula climate records (Hodgson et al., in press). However, the timing of this warm period often differs a few hundred years, e.g. starting earlier and lasting longer in the well-dated records from Signy Island (Jones et al., 2000; Hodgson & Convey, 2005) than on Livingston Island (Björck et al., 1991). Moreover, on James Ross Island an increase in lake productivity was interpreted in terms of a cooling climate between c. 3.0 and 1.4 cal. ka BP (Björck et al., 1996). In marine records from the northeast AP, ice shelf collapses or fluctuations were recorded between c. 5.0 and 1.4 cal. ka BP (Brachfeld et al., 2003; Pudsey & Evans, 2001; Hodgson et al., in press).

This Mid-Holocene 'Hypsithermal' (MHH) was followed by a climate deterioration or neoglacial cooling in all regions of the Antarctic Peninsula (Fig. 2). Lake sediment studies from Livingston Island recorded a gradually deteriorating climate, with a warm pulse centred around c. 2.0 cal. ka BP, and a cold pulse between 1.5 and 0.5 cal. ka BP (Björck et al., 1991). In the South Orkneys the hypsithermal ended, and penguin populations declined at c. 1.4-1.3 cal. ka BP (Jones et al., 2000; Hodgson & Convey, 2005; Liu et al., 2006). This timing corresponds with the timing of ice shelf reformation in the northeastern AP (Pudsey & Evans, 2001; Brachfeld et al., 2003), but is

[3] Under the assumption that sea level changes did not have an impact on the marine-based glaciers (Hjört et al., 1997)

significantly later than the cooling conditions observed in marine sites to the south and west of the AP (c. 2.7 cal. ka BP; see Fig. 2 and Taylor et al., 2001; Domack et al., 2001). Further, ice shelf advances, glacier oscillations and penguin population declines in recent times have been associated with the Little Ice Age (Domack et al., 1995; Björck et al., 1996; Fabrés et al., 2000; Liu et al., 2006).

8.3.2.2. Beak Island: Early Holocene period

Results of lithological, diatom and fossil pigment analyses showed that Lake Beak-1 was below sea level between c. 10.6 cal. ka BP and 6.0 cal. ka BP (Chapter 7). The presence of marine sediments at c. 10.6 cal. ka BP provided a minimum age for deglaciation near the site. The geomorphology of the basin excluded the possibility of an ice sheet or shelf over the site at any time, but high amounts of coarse sediments, very low diatom and pigment abundances and bad preservation of the diatoms pointed towards the presence of high iceberg concentrations at the site, which explained the rapid sedimentation rates observed in the bottom part of the core. The near absence of open water diatom species suggests that this occurred under cold conditions (Chapter 7).

Our minimum age for deglaciation corresponds relatively well with other dates given for deglaciation in the shelf regions to the east and south of Beak Island (see Fig. 2; c. 10,500 - 10,700 ^{14}C BP and 10,700 BP for the Larsen-B region, Erebus and Terror Gulf, and Greenpeace Trough respectively; Heroy & Anderson, 2005; Domack et al., 2005; Brachfeld et al., 2003). Minimum deglaciation of nearby terrestrial sites was dated later (e.g. Hope Bay: c. 6300-5500 ^{14}C BP; Zale 1994; northern James Ross: 7.4 cal. ka BP; Hjort et al., 1997), and could be explained by the particular morphology of Beak Island, and its northeastwards position with respect to to James Ross Island.

At c. 9.2 cal. ka BP, seasonally open marine conditions were deduced from the high abundances of *Chaetoceros* resting spores, higher concentrations of (unbroken) valves, and smaller sediment grain size. This broadly corresponded with the early retreat/disintegration of the ice shelf in the southern Prince Gustav Channel around 8.7-7.4 cal. ka BP (Hey et al., pers. comm.), and with the onset of a prolonged ‘warm’ period in the Palmer Deep marine record (Domack et al., 2001; Fig. 2). These conditions of high diatom productivity remained until the isolation of the Beak-1 basin, at c. 6.0 cal. ka BP.

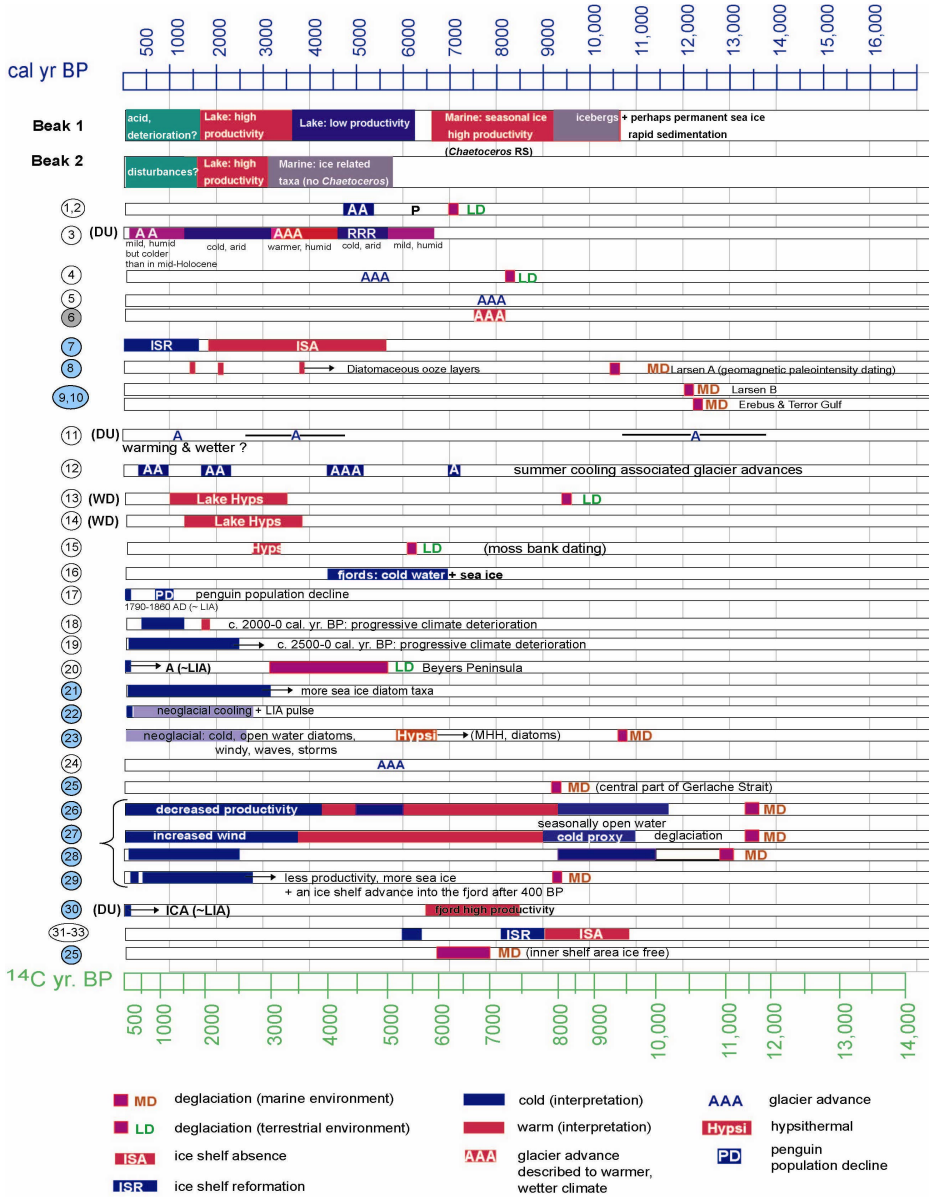

Figure 2: Overview of recent literature on the deglacial and Holocene climate variability recorded in the Antarctic Peninsula. The locations of the sites are shown in Fig. 3, the respective publications and authors are listed in Table 2. Blue circles represent marine cores, grey circles represent summaries, reviews or references to other literature sources. Black horizontal lines in site (11) represent dating error bars.

Table 2: List of references shown in Figs. 2 and 3, and their corresponding study area or site names.

1	Zale, 1994	Hope Bay
2	Gibson & Zale, 2006	Hope Bay
3	Björck et al., 1996	James Ross Island
4	Hjort et al., 1997	James Ross Island
5	Ingólfsson et al., 1992	James Ross Island
6	Ingólfsson et al., 1998	review
7	Pudsey & Evans, 2001	Prince Gustav Channel
8	Brachfeld et al., 2003	Larsen A
9	Domack et al., 2005	Larsen region
10	Heroy & Anderson, 2005	Larsen region
11	Bentley et al., 2007	South Georgia
12	Rosqvist & Schuber, 2003	South Georgia
13	Jones et al., 2000	Signy Island
14	Hodgson & Convey, 2005	Signy Island
15	Björck et al., 1991a	Elephant Island
16	Yoon et al., 2000	South Shetlands
17	Liu et al., 2006	King George
18	Björck et al., 1991b	Livingston
19	Björck et al., 1993	Livingston
20	Björck et al., 1996	Livingston
21	Barcena et al. 2006	Bransfield Strait
22	Fabrés et al., 2000	Bransfield Strait
23	Heroy et al., 2008	Bransfield Strait
24	Hansom & Flint, 2004	Brabant Island
25	Harden et al., 1992	Gerlache Strait
26	Sjunneskog & Taylor, 2002	Palmer Deep
27	Taylor & Sjunneskog, 2002	Palmer Deep
28	Domack et al., 2001	Palmer Deep
29	Shevenell et al., 1996	Lallemand fjord
30	Domack et al., 1995	Muller Ice Shelf
31	Bentley et al., 2005	George VI
32	Smith et al., 2007	George VI
33	Roberts et al., 2008	George VI

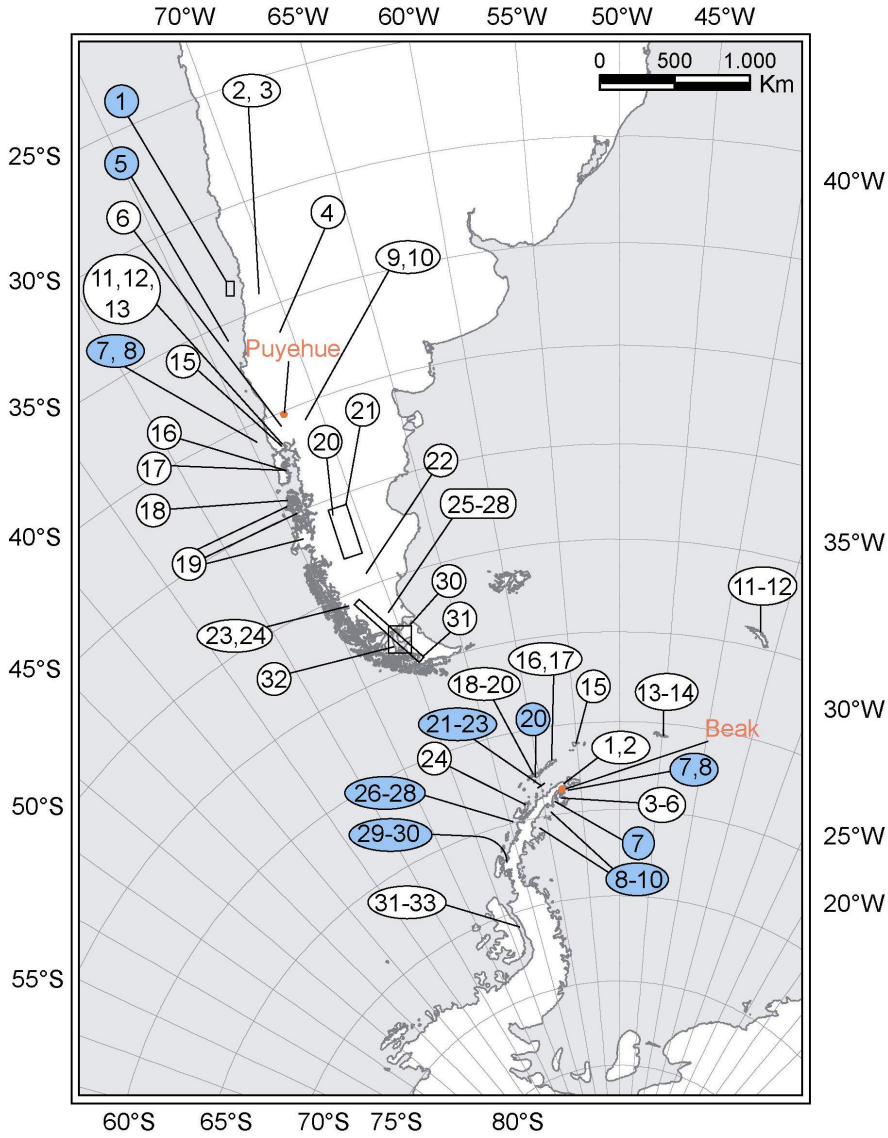

***Figure 3*:** Location of the study sites mentioned in Figs. 1 and 2. Blue circles represent marine cores.

8.3.2.3. Beak Island: Mid-Holocene and Late-Holocene periods

Between c. 6.0 and 3.5 cal. ka BP a return to cold conditions was tentatively inferred from reduced algal productivity and diversity in Lake Beak-1. At the same time, (c. 5.9-3.0 cal. ka BP) oceanographic conditions in the submerged Beak-2 basin (Chapter 6) were inferred to be 'colder' than before; the presence of a high amount of ice-related taxa, fluctuating grain sizes and high percentages of broken diatom valves pointed towards conditions that were more similar to those before 9.2 cal. ka BP than those between 9.2 and 6.9 cal. ka BP in Beak-1 (Chapters 6 and 7). The terrestrial glacier advances observed on northern James Ross Island (Hjort et al., 1997) and in Hope Bay (Zale, 1994) fall within this period, but caution is still needed when trying to explain these advances in terms of climate change, as many factors could regulate their mass balance (Hjort et al., 1997) and the exact timing of the glacier advances should be better constrained. A similar cooling in the marine environment was not recorded in the Palmer Deep record on the northwestern side of the AP (Domack et al., 2001).

During the Mid-Holocene between c. 3.5 and 1.7 cal. ka BP, a milder climate was tentatively inferred from higher organic sedimentation rates and the diatom and pigment data in Beak-1 (Chapter 7). However, some appearant discrepancies, such as the low reconstructed NH_4^+ levels in both cores, and the conflicting paleoclimatic inferences of Björck et al. (1997) for James Ross Island, call for further analysis.

In Beak-1, a gradual decrease in organic content at c. 2.0 cal. ka BP was followed by a very abrupt change in diatom composition between 1.7 and 1.4 cal. ka BP, where a high peak in *Brachysira minor* was observed, and the lake turned into more acid conditions (Chapter 7). This change coincided with a major change in diatom and pigment compositions in core Beak-2 (if we can assume that the currently constructed age-depth model for Beak-2 is correct; see Chapter 6). These changes may have reflected increased climate instability and disturbance in precipitation, but are difficult to interpret in terms of temperature, and could as well reflect a shift in the lake's ecology after some threshold was reached.

An increasing climate deterioration during the Late-Holocene was observed on Livingston Island (Björck et al., 1991), and both ice shelves in the Prince Gustav Channel and Larsen A region reformed at c. 1900 and 1400 ^{14}C BP respectively, although dating in the latter two studies was less certain (Pudsey & Evans, 2001; Brachfeld et al., 2003).

8.3.2.4. Beak Island: summary

In the Antarctic Peninsula, the Early Holocene climatic optimum (c. 11.5-9.2 ka BP; Fig. 4) coincided with the deglaciation of many middle- and inner shelf areas, including the region around our study site, Beak Island. However, data on Early Holocene climate conditions in the Peninsula are scarce. One marine study from the northwest of the AP (Palmer Deep) revealed cold marine conditions between c. 11 and 9 ka BP (Domack et al., 2001). In our record from Beak Island, similar conditions may have prevailed until c. 9.2 ka BP. From then, high productivity and open seasonal marine conditions were observed in our record. This is slightly earlier than the start of seasonally open marine conditions in the southern Prince Gustav Channel (8.7-7.4 cal. ka BP), and is in synchrony with the Palmer Deep record at the western side of the AP. At first sight, this seems to contradict the reported steepening of thermal gradients between the east and west Antarctic Peninsula regions in the Early Holocene (see Hodgson et al., in press). However, this could be partly explained by the very northern position of both the Beak and the Palmer Deep sites, and by the fact that Beak was a shallow coastal environment, that has never been covered by an ice shelf, and thus probably responded relatively fast to climate and oceanic temperature changes (see also 8.4.).

In the Mid-Holocene, glacier advances were reported from the northern AP and from Islands to the east (Fig. 4). These have been ascribed to either a cooling or a precipitation increase. On Beak Island, the period between c. 6.0 and 3.5 cal. ka BP was cautiously interpreted as a cooler period, and this may indicate that the glacier advances previously observed on James Ross and in Hope Bay were possibly caused by a temperature decline.

Between 3.5 and 1.7 cal. ka BP, a milder climate was tentatively inferred from higher organic sedimentation rates and pigment concentrations in Beak-1, after which the lake abruptly turned into acid conditions. A deteriorating climate was inferred, but more analyses are needed for the whole period after 6.0 cal. ka BP. An increasing climate deterioration during the Late-Holocene was observed on Livingston Island (Björck et al., 1991), and a ‘neoglacial cooling’ is inferred in many sites in the Antarctic Peninsula, as well as the whole Antarctic continent (Hodgson et al., in press).

8.4. Forcing factors and teleconnections

In general, insolation changes are recognized to be one of the major forcing factors for global scale postglacial climate changes (Bentley et al., 2009; Beer & van Geel, 2008). However, the way in which these variations are translated into climate changes, i.e. the feed-back mechanisms involved are to date insufficiently understood. In this context, as stated in 8.1., much attention has been given to the North Atlantic region, where changes in the influx of melt-water modulate the strength of the thermohaline circulation (THC), which, in turn, distributes heat (hence heat anomalies) around the world (Knorr & Lohmann, 2003).

This has, amongst others, lead to scientific discussions about the (semi-)global extent of the Younger Dryas cooling, which was observed in the Northern Hemisphere, the tropics, and parts of the Southern Hemisphere up to c. 40-55°S, where the Southern Westerlies prevail.

Recent research has highlighted that the Southern Westerlies themselves respond quickly to e.g. changes in atmospheric ozone concentration and hence solar variability (Gillett & Thompson, 2003; Rozema et al., 2002). They also provide important feed-back effects on the strength of the oceanic Antarctic Circumpolar Current (ACC) and hence influence the rate of upwelling of CO_2-rich Antarctic Bottom Water (Anderson et al., 2009; Toggweiler, 2009). Their importance in hemispheric/global climate regulation is well recognized in current short-term climate dynamics of the Southern Hemisphere, but recent ice-core based reconstructions of Westerly Wind strength have also shown that the Westerlies have significantly shifted in intensity at decennial and longer time scales during the Holocene (Mayewski et al., 2009 and references therein). Hence, they may have been an important factor in teleconnecting between millennial-scale climate changes in the tropics, mid-latitudes and at high latitudes in the Southern Hemisphere.

On short time scales, the link between tropical, mid-latitudinal and high latitude climates has been studied extensively (e.g. Trenberth & Caron, 2000; Stammerjohn et al., 2008; Carvalho et al., 2005). On longer time-scales these teleconnections are not known, although very recent reviews have focused on the forcing mechanisms on Antarctic Peninsula climate changes during the Holocene (e.g. Bentley et al., 2009; Mayewski et al., 2009), and on mid-latitudinal and tropical changes (Kaiser & Lamy, 2008; Pena & Cacho, 2009).

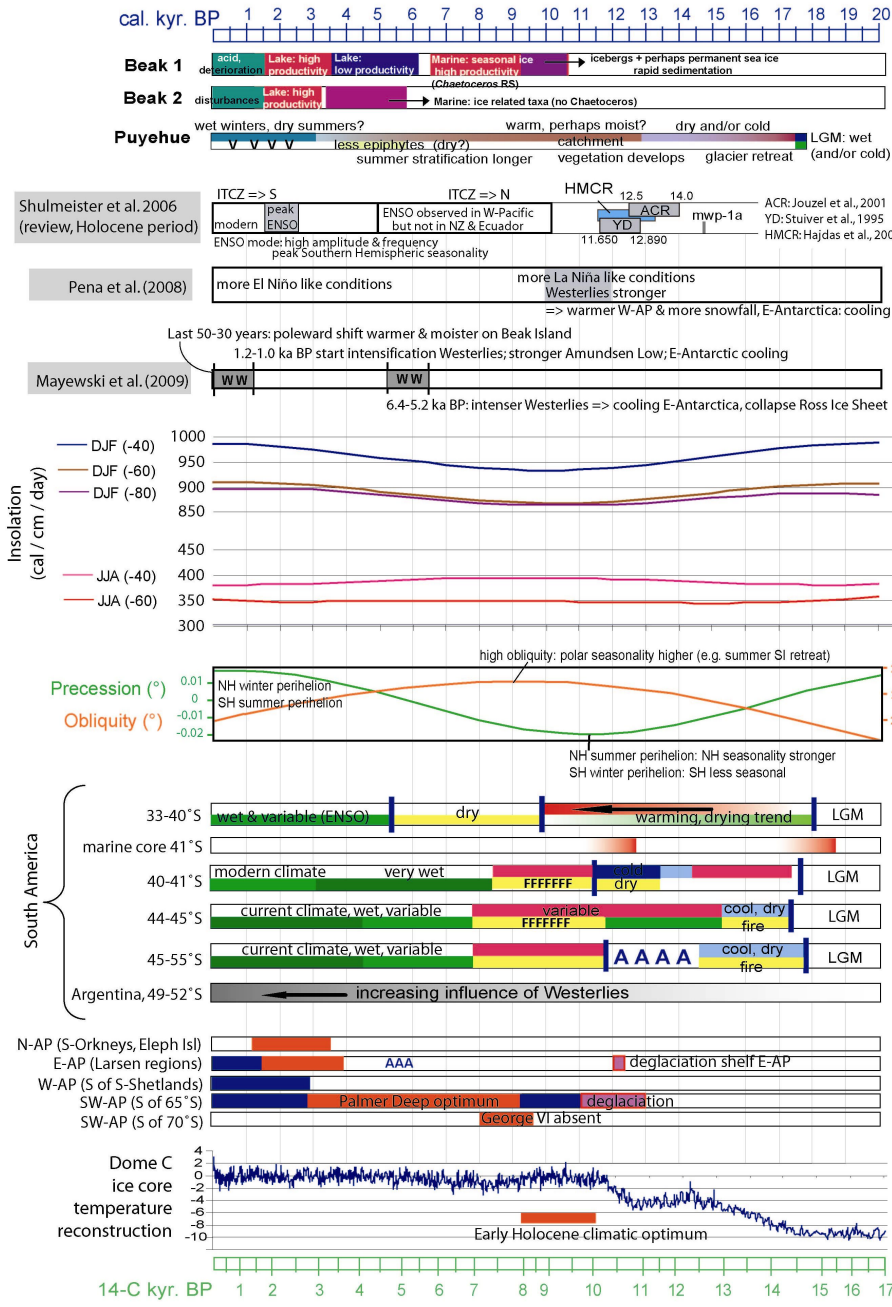
cal. kyr. BP 1 2 3 4 5 6 7 8 9 10 11 12 13 14 15 16 17 18 19 20
Beak 1
acid, deterioration
Lake: high productivity
Lake: low productivity
Marine: seasonal ice high productivity
icebergs + perhaps permanent sea ice
rapid sedimentation
(Chaetoceros RS)
Beak 2
disturbances
Lake: high productivity
Marine: ice related taxa (no Chaetoceros)
Puyehue
wet winters, dry summers?
warm, perhaps moist?
dry and/or cold
less epiphytes (dry?)
summer stratification longer
catchment vegetation develops
glacier retreat
LGM: wet (and/or cold)
Shulmeister et al. 2006 (review, Holocene period)
ITCZ => S
ITCZ => N
HMCR
12.5
14.0
modern
peak ENSO
ENSO observed in W-Pacific but not in NZ & Ecuador
ACR
YD
mwp-1a
11.650
12.890
ENSO mode: high amplitude & frequency
peak Southern Hemispheric seasonality
ACR: Jouzel et al., 2001
YD: Stuiver et al., 1995
HMCR: Hajdas et al., 2003
Pena et al. (2008)
more El Niño like conditions
more La Niña like conditions
Westerlies stronger
=> warmer W-AP & more snowfall, E-Antarctica: cooling
Mayewski et al. (2009)
Last 50-30 years: poleward shift warmer & moister on Beak Island
1.2-1.0 ka BP start intensification Westerlies; stronger Amundsen Low; E-Antarctic cooling
W W
W W
6.4-5.2 ka BP: intenser Westerlies => cooling E-Antarctica, collapse Ross Ice Sheet
Insolation (cal / cm / day)
DJF (-40)
DJF (-60)
DJF (-80)
JJA (-40)
JJA (-60)
1000
950
900
850
450
400
350
300
high obliquity: polar seasonality higher (e.g. summer SI retreat)
Precession (°)
Obliquity (°)
0.01
0
-0.01
-0.02
NH winter perihelion
SH summer perihelion
24.5
24.0
23.5
NH summer perihelion: NH seasonality stronger
SH winter perihelion: SH less seasonal
South America
33-40°S
wet & variable (ENSO)
dry
warming, drying trend
LGM
marine core 41°S
40-41°S
modern climate
very wet
FFFFFFF
cold
dry
LGM
44-45°S
current climate, wet, variable
variable
FFFFFFF
cool, dry
fire
LGM
45-55°S
current climate, wet, variable
A A A A
cool, dry
fire
LGM
Argentina, 49-52°S
increasing influence of Westerlies
N-AP (S-Orkneys, Eleph Isl)
E-AP (Larsen regions)
AAA
deglaciation shelf E-AP
W-AP (S of S-Shetlands)
SW-AP (S of 65°S)
Palmer Deep optimum
deglaciation
SW-AP (S of 70°S)
George VI absent
Dome C ice core temperature reconstruction
4
2
0
-2
-4
-6
-8
-10
Early Holocene climatic optimum
14-C kyr. BP 1 2 3 4 5 6 7 8 9 10 11 12 13 14 15 16 17

Figure 4 *(opposite page)*: Synthesis of Late-Quaternary paleoclimatic changes in South America and the Antarctic Peninsula, as summarized from Figs. 1 and 3. From top to bottom: - Paleoclimatic interpretations of our study sites; - Overview of important climate changes in a wider (semi-global) context based on Shulmeister et al. (2006), Pena et al. (2008) and Mayewski et al. (2009); - Solar insolation for the past 20,000 years, respectively for summer (DJF) and winter (JJA) for the latitudes 40°, 60°, 80°S (note that the winter insolation at 80°S is zero), data from Berger & Loutre (1991);
- Obliquity and precession values (Berger & Loutre, 1991); - Synthesis of paleoclimatic changes in South America and the Antarctic Peninsula; symbols and colors as in the legends of Figs. 1 and 2; note that caution is needed when addressing the syntheses of paleoclimatic reconstructions, because these are based on literature sources, without quantitative calibration of paleoclimatic proxy indicators and chronologies (see Verschuren & Charman, 2008) - Dome-C ice core record of temperature changes for the past 20,000 years, the plotted temperatures (°C) are deviations from the mean annual temperature of the last 1000 years (Jouzel et al., 2007).

Studies of ice-core proxies have recently shown that for the last 2000 years, major changes in Antarctic temperatures were correlated with the strength of the Westerly circulation (Mayewski & Maasch, 2006). An intensification of the Westerlies was linked to overall cooler temperatures, especially in East Antarctica, and to an intensification of the Amundsen Sea Low in West-Antarctica (Mayewski & Maasch, 2006). Similar mechanisms may have been active at longer time scales during the Holocene (Mayewski et al., 2009; Hodgson et al., in press). Two large intensifications of the southern circumpolar Westerlies are recorded, i.e. one between 6.4 and 5.6-5.2 ka BP and one starting at c. 1.2-1.0 ka BP. A less pronounced intensification was detected at c. 8.4-8.2 ka BP (Mayewski & Maasch, 2006). These changes were linked to a reverse in the trend of orbitally forced insolation (see Fig. 4), and a decrease in output of solar energy (Mayewski et al., 2009).

Pena & Cacho (2009) have similarly linked changes in El Niño occurrences to insolation changes, and more specifically orbital forcing, while El Niño is known to have an influence on climate and sea-ice dynamics in the western Antarctic Peninsula (Turner, 2004; Trenberth & Caron, 2000; Stammerjohn et al., 2008).

From the Early Holocene to the Late Holocene, orbital parameters changed from a low precession index and a high obliquity, towards a high precession index and a lower obliquity. A high precession index indicates that the perihelion (the point in the Earth's orbit nearest to the sun) occurred during Southern Hemispheric (SH) summer, and thus implies an increased Southern Hemispheric insolation seasonality (Fig. 4). The low obliquity causes a less pronounced increase in Late Holocene Southern Hemispheric summer insolation in comparison with that of Early Holocene Northern Hemispheric summer insolation, and a more pronounced decline in Northern Hemispheric summer insolation during the Late Holocene. These conditions caused a system shift to increased

La Niña-like conditions [hence a stronger Pacific Subtropical High Pressure Cell (STHP)] during the Early Holocene, a poleward shift of the Southern Westerlies, and an increased sea ice retreat around Antarctica during summer (Pena & Cacho, 2009). In the Late Holocene, the frequency and amplitude of El Niño events increased, and may have been associated with increased blocking of the Westerlies in the Amundsen-Bellingshausen region where the Low becomes less strong, as is observed in the climate today (see Fig. 5; Trenberth & Caron, 2000).

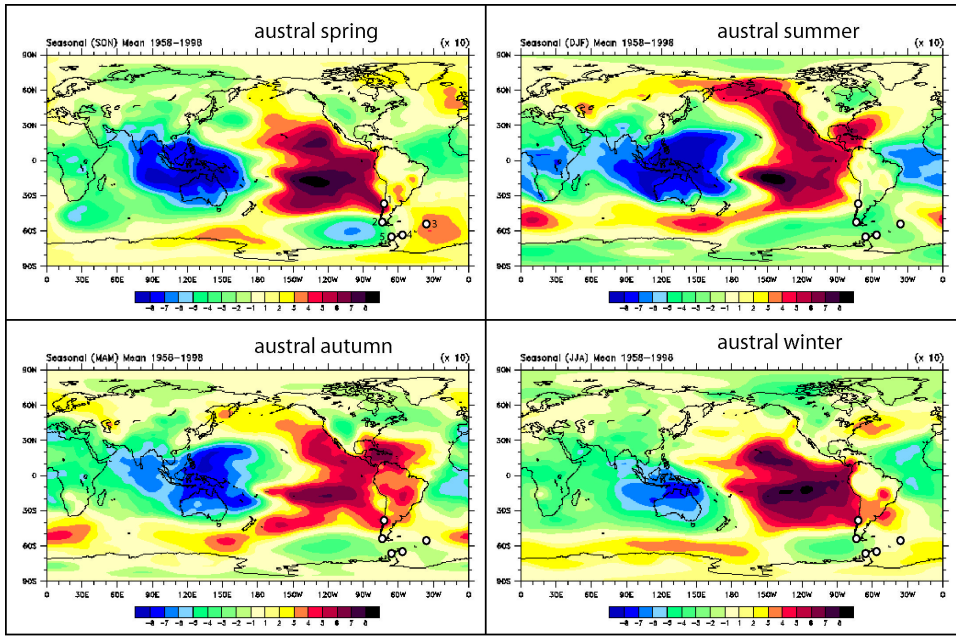

Figure 5: Correlations of four seasonal means of Sea Level Pressure (SLP) with the Southern Oscillation Index (SOI) for 1958-1998. Figure from Trenberth & Caron (2000). Negative correlations correspond with an increase in SLP during warm (El Niño) events. Some study sites of the Holant and Cache-PEP projects are indicated with a white dot: 1. Lago Puyehue (Chilean Lake District), 2. Lagos Bulnes, Pato & Parrillar (south Patagonia), 3. Fan Lake (Annenkov Island, South Georgia), 4. Lakes Beak-1,2, 3 (Beak Island, Antarctic Peninsula), 5. Narrows Lake (Pourquoi-Pas Island, west Antarctic Peninsula).

The observations of Mayewski et al. (2009) and Pena & Cacho (2009) may partly explain the observations seen in both the Antarctic Peninsula and South America (Fig. 4). The Early Holocene collapse of ice shelves on the western side of the Antarctic Peninsula (Bentley et al., 2005; Roberts et al., 2008) may be explained by these increased La Niña-like conditions. The similarities between the Palmer Deep record and the reconstruction

for Beak Island between c. 10.6 and 6.0 cal. ka BP may be explained by the stronger Westerlies being able to break through the northern tip of the Antarctic Peninsula and influencing the northeastern side. This would imply that the steepening of the thermal gradient between the east and west of the AP (see Hodgson et al., in press) is mainly caused by the warming on the western side, while ice shelves on the eastern side, south of the Prince Gustav Channel, remained under influence of the cold Weddel Gyre.

The strengthening of the Westerlies between 6.4 and 5.2 ka BP, as reconstructed by Mayewski & Maasch (2006) coincided with the advance of glaciers on James Ross Island and Hope Bay (Hjort et al., 1997; Zale, 1994; Gibson & Zale, 2006), and on South Georgia (Rosqvis & Schuber, 2003), although the latter ascribed these advances to a cooler summer temperature, because their mass balance is temperature-dependent today. Our record from Beak Island, however, indicates a period of low productivity between c. 6.0 and 3.5 ka BP, which we tentatively interpreted as a cool period, and which calls for further research in order to resolve this issue.

The intensification of the Westerlies starting at c. 1.2 ka BP (Mayewski & Maasch, 2006) seems to be contradicting with the neoglacial cooling and reformation of many ice shelves around the Antarctic Peninsula during the Late Holocene, and with the increased El Niño occurrences observed in the tropical Pacific and in South America (Fig. 5; Pena et al., 2008; Shulmeister et al., 2006). In Beak Island, a deteriorating climate was inferred, but diatom compositions pointed towards more acid and perhaps moister conditions than in the periods between 6.0 and 1.7 ka BP. Note that not only the climate circulation patterns, but also the lake biota themselves were probably directly influenced by the changes in insolation between the Early and Late Holocene (Bentley et al., 2009), although regional climate changes may have been dominant.

An increase in El Niño occurrences during the Late Holocene has been tentatively inferred from our Puyehue record, and the increased variability and/or precipitation seasonality, as seen in almost all records, may indicate a generally weaker Pacific STHP, and associated Westerlies.

8.5. Future perspectives

As outlined in the introduction, scientific focus is currently shifting from both Southern tropics and high latitudes towards the Southern mid-latitudes, especially in South America. This has three reasons: (1) the strength and position of the Southern Westerlies is directly linked with both tropical (ENSO) and high-latitude (e.g. SAM) climate oscillations (2) the Westerlies (and associated oceanic ACC) play a key-role in global climate modulation, and (3) the Westerlies have a direct impact on the regional climate west of the Andes, and can thus well be reconstructed through terrestrial records from that area. Although an increasing number of paleoclimate studies have been carried out in both southern South America and the Antarctic Peninsula, there is still a need for high-resolution well-dated archives from climate-sensitive locations to decipher past variations of the Southern Westerly Winds at millennial and sub-millennial timescales (Moreno et al., 2008).

Considering the overview in 8.2.2.1., specifically more marine records from sites off the Chilean coast would be useful, in order to reconstruct SST changes covering a meridional transect across the Pacific Eastern Boundary Current System, and to compare these with terrestrial climate shifts at corresponding latitudes. In this context, scientists have recently recovered ultra high-resolution sediment records from the Chilean fjords and the adjacent continental margin, that may yield promising results (Kaiser & Lamy, 2008). The terrestrial records would benefit from more paleolimnological reconstructions from between 40 and 36°S, where a gap seems to exist (Fig. 1), and of new high-resolution studies further south. To accomplish the latter, a number of concrete research initiatives has already been taken in the framework of the Bilateral Research Project 'Building a north-south transect for the reconstruction of late Quaternary climate and environmental change in southern Chile: (paleo)limnological and limnogeological reconnaissance', and in the framework of the British Antarctic Survey CACHE-PEP project (see Chapter 1); i.e. a field campaign was organized in southern Chilean Patagonia in 2007, where two long cores[4] and one short core were taken at different locations between 42 and 54°S (see Fig. 1 in Chapter 1), and a minimum of 25 lakes was sampled in order to start building a calibration dataset. We are convinced that the lakes

[4] Lago Pato (unofficial name) is a small lake (0.15 km^2; 51°18'S, 72°41'W; Fig. 2), immediately southeast of Lago del Toro (E- Torres del Paine), which may have been isolated from the latter during the late- or deglacial period. Lago Bulnes (unofficial name; Magellan region, 53°40'S, 70°58'W) is situated near the coast of the Magellan Streat, and has probably been submerged under a large ice-dammed paleolake at some point during the Holocene. The larger Laguna Parrillar (53°25'S, 71°16'W) was considered as a potentially promising lake for obtaining long-term paleoclimate records, and a long core is now retrieved during a new fieldwork campaign early 2009 (Heirman K., pers. comm.).

have potential to bear long sediment records. Multiproxy analyses on these cores could add to the history of local relative sea level changes, neotectonics and climate change (e.g. Bentley et al., 2005a; Bentley & McCulloch, 2005). Dating and preliminary sedimentological analyses on these Patagonian cores are being done (Roberts S., Heirman K., pers. comm.) and may yield interesting results and contributions to the paleoclimate records along the South American - Antarctic transect.

Likewise, more climate reconstructions are needed from the Antarctic Peninsula region, where especially more reliably dated sites should be investigated. Coastal lake records provide good opportunities for this, and particularly records from the western margin of the AP should be sought, in order to investigate the possible influence of e.g. circumpolar deep water on the manifestation of the Early Holocene climatic optimum on regional Antarctic Peninsula climates. Further, additional records from the western Weddell margin would help to constrain the ages and climatic interpretations of the Mid-Holocene glacier advances observed on James Ross Island and in Hope Bay. Also, detailed, continuous and well-dated records from maritime Antarctic and sub-Antarctic islands would add to the continuity of the Antarctic Peninsula - South American transect, as it has been proven that the current climate dynamics in these regions is often correlated, but not necessarily positively along the same latitude (Trenberth & Caron, 2000). Moreover, high-resolution and well-dated climate reconstructions from both sides of the Antarctic Peninsula and from the sub-Antarctic region may also permit comparisons with ice-core based reconstructions of Westerly Wind activity in both hemispheres (EPICA, 2006; Mayewski & Maasch, 2006). Concrete, in the framework of the Holant and CACHE-PEP projects, lakes have been cored and are being analyzed on Annenkov Island (South Georgia) and in the Marguerite Bay region (Hodgson D., Roberts S., pers. comm.). Further, ice cores have recently been taken in the Antarctic Peninsula (e.g. James Ross: McConnell et al., 2007; and Berkner Island; see Hodgson et al. (2007) for a good overview of current and prospective projects in the region), which may reveal more regional scale information about temperature, precipitation and sea-ice changes in the past.

In the past ten years, the number of studies on the taxonomy, systematics and biogeography of freshwater diatoms in Antarctica and sub-Antarctica has increased, especially for the northeastern Antarctic Peninsula region, Maritime Antarctica and sub-Antarctica (e.g. Oppenheim, 1994; Van de Vijver et al., 2006; Van de Vijver & Mataloni, 2008). This is partly due to the increasing recognition of the need of intercalibrated

diatom datasets, both for paleo-environmental and biogeographical studies (Hübener et al., 2008; Vyverman et al., 2007). Our checklist of freshwater diatom species from Livingston, Signy and Beak Islands, is up to current taxonomical standards and is fully intercalibrated with other diatom datasets from continental Antarctic and sub-Antarctia. However, while we described five new species occurring in this dataset, many other taxa and species complexes remain to be revised.

Furthermore, there is a need for systematic studies of diatoms in (southern) South America. To date, little is known about the taxonomy and ecology of diatoms in this region (but see Maidana et al., 2005), and much of the literature is old and/or does not contain detailed descriptions and illustrations (e.g. Frenguelli, 1942; Krasske, 1939). As the recent studies of (sub-) Antarctic diatom communities has resulted in the discovery of many new (and often endemic) species, we predict that this will also be the case in South America. Moreover, southern South America has often been referred to as a possible source for (Maritime) Antarctic diatoms (together with dust and pollen, e.g. Björck et al., 1993; Gasso & Stein, 2007; McConnell et al., 2007; Gaiero et al., 2004). Critical revision and intercalibration of existing data will be needed to better quantify exchanges of diatom floras between these regions and to determine to what extent they have had independent evolutionary histories. Furthermore, the construction of a Patagonian diatom surface dataset for developing transfer functions is also needed to allow more quantitative environmental reconstructions in future paleolimnological studies. During the fieldwork campaign (2007) described above, a total of 25 lakes between 51 and 53°S was sampled for this purpose. It would be interesting, both for quantitative and qualitative environmental reconstructions, to analyze diatoms from these lakes and to extend the dataset with other lakes in order to cover the major environmental gradients that occur in the southern part of South America. Only then will it be possible to take full advantage of the typically close match between diatom species distribution and environmental conditions in future paleo-environmental reconstructions.

References:

Abarzúa A.M., Moreno P.I. 2008. Changing fire regimes in the temperate rainforest region of southern Chile over the last 16,000 yr. Quaternary Research. 69: 62-71.

Abarzúa A.M., Villagrán C., Moreno P. 2004. Deglacial and postglacial climate history in east-central Isla Grande de Chiloé, southern Chile (43°S). Quaternary Research. 62: 49-59.

Ackert R.P., Becker R.A., Singer B.S., Kurz M.D., Caffee M.W., Mickelson D.M. 2008. Patagonian glacier response during the Late Glacial – Holocene transition. Science. 321: 392-395.

Anderson R.F., Ali S., Bradtmiller L.I., Nielsen S.H.H., Fleisher M.Q., Anderson B.E., Burckle L.H. 2009. Wind-driven upwelling in the Southern Ocean and the Deglacial rise in Atmospheric CO2. Science. 323: 1443-1448.

Ariztegui D., Bianchi M.M., Masaferro J., Lafargue E., Niessen F. 1997. Interhemispheric synchony of late-glacial climatic instability as recorded in proglacial Lake Mascardi, Argentina. Journal of Quaternary Science. 12: 333-338.

Ariztegui D., Anselmetti F.S., Gilli A., Waldmann N. 2008. Late Pleistocene environmental change in eastern Patagonia and Tierra del Fuego – A limnological approach. Chapter 11, 241-251. In: Rabassa J. (Ed.): The Late Cenozoic of Patagonia and Tierra del Fuego. Developments in Quaternary Science, 11 (series editor: J.J.M. Van der Meer). Elsevier.

Bárcena M.A., Fabrés J., Isla E., Flores J.A., Sierro F.J., Canals M., Palanques A. 2006. Holocene neoglacial events in the Bransfield Strait (Antarctica). Palaeoceanographic and palaeoclimatic significance. Scientia Marina. 70 (4): 607-619.

Beer J., van Geel B. 2008. Holocene climate change and the evidence for solar and other forcings. Chapter 6, In: Battarbee R.W., Binney H.A. (Eds.): Natural climate variability and global warming. A Holocene perspective. Wiley-Blackwell, Chichester, United Kingdom: 139-162.

Bennett K.D., Haberle S.G., Lumley S.H. 2000. The last glacial-Holocene transition in Southern Chile. Science. 290: 325-328.

Bentley M.J. 1997. Relative and radiocarbon chronology of two former glaciers in the Chilean Lake District. Journal of Quaternary Science. 12: 25-33.

Bentley M.J. & McCulloch R.D. 2005. Impact of neotectonics on the record of glacier and sea level fluctuations, Strait of Magellan, Southern Chile. Geografiska Annaler. 87A (2): 393-402.

Bentley M.J., Sugden D.E., Hulton N.R.J., McCulloch R.D. 2005a. The landforms and pattern of deglaciation in the Strait of Magellan and Bahía Inútil, southernmost South America. Geografiska Annaler. 87A (2): 313-333.

Bentley M.J., Hodgson D.A., Sugden D.E., Roberts S.J., Smith J.A., Leng M.J., Bryant C. 2005b. Early Holocene Retreat of the George Vi Ice Shelf, Antarctic Peninsula. Geology. 33: 173-176.

Bentley M.J., Evans D.J.A., Fogwill C.J., Hansom J.D., Sugden D.E., Kubik P.W. 2007. Glacial geomorphology and chronology of deglaciation, South Georgia, sub-Antarctica. Quaternary Science Reviews. 26: 644-677.

Bentley M.J., Hodgson D.A., Smith J.A., Ó Cofaigh C., Domack E.W., Larter R.D., Roberts S.J., Brachfeld S., Leventer A., Hjort C., Hillenbrand C-D., Evans J. 2009. Mechanisms of Holocene palaeoenvironmental change in the Antarctic Peninsula region. The Holocene. 19: 51-69.

Berger A., Loutre M.F. 1991. Insolation values for the climate of the last 10 million years. Quaternary Sciences Reviews. 10 (4): 297-317.

Bertrand S., Boës X., Castiaux J., Charlet F., Urrutia R., Espinoza C., Lepoint G., Charlier B., Fagel N. 2005. Temporal evolution of sediment supply in Lago Puyehue (Southern Chile) during the last 600 yr. and its climatic significance. Quaternary Research. 64: 163-175.

Bertrand S., Charlet F., Charlier B., Renson V., Fagel, N. 2008. Climate variability of southern Chile since the Last Glacial Maximum: a continuous sedimentological record from Lago Puyehue (40°S). Journal of Paleolimnology. 39 (2): 179-195.

Björck S., H°akansson H., Zale R., Karlén W., Jönsson B.L. 1991a. A Late Holocene lake sediment sequence from Livingston Island, South Shetland Islands, with palaeoclimatic implications. Antarctic Science. 3: 61-72.

Björck S., Malmer N., Hjort C., Sandgren P., Ingólfsson Ó., Wallzn B., Smith R.I.L., Jönsson B.L. 1991b. Stratigraphic and plaeoclimatic studies of a 5500-year-old moss bank on Elephant Island. Antarctica. Arctic and Alpine Research. 23: 361-374.

Björck S., Håkansson H., Olssen S., Banekow L., Janssens J. 1993. Palaeoclimatic studies in South Shetland Islands, Antarctica, base don numerous stratigraphic variables in lake sediments. Journal of Paleolimnology. 8: 233-272.

Björck S., Olsson S., Ellis-Evans C., Håkansson H., Humlum O., de Lirio J.M. 1996. Late Holocene palaeoclimatic records from lake sediments on James Ross Island, Antarctica. Palaeogeography, Palaeoclimatology, Palaeoecology. 121: 195-220.

Boës X., Fagel N. 2008. Timing of the late glacial and Younger Dryas cold reversal in southern Chile varved sediments. Journal of Paleolimnology. 39 (2): 267-281.

Bonilla S., Villeneuve V., Vincent W.F. 2005. Benthic and planktonic algal communities in a high Arctic lake : pigment structure and contrasting responses to nutrient enrichment. Journal of Phycology. 41: 1120-1130.

Boyd B.L., Anderson J.B., Wellner J.S., Fernández R.A. 2008. The sedimentary record of glacial retreat, Marinelli Fjord, Patagonia: Regional correlations and climate ties. Marine Geology. 255: 165-178.

Brachfeld S., Domack E.W., Kissel C., Laj C., Leventer A., Ishman S., Gilbert R., Camerlenghi A., Eglinton L. 2003. Holocene history of the Larsen-A Ice Shelf constrained by geomagnetic paleointensity dating. Geology. 31: 749-752.

Campos H., Steffen W., Agüero G., Parra O., Zúñiga L. 1989. Estudios limnologicos en el Lago Puyehue (Chile): Morfometria, factores fisicos y quimicos, plancton y productividad primaria. Medio Ambiente. 10: 36-53.

Cruces F., Urrutia R., Araneda A., Pozo K., Debels P., Vyverman W., Sabbe K. 2001. Trophic evolution of Laguna Grande de San Pedro (8^{th} Region, Chile) during the last century, by means of the analysis of sedimentary records. Revista Chilena de Historia Natural. 74 (2): 407-418.

Denton G.H., Lowell T.V., Heusser C.J., Schlüchter C., Andersen B.G., Heusser L.E., Moreno P.I., Marchant D.R. 1999. Geomorphology, stratigraphy, and radiocarbon chronology of Llanquihue drif in the area of the southern lake district, Seno Reloncaví, and Isla Grande de Chiloé, Chile. Geografiska Annaler, 81A (2), 167-229.

Domack E.W. 2002. A synthesis for site 1098: Palmer Deep. In: Barker P.F., Camerlenghi A., Acton G.D., Ramsay A.T.S. (Eds). Proceedings of the Ocean Drilling Program, Scientific Results. Ocean Drilling Program, Texas A&M University, College Station, TX 77843-9547, USA.

Domack E.W., Ishman S.E., Stein A.B., McClennen C.E., Jull A.J.T. 1995. Late Holocene advance of the Muller Ice Shelf, Antarctic Peninsula – sedimentological, geochemical and paleontological evidence. Antarctic Science. 7: 159-170.

Domack E., Leventer A., Dunbar R., Taylor F., Brachfeld S., Sjunneskog C., ODP Leg 178 Scientific Party. 2001. Chronology of the Palmer Deep Site, Antarctic Peninsula: a Holocene Palaeoenvironmental Reference for the Circum-Antarctic. Holocene. 11: 1-9.

Domack E.W., Duran D., Leventer A., Ishman S., Doane S., McCallum S., Amblas D., Ring J., Gilbert R., Prentice M. 2005 Stability of the Larsen B ice shelf on the Antarctic Peninsula during the Holocene epoch. Nature. 436: doi. 10.1038.

EPICA Community Members. 2006. One-to-one coupling of glacial climate variability in Greenland and Antarctica. Nature. 444 (9): 195-198.

Fabrés J., Calafat A.M., Canals M., Bárcena M.A., Flores J.A. 2000. Bransfield Basin fine grained sediments: Late Holocene sedimentary processes and oceanographic and climatic conditions. Holocene. 10 (9): 703-718.

Fogwill C.J. & Kubik P.W. 2005. A glacial stage spanning the Antarctic Cold Reversal in Torres del Paine (51°S), Chile, based on preliminary cosmogenic exposure ages. Geografiska Annaler. 87A (2): 403-408.

Frenguelli J. 1942. Diatomeas del Neuquen (Patagonia). Rev. Museo Plata Sección Botanica. 5: 73-219.

Fundell F., Fischer H., Weller R., Traufetter F., Oerter H., Miller H. 2006. Influence of large-scale teleconnection patterns on methane sulfonate ice core records in Dronning Maud Land. Journal of Geophysical Research. 111: D04103, doi: 1029/2005JD005872.

Gaiero D.M., Depetris P.J., Probst J.L., Bidart S.M., Leleyter L. 2004. The signature of river- and wind-borne materials exported from Patagonia to the southern latitudes: a view from REEs and implications for paleoclimatic interpretations. Earth and Planetary Science Letters. 219: 357-376.

Gasso S. & Stein A.F. 2007. Does dust from Patagonia reach the sub-Antarctic Atlantic Ocean? Geophysical Research Letters. 34 (1): Art. n° L01801.

Gillett N.P., Thompson D.W.J. 2003. Simulation of Recent Southern Hemisphere Climate Change. Science. 302: 273-275.

Gilli A., Ariztegui D., Anselmetti F.S., McKenzie J.A., Markgraf V., Hajdas I., McCulloch R.D. 2005. Mid-Holocene strengthening of the Southern Westerlies in South America – Sedimentological evidences from Lago Cardiel, Argentina (49°S). Global and Planetary Change. 49: 75-93.

Haberle S.G. & Bennett K.D. 2004. Postglacial formation and dynamics of North Patagonian Rainforest in the Chonos Archipelago, Southern Chile. Quaternary Science Reviews. 23: 2433-2452.

Haberzettl T., Fey M., Lücke A., Maidana N.I., Mayr C., Ohlendorf C., Schäblitz F., Schleser G.H., Wille M., Zolitschka B. 2005. Climatically induced lake level changes during the last two millennia as reflected in sediments of Laguna Potrok Aike, southern Patagonia (Santa Cruz, Argentina). Journal of Paleolimnology. 33: 283-302.

Haberzettl T., Corbella H., Fey M., Janssen S., Lücke A., Mayr A., Ohlendorf C., Schäblitz F., Schleser G.H., Wille M., Wulf S., Zolitschka B. 2007. Late Glacial and Holocene wet-dry cycles in southern Patagonia – Chronology, sedimentology and geochemistry of a lacustrine sediment record from Laguna Potrok Aike (Argentina). The Holocene. 17: 297-310.

Haberzettl T., Kück B., Wulf S., Anselmetti F., Ariztegui D., Corbella H., Fey M., Janssen S., Lücke A., Mayr C., Ohlendorf C., Schäbitz F., Schleser G., Wille M., Zolitschka B. 2008. Hydrological variability in southeastern Patagonia during Oxygen Isotope Stage 3 and the Holocene. Palaeogeography, Palaeoclimatology, Palaeoecology. 259: 213-229.

Hajdas I., Bonani G., Moreno P.I. and Ariztegui D. 2003. Precise radiocarbon dating of Late-Glacial cooling in mid-latitude South America. Quaternary Research. 59: 70-78.

Hansom J.D., Flint C.P. 1989. Short notes. Holocene ice fluctuations on Brabant Island, Antarctic Peninsula. Antarctic Science. 1: 165-166.

Harden S.L., DeMaster D.J., Nittrouer C.A. 1992. Developing sediment geochronologies for high-latitude continental shelf deposits: a radiochemical approach. Marine Geology. 103: 69-97.

Heroy D.C., Anderson J.B. 2005. Ice-sheet extent of the Antarctic Peninsula region during the Last Glacial Maximum (LGM) – Insights from glacial geomorphology. Geological Society of America Bulletin. 117: 1497-1512.

Heroy D.C., Sjunneskog C., Anderson J.B. 2007. Holocene climate change in the Bransfield Basin, Antarctic Peninsula: evidence from sediment and diatom analysis. Antarctic Science. DOI: 10.1017/S0954102007000788.

Hjort C., Ingólfsson Ó., Möller P., Lirio J.M. 1997. Holocene glacial history and sea-level changes on James Ross Island, Antarctic Peninsula. Journal of Quaternary Science. 12 (4): 259-273.

Hodgson D.A., Convey P. 2005. A 7000-year Record of Oribatid Mite Communities on a Maritime-Antarctic Island: Responses to Climate Change. Arctic, Antarctic, and Alpine Research. 37 (2): 239-245.

Hodgson D., Wolff E., Mulvaney R., Allen C. 2007. Extending the Americas paleoclimate transect through the Antarctic Peninsula to the Pole. PAGES news. 15 (1): 6-7.

Hodgson D.A., Abram N., Anderson J., Bargelloni L., Barrett P., Bentley M.J., Bertler N.A.N., Chown S., Clarke A., Convey P., Crame A., Crosta X., Curran M., di Prisco G., Francis J.E., Goodwin I., Gutt J., Massé G., Masson-Delmotte V., Mayewski P.A., Mulvaney R., Peck L., Pörtner H-O., Röthlisberger R., Stevens M.I., Summerhayes C.P., van Ommen T., Verde C., Verleyen E., Vyverman W., Wiencke C., Zane L. In Press. Antarctic climate and environment history in the pre-instrumental period. In: Turner J., Convey P., di Prisco G., Mayewski P.A., Hodgson D.A., Fahrbach E., Bindschadler R., Gutt J. (Eds.). Antarctic Climate Change and the Environment. Scientific Committee for Antarctic Research, Cambridge.

Hübener T., Dreßler M., Schwarz A., Langner K., Adler S. 2008. Dynamic adjustment of training sets (‚moving-window' reconstruction) by using transfer functions in paleolimnology – a new approach. Journal of Paleolimnology. 40 (1): 79-95.

Huber U.M., Markgraf V., Schäbitz F. 2004. Geographical and temporal trends in Late Quaternary fire histories of Fuego-Patagonia, South America. Quaternay Science Reviews. 23: 1079-1097.

Ingólfsson O. 2004. Quaternary glacial and climate history of Antarctica. In: Ehlers J., Gibbard P.L. (Eds.): Quaternary glaciations – Extent and Chronology, III. Elsevier: 3-43.

Ingólfsson O., Hjort C., Björck S., Smith R.I.L. 1992. Late Pleistocene and Holocene Glacial History of James-Ross-Island, Antarctic Peninsula. Boreas. 21: 209-222.

Ingólfsson O., Hjort C., Berkman P., Björck S., Colhoun E., Goodwin I.D., Hall B., Hirakawa K., Melles M., Möller P., Prentice M. 1998. Antarctic glacial history since the Last Glacial Maximum: an overview of the record on land. Antarctic Science. 10: 326-344.

Jenny B., Wilhelm D., Valero-Garcés B.L. 2003. The Southern Westerlies in Central Chile: Holocene precipitation estimates based on a water balance model for Laguna Aculeo (33°50'S). Climate Dynamics. 20: 269-280.

Jones V., Juggins S, Ellis-Evans JC. 1993. The relationship between water chemistry and surface sediment diatom assemblages in maritime Antarctic lakes. Antarctic Science. 5 (4): 339-348.

Jones V., Juggins S. 1995. The construction of a diatom-based chlorophyll *a* transfer function and its application at three lakes on Signy Island (maritime Antarctic) subject to differing degrees of nutrient enrichment. Freshwater biology. 34: 433-445.

Jones V.J., Hodgson D.A., Chepstow-Lusty A. 2000. Palaeolimnological evidence for marked Holocene environmental changes on Signy Island, Antarctica. The Holocene. 10 (1): 43-60.

Jouzel J., Masson V., Cattani O., Falourd S., Stievenard M., Stenni B., Longinelli A. Johnsen S.J., Steffensen J.P., Petit J.-R., Schwander J., Souchez R. and Barkov N.I. 2001. A new 27 ky high resolution East Antarctic climate record. Geophysical Research Letters. 28: 3199-3202.

Jouzel, J., Masson-Delmotte V., Cattani O., Dreyfus G., Falourd S., Hoffmann G., Minster B., Nouet J., Barnola J.M., Chappellaz J., Fischer H., Gallet J.C., Johnsen S., Leuenberger M., Loulergue L., Luethi D., Oerter H., Parrenin F., Raisbeck G., Raynaud D., Schilt A., Schwander J., Selmo E., Souchez R., Spahni R., Stauffer B., Steffensen J.P., Stenni B., Stocker T.F., Tison J.L., Werner M., Wolff E.W. 2007. Orbital and Millennial Antarctic Climate Variability over the Past 800,000 Years. Science. 317 (5839): 793-797.

Kaiser J., Lamy F. 2008. Last glacial SST changes in the SE Pacific – a bipolar see-saw perspective. PAGES News. 16 (1): 20-22.

Krasske G. 1939. Zur Kieselalgenflora Sudchiles. Archiv für Hydrobiologie. 35: 349-468.

Lamy F., Hebbeln D., Wefer G. 1999. High-resolution marine record of climatic change in mid-latitude Chile during the last 28,000 years based on terrigenous sediment parameters. Quaternary Research. 51: 83-93.

Lamy F., Kaiser J., Ninnemann U., Hebbeln D., Arz H.W., Stoner J. 2004. Antarctic timing of surface water changes off Chile and Patagonian Ice Sheet response. Science. 304: 1959-1962.

Lamy F., Kaiser J., Arz H.W., Hebbeln D., Ninnemann U., Timm O., Timmermann A., Toggweiler J.R.. 2007. Modulation of the bipolar seesaw in the Southeast Pacific during Termination 1. Earth and Planetary Science Letters. 259: 400-413.

Liu X.-D., Li H.-C., Sun L.-G., Yin X.-B., Zhao S.-P., Wang Y.-H. 2006. d13C and d15N in the ornithogenic sediments from the Antarctic maritime as palaeoecological proxies during the past 2000 yr. Earth and Planetary Science Letters. 243: 424-438.

Maidana N.I., Izaguirre I., Vinocur A., Mataloni G., Pizarro H. 2005. Diatomeas en una transecta patagónico-antártica. Ecología Austral. 15: 159-176.

Marden C.J. 1997. Late-glacial fluctuations of South Patagonian Icefield, Torres del Paine National Park, Southern Chile. Quaternary International. 38-39: 61-68.

Marden C.J. & Clapperton C.M. 1995. Fluctuations of the South Patagonian Icefield during the last glaciation and the Holocene. Journal of Quaternary Science. 10: 197-210.

Markgraf V., Bradbury J.P., Schwalb A., Burns S.J., Stern C., Ariztegui D., Gilli A., Anselmetti F.S., Stine S., Maidana N. 2003. Holocene palaeoclimates of southern Patagonia: limnological and environmental history of Lago Cardiel, Argentina. The Holocene. 13 (4), 581-591.

Markgraf V., Whitlock C., Haberle S.G. 2007. Vegetation and fire history during the last 18,000 cal yr B.P. in southern Patagonia: Mallin Pollux, Coyhaique, Province Aisén (45°41'30"; S, 71°50'30"; W, 640m elevation. Palaeogeography, Palaeoclimatology, Palaeoecology. 254: 492-507.

Markgraf V., Whitlock C., Anderson R.S., García A. 2009. Late Quaternary vegetation and fire history in the northernmost *Nothofagus* forest region: Mallín Vaca Lauquen, Neuquén Province, Argentina. Journal of Quaternary Science. 24 (3): 248-258.

Massaferro J., Brooks S.J., Haberle S.G. 2005. The dynamics of chironomid assemblages and vegetation during the Late Quaternary at Laguna Facil, Chonos Archipelago, southern Chile. Quaternary Science Reviews. 24: 2510-2522.

Massaferro J.L., Moreno P.I., Denton G.H., Vandergoes M., Dieffenbacher-Krall A. 2009.Chironomid and pollen evidence for climate fluctuations during the Last Glacial Termination in NW Patagonia. Quaternary Science Reviews, 28 (5-6): 517-525.

Masson V., Vimeux F., Jouzel J., Morgan V., Delmotte M.., Ciais P., Hammer C., Johnsen S., Lipenkov V., Mosley-Thompson E., Petit J.R., Steig E.J., Stievenard M., Vaikmae R. 2000. Holocene climate variability in Antarctica based on 11 ice-core isotopic records. Quaternary Research. 54: 348-358.

Mayewski P.A., Maasch K. 2006. Recent warming inconsistent with natural association between temperature and atmospheric circulation over the last 2000 years. Climates of the Past Discussions. 10: 327-355.

Mayewski P.A., Meredith M.P., Summerhayes C.P., Turner J., Worby A., Barrett P.J., Casassa G., Bertler N.A.N., Bracegirdle T., Naveira Garabato A.C., Bromwich D., Campbell H., Hamilton G.S., Lyons W.B., Maasch K.A., Aoki S., Xiao C., van Ommen T. 2009. State of the Antarctic and Southern Ocean Climate system. Reviews of Geophysics. 47: RG1003 (38 pp.).

Mayr C., Fey M., Haberzettl T., Janssen S., Lücke A., Maidana N.I., Ohlendorf C., Schäbitz F., Schleser G.H., Struck U., Wille M., Zolitschka B. 2005. Palaeoenvironmental changes in southern Patagonia during the last millennium recorded in lake sediments from Laguna Azul (Argentina). Palaeogeography, Palaeoclimatology, Palaeoecology. 228: 203-227.

Mayr C., Wille M., Haberzettl T., Fey M., Janssen S., Lücke A., Ohlendorf C., Oliva G., Schäblitz F., Schleser G.H., Zolitschka B. 2007. Holocene variability of the Southern Hemisphere westerlies in Argentinean Patagonia (52°S). Quaternary Science Reviews. 26: 579-584.

McConnell J.R., Aristarain A.J., Banta J.R., Edwards P.R., Simões J.C. 2007. 20th-Century doubling in dust archived in an Antarctic Peninsula ice core parallels climate change and desertification in South America. Proceedings of the National Academy of Sciences of the USA (PNAS). 104 (14): 5743-5748.

McCulloch R.D. & Davies S.J. 2001. Late-glacial and Holocene palaeoenvironmental change in the central Strait of Magellan, southern Patagonia. Palaeogeography, Palaeoclimatology, Palaeoecology. 173: 143-173.

McCulloch R.D., Bentley M.J., Purves R.S., Hulton N.R.J., Sudgen D.E., Clapperton C.M. 2000. Climatic inferences from glacial and palaeoecological evidence at the last glacial termination, southern South America. Journal of Quaternary Science. 15: 409-417.

Montecinos A., Aceituno P. 2003. Seasonality of the ENSO-related rainfall variability in central Chile and associated circulation anomalies. Journal of Climate. 16: 281- 296.

Mohtadi M., Rossel P., Lange C.B., Pantoja S., Böning P., Repeta D.J., Grunwald M., Lamy F., Hebbeln D., Brumsack H.-J. 2008. Deglacial pattern of circulation and marine productivity in the upwelling region off central-south Chile. Earth and Planetary Science Letters. 272: 221-230.

Moreno P.I. 2004. Millennial-scale climate variability in Northwest Patagonia over the last 15 000 yr. Journal of Quaternary Science. 19: 35-47.

Moreno P.I., Léon A.L. 2003. Abrupt vegetation changes during the last glacial to Holocene transition in mid-latitude South America. Journal of Quaternary Science. 18: 787-800.

Moreno P.I., Jacobson G.L., Andersen B.G., Lowell T.V., Denton G.H. 1999. Vegetation and climate changes during the last glacial maximum and the last termination in the Chilean Lake District: A case study from Canal de la Puntilla (41°S). Geografiska Annaler. 81A: 285-311.

Moreno P.I., Jacobson G.L., Lowell T.V., Denton G.M. 2001. Interhemispheric climate links revealed by a late-glacial cooling episode in southern Chile. Nature. 409: 804-808.

Moreno P.I., Kaplan M.R., François J.P., Villa-Martínez R., Moy C.M., Stern C.R., Kubik P.W. 2009. Renewed glacial activity during the Antarctic cold reversal and persistence of cold conditions until 11.5 ka in southwestern Patagonia. Geology. 37 (4): 375-378.

Moreno P.I., Francois J.P., Villa-Martinez R.P., Moy C.M. 2008. Millennial-scale variability in Southern Hemisphere westerly wind activity over the last 5000 years in SW Patagonia. Quaternary Science Reviews. : 1-14.

Oppenheim DR. 1994. Taxonomic studies of *Achnanthes* (Bacillariophyta) in freshwater maritime antarctic lakes. Canadian Journal of Botany. 72: 1735-1748.

Pena L.D. & Cacho I. 2009. High-to low-latitude teleconnections during glacial terminations associated with ENSO-like variability. PAGES Newsletter. 17 (1): 5-7.

Pudsey C.J., Evans J. 2001. First survey of Antarctic sub-ice shelf sediments reveals mid-Holocene ice shelf retreat. Geology. 29 (9): 787-790.

Roberts S.J., Hodgson D.A., Bentley M.J., Smith J.A., Millar I.L., Olive V., Sugden D.E. 2008. The Holocene history of George VI Ice Shelf, Antarctic Peninsula from clast-provenance analysis of epishelf lake sediments. Palaeogeography, Palaeoclimatology, Palaeoecology. 259: 258-283.

Rosqvist G.C., Schuber P. 2003. Millennial-scale climate changes on South Georgia, Southern Ocean. Quaternary Research. 59: 470-475.

Rozema J., van Geel B., Björn L.O., Lean J., Madronich S. 2002. Paleoclimate: Toward solving the UV puzzle. Science. 296 (5573): 1621-1622.

Sabbe K., Verleyen E., Hodgson D.A., Vanhoutte K., Vyverman W. 2003. Benthic diatom flora of freshwater and saline lakes in the Larsemann Hills and Rauer Islands, East Antarctica. Antarctic Science. 15 (2): 227-248.

Sicko-Goad L., Stoermer E.F., Ladewski B.G. 1977. A morphometric method for correcting phytoplankton cell volume estimates. Protoplasma. 93: 147-163.

Sicko-Goad L., Schelske C.L., Stoermer E.F. 1984. Estimations of intracellular carbon and silica content of diatoms from natural assemblages using morphometric techniques. Limnology & Oceanography. 29 (6): 1170-1178.

Shevenell A.E., Domack E.W., Kernan G. 1996: Record of Holocene paleoclimate change along the Antarctic Peninsula: Evidence from glacial marine sediments, Lallemand Fjord. In: Banks M.R., Brown M.J. (Eds.). Climate succession and glacial record of the Southern Hemisphere, Papers Proceedings of the Royal Society of Tasmania. 130: 55-64.

Shulmeister J. R., Rodbell D.T., Gagan M.K., Seltzer G.O. 2006. Inter-hemispheric linkages in climate change: paleo-perspectives for future climate change. Climate of the Past Discussions. 2: 79-122.

Sjunneskog C., Taylor F. 2002. Postglacial marine diatom record of the Palmer Deep, Antarctic Peninsula (ODP Leg 178, Site 1098). 1. Total diatom abundance. Paleoceanography. 17: doi: 10.1029/2000PA000563.

Smith J.A., Bentley M.J., Hodgson D.A., Roberts S.J., Leng M.J., Lloyd J.M., Barrett M.S., Bryant C., Sugden D.E. 2007. Oceanic and Atmospheric Forcing of Early Holocene Ice Shelf Retreat, George Vi Ice Shelf, Antarctica Peninsula. Quaternary Science Reviews. 26: 500-516.

Sterken M., Verleyen E., Sabbe K., Terryn G., Charlet F., Bertrand S., Boës X., Fagel N., De Batist M., Vyverman W. 2008. Late Quaternary climatic changes in southern Chile, as recorded in a diatom sequence of Lago Puyehue (40°40'S). Journal of Paleolimnology. 39: 219-235

Stuiver M., Grootes P.M., Braziunas T.F. 1995. The GISP2 $\delta^{18}O$ climate record of the past 16,500 years and the role of the sun, ocean, and volcanoes. Quaternary Research. 44: 341-354.

Sugden D.E., Bentley M.J., Fogwill C.J., Hulton N.R.J., McCulloch R.D., Purves R.S. 2005. Late-glacial glacier events in southernmost South America: a blend of 'northern' and 'southern' hemispheric climatic signals? Geografiska Annaler A. 87A: 273-288.

Taylor F., Sjunneskog C. 2002. Postglacial marine diatom record of the Palmer Deep, Antarctic Peninsula (ODP Leg 178, Site 1098) 2. Diatom assemblages. Paleoceanography. 17 (3): Art. N°8001.

Toggweiler J.R. 2009. Shifting Westerlies. Science. 323: 1434-1435.

Trenberth K.E., Caron J.M. 2000. The Southern Oscillation Revisited: Sea Level Pressure, Surface Temperatures, and Precipitation. Journal of Climate. 13: 4358-4365.

Turner J., Colwell S.R., Marshall G.J., Lachlan-Cope T.A., Carleton A.M., Jones P.D., Lagun V., Reid P.A., Iagovkina S. 2005a. Antarctic climate change during the last 50 years. International Journal of Climatology. 25: 279-294.

Turner K.J., Fogwill C.J., McCulloch R.D., Sugden D.E. 2005b. Deglaciation of the eastern flank of the North Patagonian Icefield and associated continental-scale lake diversions. Geografiska Annaler. 87A: 363-374.

Urrutia R., Sabbe K., Cruces F., Pozo K., Becerra J., Araneda A., Vyverman W., Parra O. 2000. Paleolimnological studies of Laguna Chica de San Pedro (VIII Region): Diatoms, hydrocarbons and fatty acid records. Revista Chilena de Historia Natural. 73 (4): 717-728.

Van de Vijver B., Van Dam H., Beyens L. 2006. *Luticola higleri sp. nov.*, a new diatom species from King George Island (South Shetland Islands, Antarctica. Nova Hedwigia. 82(1-2): 69-79.

Van de Vijver B., Mataloni G. 2008. New and interesting species in the genus *Luticola* D.G. Mann (Bacillariophyta) from Deception Island (South Shetland Islands). Phycologia. 47: 451-467.

Vargas-Ramirez L., Roche E., Gerrienne P., Hooghiemstra, H. 2008. Pollen-based record of Lateglacial-Holocene climatic variability on southern Lake District, Chile. Journal of Paleolimnology. 39 (2): 197-217.

Verleyen E., Vyverman W., Sterken M., Hodgson D.A., De Wever A., Juggins S., Van de Vijver B., Jones V.J., Vanormelingen P., Roberts D., Flower R., Kilroy C., Souffreau C., Sabbe K. In Press. The importance of dispersal related and local factors in shaping the taxonomic structure of diatom metacommunities. Oikos. DOI: 10.1111/j.1600-0706.2009.17575.x

Verschuren D., Charman D.J. 2008. Latitudinal linkages in moisture-balance variation. Chapter 8, In: Battarbee R.W., Binney H.A. (Eds.): Natural climate variability and global warming. A Holocene perspective. Wiley-Blackwell, Chichester, United Kingdom: 189-231.

Villalba R. 2007. Tree-ring evidence for tropical-extratropical influences on climate variability along the Andes in South-America. PAGES News. 15 (2): 23-25.

Villa-Martinez R., Villagrán C., Jenny B. 2004. Pollen evidence for late-Holocene climatic variability at Laguna de Aculeo, Central Chile (lat. 34°S). The Holocene. 14 (3): 363-369.

Villa-Martinez R., Moreno P.I. 2007. Pollen evidence for variations in the southern margin of the westerly winds in SW Patagonia over the last 12,600 years. Quaternary Research. 68: 400-409.

Vyverman W., Verleyen E., Sabbe K., Vanhoutte K., Sterken M., Hodgson D.A., Mann D.G., Juggins S., Van de Vijver B., Jones V., Flower R., Roberts D., Chepurnov V.A., Kilroy C., Vanormelingen P., De Wever A. 2007. Historical processes constrain patterns in global diatom diversity. Ecology. 88 (8): 1924-1931.

Whitlock C., Bianchi M.M., Bartlein P.J., Markgraf V., Marlon J., Walsh M., McCoy N. 2006. Postglacial vegetation, climate, and fire history along the east side of the Andes (lat 41-42.5°S), Argentina. Quaternary Research. 66: 187-201.

Wille M., Maidana N.I., Schäblitz F., Fey M., Haberzettl T., Janssen S., Lücke A., Mayr C., Ohlendorf C., Schleser G.H., Zolitschka B. 2007. Review of Palaeobotany and Palynology. 146: 234-246.

Yoon H.I., Park B.K., Kim Y., Kim D. 2000. Glaciomarine sedimentation and its palaeoceanographic implications along the fjord margins in the South Shetland Islands, Antarctica, during the last 6000 years. Palaeogeography, Palaeoclimatology, Palaeoecology. 157: 189-211.

Zale R. 1994. Changes in size of the Hope Bay Adélie penguin rookery as inferred from Lake Boeckella sediment. Ecography. 17: 297-304.

Summary

In order to frame the recent global climatic changes, climate and oceanic models need to be tested against known climatic variations in the past. Recently, deglacial and Holocene paleo-environmental related research has shifted its main focus from the North-Atlantic region to the Southern Hemispheric high latitudes, as Antarctica and the Southern Ocean have shown to play an important role in global climate regulation (e.g. Knorr & Lohman, 2003). Very recently, the tropical (mainly Pacific) latitudes have been evenly recognized as potentially playing a large role in global climate modulation, both at interannual-decadal (e.g. El Niño Southern Oscillation) and century to millennial time scales (e.g. long-term changes in ENSO variability; Shulmeister et al., 2006; Pena & Cacho, 2009). Pacific tropical and Antarctic climate anomalies are physically linked with each other through the strength and the position of the Antarctic Circumpolar Current (ACC) and Southern Westerly Wind belt (SWW). Therefore, recent climate reconstructions are focused on past changes in position and strength of these winds, which have a direct impact on local and/or regional weather patterns along the westcoast of South America, and the Antarctic Peninsula.

In this thesis, lake sediments were analyzed for biological, sedimentological and geochemical proxies, in order to infer past climatic changes at two key sites along a latitudinal transect from southern South America (40°S) through the Antarctic Peninsula (63°S).

The first two chapters of this thesis are dedicated to postglacial paleoenvironmental and related paleoclimatic changes, inferred from an 11.22 m sediment core from Lake Puyehue (Chilean Lake District, 40°S), located at the northern boundary of the Southern Westerly Wind belt.

In **Chapter 2**, we used fossil diatom assemblages from the Puyehue sediment record in order to reconstruct past changes in the lake environment (amounts of mixing and nutrients in the lake, as a function of changing temperature and/or wind/precipitation regimes linked with the Southern Westerlies). In **Chapter 3** we analysed the N/C content in the Puyehue core sediments, in order to detect changes in the main source (terrestrial versus aquatic) of organic matter throughout time, and compare this with the pollen and diatom concentrations in the core. For this, we first measured N/C ratios in different

terrestrial and aquatic sources, and the most appropriate sources were used as parameters in a mixing equation for calculating the terrestrial and aquatic fractions of organic matter in the core.

These studies revealed that the lake was probably already deglaciated before 17.9 ka BP, and that two important warming steps may have occurred at c. 17.3 BP and 12.8 ka BP, the latter indicating the start of extensive catchment vegetation development. These steps are evenly observed in other marine and terrestrial records in Patagonia, indicating a stepped southward shift of the Southern Westerlies during deglaciation. Towards the end of the Holocene (c. 3 ka BP) diatom data are tentatively interpreted in terms of a higher frequency of El Niño; an evolution that has also been observed in the tropical East Pacific area.

Chapters 4 to 7 are dedicated to the Antarctic Peninsula, where we first studied in detail the diatom communities currently living in Maritime Antarctica and Beak Island (NE-Antarctic Peninsula, 63°S), in order to better constrain the ecological preferences of the diatoms found in the fossil assemblages from Beak Island lake sediment cores (Chapters 6 and 7). For this, we screened the diatom communities from six surface samples from Beak Island, and from an existing database of 69 samples from Signy and Livingston Islands (Jones et al., 1993; Jones & Juggins, 1995), intercalibrating/identifying the species and providing an update on the systematics of the diatoms found on these Islands (**Chapter 4**). This has lead us to identify at least 14 species that recently appeared to be Antarctic endemes. Five of the species in our dataset were described as new species (**Chapter 5),** belonging to the genera *Chamaepinnularia*, *Craticula*, *Diadesmis* and *Navicula*. In **Chapter 6**, we explored the diatom species compositions in our intercalibrated dataset, and constructed a transfer function for NH_4^+ concentrations, which was then applied to the fossil diatom assemblages in a sediment core from Lake Beak-2 (Beak Island). This lake is essentially a shallow isolation basin, and its bottom sediments pointed to cold oceanographic coastal conditions between c. 5.9 and 3.0 ka BP.

Similarly, in **Chapter 7**, we reconstructed changes in sea-ice conditions and climate, by analyzing fossil diatom and pigment compositions from the highest (and deepest) isolation lake on Beak Island (Beak-1). This record extended back to 10.6 ka BP, and provided one of the few early-Holocene coastal marine paleoenvironmental records in the northeastern Antarctc Peninslua. A quick deposition of sediments was observed for the Early Holocene, and was followed by a period with seasonally open marine conditions

between c. 9.2 and 6.9 ka BP, providing evidence for relatively warm conditions in the Early Holocene. This broadly corresponded with the early retreat/disintegration of the ice shelf in the southern Prince Gustav Channel around 8.7-7.4 cal. ka BP. After the isolation of the basin, fluctuations in diatom productivity and pigment concentrations were tentatively linked to climatic optima (e.g. between c. 3.5 and 1.2 ka BP), which have also been detected in other records in the South Orkneys and on the Antarctic Peninsula. A subsequent decrease in organic content at c. 1.7-2.0 cal. ka BP broadly corresponded with the timing of ice shelf reformation in the Prince Gustav Channel and Larsen A area. This decrease was also marked by a change towards acid conditions between c. 1.7 and 1.5 cal. ka BP, and could be linked with a deteriorating/cooling climate. This timing corresponds with the onset of a neoglacial cooling as inferred from different studies in the Antarctic Peninsula region. A strong increase in productivity is observed in the upper centimeters of the core, and could be related to the recent warming observed in the Antarctic Peninsula, showing that this lake is one of the ecosystems that have already undergone a strong change under the influence of the recent rapid regional climate warming.

Samenvatting

Om de huidige globale klimaatveranderingen beter te kunnen begrijpen en te kaderen, worden klimaatmodellen ontwikkeld, die echter moeten getest worden door middel van geobserveerde klimaatveranderingen doorheen de tijd. In de laatste decennia is de focus van het paleoklimaat-onderzoek verschoven van de Noord-Atlantische regio naar de hoge zuidelijke breedtegraden (Antarctica en de Zuidelijke Oceaan), omdat die gebieden belangrijker bleken te zijn in de regulatie van het klimaat op wereldschaal dan vroeger gedacht (Knorr & Lohman, 2003). Recent is ook meer erkenning gegeven aan het belang van de tropen (en vooral in de Pacifische sector) in de beïnvloeding van het klimaat op wereldschaal, en dit niet alleen op inter-annuele schaal (bv. El Niño Southern Oscillation met zijn wereldwijde atmosferische en oceanische teleconnecties), maar ook op tijdschalen van honderden tot duizenden jaren (zoals de lange termijn veranderingen in frequentie en amplitude van El Niño; Shulmeister et al., 2006; Pena & Cacho, 2009).

Klimaat-anomalieën in de Pacifische tropen en in Antarctica zijn fysiek rechstreeks aan elkaar gekoppeld, en resulteren in veranderingen in de positie en sterkte van de Antarctische Circumpolaire Stroom (oceanisch) en de Zuidelijke Westenwindgordel (atmosferisch). Deze hebben beiden een directe en sterke invloed op het klimaat aan de westkust van Zuid-Amerika (en tot op zekere hoogte in het Antarctisch Schiereiland), en de reconstructie van die winden staat tegenwoordig centraal in vele internationale paleoklimaat-programma's.

In deze thesis werden biologische, sedimentologische en geochemische proxies in lacustriene sedimenten geanalyseerd, met het oog op het reconstrueren van klimaatgebonden milieuveranderingen in twee key-sites langsheen een longitudinaal transect van zuidelijk Zuid-Amerika (40°S) over het Antarctisch Schiereiland (63°S).

De eerste twee Hoofdstukken behandelen postglaciale paleomilieu- (en ermee gerelateerde klimaat-) veranderingen, afgeleid uit een 11.22 m lange sedimentboorkern van Lago Puyehue (Chileens merendistrict, 40°S), dat gesitueerd is aan de noordrand van de zuidelijke westenwindgordel.

In **Hoofdstuk 2** werden fossiele diatomeeënassemblages in de Puyehue sedimentboorkern geanalyseerd, om vroegere veranderingen in mixing regime en nutriëntgehaltes in het meer te reconstrueren, als benadering voor de ermee gelinkte

klimaatveranderingen (temperatuur, neerslag, wind), al dan niet gelinkt met veranderingen in de sterkte en positie van de westenwinden. In **Hoofdstuk 3** werden N/C analyses uitgevoerd op het organisch materiaal uit diezelfde boorkern, om zo de veranderingen te reconstrueren in de oorsprong (terrestrisch versus aquatisch) van dat organisch materiaal. Om deze fracties te berekenen werd gebruik gemaakt van de huidige N/C waarden van verschillende bronnen (planten, water, en in deze studie eerder oudere bodems) in het stroombekken van het meer. De veranderingen in terrestrische versus aquatische oorsprong van het organisch materiaal in de boorkern werden vergeleken met pollen en diatomeeën gegevens.

De analyses van de Puyehue boorkern toonden aan dat het meer reeds gedeglacieerd was vóór 17.9 ka BP (i.e. de geïnfereerde basale ouderdom van de boorkern). In beide Hoofdstukken zijn ook twee grote veranderingen geregistreerd, die waarschijnlijk duidden op een stapsgewijze opwarming van het klimaat in zuid-Chili, namelijk rond 17.3 ka BP en 12.8 ka BP. De laatstgenoemde opwarming ging gepaard met een sterke uitbreiding en ontwikkeling van de vegetatie in het stroombekken van Puyehue, en duidt op de mogelijke aanwezigheid van een (deel van) de gletsjer tot ongeveer 12.8 ka BP.

Deze stapsgewijze opwarming is ook waargenomen in andere mariene en terrestrische records in Patagonië, en weerspiegelt de zuidwaardse verschuiving van de zuidelijke westenwinden doorheen de tijd. De diatomeeënsamenstellingen in de bovenste delen van de Puyehue core, werden voorzichtig geïnterpreteerd in termen van een mogelijke verhoging in het aantal en/of de amplitude van El Niño gebeurtenissen, wat ook uit studies in de tropen reeds gebleken is.

Hoofdstukken 4 tot 7 zijn gewijd aan het Antarctisch Schiereiland, waar we in detail de diatomeeëngemeenschappen van enkele Maritiem Antarctische eilanden (en Beak Island) bestudeerd hebben, om aldus een beter beeld te hebben van de relatie tussen verschilende diatomeeënsoorten en het milieu waarin zij het best gedijen. Hiervoor werden 69 oppervlaktestalen van meren uit Livingston en Signy Island (Jones et al., 1993; Jones & Juggins, 1995) gescreend, en geïntercalibreerd met diatomeeënassemblages uit zes oppervlaktesedimenten en verschillende fossiele stalen uit sedimentboorkernen van meren op Beak Island (**Hoofdstuk 4**). Van de 102 soorten zijn er minstens 14 geïdentificeerd die momenteel als Antarctische endemen beschouwd worden. Er werden ook vijf nieuwe soorten beschreven (behorende tot de genera *Chamaepinnularia, Craticula*, *Diadesmis* en *Navicula*) (**Hoofdstuk 5**). In **Hoofdstuk 6** onderzochten we de soortensamenstelling in deze geïntercalibreerde dataset, en gebruikten die om een transfer functie op te stellen voor de kwantitatieve reconstructie

van NH_4^+ concentraties. Deze werd vervolgens toegepast op een boorkern uit Beak-2, een ondiep isolatiemeer op Beak Island. De mariene sedimenten van deze boorkern werden geïnterpreteerd aan de hand van fossiele diatomeeën- en pigmenten-assemblages, en duidden op waarschijnlijk koude mariene condities tussen 5.9 en 3.0 ka BP.

In **Hoofdstuk 7** werden vroegere zeeijs- en klimaatcondities gereconstrueerd aan de hand van fossiele diatomeeën en pigmentconcentraties uit een boorkern afkomstig van het hoogst gelegen (en diepste) meer van Beak-Island (Beak-1). Deze reconstructie ging terug tot c. 10.6 ka BP, en vormt één van de weinige ondiep-mariene reconstructies die teruggaan tot het vroeg-Holoceen. Na een periode van snelle sedimentatie, gelinkt aan de aanwezigheid van ijsbergen in/nabij het meer, werden seizoenaal open mariene condities gereconstrueerd voor de periode tussen c. 9.2 en 6.9 ka BP. Een dergelijke vroeg-Holocene warme periode komt overeen met verschillende studies in de regio, en onder andere met het opbreken van een ice shelf in het zuidelijke Prince Gustav kanaal. Na de isolatie van het meer werd een periode met hoge diatomeeënproductiviteit en pigmentconcentraties voorzichtig gelinkt met een klimaatsoptimum (tussen 3.5 en 1.2 ka BP), wat overeen komt met ongeveer gelijktijdige klimaatsopwarmingen gedetecteerd in het Schiereiland en de South Orkney eilanden. Een verandering in milieu rond 2.0-1.7 ka BP werd gedetecteerd, en wijst op zuurdere (en mogelijks vochtigere) omstandigheden in het meer. De productiviteit in het meer daalde sterk rond 1.7 ka BP, en is mogelijks gelinkt met een koeler klimaat. Qua timing komt deze verandering overeen met het begin van een neoglaciale afkoeling zoals geïnfereerd in verschillende sites rond het Antarctisch Schiereiland. Een sterke stijging in productiviteit in de bovenste sedimenten van de boorkern werd gelinkt met de recente temperatuursstijging in de regio, was erop zou wijzen dat dit meer één van de vele ecosystemen is dat reeds sterk veranderd is onder de recente klimaatveranderingen in het Antarctisch Schiereiland.

Appendix

List of publications of the author

A1 publications: in prep. (Thesis Chapters)

Sterken M., Van de Vijver B., Jones V., Verleyen E., Hodgson D.A., Vyverman W., Sabbe K. An illustrated and annotated checklist of freshwater diatoms (Bacillariophyta) from Maritime Antarctica (Livingston, Signy and Beak Island).

Sterken M., Verleyen E., Sabbe K., Hodgson D.A., Roberts S., Jones V., Balbo A., Moreton S., Vyverman W. A diatom and pigment based reconstruction of Holocene climate change on Beak Island, the Antarctic Peninsula.

Sterken M., Roberts S.J., Hodgson D.A., Vyverman W., Balbo A., Sabbe K., Moreton S., Verleyen E. Deglaciation history and Holocene climate dynamics to the north of Prince Gustav Channel, northeastern Antarctic Peninsula.

Van de Vijver B., **Sterken M.**, Vyverman W., Mataloni G., Nedbalova L., Kopalova K., Verleyen E., Sabbe K. Five new non-marine diatom taxa from islands in the Atlantic sector of the Southern Ocean.

A1 publications

Bertrand S., **Sterken M**., Vargas-Ramirez L., De Batist M., Vyverman W., Lepoint G., Fagel N. **In Press (Thesis Chapter)**. Bulk organic geochemistry of Puyehue Lake and watershed sediments (Chile, 40°S): Implications for paleoenvironmental reconstructions. Palaeogeography, palaeoclimatology, palaeoecology.

Verleyen E., Vyverman W., **Sterken M**., Hodgson D.A., De Wever A., Juggins S., Van de Vijver B., Jones V.J., Vanormelingen P., Roberts D., Flower R., Kilroy C., Souffreau C., Sabbe K. **In Press**. The importance of dispersal related and local factors in shaping the taxonomic structure of diatom metacommunities. Oikos. DOI: 10.1111/j.1600-0706.2009.17575.x

Sterken M., Verleyen E., Sabbe K., Terryn G., Charlet F., Bertrand S., Boës X., Fagel N., De Batist M. and Vyverman W. **2008 (Thesis Chapter)**. Late Quaternary climatic changes in southern Chile, as recorded in a diatom sequence of Lago Puyehue (40°40'S). J. Paleolimnol., 39 (2): 219-235.

Vyverman W., Verleyen E., Sabbe K., Vanhoutte K., **Sterken M.**, Hodgson D.A., Mann D.G., Juggins S., Van de Vijver B., Jones V.J., Flower R., Roberts D., Chepurnov V., Kilroy C., Vanormelingen P., De Wever A. **2007**. Historical processes constrain patterns in global diatom diversity. Ecology. 88 (8): 1924-1931.

Sterken M., Sabbe K., Chepstow-Lusty A., Frogley M., Cundy A., Vanhoutte K., Verleyen E. and Vyverman W. **2006**. Climate and land use changes in the Cuzco region (Cordillera Oriental, South East Peru) during the last 1200 years: a diatom based reconstruction. Archiv. Hydrobiol. 165 (3): 289-312.

Vanhoutte K., Verleyen E., Sabbe K., Kilroy C., **Sterken M**. and Vyverman W. **2006**. Congruence and disparity in benthic diatom communities of small lakes in New Zealand and Tasmania. Marine & Freshwater Research. 57 (8): 1-13.

A4 publications

Van Wichelen J., De Coster S., De Ruysscher F., De Keyser K., van Gremberghe I., **Sterken M.**, Vanormelingen P., van der Gucht K. En Vyverman W. (**2006**). Waterbloei, een bedreiging voor natuurwaarden in Vlaanderen? (Natuur.focus, 5(3): 91-97).

Front cover pictures:
On the left: Lago Puyehue (picture: Mieke Sterken)
On the right: Lake Beak-1 (picture: Dominic Hodgson)

Pictures on the back side:
SEM micrographs of maritime Antarctic diatoms (pictures: Mieke Sterken).